Visualising Pathways for Learning about Novelty in the Rodent Brain

Submitted to Cardiff University for the Degree of Doctor of Philosophy by

Lisa Kinnavane

2015

Acknowledgements

First, I would like to thank my supervisor, John Aggleton, for so many things, for the limitless guidance and support, for always having your office door open, for sharing your music and, not least, for helping me to see the wood when all I could find was trees.

Very special thanks to Eman Amin for carrying out the behavioural training for the experiments in Chapters 3 and 5. Also, thank you for teaching me many of the techniques that I used in this thesis and for becoming a great friend.

Thanks to Murry Horne for performing the hippocampal lesion surgeries on the rats used in Chapter 3 and to Cristian Olarte-Sánchez for doing the perirhinal lesion surgeries on the rats used in Chapters 5 and 6.

Thank you so much to Andrew Nelson and Anna Powell for your advice along the way, for keeping me smiling, and for dealing with all of those commas.

Thank you to Mathieu Albasser for taking the time to teach me the structural equation modelling technique. Thank you to all my colleagues and everybody in the Behavioural Neuroscience Lab, particularly Moira and Claudia.

To my girls, Becca, Clara, Amie and Virgine, I couldn't have gotten though these four years without you. Thanks to Jamie and Ellie for putting up with an often absent sister in the name of science, to the rest of my family for always being interested in my work and to my friends in Galway for helping me to forget that work... at least sometimes.

And last, but by no means least, to my ultimate support system, Mike, Mum and Dad, thank you simply isn't enough. To my boy, my love, my partner in crime, enormous thanks for your understanding, your support, and for always knowing what to say to make me laugh. To Mum and Dad, if we grew up together I think this marks the point that we all, finally, become adults (about time too!). I am eternally grateful for everything that you have both done to get me here, for your unshakable belief in me, and for encouraging me to follow my passion. This is dedicated to you.

Summary

Recognition memory is the ability to distinguish novel from familiar stimuli. This thesis explores opposing models of recognition memory that alternatively assume that the perirhinal cortex and hippocampus (regions of the medial temporal lobe) must functionally interact to support recognition memory or that the perirhinal cortex can support this process independently. Additionally, the way in which these areas differentially interact to support learning about novel compared to familiar stimuli was examined.

To achieve this, rats with lesions to the hippocampus or perirhinal cortex were given tests of object recognition memory or allowed to explore novel stimuli, after which, regional neuronal activity and network interactions were explored. This was achieved by immediate-early gene imaging; the expression of c-*fos* was used as a marker of neuronal activity, allowing for the assessment of regional activity at an extremely high anatomical resolution. Network interactions were explored using structural equation modelling; a statistical technique that made it possible to test if the observed activity could be mapped on to known anatomical pathways. In this way, network dynamics supporting these behavioural tasks were explored. Thus, the functional interdependence of the hippocampus and perirhinal cortex was tested both when the brain was intact and following lesions. This was done at multiple levels; behaviourally, at the level of regional activation and at the level of systems interactions.

The behavioural and network analyses from the lesion studies provide evidence for the functional independence of the perirhinal cortex and hippocampus. Parallel work in the intact rats provided evidence that, under normal circumstances, novel or familiar stimuli can define patterns of parahippocampal-hippocampal interactions. Specifically, novelty engaged lateral entorhinal cortical layers II and III to recruit CA3 (the perforant path) and subsequently CA1, while familiarity was associated with the more direct route from the lateral entorhinal cortex to CA1 (the temporoammonic pathway).

Contents

Figures

Tables

1. General Introduction

1.1 Overview

The research described in this thesis focuses on elucidating the neural networks that contribute to recognition memory in rodents, and further exposing the manner in which network dynamics are altered by exposure to novel or familiar stimuli. While we have learned a huge amount about the brain and its regional specialisation from traditional lesion studies, it is clear that no single region completes even the simplest cognitive task in isolation. Thus, the overarching aim of this work is to reconstruct functional networks of anatomically connected regions. Lesion experiments are interpreted in a novel way, by assessing their impact not only on the behaviour of the animals but also on the remaining components of these functional networks.

Put simply, recognition memory is the ability to distinguish novel from familiar stimuli; this process involves stimulus identification along with a judgement of prior occurrence (Mandler, 1980) and as such it can be considered to be a component of declarative memory. This ubiquitous form of memory is shared by humans with other animals, making it an important target for neuroscientific investigation. It has many interesting features that make it a good model system for studying memory, particularly as components of recognition memory can be tested non-verbally in animals, something that is not possible for episodic memory, as this requires mental time-travel and introspection (Tulving, 1972). These are features that cannot be tested in animals. Recognition memory does, however, share characteristics with episodic memory. For example, it requires only a single exposure and so information can be retrieved following a single episode, it occurs quickly and exposures can be very short. There are several models that postulate how regions of the medal temporal lobe interact to support recognition memory and the main focus of this thesis will be to test aspects of these models.

1.2 A brief history of behavioural testing for recognition memory

The hippocampus was brought to the forefront of memory research in 1957 with the seminal paper by Scoville and Milner describing a patient, H.M., who, following the bilateral resection of his hippocampi and surrounding cortices, presented with dense

anterograde amnesia (Scoville and Milner, 1957). This, along with the discoveries of long-term potentiation in the dentate gyrus (Bliss & Lomo, 1973) and place cells in the hippocampal subfield, CA1 (O'Keefe & Dostrovsky, 1971), led to the influential notion that the hippocampus is central to mnemonic processing. A great deal of research has subsequently implicated the surrounding regions in forming subtly different forms of memories, including, memories of prior occurrence. Much of the memory-related research that followed H.M. was carried out in animal models. This necessitated the creation of appropriate tests of memory in animals that taxed the same neuropsychological mechanisms thought to support mnemonic processing in humans. This section will give a short history of recognition memory testing, beginning in humans and moving on to the development of similar tests for monkeys and then rodents, leading up to the paradigms commonly used today.

1.2.1 Delayed matching/nonmatching to sample tasks

Recognition memory has been tested in humans in a very simple manner for over 100 years. This test is known as the delayed matching-to-sample paradigm. In an example of these early tests of recognition memory, subjects were presented with a list of twenty words. Following a variable delay, they were given a second list of forty words; twenty from the list seen previously and twenty new words. This is a forced-choice paradigm as subjects were instructed to indicate 20 words they recognised as being from the original list, along with their degree of certainty, even if this involved guessing (Strange, 1913; Strange & Strange, 1916).

One of the most important challenges in recognition memory research over the last century has been to create a behavioural test for animals that closely mimics how recognition memory is tested in humans. The first such test was an object based delayed matching-to-sample paradigm in rhesus monkeys (Gaffan, 1974). The following year the delayed nonmatching-to-sample (DNMS) paradigm was introduced by Mishkin and Delacour (1975). The DNMS task (Figure 1.1A) is based on the discovery that by using a rewarded forced-choice procedure, monkeys can rapidly be trained to select a novel object in preference to a familiar object, thereby demonstrating recognition memory. Importantly, the DNMS task requires only a single exposure phase to familiarise the monkey with the initial sample stimulus, e.g., object A. After a delay, the monkey is given a choice between the now familiar object A and novel object B. Selection of object B is rewarded. In this way, the monkey is reinforced for applying a nonmatching rule to a familiar sample object after a retention delay, i.e., delayed nonmatching-to-

sample. The next trial involves a completely new pair of objects, e.g., sample object C and novel object D. Thus, a series of trials can be represented as A+ then A- vs. B+ (trial 1); C+ then C- vs. D+ (trial 2); E+ then E- vs. F+ (trial 3), and so on, where the object with a plus sign covers a food reward and the object with a negative sign is unrewarded (Figure 1.1A).

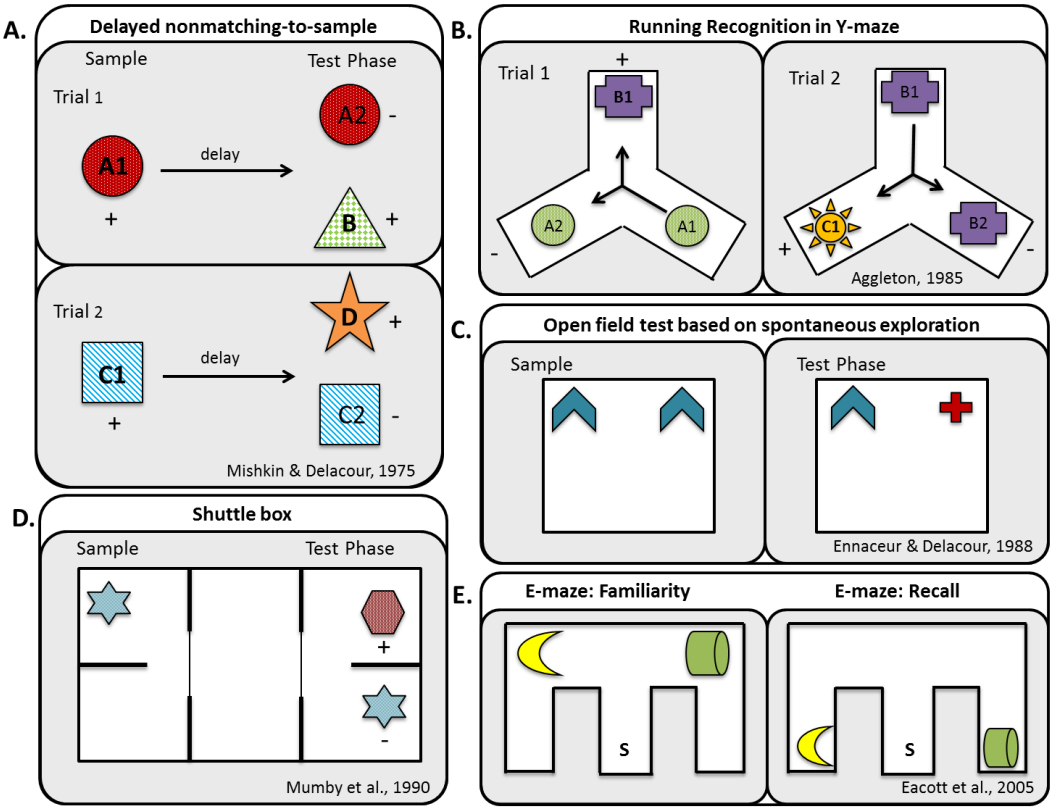

Figure 1.1. Schemata of various tests of object recognition memory.

(A) Delayed nonmatching-to-sample task designed for monkeys. (B) Running Recognition in Y-maze; arrows show direction of rats movements. (C) Open field test of object recognition memory; none of the objects are associated with a food reward. (D) Shuttle box test; two sliding doors separate the central holding area from the sample and test regions at the ends of the maze. (E) E-maze; S denotes the start arm. Configuration of sample and test phases for both familiarity and recall are as shown, upon completion of the sample phase the rat is placed in a holding cage with a copy of one of the objects from the sample phase for habituation. The animal is then returned to the maze; when the objects are placed on the backbone of the E-maze the rat can see them from the start arm and so can choose the non-habituated object based on familiarity processing whereas when the objects are placed in the outer arms they cannot be seen from the start arm and so must use recall processes to remember where the non-habituated object is located. + Objects associated with food reward. Bold letters represent novel objects.

The DNMS task not only has clear parallels with forced-choice recognition tests given to humans but also permits multiple recognition problems within a single session. As studies with monkeys inevitably rely on very small group sizes, the ability to give many

trials per session is an essential feature if the task is going to differentiate between neural manipulations. The DNMS protocol also proved to be highly versatile, as it can easily be given with varying retention intervals and altered interference between sample and recognition test (Mishkin, 1978). The task can also be given in the dark in order to test tactile recognition memory (Murray & Mishkin, 1985). By taking advantage of the monkey's spontaneous preference for novelty over familiarity, the DNMS task is not only quick to train but reduces the likelihood that deficits arise because the nonmatching rule itself has been lost. Furthermore, it proved relatively straightforward to test humans on both delayed matching-to-sample and delayed nonmatching-to-sample tasks that were deliberately modelled on DNMS tests given to monkeys. Such experiments showed, for example, that anterograde amnesia is typically sensitive to this form of recognition test (Aggleton et al., 1988; Squire et al., 1988).

The next step was to determine if rodents could also learn a DNMS task that involved a single sample exposure. In the first such experiment (Aggleton, 1985), rats ran in a Y-shaped maze where they selected between objects using a 'running recognition' protocol. Consequently, the novel stimulus for one trial became the familiar stimulus for the subsequent trial. In practice, the reinforced rule was to choose the arm with novel contents and avoid the arms with familiar contents (Figure 1.1B). As the nonmatching procedure was continuous, there was no discrete sample phase, apart from at the very start of the session (trial 0). The task design can, therefore, be represented as A+ (trial 0), A- vs. B+ (trial 1), B- vs. C+ (trial 2), D+ vs. C- (trial 3), E+ vs. D- (trial 4), and so on. The continuous testing procedure makes it possible to give multiple trials per session without having to handle the rats.

A later nonmatching task for rats (Mumby et al., 1990) included a separate sample phase at the start of each trial, so more closely following the DNMS procedures given to monkeys. The apparatus consisted of a shuttle box with a central holding area (Mumby et al., 1990; Figure 1.1D). To start each trial, the rat ran from the central holding area to the sample end to explore novel object A. This familiarisation phase was followed by a choice test at the opposite end of the shuttle box between the now familiar, object A and a novel alternative, object B. The rat was rewarded with food for selecting the novel object rather than the familiar sample object. New sets of objects were used for each trial. Again, the rats were not handled during the test session and multiple trials could be given within each session (Mumby et al., 1990).

More recently these rodent DNMS tasks have been replaced by other, simpler methods. The problem is that rodent DNMS tasks involve considerable training. Even then, some rats struggle to reach levels of performance that would be informative when trying to manipulate recognition memory. A related issue is that because task acquisition is demanding, it remains possible that neural interventions might affect performance by altering the ability to learn and apply the rule, rather than by affecting the ability to distinguish novel from familiar stimuli. These tasks also depend on the use of food rewards, meaning changes in motivation might alter performance. Thus, a simpler test was required.

1.2.2 Spontaneous object recognition

The assessment of recognition memory in rodents was transformed by the introduction of spontaneous preference tests based on measurements of exploration. This was based on work that began in the 1950's. It was first demonstrated that rats reduce time spent exploring an object over subsequent presentations (Berlyne, 1950). It was also shown in T-maze studies that rats prefer arms that have a changed appearance and so seem novel (Dember, 1956; Kivy et al., 1956). Subsequently, it was demonstrated that hamsters will spend more time exploring an object that has moved to a novel position (Poucet et al., 1986). Utilising this preference for novelty, Ennaceur and Delacour (1988) showed that if rats are given sufficient time to explore two identical copies of object A in an open rectangular arena, they will typically spend more time exploring novel object B in preference to a duplicate of object A, when placed back in that same arena following a retention delay (Figure 1.1C). This simple, but powerful, protocol has led to countless experiments into the neural basis of recognition memory. Spontaneous preference tasks are also very versatile and have been adapted to measure memory for object location (Poucet et al., 1986; Ennaceur et al., 1997) object-in-place information (Dix & Aggleton, 1999), object-in-context conjunctions (Dix & Aggleton, 1999; Norman & Eacott, 2005), object reconfigurations (Ennaceur & Aggleton, 1994) and object recency (Mitchell & Laiacona, 1998), along with various combinations of these forms (Eacott & Norman, 2004; Dere et al., 2005; Good et al., 2007; Langston & Wood, 2010).

There are several advantages of the spontaneous object recognition task. The spontaneous nature of the task rule makes the procedure simple to run; rodents require little pre-training except for habituation to the test arena. Further, normal rats require only a single exposure to a sample object to display successful recognition memory. Additionally, food or water deprivation is not required and so the results should not be

sensitive to manipulations that affect motivation. As mentioned previously, the task is also very versatile, making it easy to alter task difficulty by altering the interval between sample and test. The popularity of the spontaneous object recognition task is reflected in the fact that the initial paper by Ennaceur and Delacour (1988) has been cited over a thousand times (ISI, Web of Science). It has also been estimated that approximately 43,000 animals were used in this type of task or its close variants in the years 2007-2012 (Ameen-Ali et al., 2012).

Despite these procedural advantages, in order for a behavioural paradigm to be truly useful, construct validity must be demonstrated; i.e., that the task taxes the cognitive processes that are thought to support recognition memory and so relies on the same neural substrates. For example, it could be argued that the spontaneous recognition test simply measures habituation to repeated stimuli, a form of implicit learning, and as such, is not comparable to the explicit tests of recognition memory given to humans. However, studies with rodents have shown that perirhinal lesions do not affect the decrease in exploration that occurs with repeated presentation of the same stimulus (i.e., habituation), while concurrently the lesions impair object recognition based on the preference between two objects presented simultaneously (Mumby et al., 2007; Albasser et al., 2009; 2011b).

It is possible to examine if spontaneous tests of recognition memory involve similar neural structures to those required for forced-choice tests of recognition. One source of evidence comes from comparing the outcome of DNMS experiments with those using spontaneous object preference tasks. Taking the example of brain lesions in rats, it can be seen that perirhinal cortex lesions impair object recognition whether tested using spontaneous tasks (Aggleton et al., 1997; Winters et al., 2008; Aggleton et al., 2010) or DNMS procedures (Mumby & Pinel, 1994). Similarly, perirhinal lesions in monkeys disrupt both DNMS and visual-paired comparison tasks, which compare the times spent looking at novel and familiar stimuli (Nemanic et al., 2004). Further, lesions in sites such as the fornix, medial prefrontal cortex, and mammillary bodies spare object recognition in rats whether tested using nonmatching-to-sample (Aggleton et al., 1990; Shaw & Aggleton, 1990) or spontaneous preference tests (Ennaceur & Aggleton, 1994; Aggleton et al., 1995; Ennaceur et al., 1996, 1997; Barker at al., 2007). Comparisons between the consequences of hippocampal lesions in rats are more difficult to interpret as the majority of both spontaneous and reinforced nonmatching studies describe sparing of recognition memory, while some studies report deficits (Aggleton et al., 1986;

Mumby et al., 1992; Clark et al., 2000; Mumby et al., 2001; Forwood et al., 2005; Ainge et al., 2006; Winters et al., 2008; Broadbent et al., 2010; Barker & Warburton, 2011b). There is, however, evidence from a study in monkeys that hippocampal lesions cause profound deficits in the visual paired comparison task while sparing performance in a DNMS task, except under the most difficult test conditions, suggesting that these task do not tax the same neural processes (Nemanic et al., 2004). A similar result was also seen in humans (Pascalis et al., 2004). These results will be discussed more extensively in the next section, but taken overall, spontaneous preference tests of recognition memory for rodents give comparable results to those found with reinforced nonmatching procedures.

1.3 Neural basis of recognition memory

This section will further discuss insights into the neural substrates of recognition memory obtained from spontaneous object recognition tasks along with several other informative paradigms in both primates and rodents. First, however, a description of the neuroanatomy relevant to the following arguments will be given.

1.3.1 Anatomy of the rodent medial temporal lobe

Despite debate over the specific functions of component parts of the medial temporal lobe there is consensus that this region is highly important for memory, notably recognition memory (Brown & Aggleton, 2001; Eichenbaum et al., 2007; Wixted & Squire, 2011; Ranganath & Ritchey, 2014). Consequently, an understanding of the underlying anatomy and connections of this region is particularly important when trying to interpret the results of lesion and electrophysiological studies. The rodent medial temporal lobe includes the hippocampal formation and the adjacent rhinal cortices (Figure 1.2). The hippocampal formation can be divided into the hippocampus proper and the subicular cortices. The hippocampus proper comprises the CA fields 1-3 and the dentate gyrus. The subicular cortices can also be further subdivided into the subiculum, presubiculum, parasubiculum and postsubiculum (Figure 1.2; Aggleton, 2012). The rodent rhinal cortices are divided into areas 35 and 36, composite parts of the perirhinal cortex (PRH), postrhinal cortex (POR), lateral entorhinal cortex (LEC) and medial entorhinal cortex (MEC) (Figure 1.2; van Strien et al., 2009). These various regions can be differentiated based on their laminar structure; the dentate gyrus, CA1-3 and the subiculum are formed of three layers, while the pre-, para- and postsubiculum and the rhinal cortices have six layers (Amaral & Lavenex, 2007). In the rodent, the cortical regions listed above can be collectively referred to as the parahippocampal cortex. This

is noteworthy as in the primate brain the ‘parahippocampal cortex’ is a defined region in and of itself (areas TF, TH); it is homologue of the rodent postrhinal cortex (Aggleton, 2012).

In simplified terms, the anatomical connections in this region can be thought of as following two streams, although these are by no means completely segregated (Figure 1.3; VanStrien et al., 2009). The postrhinal and perirhinal have differences in the origin of their afferents but can generally be thought of as receiving inputs from unimodal and polymodal association areas (Burwell & Amaral, 1998a,b). The perirhinal cortex is densely reciprocally connected with the lateral entorhinal cortex, while the medial entorhinal cortex has stronger connections with the postrhinal cortex (Naber et al., 1997; Burwell & Amaral, 1998a,b). The medial and lateral entorhinal cortices then, in turn, provide the main hippocampal afferent connections (Amaral, 1993; Witter, 1993).

The perirhinal cortex is important to many of the arguments that follow. Together with the postrhinal cortex, it can be viewed as one of the input regions of this system and so a detailed description of their connections beyond the parahippocampal region is given. The perirhinal cortex lines the banks of the posterior third of the rhinal sulcus (Figure 1.2). Rostral to it lies the insular cortex and it begins where the claustrum ends. It is bound dorsally by the ventral temporal association area (also known as TE/Te2/Tev), ventrally by the lateral entorhinal cortex and caudally by the both the lateral entorhinal and postrhinal cortices (Burwell, 2001). It consists of two cytoarchitecturally distinct regions; the dorsal area 36 and ventral area 35 (Figure 1.2), each having different efferent and afferent patterns of connectivity (Burwell and Amaral, 1998a,b; Burwell, 2001; Furtak et al., 2007).

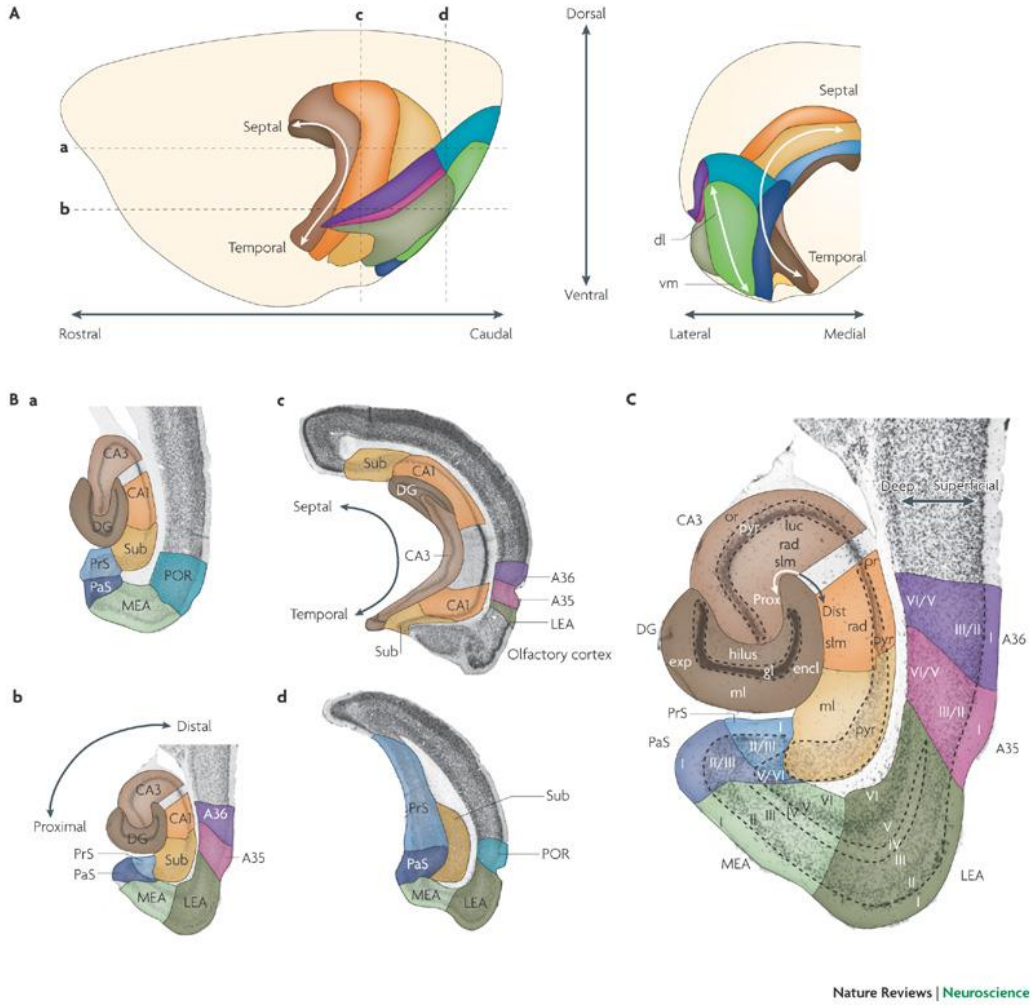

Figure 1.2. Depiction of the hippocampal formation and parahippocampal region in the rat brain.

Part A: Lateral (left panel) and caudal (right panel) views. For orientation in the hippocampal formation (consisting of the dentate gyrus (DG; dark brown), CA3 (medium brown), CA2 (not indicated), CA1 (orange) and the subiculum (Sub; yellow), three axes are indicated: the long or septotemporal axis (also referred to as the dorsoventral axis); the transverse or proximodistal axis, which runs parallel to the cell layer and starts at the DG; and the radial or superficial-to-deep axis, which is defined as being perpendicular to the transverse axis. In the parahippocampal region (green, blue, pink and purple shaded areas), a similar superficial-to-deep axis is used. Additionally, the presubiculum (PrS; medium blue) and parasubiculum (PaS; dark blue) are described by a septotemporal and proximodistal axis. The entorhinal cortex, which has a lateral (LEA; dark green) and a medial (MEA; light green) aspect, is described by a dorsolateral-to-ventromedial gradient and a rostrocaudal axis. The perirhinal cortex (consisting of Brodmann areas (A) 35 (pink) and 36 (purple)) and the postrhinal cortex (POR; blue-green) share the latter axis with the entorhinal cortex and are additionally defined by a dorsoventral orientation. The dashed lines in the left panel indicate the levels of two horizontal sections (a,b) and two coronal sections (c,d), which are shown in part B. Part C: A Nissl-stained horizontal cross section (enlarged from part Bb) in which the cortical layers and three-dimensional axes are marked. The Roman numerals indicate cortical layers. CA, cornu ammonis; dist, distal; dl, dorsolateral part of the entorhinal cortex; encl, enclosed blade of the DG; exp, exposed blade of the DG; gl, granule cell layer; luc, stratum lucidum; ml, molecular layer; or, stratum oriens; prox, proximal; pyr, pyramidal cell layer; rad, stratum radiatum; slm, stratum lacunosum-moleculare; vm, ventromedial part of the entorhinal cortex. Reproduced from VanStrien et al. (2009).

Area 36 receives over half of its inputs from surrounding temporal regions such as the ventral temporal association cortex; it also receives projections from the insular cortex, visual association regions of the occipital cortex as well as frontal and parietal multimodal areas, but these are somewhat less dense than the temporal connections. The main inputs into area 35 are from the piriform and insular cortices with less numerous projections from olfactory regions, temporal, parietal and frontal association areas. Additionally, both areas are reciprocally connected to the amygdala, (Burwell and Amaral, 1998b; Furtak et al., 2007). The extrinsic cortical efferent connections of areas 35 and 36 generally follow the pattern of their afferent connections. Area 35 sends a dense projection to the insula while the most numerous projection from area 36 is to the ventral temporal association area. They also both send efferents to frontal temporal and parietal association areas, including the secondary somatisensory cortex (Agster & Burwell, 2009). The postrhinal cortex receives a high proportion of its inputs from visual areas in the occipital cortex, mainly from association areas but to a lesser extent from primary visual cortex. It also receives inputs from visuospatial areas, including posterior parietal and ventral temporal cortex as well as the retrosplenial cortex (Burwell and Amaral, 1998b; Furtak et al., 2007). The majority of postrhinal connections are highly reciprocal; thus the densest output is to the visual association areas in the occipital cortex with other strong projections to ventral temporal cortex, posterior parietal cortex and cingulate cortex (Agster & Burwell, 2009). On the whole, the perirhinal cortex receives multimodal sensory related inputs and as such has been described as “the locus of a convergence of perceptual information”, while the majority of regions that the postrhinal cortex is connected to are related to visual processing (Furtak et al., 2007; Burwell & Agster, 2008).

Area 36 is more heavily reciprocally connected with the postrhinal cortex than is area 35 (Burwell & Amaral, 1998a). The connections between the perirhinal cortex and lateral entorhinal cortex follow a ventral to dorsal gradient, which gives them a degree of directionality. The strongest projections are from area 36 to area 35 and from area 35 to lateral entorhinal cortex. The projections to lateral entorhinal cortex originate predominantly in layers III and V of area 35 (although area 36 does send a weaker projection) and converge on layers II and III of the lateral entorhinal cortex (Figure 1.3; Burwell & Amaral, 1998a; Kerr et al., 2007). Area 35 receives relatively strong projections back from the lateral entorhinal cortex while area 36 receives a much weaker back projection; both originating predominantly in cortical layers III and V of the lateral entorhinal cortex. Both of these connections are less numerous than the reciprocal ones

into the lateral entorhinal cortex (Burwell & Amaral, 1998b). Additionally, a small proportion of the cortical input to both area 35 and 36 arises in the medial entorhinal cortex (Burwell & Amaral, 1998b). Both areas 35 and 36 have a reciprocal connection with CA1 and to a lesser extent, with the subiculum (Furtak et al., 2007).

The postrhinal cortex is predominantly connected to the medial entorhinal cortex (Figure 1.3), although it does have a lighter connection with lateral entorhinal cortex (Naber et al., 1997; Burwell & Amaral, 1998a). These projections originate in cortical layers II, III and V and converge on layers II and III of the entorhinal cortex (Burwell & Amaral, 1998a; Furtak et al., 2007; Kerr et al., 2007). The postrhinal cortex also has modest connections with the septal region of CA1 (Furtak et al., 2007). Additionally, there are dense reciprocal connections between areas of the entorhinal cortex. In the medial area, neurons in cortical layers II, III, V and VI project to layers II and III of the lateral region. The return projections are slightly more complicated; cells in layers II and V of the lateral entorhinal cortex project to layers II and III of the medial entorhinal cortex while layers III and VI of the lateral region project across the depth of the medial entorhinal cortex (VanStrien et al., 2009).

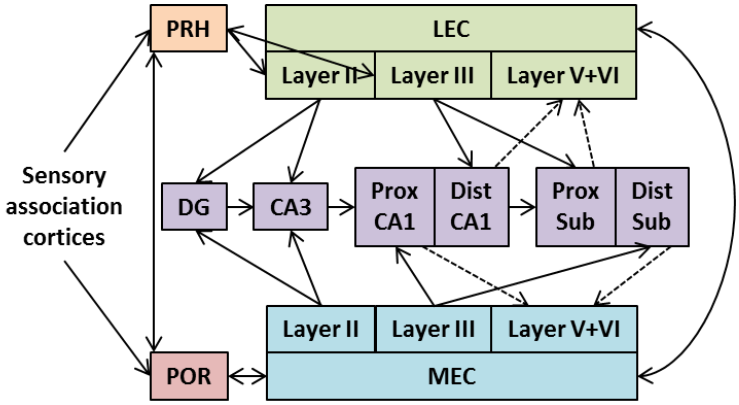

Figure 1.3. Simplified schematic of the prevailing connections of the medial temporal lobe.

Abbreviations: CA = Cornu Ammonis; Dist = distal; DG = denate gyrus; LEC = lateral entorhinal cortex; MEC = medial entorhinal cortex; POR = postrhinal cortex; PRH = perirhinal cortex; Prox = proximal. For simplicity the schematic does not include the direct connections linking PRH (and POR) with CA1/subiculum.

The hippocampus proper is traditionally thought of as being a unidirectional trisynaptic loop. This loop can be thought of as beginning with neurons in cortical layer II (although other layers contribute sparsely; VanStrien et al, 2009) of the both the medial and lateral entorhinal cortices; these axons travel in a projection known as the perforant pathway

and synapse with the granule cells of the dentate gyrus (Steward & Scoville, 1976; Amaral, 1993; Dolorfo & Amaral, 1998). These excitatory synapses follow a well-defined organisation; axons from the lateral entorhinal cortex make contact with the outer third of the granule dendritic tree, while axons from the medial entorhinal cortex make contact with the middle third of the dendritic arbour. The granule cells of the dentate gyrus then project to CA3; these axons are known as mossy fibres. Mossy fibres make synaptic contact with proximal apical dendrites of the pyramidal cells in CA3 which, in turn, send Schaffer collaterals to the pyramidal cells of the ipsilateral CA1. In addition, CA3 neurons send commissural projections to the contralateral CA3 and CA1 pyramidal cells. To summarise, the canonical trisyanaptic loop can be represented as: entorhinal cortex → dentate gyrus (synapse 1), dentate gyrus → CA3 (synapse 2), CA3 → CA1 (synapse 3) (Amaral & Lavenex, 2007; Burwell & Agster, 2008). These connections have a well-defined topography across the transverse axis of the hippocampus, which is defined in relation to the dentate gyrus. In this dimension, non-adjacent regions are more densely connected. That is, neurons in the proximal region (closer to dentate gyrus) of CA3 project to the distal region of CA1 while distal CA3 cells project to proximal CA1 (Amaral, 1993; VanStrien et al., 2009).

To complete the picture, there are additional pathways to be included that are not set out in this conventional trisynaptic view. These include the temporoammonic pathway which carries axons that originate in cortical layer III of the entorhinal cortex and terminate bilaterally on distal apical dendrites of CA1 pyramidal neurons (Steward & Scoville, 1976; Amaral, 1993; Amaral & Lavenex, 2007). An additional layer of complexity comes from the fact that the lateral entorhinal cortex has a stronger projection to distal CA1 and proximal subiculum (i.e. inputs terminate around the border between CA1 and subiculum) while MEC preferentially projects to proximal CA1 and distal subiculum (Amaral, 1993; Witter, 1993). The projection from CA1 to the subiculum has a similar transverse topography, in that neurons in the proximal region of CA1 synapse on neurons in the distal regions of the subiculum and *vice versa*. Together with the trisynaptic loop, these connections can be termed the polysynaptic pathway (VanStrien et al., 2009). Further, it should be noted that while the predominant direction of connections is as described here, more modest back-projections have also been reported from CA3 back to the dentate gyrus, as well as from CA1 to CA3 (reviewed in VanStrien at al., 2009).

The main output from the hippocampal formation is from CA1 and subiculum to cortical layers V and VI of the entorhinal cortex (Tamamaki & Nojyo, 1995), although fibres can terminate sparsely in the more superficial layers (VanStrien et al., 2009). As is often the case, the efferents follow the same pattern as the afferents. Accordingly, the proximal region of CA1 and distal subiculum project to the medial entorhinal cortex while distal CA1 and proximal subiculum send return projections to the lateral entorhinal cortex (VanStrien et al., 2009).

1.3.2 Recognition memory: Single vs. dual process models

When we observe an item, we often instinctively know whether we have encountered that item before, i.e. if it is novel or familiar. Subjective experience indicates that this type of memory can come in two forms; remembering an item along with associated information, for example, when and where the item was last seen, or simply knowing an item has been experienced before. This dichotomy is captured by 'dual-process' models of recognition memory. These two-process models typically assume the existence of familiarity-based as well as recollective-based recognition. Familiarity involves knowing an item has been encountered before, without any additional information. Recollection-based recognition is thought to be more complex as it involves remembering associated contextual information related to the target object. Advocates of dual-process models assume that familiarity and recollection reflect independent neural processes (Yonelinas, 2002). It has, however, been suggested that recognition memory is a unitary process (Squire et al., 2007; Wixted & Squire, 2011).

A second, somewhat related debate, concerns the extent to which regions of the medial temporal lobe show functional heterogeneity; that is, do these regions make different contributions to recognition memory (Squire, 2004; Brown & Aggleton, 2001; Aggleton, 2012). Proponents of dual-process models of recognition memory often argue that recollection and familiarity have distinct neural substrates (Brown & Aggleton, 2001; Yonelinas, 2002). In contrast, there are those that suggest that functional distinctions cannot be made between the contributions of regions of the medial temporal lobe to recognition memory (Squire et al., 2007; Wixted & Squire, 2011). Several variations exist based on single or dual-process accounts of recognition memory. What follows is a more detailed description of two influential models; the first supporting a dual-process and the second, a single-process account of recognition memory.

1.3.2.1 Multiple anatomical systems within the medial temporal lobe

The "extended hippocampal system" is postulated to support episodic memory. This system was initially proposed by Aggleton and Brown (1999) and is composed of the fornix, mammillary bodies, and anterior thalamic nuclei, in addition to the hippocampus (Aggleton & Brown, 1999). Later, the retrosplenial cortex was also included (Aggleton & Brown, 2006). This model proposes that the different regions within the temporal lobe are functionally heterogeneous and so make dissociable contributions to memory and, further, that under certain circumstances regions can function independently. This is based on experimental dissociations from lesion studies in rodent and non-human primates, as well as variable deficits seen in amnesic patients with damage centred on different regions within the medial temporal lobe (Aggleton & Brown, 1999; Brown & Aggleton, 2001). Aggleton & Brown further suppose that recognition memory is composed of two distinct neural processes; recollection and familiarity. In this view, recollection is related to episodic memory and so is supported by this extended hippocampal system, while familiarity is assumed to be an independent process predominantly maintained by the perirhinal cortex. Thus, this model is consistent with dual-process views of recognition memory (Aggleton & Brown, 1999; Brown & Aggleton, 2001; Aggleton & Brown, 2006). Hippocampal damage would be predicted to affect recognition memory for episodes (Brown & Aggleton, 2001).

More recently, this idea of the extended hippocampal system was further expanded. In a detailed review of the current anatomical data of both intrinsic and extrinsic connections of the medial temporal lobe, Aggleton (2012) suggests that there are in fact four dissociable systems residing within the medial temporal lobe, each supporting diverse mnemonic functions. In addition to the extended-hippocampal system these are; the parahippocampal–prefrontal system for familiarity-based recognition and retrieval processing, the rostral hippocampal system for affective and social learning and the reciprocal hippocampal–parahippocampal system for sensory information and integration (Aggleton, 2012). These networks are not presumed to be mutually exclusive, but it is proposed that they have the capacity to function independently.

The parahippocampal–prefrontal network (Figure 1.4) is concerned with discriminating both the familiarity and recency of occurrence of objects. The system is centred on the perirhinal cortex and its connections with surrounding cortical regions (TE and LEC) as well as the medial prefrontal cortex and medial dorsal nucleus of the thalamus (Aggleton, 2012).

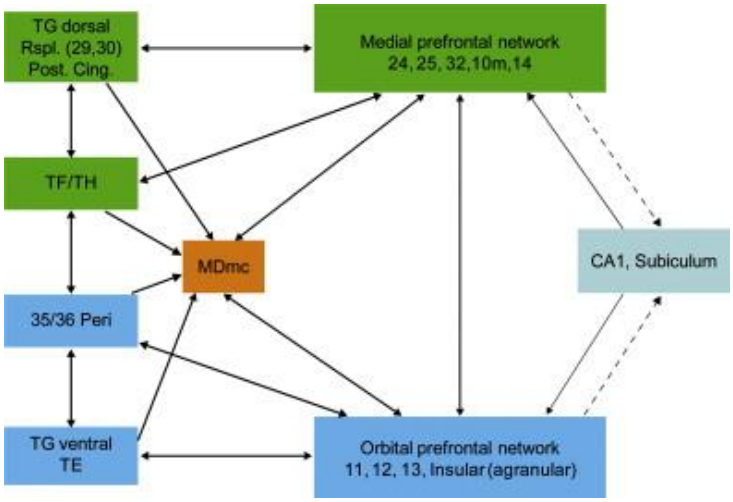

Figure 1.4. The parahippocampal–prefrontal system for familiarity.

The left side of the figure shows the main connections comprising the parahippocampal–prefrontal system. For purposes of contrast, the respective connections of the hippocampus (CA1, subiculum) are shown on the right. Abbreviations: MDmc, magnocellular part of the medial dorsal nucleus of the thalamus; Post Cing, posterior cingulate region. All other numbers and letters refer to cortical area designations. Adapted from Aggleton, 2012.

1.3.2.2 The medial temporal memory system

Squire and Zola-Morgan (1991) proposed "the medial temporal memory system", a model in which the hippocampus resides at the apex of a hierarchical structure and information is supplied to it by the perirhinal cortex and parahippocampal cortex, via the entorhinal cortex (Figure 1.5; Squire & Zola-Morgan, 1991). In contrast to Aggleton and Brown's model, mnemonic functions of the medial temporal lobe are seen to be more functionally distributed. The component regions are presumed to operate in concert to support memory in general and cannot be dissociated based on their contributions to differing memory processes. More severe memory deficits are predicted based on the size of the lesion rather than which components parts are damaged (Squire & Zola-Morgan, 1991). As such, recognition memory is supposed to be a unitary process and the perceived distinction between recall and familiarity is simply that, perceived. In this view, recognition memory varies simply on a scale of strength. Furthermore, hippocampal activity is proposed to be associated with encoding and retrieval of strong memories, whether contextual information about the learning experience is remembered or not (Squire at al., 2007). Indeed, this model also supposes that weak recollective processes can occur in the absence of the hippocampus (Wais et al., 2006; Squire at al., 2007). Thus, this single process account of recognition memory predicts that damage to these regions leads to equivalent deficits in recollection and familiarity (Squire at al., 2004, 2007).

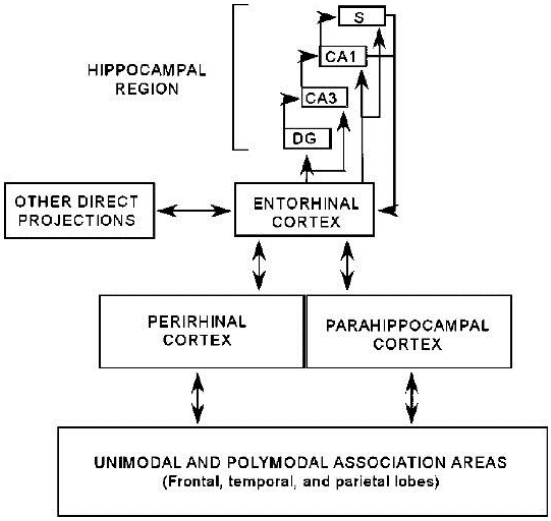

Figure 1.5. A schematic view of the medial temporal lobe memory system.

Abbreviations: CA1, CA3, the CA fields of the hippocampus; DG, dentate gyrus; S, subicular complex. Adapted from Squire et al., 2004.

Elaborations on the original model propose that the assumption that recollection leads to high confidence, high accuracy judgements, while familiarity leads to low confidence, low accuracy decisions is incorrect. More specifically, it is hypothesised that judgements of prior occurrence that are not associated with contextual information can be done so with high confidence and additionally that contextual retrieval can be associated with low confidence memories (Squire at al., 2007; Wixted & Squire, 2011). It is acknowledged that the perirhinal cortex and hippocampus make subtly different contribution to memory but these are proposed to be based on the attributes of the memory. The perirhinal cortex is described as responding primarily to visual attributes or stimulus identity (with the possibility that other sensory modalities can be bound to these visual representations). Hippocampal activity is proposed to be associated with encoding based on multiple stimulus attributes, for example; visual, spatial, tactile and temporal attributes (Wixted & Squire, 2011). This model cannot, however, account for dissociations that have been demonstrated between recollection and familiarity for the hippocampus and perirhinal cortex.

From these differing accounts of recognition memory, it is clear that debate continues over the relationship of these putative mnemonic processes and their anatomical substrates; whether recognition memory is underpinned by complementary interactions between relatively specialized regions or, alternatively, is distributed throughout a functionally homogenous medial temporal lobe. The following sections will discuss experimental evidence for these theories.

1.3.4 Perirhinal lesion studies

Support for perirhinal based familiarity detection comes from several experimental paradigms. Earlier experiments involved visual delayed nonmatch (or match) to sample studies of monkeys with lesions of the rhinal cortices. They concluded that an intact perirhinal cortex is a requirement for successful recognition memory of infrequently encountered single objects (Zola-Morgan et al., 1989; Gaffan & Murray, 1992; Suzuki et al., 1993; Meunier et al., 1993; Eacott et a., 1994). Similar results have been reported for olfactory and tactile recognition memory, implicating the perirhinal cortex in recognition memory for several modalities (Suzuki et al., 1993). Impairments in the DNMS task following perirhinal lesions were replicated in the rat (Mumby & Pinel, 1994) and were extended to show that perirhinal lesions also impair recognition memory in rats when tested on the spontaneous object recognition paradigm (Ennaceur et al., 1996; Aggleton et al, 1997; Ennaceur & Aggleton, 1997; O'Brien et al., 2006; Albasser et al., 2009).

Additionally, temporary inactivation of the perirhinal cortex, using the sodium channel blocker, lidocaine, implicated the perirhinal cortex in encoding, consolidation and retrieval of object recognition memories (Winters & Bussey, 2005; for review see Winters et al., 2008).

1.3.5 Hippocampal lesion studies

Early studies tested monkeys on the visual DNMS paradigm following combined lesions to the hippocampus and amygdala, and found deficits (Mishkin, 1978; Murray & Mishkin, 1986). However, based on the observation that aspiration lesions of the amygdala damaged projection fibres originating in the rhinal cortices and area TE (Goulet et al., 1998) this result was investigated further. Combined hippocampal-amygdala lesions created with a neurotoxin, rather than by aspiration (to spare the adjacent cortex) dissipated the previously observed DNMS impairment (Murray & Mishkin, 1998). Murray and Mishkin concluded that the deficits seen in their earlier experiments were due to inadvertent damage to the perirhinal cortex caused by the aspiration lesion technique (Murray & Mishkin, 1998). Indeed, this study actually reported a negative correlation between the extent of hippocampal damage and recognition memory impairment (Murray & Mishkin, 1998). This result was extended by a meta-analysis of three experiments on the effects of hippocampal lesions on the DNMS task in monkeys. This meta-analysis concluded that greater impairments in

DNMS were associated with smaller hippocampal lesions (Baxter & Murray, 2001); although this result is disputed on methodological grounds by Zola & Squire (2001).

Deficits in visual recognition memory following hippocampal lesion have been reported although often the impairments were mild and evident only at longer retention delays (Zola-Morgan et al., 1992; Alvarez et al., 1995; Beason-Held et al., 1999; Zola et al., 2000; Nemanic et al., 2004). Indeed, there are studies that simultaneously reported a DNMS deficit in monkeys with hippocampal lesions that was significantly exacerbated by perirhinal lesions (Zola-Morgan et al., 1993, 1994; Nemanic et al., 2004). Further, fornix transection in monkeys caused deficits in delayed match (or nonmatch) to sample that were minor in comparison to cases in which the surrounding cortex was damaged (Bachevalier et al., 1985, Gaffan, 1994). Although caution must be taken when interpreting these fornix related results, as some deficits due to fornix lesions can be dissociated from the effects of hippocampal lesions (Clarke et al., 2000).

A similar pattern of results is seen in rodent tests of recognition memory; many studies have reported no effect of hippocampal lesions on various behavioural paradigms that test this form of memory (Aggleton et al., 1986; Rothblat & Kromer, 1991; Jackson-Smith et al., 1993; Kesner et al., 1993; Rawlins et al., 1993; Steele and Rawlins, 1993; Mumby et al., 1995, 1996; Glenn & Mumby, 1996; Duva et al., 1997; Cassaday & Rawlins, 1997; Winters et al., 2004; Forwood et al., 2005; Ainge et al., 2006; Langston & Wood, 2010; Barker & Warburton, 2011b; Albasser et al., 2012). However, there are also reports of hippocampal lesion induced deficits in rodents (Mumby et al., 1992; Clark et al., 2000; Gaskin et al., 2003; Broadbent et al., 2004, 2010; Hammond et al., 2004; Prusky et al., 2004; de Lima et al., 2006; Rossato et al., 2007; Cohen et al., 2013).

As was the case with the non-human primate studies, when hippocampal damage disrupted rodent object recognition, this deficit was often minimal. For example, Mumby et al., (1992) reported a deficit in DNMS at the longest delay tested when rats with hippocampal lesions were compared to controls. However, as Mumby (2001) explained in a review that followed, the rats with lesions were not impaired when compared to their own pre-surgery scores for the same time point. The deficit was actually due to an increase in performance of the control group compared to their own pre-surgery scores (Mumby, 2001). Further, a single study demonstrated that the recognition memory deficit following hippocampal lesions is much less severe than the deficit caused by perirhinal lesions (Prusky et al., 2004). Temporary inactivation of the hippocampus in both mice and rats reduced spontaneous preference for novelty but

discrimination remained above chance levels (Hammond et al., 2004; de Lima et al., 2006). Protein synthesis inhibition in dorsal CA1 did not affect successful novel object preference at three hours but prevented it at 24 hours (Rossato et al., 2007).

These variable hippocampal lesion results could indicate that under normal circumstances the hippocampus and parahippocampal cortex cooperate to support recognition memory but the perirhinal cortex can do this in isolation if necessary. Nevertheless, a consensus has not been reached.

1.3.6 Dissociations and double dissociation studies

The lesion evidence discussed thus far suggests that the perirhinal cortex and hippocampus do not contribute equally to recognition memory. However, this inference is based on different cohorts of animals with lesions of varying sizes produced by different methods in rats that may or may not have received pre-surgery training. Additionally, various behavioural paradigms have been employed. These methodological variations are addressed by studies that demonstrate a behavioural dissociation; that is sparing in one task with a simultaneous deficit in another task following a lesion. Several studies have reported that hippocampal lesions cause deficits in spatial memory tasks while leaving recognition memory unaffected (Aggleton et al., 1986; Jackson-Smith et al., 1993; Duva et al., 1997). Indeed, rats with hippocampal lesions were shown to be impaired on a spatial nonmatching-to-place task both before and after demonstrating intact object recognition memory, verifying that the spared behaviour was not due to functional recovery in the time since the first spatial test (Forwood et al., 2005). There is also evidence for the complementary behavioural pattern; i.e., that perirhinal lesions impair object recognition but spare spatial memory (Aggleton et al., 1997; Bussey et al., 1999).

Another informative class of studies involve functional dissociations; demonstrating that lesions in different region have opposing effects on the same behavioural task. Rats with hippocampal lesions took significantly longer than control rats and those with perirhinal lesions to find the target platform in a delayed matching-to-place task, while the perirhinal rats were no different to the sham controls, (Glenn & Mumby, 1998). Further, there are studies that have shown lesions to the perirhinal cortex impair object recognition memory but spare spatial tasks, while fornix lesions have the opposite effects (Ennaceur et al., 1996; Ennaceur & Aggleton, 1997; Bussey et al., 2000). However, as mentioned above, the effects of hippocampal and fornix lesions can be

dissociated (Clark et al., 2000) and so the most convincing evidence comes from a study that demonstrated a double dissociation within the same experiment.

Winters et al. (2004) found a clear double dissociation between lesion groups. Rats with hippocampal lesions were impaired relative to both sham controls and rats with rhinal lesions when tested in the radial arm maze, while the rats with perirhinal lesions did not differ from the controls. The same rats with perirhinal lesions were impaired on spontaneous object recognition tested in the Y-maze relative to sham controls, while those with hippocampal lesions were not (Winters et al., 2004). Additionally, monkeys with hippocampal or perirhinal lesions were impaired on an object-in-place variation of the visual-paired comparison task, while only those with perirhinal lesions were impaired on the novel item version of the task (Bachevalier & Nemanic, 2008).

It should be noted that there are studies that have reported impairments in spatial memory tasks following perirhinal lesions (Wiig & Bilkey, 1994a,b; Liu & Bilkey, 1998a,b, 2001). However, a detailed review of the mnemonic consequences of perirhinal lesions on spatial tasks concluded that in the cases in which deficits were observed, they were minor in comparison to the effects of hippocampal or fornix lesions (Aggleton et al., 2004). For example, Liu and Bilkey (2001) demonstrated in a single study that hippocampal lesions severely impaired performance in all tasks in a spatial battery, while perirhinal lesions had much more restricted effects in spatial working memory tested at longer delays (Liu & Bilkey, 2001).

Disconnection analyses have also generated pertinent results. These experiments involved lesions to the perirhinal cortex in one hemisphere with hippocampal lesions in the ipsilateral or contralateral hemisphere (Barker & Warburton, 2011). This allows for the assessment of functional circuits. If a connection is required between these regions to support a task, the deficit will be worse in rats that received contralateral rather than ipsilateral lesions, as the circuit is disrupted in both hemispheres as opposed to just one (Warburton & Brown, 2010). It has been found that a functional connection between the perirhinal cortex and the hippocampus was not required for object recognition memory but was necessary for successful object-in-place memory, object recency memory and object paired associate learning (Jo & Lee, 2010; Barker & Warburton, 2011). These are examples of associative recognition, which refers to when the individual components are familiar but their altered location or element re-combination creates a novel configuration (Mayes et al., 2007; Barker & Warburton, 2011). It should be noted that there is a hippocampal lesion study that reported spared object-place and object-context

associations but found deficits in the three-way association between object, place and context. Thus, although the results are somewhat inconsistent, they still highlight a specific role for the hippocampus in associative memory (Langston & Wood, 2010).

Taken together, the lesion evidence suggests that although the hippocampus may have some involvement in the memory of prior occurrence, the perirhinal cortex has a more pivotal role; such dissociations would not be possible if the medial temporal lobe processed these types of memories in a functionally homogenous manner. These functional dissociations can only be possible if components of the network make separate contributions to recognition memory, supporting dual-process views. However, the precise nature of the hippocampal contribution is still to be elucidated.

1.3.7 Neuronal recording studies

Further evidence for the role of the perirhinal cortex in familiarity comes from electrophysiological studies. Neuronal recordings in monkeys have found different neuronal firing patterns based on the relative familiarity, recency or novelty of a presented stimulus (Fahy et al., 1993; Xiang & Brown, 1998). One such study involved a serial recognition task. Conscious monkeys were presented with a series of images; for each image they had to indicate if it had been previously encountered (Xiang & Brown, 1998). The neuronal responses to these images were recorded in area TE, the perirhinal cortex, entorhinal cortex and the hippocampus. The vast majority of neurons that displayed differential firing patterns based on the relative familiarity or recency of an image did so by repetition suppression; the neurons were highly active when they first encountered a stimulus but subsequent presentations elicited an attenuated response.

Based on their firing patterns, the differentially responsive neurons in the perirhinal cortex were sub-divided into three distinct categories (Figure 1.6). ‘Novelty neurons’ are highly active when initially exposed to a stimulus but rapidly diminish their activity upon a second exposure to that stimulus (Figure 1.6). ‘Novelty neurons’ will also respond to very familiar items that have not been encountered recently but this response is much shorter. ‘Familiarity neurons’ require more time for the response decrement to be observed; the magnitude of their response is no different between first and second presentations of a new stimulus. However, if the stimulus is highly familiar, activity levels of ‘familiarity neurons’ fall and this reduction is maintained over multiple presentations of the stimulus, regardless of how recently it was last seen (Figure 1.6). ‘Recency neurons’ also reduce their activity quickly upon a second exposure to an item

but this occurs in the same manner for both novel as well as highly familiar items that have not been encountered recently (Figure 1.6).

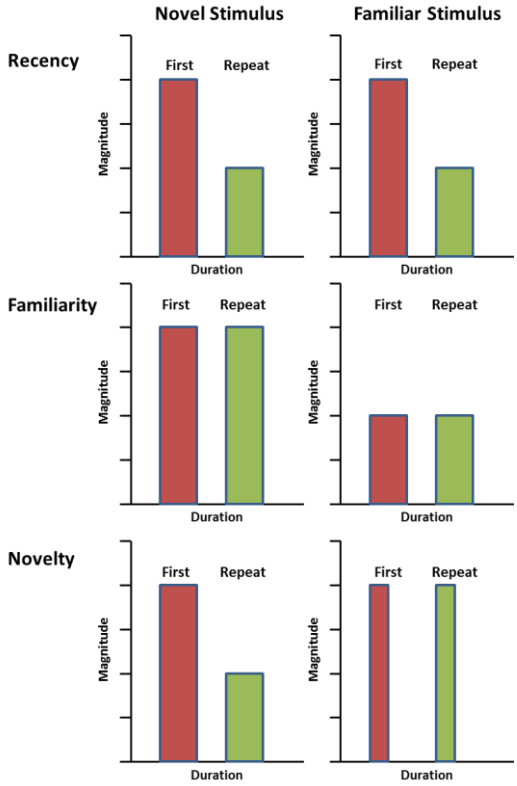

Figure 1.6. Three patterns of response decrements in the perirhianl cortex upon stimulus repetition.

Patterns of responsiveness for idealised recency, familiarity and novelty neurones (bars representing the magnitude and duration of responses to first and repeat presentations of novel and familiar stimuli). Adapted from Brown & Xiang, 1998.

Interestingly, in the cortical areas examined, over a third of the visually responsive neurons displayed differential firing patterns based on the relative familiarity or recency of the image (Xiang & Brown, 1998). This repetition suppression effect is strongest when the interval between first and subsequent presentations is short and familiar stimuli are presented frequently. It was calculated in a review paper that in the perirhinal cortex under these optimal conditions, approximately half of the visually responsive neurons, that is a quarter of the total number of recorded neurons, demonstrated this repetition suppression effect (Brown & Xiang, 1998). The same group obtained similar results concerning 'recency' and 'familiarly neurons' from single unit recordings in the perirhinal cortex of the rat (Zhu et al., 1995a). A recent study demonstrated similar response decrement effects to familiar images in monkey TE (Meyer et al., 2014).

It is striking that this response decrement can occur after a single presentation of a stimulus as it represents a tangible relationship between rapid learning and the activity of a single neuron (Brown & Xiang, 1998) and importantly, the responses are stimulus bound (Brown et al., 1987; Xiang & Brown; 1998; Naya et al., 2003). Also, at the population level, these described neuronal responses took place rapidly. In the perirhinal cortex, response followed stimulus presentation by only 75 - 135 ms depending on the class of neuron (novelty neurons being fastest; Xiang & Brown; 1998). There was also evidence of long-term storage of visual information. Familiarity neurons in the perirhinal cortex were found that maintained a differential response to stimuli for more than 24 hours and this response was stable despite the presentation of many intervening stimuli (Fahy et al., 1993; Xiang & Brown, 1998). Finally, these responses occur automatically, whether the stimuli have behavioural relevance or not and do not require training (Fahy et al., 1993; Brown & Xiang, 1998; Xiang & Brown, 1998). All of these features make the perirhinal cortex an ideal candidate for being the neural substrate of familiarity processing (Brown & Aggleton, 2001; Brown et al., 2010).

More recent unit recording studies have employed spontaneous object exploration paradigms. In these studies, neuronal recordings were made in freely moving rats while they explored objects in an open field (Deshmukh et al., 2012). Perirhinal units increased firing only in relation to objects. Although not calculated in the paper, the rate maps indicated that greater activity was seen when novel objects were added to the arena (Deshmukh et al., 2012). A similar study involved allowing rats to freely explore objects on a circular track (Burke et al., 2012). Again, perirhinal neurons increased their firing rate when in close proximity to objects (Burke et al., 2012). It should be noted that the repetition dependent response decrement of neuronal activity due to familiar stimuli was not observed (Burke et al., 2012). However, Burke et al., (2012) excluded interneurons from their analyses, while another study has suggested that the repetition suppression effect is exhibited specifically by inhibitory interneurons rather than excitatory neurons of the inferior temporal cortex (Woloszyn & Sheinberg, 2012).

A recent single unit recording study in rats suggested that rather than signalling stimulus identity, perirhinal units encode stimulus-outcome associations (Ahn & Lee, 2015). However, this was based on highly familiar stimuli that were only encountered in association with a response rule (Ahn & Lee, 2015). It has been shown in monkeys that some units in area 36 of the perirhinal cortex encode stimulus associations but only after they have encoded the stimulus itself; indeed, less than half of the stimulus specific

neurons went on to signal information on the association (Naya et al., 2003). Similarly, another recent study recorded units in the monkey perirhinal cortex and TE during a task in which similar visual stimuli were differentially associated with reward. They found that perirhinal units only signalled stimulus reward outcome when the reward contingency was deterministic and not when it was random (Eradath et al., 2015). These results could be interpreted as indicating that the perirhinal cortex only encodes object-outcome associations when this relationship is evident and not when it is ambiguous (Inhoff & Ranganath, 2015). Interestingly, it was reported in the rat study that feature ambiguity was encoded at the population level in the perirhinal cortex (Ahn & Lee, 2015). Thus, although the perirhinal cortex is undoubtedly involved in processing visual stimuli, the precise nature of this contribution is still to be elucidated. Nonetheless, this evidence does not preclude the perirhinal cortex from signalling stimulus familiarity upon subsequent presentations of a stimulus, it does however suggest that this is not its the only role.

The serial recognition task in monkeys (described above) has also been used to explore differential responses to novel and familiar stimuli in the hippocampus. The repetition suppression effect was observed in less than 3% of neurons in the hippocampus (in one study, 0%); that is below the generally accepted level of chance, i.e., 5% (Brown et al., 1987; Rolls et al., 1993; Xiang & Brown, 1998). Further, the time taken for a neuron to respond following stimulus onset is known as the response latency. Xiang & Brown (1998) reported response latencies were shortest in area Te2 (75 ms) and progressively longer in perirhinal cortex (75 – 135 ms) and entorhinal cortex (135 – 225ms). In the hippocampus, response latencies were typically 140 – 260 ms (Rolls et al., 1993). Thus, it seems unlikely that the responses seen in the hippocampus were generated up-stream of those in the perirhinal cortex (Brown & Aggleton, 2001). The main information reported to be encoded by these few differentially responsive neurons in the hippocampus was on the relative recency of the stimulus (Rolls et al., 1993). Another study reported that hippocampal neurons encode information on highly familiar images of scenes but they found no difference in the magnitude of response between novel and highly familiar images (Yanike et al., 2004). It should be noted, that there is a vast literature on hippocampal place cells and their contribution to spatial memory (O'Keefe & Dostrovsky, 1971; O'Keefe & Burgess, 1996; McNaughton et al., 2006; Moser et al., 2008). Additionally, when the spatial location or the temporal order of stimulus presentation is relevant then hippocampal encoding also occurs (Knierim et al., 2006; Manns et al., 2007; Manns & Eichenbaum, 2009; Komorowski et al., 2009; McKenzie et

al., 2014). Thus, neuronal recording evidence suggests that the hippocampus is not involved in discriminating whether a stimulus is novel or familiar but rather is involved in associative learning about these stimuli. This evidence is consistent with dual-process models of recognition memory.

1.3.8 Behavioural distinctions between recollection and familiarity

1.3.8.1 E-maze

Behavioural dissociations between recollection and familiarity have been achieved using a paradigm known as the E-maze (Figure 1.1E; Eacott et al., 2005). In the first sample phase, rats are exposed to a pair of objects located as illustrated in the left panel of Figure 1.1E. In the second sample phase the context (appearance of the maze) is changed and the locations of the objects are swapped. During a second retention interval the rat is habituated to one of the objects in a holding cage. The subsequent test phase can take one of two forms; in a familiarity test the objects are placed in the same locations as they were during the sample phase with the associated context (Figure 1.1E, left panel). This variant of the task can be solved based on familiarity as rats can see the objects from the start point in the maze and intact rats will preferentially explore the non-habituated, less familiar object (Eacott et al., 2005). In a recall test, objects are placed in the two outer arms where they cannot be seen directly from the start point (Figure 1.1E, right panel). The side they are placed on is congruous with the sample phase in the same context. As the rats cannot see the objects from the start point, they must use the context to guide their decision on which arm to turn down to reach the non-habituated object. Thus, this form of the task cannot be solved simply using familiarity but must involve recollection. Again, intact rats can use these contextual cues to guide their behaviour (Eacott et al., 2005). Using this paradigm, recollection and familiarity have been tested and dissociated, not only in the same animal but in the same trial. It was shown that rats with lesions to the fornix had no preference for turning towards the correct arm, demonstrating impaired recall. In the same trials, object preference was then measured based on subsequent preferential exploration and it was found that they spent a greater amount of time exploring the non-habituated object so demonstrating intact familiarity (Eacott & Easton, 2007; Easton et al., 2009). This behavioural dissociation provides further evidence for the dual-process view of recognition memory. Additionally, this paradigm has been used to demonstrate that recollection was impaired in rats with fornix lesions that disconnect the hippocampus while familiarly was spared.

1.3.8.2 Rodent receiver operating characteristics

The implication that hippocampal lesions have little effect on a rat's ability to successfully discriminate novel from familiar objects has been extended beyond visual recognition. Paralleling the results of visual recognition memory, hippocampal lesions induced a minor impairment in an odour DNMS task that was only evident at long delays (Dudchenko et al., 2000). It was then demonstrated, at shorter delays, that lesions to the hippocampus do not impair a rat's ability to distinguish novel from familiar odours but simultaneously impair their capacity to remember the temporal order of these presentations (Fortin et al., 2002). This odour-based paradigm was developed to generate an interesting set of studies that employed analysis of receiver operating characteristics (ROCs).

An ROC is a function that plots the probability of a 'hit' against the probability of a 'false alarm' across different response criteria (Figure 1.7). A 'hit' corresponds to a subject correctly categorising a previously encountered item as familiar, while a 'false alarm' occurs when they incorrectly classify a new stimulus as familiar. The response criteria reflect the confidence with which the recognition decision is made. The left side of an ROC curve corresponds to choices made with a strict response criterion; i.e., few hits but also few false alarms. The right side of an ROC represents progressively lenient response criteria, a situation in which there are a high number of hits with a correspondingly high number of false alarms. Chance performance is represented by a diagonal symmetrical line through the origin as it reflects an equal number of hits and false alarms occurring at any given confidence level. Successful recognition memory, that is, a greater number of 'hits' than 'false alarms', results in a function that lies above this chance line. ROCs derived from normal subjects engaged in a recognition memory task display a characteristic shape; an asymmetric (above origin Y-intercept) curvilinear function (Figure 1.7A). The Dual Process Signal Detection model supports dual-process theories of recognition memory. This model proposes that recollection is represented by an asymmetric linear function reflecting the threshold nature of recollection (Figure 1.7B) while familiarity is characterised by a symmetrical curvilinear function (Figure 1.7C; Yonelinas & Parks, 2007).

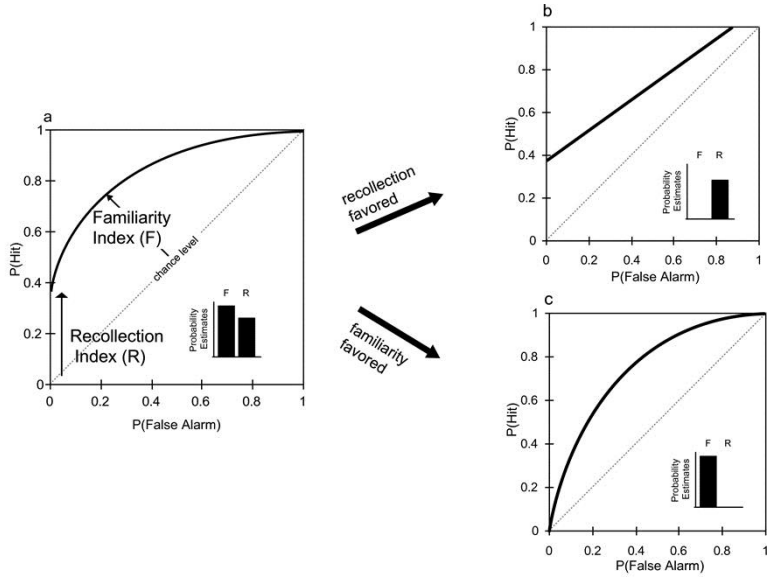

Figure 1.7. Idealised ROC functions for item recognition memory.

(A) The ROC curve for recognition memory is typically asymmetrical and curvilinear. (B) ROC function observed when performance is based only on recollection. (C) ROC function observed when performance is based only on familiarity. Adapted from Eichenbaum et al., 2012.

This type of ROC analysis was originally developed in humans but has been adapted for odour recognition memory testing in rodents. Rats were initially presented with a sequence of digging cups with different odours mixed in the digging media. Following a delay, the rats were presented with another sequence of digging cups; some with familiar odours, some with novel odours. Selection of a novel odour was reinforced by a food reward buried in the associated digging cup. If the presented odours were familiar, then the rat was rewarded for digging in an alternative cup that was not scented. The response criteria or confidence levels with which the decisions were made was experimentally manipulated by varying the effort the rats had to expend to retrieve the rewards. This was achieved by systematically altering the height of the digging cups as well as varying ratio of the food reward available in the presented vs. alternative cup (Eichenbaum et al., 2010). It was demonstrated in intact rats that this behavioural protocol produced an ROC with the asymmetrical, curvilinear function predicted by normal recognition memory (Fortin et al., 2004). Interestingly, when the rats subsequently received hippocampal lesions the resulting ROC functions retained the curvilinear shape but were no longer asymmetrical. It was concluded that this reflected a loss of recollection and a reliance on familiarity-based processing in the absence of the hippocampus. The opposite effect of increased reliance on recollection was seen in intact rats when the retention interval was increased (Fortin et al., 2004).

The task was further developed by adding an associative component; in the sample phase the rats had to learn about stimulus pairs – an odour paired with a particular digging media. In the test phase rats were presented with either familiar or rearranged, thus relatively novel, odour media pairings. Due to the associative nature of this type of task, it should be more reliant on recollection than familiarity processing. As predicted, the results indicated that the ROC functions from intact rats remained asymmetric but became linear, reflecting the proposed reliance on recollection and absent familiarity processing (Sauvage et al., 2008). Even given the task bias towards recollection, rats with hippocampal lesions could successfully perform the task but simultaneously displayed enhanced familiarly and reduced recollection as their ROC functions were more curvilinear and their asymmetry was diminished (Sauvage et al., 2008). It was suggested that this occurred as rats with hippocampal lesions unitised the pairs of stimuli into a single item (Sauvage et al., 2008); although this interpretation has been criticised by proponents of the single process view of recognition memory (Wixted & Squire, 2011). Another experimental manipulation, namely adding a response deadline, altered the ROC functions of intact rats in the opposite manner to the associative task. Allowing only a short amount of time in which to make a recognition memory judgement biased responding to rely more on familiarity, reflected by a curvilinear, symmetrical ROC (Sauvage et al., 2010). The associative behavioural paradigm described above was also given to aged rats; their overall performance on the task was no different to that of young rats; however, their ROC functions indicated a greater reliance on familiarity processing and a loss of the asymmetric recollective component (Robitsek et al., 2008). The loss of recall, but not familiarity was associated with a simultaneous spatial memory deficit; one less controversially associated with hippocampal damage (Robitsek et al., 2008).

Taken together, these results indicate that recognition memory is composed of two processes that can be separated by experimental manipulation; forcing rapid recognition judgements causes reliance on familiarity while increasing the retention interval or adding an associative component to the task predispose to recollection (Eichenbaum et al., 2010; Sauvage et al., 2010). Furthermore, hippocampal lesions preferentially affect the recollective component (Fortin et al., 2004; Sauvage et al., 2008). Thus, this set of studies provides further evidence for the dual-process view of recognition memory.

An opposing model that supports single-process models of recognition memory - the Unequal Variance Signal Detection (UVSD) model – can also account for the shape of

standard recognition related ROC functions. This model proposes that the curvilinear nature of the ROC function is due to memory strength and the asymmetry is caused by greater variability in the memory strength of previously encountered items over new ones (Yonelinas & Parks, 2007). However, as described above, these two components have been demonstrated to be dissociable and the UVSD model cannot account for opposing effects on these two components of the function (Eichenbaum et al., 2010).

1.3.9 Human studies

1.3.9.1 Patient studies

There are also insights to be gained from studying patients with damage to the medial temporal lobe. Of particular interest are those patients with damage confined to the hippocampus and sparing of the surrounding cortices. The Doors and People test is often used to test amnesic patients in order to distinguish between recall and recognition. It involves four subtests; two visual based tests, one of recall and one of recognition as well as verbal based tests of both recall and recognition (Baddeley et al., 1994). This test has been administered to patients with pathology restricted to the hippocampus, who demonstrated impairments on the recollection subtests with relatively spared recognition (Baddeley et al., 2001; Mayes et al., 2002; Aggleton et al., 2005; Barbeau et al., 2005; Adlam et al., 2009).

Studies employing signal detection analyses in humans have also demonstrated that recollection and familiarity can be separated based on the shape of their ROC curves (Yonelinas, 2002; Yonelinas & Parks, 2007). These functions are derived in the same manner as that described for rats (Section 1.3.4); although response criteria are often obtained by asking the subject to rate how confident they are in their decision of prior occurrence on a scale from one (definitely novel) to six (definitely familiar). ROC curves derived for patients with circumscribed hippocampal pathology have been shown to be curvilinear and symmetric, demonstrating reliance on familiarity over recollection (Yonelinas et al, 1998, 2002; Aggleton et al., 2005; Peters et al., 2009). However, this loss of asymmetry has been interpreted as a general reduction in memory strength due to hippocampal damage rather than a specific loss of recollection (Wais et al., 2006; Squire at al., 2007; Dede et al., 2013). In this latter interpretation, consistent with a single-process recognition view, a symmetrical ROC curve indexes weak memory. On the other hand, an asymmetrical ROC curve denotes a strong memory due to the fact that the previously encountered stimuli will have greater variance associated with them than the

new stimuli. Further, this implies that recollective processes can occur in the absence of the hippocampus (Squire at al., 2007). Although care is required when interpreting these results as it has been demonstrated that ROC analyses may not be suitable for testing long-term amnesic patients, who may have developed alternative coping strategies (Bird et al., 2008).

Another common paradigm used to differentiate recollection from familiarity in humans is the remember/know task in which subjects are asked if an item is new, or if it was encountered in the sample phase, and further, whether they actually recall seeing the test item previously (remember) or if it simply feels familiar (know). In source memory or associative recognition tasks, recollection is confirmed by asking the subject to indicate not only if the stimulus has been encountered previously, but if so, the experimental situation in which this occurred. An example would be asking the participant the colour of the background on which the stimulus was seen or which stimuli were shown simultaneously. These, along with similar paradigms, have been utilised in single patient case studies as well as larger group studies. These studies have demonstrated that amnesic patients with damage restricted to the hippocampus have impairments in tests of recall with relative preservation of familiarity, while damage that encompasses the hippocampus and surrounding cortices results in diminished performance in both forms of memory (Aggleton & Shaw, 1996; Yonelinas et al, 1998; Mayes et al., 2002, 2004; King et al., 2004; Pascalis et al., 2004; Turriziani et al., 2004; Aggleton et al., 2005; Barbeau et al., 2005; Holdstock et al., 2005; Uncapher et al., 2006; Bowles et al., 2010). However, the construct validity of the remember/know paradigm has been questioned; it has been suggested that this paradigm probes memory strength rather than recall and familiarity (Wais et al., 2008).

The complementary pattern has also been demonstrated, i.e., impaired familiarity and preserved recollection. Patient, NB, received a resection of left her temporal cortex that included perirhinal and entorhinal cortices, while her hippocampus remained functional (Bowles et al. 2007, 2011). The same research group went on to demonstrate an interesting double dissociation between NB and a patient lacking their hippocampus. While their overall recognition performance was matched, their greater deficits were in familiarity and recollection respectively (Bowles et al., 2010). Damage to the surrounding cortex that spares the hippocampus is rare but insights can also be gained by comparing patients with hippocampal damage to those with hippocampal plus cortical damage. Patients with more widespread medial temporal lobe damage have been shown

to be more severely impaired in object recognition and object discrimination tasks than patients with damage confined to the hippocampus (Buffalo et al., 1998; Barense et al., 2005; Lee et al., 2005b).

Of potential relevance are contrasts between patients with semantic dementia (the temporal lobe variant of frontotemporal dementia) and those with Alzheimer's disease. Generalised medial temporal lobe atrophy is common to both of these pathologies but greater perirhinal and entorhinal degeneration is associated with semantic dementia while hippocampal atrophy is more common in Alzheimer's disease (Davies et al., 2004). A double dissociation has been demonstrated; Alzheimer's disease is associated with impaired discrimination of landscape scenes while semantic dementia is associated with compromised face discrimination (Lee et al., 2006, 2007). Semantic dementia is not associated with object recognition memory deficits when sample and test items are identical, however, altering perceptual features of the items (e.g. colour) induces deficits (Graham et al., 1997, 2000) and under these perceptually demanding conditions, semantic dementia patients display high false recognition rates (Simons et al., 2005). Additionally, a subset of patients with temporal lobe epilepsy experience déjà vu (inappropriate feeling of familiarity) during their seizures, this has been linked to metabolic changes in the perirhinal and entorhinal cortices (Guedj et al., 2010) and further, a group of these patients demonstrated familiarity deficits during an interictal period (Martin et al., 2012).

As with animal studies, amnesic patient data are not definitive; there are human studies which have demonstrated that some patients with focal hippocampal damage display similar deficits in tasks that tax recollection or familiarity (Stark et al., 2002, Manns et al., 2003; Cipoletti et al., 2006; Kirwan et al., 2010; Smith et al., 2011; Dede et al., 2013). An additional layer of complexity is added by the finding that hippocampal damage can be associated with familiarity impairments for some stimulus types but not others (Cipoletti et al., 2006; Smith et al., 2014) with a similar result following perirhinal damage (Martin et al., 2011).

1.3.9.2 Functional imaging studies

More compelling evidence comes from human functional and event-related MRI studies in healthy participants. Both single and double dissociations of function and anatomy have been reported based on variants of the remember/know or source memory paradigms described above. Familiarity processing is associated with cortical activity adjacent to the hippocampus (generally presumed to be perirhinal cortex) while

processing of contextual information (recollection) is associated with hippocampal activity (Davachi et al., 2003; Henson et al., 2003 Ranganath et al., 2003; Gonsalves et al., 2005; Yonelinas et al. 2005; Daselaar et al. 2006; Kensinger & Schacter 2006; Montaldi et al., 2006; Diana et al., 2007, 2010; Flegal et al., 2014). Further, greater activation in the perirhinal cortex at the time of encoding is associated with stimuli that are later judged to be highly familiar (Davachi et al., 2003; Ranganath et al., 2003; Kensinger & Schacter, 2006) whereas during retrieval, highly familiar stimuli are associated with reduced perirhinal activity (Henson et al., 2003; Gonsalves et al. 2005; Daselaar et al. 2006; Montaldi et al. 2006). Greater hippocampal involvement has been observed during a test of recognition that taxed context retrieval (Flegal et al., 2014). This parallels results obtained from neuronal recording studies in animals (discussed above). A study involving both functional MRI and intracranial electroencephalography (iEEG) recordings is of particular note as iEEG recordings have much better temporal resolution than any MR-based technique. It was reported that item processing occurs initially in the perirhinal cortex, while hippocampal activity appears after a novelty decision has already been made and so is likely to be post-processing (Staresina et al., 2012).

In contradistinction are fMRI studies that have reported similar activity levels in the hippocampus and the surrounding cortices when subjects encode items that will subsequently be remembered in isolation (familiarity) or remembered along with source information (recall) (Gold et al., 2006; Shrager et al. 2008). Further, a study found that hippocampal activity at retrieval is equivalent for both recollection and familiarity when the memory is strong (Smith et al., 2011). Additionally, single unit recordings in the hippocampus of epileptic patients identified a population of neurons that increased their firing rate in response to novel stimuli as well as those that increased firing in response to familiar stimuli, even when behavioural performance on the spatial attributes of the task were at chance (Rutishauser et al., 2006).

In summary, a large body of evidence from a diverse set of experimental paradigms exists to support dual-process accounts of recognition memory but there is also evidence to support single-process, memory strength based accounts. Thus, further investigation is required. Addressing this issue by looking at functional networks, rather than assessing individual regions may aid in clarifying the matter.

1.4 Use of the 'bow-tie' maze for testing rodent recognition memory

Some of the main advantages of the spontaneous object recognition task (described in section 1.2.2) are the same features that bring potential problems. One issue is that the task is based around spontaneous behaviour. This feature inevitably contributes to variance between subjects, so decreasing statistical power. A further issue is that the amount of exploration given to a particular novel or particular familiar object might be biased by individual preferences to specific types of objects. The solution is to counterbalance the choice of novel and familiar objects within a study, but this arrangement still adds variance, unless the test objects are equivalently matched for their attractiveness. A consequence of the inter-animal and inter-stimulus variance is the frequent need for additional trials, additional rodents, or both.

Another problem is that the length of time taken to run a single recognition test means that experimenters typically complete no more than one trial per day. This limitation means that test sessions often have to be repeated to combat variance. It also means that added importance is attached to the particular choice of the individual objects used for the familiar and novel stimuli. The second problem is that the test animals are repeatedly handled, not just before and after testing, but also in the middle of testing (to begin and end the retention interval). The individual reaction of the test animals to being held is again likely to increase variance, especially as both individual rodents and individual experimenters may behave differently. This problem is compounded further if the brain manipulation under investigation affects stress or affect. To counteract both problems it is often necessary to use relatively large group sizes or risk the problem of having insufficient power to detect real effects.

In order to address these concerns, the 'bow-tie maze', introduced by Albasser et al. (2010a) was chosen as the test apparatus for all object-based memory tests described in this thesis. This was selected as the task utilises the strongest features of the spontaneous object recognition task while addressing as many of its shortcomings as possible. This task is a hybrid of DNMS and spontaneous object recognition, drawing key elements from both tasks. The central feature is that rodents repeatedly explore pairs of objects at opposite ends of an enclosed maze shaped like a bow-tie. Each pair of stimuli consists of one novel object and one familiar object (Figure 1.8). A sliding door in the middle of the maze separates the two ends, so ensuring discrete trials. This arrangement makes it possible to run multiple trials within a session without handling the rodents. Although

the animals have to be pre-trained to run from one end of the maze to the other for food rewards, this pre-training helps to ensure that the animals are well habituated to the test environment and so reduces stress.

Food rewards are placed under the test objects to encourage their investigation and to ensure that the rats shuttle up and down the apparatus. The animals do not, however, learn a reinforced matching or nonmatching rule as both novel and familiar objects are equally associated with reward (Albasser et al. 2010a). Instead, recognition is still signalled by spontaneous exploration preferences. Each trial is typically just one minute long, i.e., much shorter than a normal spontaneous recognition trial tested in an open field. This is possible as rodents approach the objects almost immediately in order to retrieve food rewards, and so explore from the outset of the trial. The one minute trial time also takes advantage of the finding that in standard spontaneous object recognition tasks the most discriminatory period of exploration between novel and familiar objects often takes place at the beginning of the test session (Dix & Aggleton, 1999). Exploiting these features, a rat in the bow-tie maze can, for example, receive twenty recognition trials in twenty-one minutes. In contrast, the same duration of testing in a standard spontaneous exploration task would normally allow just one trial.

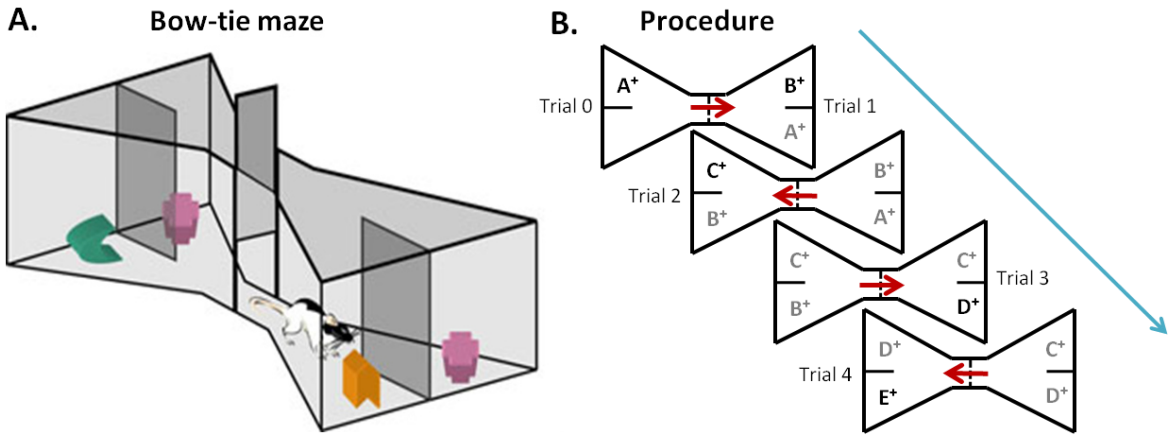

Figure 1.8. The 'bow-tie' maze.

(A) Schematic of the bow-tie maze. A central sliding door separates the two ends of the maze in which two objects are placed. (B) General procedure for running the standard object recognition test showing the presentation order of the objects. All objects are rewarded. Arrows show direction of rat movements. Bold letters represent novel objects and grey letters represent familiar objects. Adapted from Albasser et al., (2011a).

The bow-tie maze has high plain sides to limit distracting visual stimuli and reduce spatial cues (Figure 1.8A). To begin a session (trial 0), the rat is put into one end of the

maze, which also contains an object (A) that covers a food reward (Albasser et al., 2010a; Figure 1.8B). The animal is allowed to retrieve the food reward and will then explore the object. One minute after being placed in the maze, the central sliding door is opened and the animal runs to the opposite end for more food rewards. In the simplest task design, the rodent finds novel object B and an identical copy of the now familiar, object A (trial 1). Successful recognition is reflected in the greater amount of time spent exploring novel object B. After a further minute, the central door is raised and the animal runs back to the opposite end, where it can explore object B (now familiar) and novel object C (trial 2). Recognition is measured by calculating the cumulative difference in time spent exploring the novel and familiar objects ('cumulative D1') over successive trials. In addition, this D1 score can be divided by the total amount of object exploration ('updated D2') to give a D2 score; a ratio that ranges between +1 and -1 (Figure 1.9).

Experiments run in the bow-tie maze have typically used this 'running recognition' protocol (Figure 1.8B). This design has several benefits; first, it increases the numbers of trials that can be given within a set period as there is no discrete sample phase. Also, importantly, by ensuring that every object serves as both a familiar and a novel stimulus, the influence of any individual object that might be particularly attractive or aversive to the test animals are cancelled out as any such effects should be counteracted across subsequent trials. A further benefit is that over the course of several sessions the task could use over a hundred different objects, rather than repeatedly use a very limited sample of objects. Again, the increase in the number of stimuli helps to remove any biases associated with particular objects. Using these designs it has been found that perirhinal cortex lesions impair object recognition (Figure 1.9A) while hippocampal lesions appear to spare recognition memory (Figure 1.9B,C; Albasser et al., 2010b, 2011a, 2012, 2013a). This pattern is consistent with many studies using spontaneous object recognition and DNMS tasks.

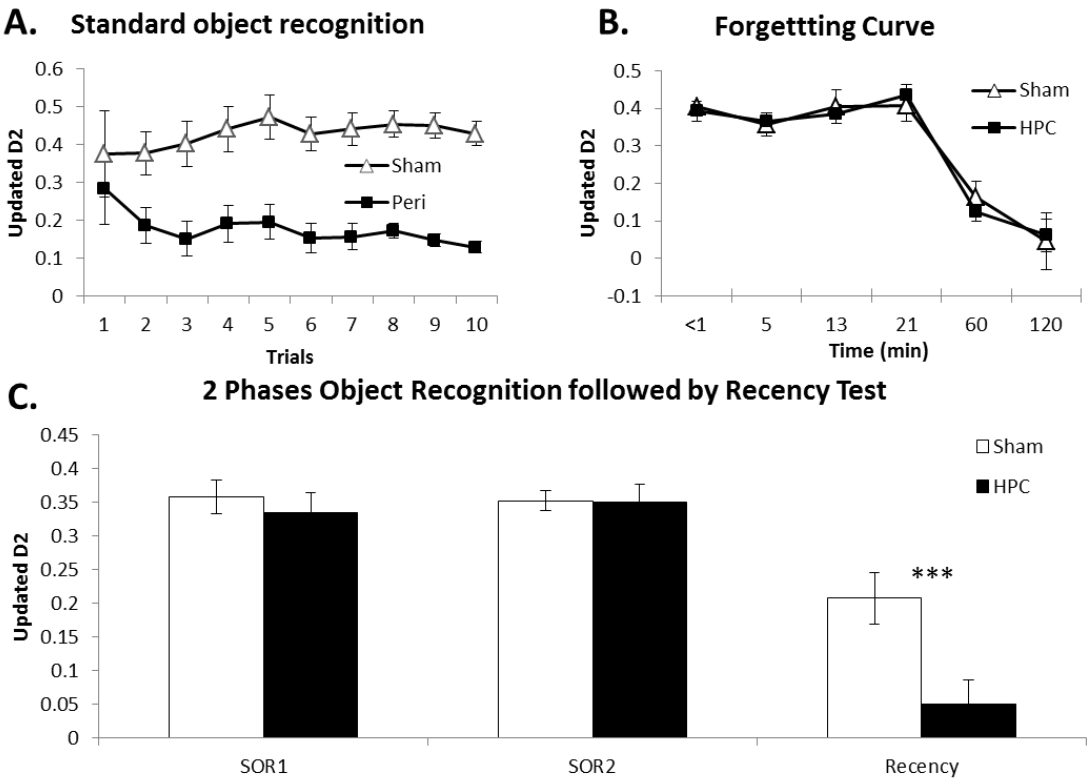

Figure 1.9. Recognition memory results obtained in the bow-tie maze.

(A) Object recognition by rats with perirhinal cortex lesions (black square) and surgical controls (white triangle); graph shows the updated D2 scores over successive trials. D2 is the time exploring the novel object minus the time exploring the familiar object, divided by total exploration. Scores can range from +1 to -1. Adapted from Albasser et al., (2011b). (B) Object recognition forgetting curve: Graph shows updated D2 scores of composite object recognition memory performance of rats with hippocampal lesions (black square) and their controls (white triangle) across various retention intervals used in separate experiments. (C) Object recency: graph showing the mean performance of rats with hippocampal lesions (black) and their surgical controls (white) on recency discrimination performance. Only the control group performed above chance. In addition, recognition performance is given for the two blocks of stimulus familiarization (SOR1 and SOR2) that included object recognition (retention delay 1 min). B, C. Adapted from Albasser et al. (2012). Data shown are mean ±standard error of the mean. Group differences ***$p < 0.001$.

Additionally, the bow-tie maze offers several procedural variants that have been employed to test different aspects of object based memory. Retention delays have been increased by delaying the repeat of a stimulus to nearer the end of the series of continuous trials. In this way, both interference and retention delays can be varied by interposing other trials before returning to the now familiar object. Consequently, forgetting curves can be derived from the results of a single session (Albasser et al., 2010a; Figure 1.9B). The fact that the test objects are immediately adjacent to food rewards means that the rats are encouraged to approach the objects, which are in constant locations. Consequently, once rodents are habituated to the bow-tie maze in the

light, it can also be used to examine non-visual object recognition (Albasser et al., 2011b, 2013b). Additionally, identical pairs of objects, either novel or familiar, can be presented in order to further familiarise the animals with a particular set of objects or to increase the amount of time between discrimination trials (Albasser et al., 2012).

The bow-tie maze can also be used to test recency memory (Albasser et al., 2012). Recency memory is the ability to discriminate between familiar stimuli based on the relative distance in time since they were last encountered; also known as temporal order memory. A common approach to testing recency memory is to divide the test session into multiple stages. In the first phase the rat is exposed to multiple stimuli, and then removed from the apparatus so that the test session can follow at whatever interval is required. Further, it was also possible to test both recognition and recency of the same objects within a single test session (Albasser et al., 2012). Although the preferred behavioural procedure within the bow-tie maze has been a running recognition design, discrete sample and test phases could readily be run at opposite ends of the apparatus, i.e., more akin to DNMS. The apparatus has also been used for object-in-place recognition (Nelson & Vann, 2014).

Another benefit of the bow-tie maze is its reliability in generating recognition discrimination scores (D1 and D2) that are significantly above chance with modest sized groups of animals (Albasser et al., 2010a; see also Ameen-Ali et al., 2012). The multiple trials mean that individual control rats typically perform above chance with short retention delays (Albasser et al., 2010a). A closely related feature is that the variance of the updated D2 scores for any group of animals decreases as the trial numbers within a session increase (Figure 1.9A; Albasser et al., 2010a, 2011b).

The gain in power provided by such hybrid tasks has been examined more formally by Ameen-Ali et al. (2012). These researchers devised a slightly more elaborate task, known as the E-maze (similar to that depicted in Figure 1.1E but with an additional holding area attached at the end of the arms), which shares many of the key features of the bow-tie maze. In their task there are several compartments but, like the bow-tie maze, the rat is trained to run through the apparatus where it receives sample and test trials without being handled. The animals also receive multiple trials in a session (Ameen-Ali et al., 2012, 2015). The test objects are again associated with food rewards, while recognition is determined on the basis of preferred exploration. Comparisons with previous spontaneous object recognition studies by the same group helped to confirm the gain in statistical power associated with such hybrid methods (Ameen-Ali et al., 2012).

1.5 The functional imaging of rodent recognition memory: Immediate-early gene mapping

A key advantage of these relatively new recognition memory task variants is the ability to give multiple test trials within a single session. This section describes investigations into the study of recognition memory that could not be conducted without this particular feature.

The term immediate-early gene (IEG) refers to a particular group of genes that do not require previous protein synthesis to be activated (Herrera & Robertson, 1996). For this reason, they have a temporal advantage over other genes, so giving the term 'immediate'. There are numerous immediate-early genes, which can be categorised into two groups. One group, the 'regulatory transcription factors', influence cell function through the downstream genes that they regulate. The second group, 'effector factors' can directly control specific cellular functions. There are thought to be between 10-15 IEGs that are regulatory transcription factors (Lanahan & Worley, 1998). Two of these are the genes c-*fos* and zif268, both of which are assumed to have roles in long term plasticity (Abraham & Dragunow, 1991; Guzowski, 2002; Tischmeyer & Grimm, 1999).

Expression of c-*fos* has commonly been used as a proxy marker of neuronal activity, as increased neuronal activity causes its up-regulation and expression of its protein product, Fos (Herrera & Robertson, 1996; Chaudhuri, 1997). This IEG is commonly chosen for use in conjunction with behavioural tests as it has relatively low baseline expression levels that increase quickly following neuronal activation and then again return to baseline due to tight auto-regulatory control (Chaudhuri, 1997; Zangenehpour & Chaudhuri, 2002). Indeed, the temporal profile of this expression has been characterised; Fos, the protein product of c-*fos*, peaks between 60 and 120 minutes after the inducing event (Bisler et al., 2002; Zangenehpour & Chaudhuri, 2002). Studies have shown that expression of c-*fos* is related to synaptic plasticity associated with learning and memory processes (Swank et al., 1996; Tischmeyer & Grimm, 1999; Guzowski, 2002; He et al., 2002; Countryman et al., 2005; Guzowski et al., 2005; Katche et al., 2010 Liu et al., 2012; Ramirez et al., 2013). Importantly, it has been demonstrated that c-*fos* expression is required for effective long term recognition memory (Seoane et al., 2012), i.e., it has an integral role within this form of memory. Furthermore, contextual fear related memory engrams in the hippocampus have been optogenetically re-activated based on the activity of c-*fos*, and shown to affect behaviour, further implicating it in mnemonic processes (Liu et al., 2012).

1.5.1 Comparing c-*fos* expression for novel and familiar stimuli

It has been demonstrated that when rats see novel visual stimuli there is increased expression of c-*fos* in the perirhinal cortex (Wan et al., 1999, 2004; Zhu et al., 1995b, 1996, 1997), which parallels the increased single-unit activity also observed in the perirhinal cortex (Zhu et al., 1995a). Of particular significance is the finding that knocking down c-*fos* expression by infusion of antisense Fos oligodeoxynucleotides into the rat perirhinal cortex immediately before or after the sample phase of a spontaneous novel object preference test disrupts the stabilisation of long term recognition memory (Seoane et al., 2012). For these reasons, expression of c-*fos* in the perirhinal cortex is seen as a proxy marker for neural activity closely involved with recognition memory.

Although immediate-early gene imaging provides exceptional anatomical resolution (down to individual neurons) it has much poorer temporal resolution. For example, in experiments that examine levels of Fos protein, there is often a gap of around 90 minutes between the target learning behaviour and the sacrifice of the animal. While this interval is designed to capture peak production of Fos (Guzowski, 2002; Zangenehpour & Chaudhuri, 2002) it means that the source of the signal can become blurred. A further issue is that most IEG imaging studies require a control group that is matched for sensorimotor demands but is expected to show little or no learning when compared with the experimental group. Differential Fos levels are then assumed to reflect the learning condition. Thus, the validity of this subtraction method depends on the appropriateness of the control condition.

Initial studies of c-*fos* expression simply compared IEG activity levels in rats shown either novel or familiar stimuli (Zhu et al., 1995b, 1996, 1997). These studies found raised c-*fos* expression associated with novel stimuli in the perirhinal cortex and visual association area Te2, but not in the hippocampus (Zhu et al., 1995b, 1996, 1997). A refinement, the 'split-viewing' procedure, involved presenting novel visual stimuli to one eye of the rat and familiar stimuli to the other eye of the same rat (Wan et al., 1999; Warburton et al., 2003; Wan et al., 2004). Inter-hemispheric comparisons again showed that viewing novel stimuli was associated with raised c-*fos* expression in the perirhinal cortex and area Te2, but not in the hippocampus (Table 1.1; Wan et al., 1999). Changes in hippocampal activity were found, however, when stimulus novelty was introduced by rearranging the spatial configurations of familiar groups of stimuli, i.e., associative recognition (Table 1.1; Wan et al., 1999; Aggleton et al., 2012).

Table 1.1. Summary table of c-*fos* expression studies showing the patterns of Fos changes in tests of recognition memory.

Brain region	Novel object bowtie maze in the light (Albasser et al., 2010b)	Novel object bowtie maze in the dark (Albasser et al., 2013)	Paired viewing: Novel/familiar single images (Wan et al., 1999)	Paired viewing: Novel spatial arrangement of familiar images (Wan et al., 1999)
CA1	↑	↑	No change	↑
CA3	↑	↑	No change	No change
Dentate gyrus	↓	↑	No change	↓
Subiculum	No change	-	No change	↓
Lateral Entorhinal	No change	↑	No change	No change
Medial Entorhinal	No change	No change	-	-
Rostral Perirhinal	No change	↑	-	-
Caudal Perirhinal	↑	No change	↑	No change
Area Te	↑	No change	↑	No change

Symbols: ↑ increased Fos counts with associative novelty; ↓ decreased Fos counts with novelty; — Fos counts were not made in the structure.

A drawback of the c-*fos* imaging studies discussed so far is that there was no concomitant behavioural evidence to show that the rats could actually distinguish the novel from the familiar visual stimuli. It is most unlikely that this would be possible using the standard spontaneous recognition task (Ennaceur & Delacour, 1988), as animals normally experience a very small number of novel stimuli within a test session,

making it unlikely that the neural Fos signal would be sufficiently large to be detected. There may also be individual biasing effects caused by the particular objects selected for the task. Problems could also occur with individual animals that fail to show a clear preference for the novel stimuli. Additionally, the need to handle the rat repeatedly would add further noise to the c-*fos* signal.

The bow-tie maze provides a means to examine c-*fos* expression associated with recognition memory (Albasser et al., 2010b, 2013b). The apparatus allows for the presentation of multiple stimuli within a single recognition session, so increasing signal strength, while also increasing the likelihood of deriving clear preference measures for novel over familiar stimuli for individual animals. In studies using this apparatus, rats have been given 20 recognition trials, i.e., 20 novel objects vs. 20 familiar objects, and then perfused 90 minutes later for the immunohistochemical visualisation of the Fos protein. The use of this task raises two important procedural considerations. The first is that the recognition test must contain both novel and familiar stimuli to make it possible to behaviourally confirm the recognition of repeated stimuli, i.e., the test cannot solely contain novel stimuli. The second is the issue of how best to design a control condition that isolates those changes in c-*fos* activity associated with recognition memory. This control condition needs to be matched to the visuo-motor demands of the recognition condition. In the first study to examine c-*fos* expression associated with behavioural measures of recognition (Albasser et al., 2010b), the control rats were given the same 20 recognition trials with the same set of 20 objects as those given to the experimental (recognition) group on the final test day. The critical difference was that these control rats had repeatedly been exposed to the same set of 20 objects over numerous, previous sessions, ensuring that all stimuli were familiar on the final test day. The impact of this familiarisation procedure could be seen in the final test session. The recognition memory group showed a strong preference for the novel over the familiar stimuli. In contrast, the familiar object control group showed no clear preference between the test objects, presumably reflecting their acquired familiarity (Albasser et al., 2010b).

Comparisons of c-*fos* expression after recognition testing in the bow-tie maze (novel object recognition condition vs. familiar object control condition) revealed that recognition was associated with raised Fos counts (Table 1.1) in the caudal perirhinal cortex (areas 35 and 36), as well as area Te2 (Albasser et al., 2010b). Other sites such as the prelimbic, infralimbic and anterior cingulate cortices did not show differential Fos levels. These results are very similar to those from c-*fos* studies in which rats were

passively shown either novel or familiar stimuli (Zhu et al., 1995b; Wan et al., 1999, 2004), as well as paralleling the outcome of lesion studies in these same areas (Barker et al., 2007; Winters et al., 2008; Warburton & Brown, 2010; Ho et al., 2011). There was, however, one main difference; hippocampal changes in c-*fos* expression were found in the bow-tie maze task that had not been observed in the previous procedures that passively presented novel stimuli (e.g., Zhu et al., 1995b; Wan et al., 1999, 2004). Comparisons between rats in the bow-tie maze that explored either novel objects or only familiar objects (Table 1.1), revealed that in the novel object group the hippocampal subfields CA3 (septal) and CA1 (temporal) showed significant Fos increases, while the dentate gyrus (septal and intermediate) showed a Fos decrease (Albasser et al., 2010b). This pattern of hippocampal changes (Table 1.1) matches the Fos findings when rats are passively shown spatially rearranged familiar visual stimuli in the split-hemisphere procedure (Wan et al., 1999). That is, relatively increased Fos counts were again seen in CA3 and CA1, while relatively decreased Fos counts were seen in the dentate gyrus (Wan et al., 1999; Albasser et al., 2010b). One interpretation, is that by exploring objects in the bow-tie maze the rats not only showed differential neural responses associated with novelty vs. familiarity, but also showed additional neural changes arising from the learning of other information associated with individual objects, e.g., their spatial or temporal attributes (Warburton & Brown, 2010).

In a complementary bow-tie maze study, c-*fos* expression was examined after rats had discriminated novel from familiar objects in the dark (Albasser et al., 2013b). This study used essentially the same experimental and control protocols as described above, though all testing was carried out in the dark. Thus, in the final session, one group experienced novel objects while the control group experienced the same set of familiar objects that had been given on all of the preceding sessions (Albasser et al., 2010b). Comparisons between these two groups showed increased c-*fos* activity in rostral perirhinal cortex, but not in caudal perirhinal cortex, of those rats discriminating novel from familiar objects in the dark. This rostral-caudal perirhinal pattern is the opposite of that found for object recognition in the light (Albasser et al., 2010b), creating a potential double dissociation (Table 1.1). Novel objects in the dark were again associated with increased c-*fos* activity in the hippocampus, but the pattern of subfield change was also different to that seen the light (Table 1.1). In the dark there were significant Fos increases in the dentate gyrus, CA1 and CA3 (Albasser et al., 2013b), whilst in the light there was a Fos decrease in the dentate gyrus, as well as Fos increases in CA1 and CA3 (Albasser et al., 2010b). In addition, a wider array of other brain regions, some involved in spatial memory, were

activated by exploring novel objects in the dark in a bow-tie maze, e.g., the anterior thalamic nuclei, retrosplenial granular cortex, anterior cingulate cortex, and lateral entorhinal cortex (Albasser et al., 2013b).

1.5.2 Network analyses based on structural equation modelling

The main behavioural contrast that has been investigated in these c-*fos* expression studies (Albasser et al., 2010b, 2013b) is between rats that discriminate novel from familiar objects (recognition memory) and rats that only explore familiar objects. In order to investigate if the regional Fos differences observed in the medial temporal lobe reflect changes in networks of activity, an additional form of statistical analysis was employed.

For these network analyses, the relationship between the activity-related Fos counts in different brain sites were examined using structural equation modelling (SEM). Structural equation models are multiple-equation regression models that can quantify causal (structural) relationships between a set of variables. This technique was originally developed for use in social psychology studies in which it is used to test theoretical relationships among several observed variables as well as using observed variables to estimate unobservable (latent) variables (Bollen & Long, 1993; Tabachnick & Fidell, 2001; Schumacker & Lomax, 2010). Although SEM is the commonly used nomenclature, the more precise term for the technique used here is path analysis, as the theoretical models to be tested involve relationships between observed, and not latent, variables. Consequently, this type of analysis can be thought of as a set of multiple equation regression models that can confirm or reject theoretical relationships between these observed variables. These relationships include inferring the potential direction of influence between two regions (Schumacker & Lomax, 2010). The strength of a relationship (path) between regions is estimated based on the covariance matrix of the observed data (Protzner & McIntosh, 2006). A model is assessed on how well it replicates the variance-covariance matrices of the observed data (Tabachnick & Fidell, 2001).

SEM is commonly used to test models of neuronal activity in distributed networks in the brain based on regional activity obtained from positron emission tomography and functional magnetic resonance imaging studies (McIntosh & Gonzalez-Lima, 1991, 1994; Friston et al., 1993, Friston, 1994; Kim & Horwitz, 2009). It is used to study network dynamics based on the assumption that covariance between the activity of

different brain regions reflects neuronal interactions; i.e., that activity changes in one area are generated by alterations in the influence of a connected region (McIntosh, 2002). It can be used to estimate effective connectivity; that is the influence one neuronal system exerts over another (Friston, 1994). Further, it can be used to estimate alterations in effective connectivity within an anatomically defined network based on task or group differences (Protzner & McIntosh, 2006; Kim & Horwitz, 2009). Indeed, relevant to the current work, it has been used to identify differences in the functional networks associated with visual processing of objects or spatial locations (McIntosh & Gonzalez-Lima, 1994) It has also been used to identify patterns of effective connectivity in a given data set (Bullmore et al., 2000). In these types of studies, when sample size is small, caution must be taken when interpreting the absolute numbers of the estimated path coefficients. However, it has been demonstrated that the relative strength of path coefficients usually recapitulate the strength of the underlying relationship when models are non-recursive (Boucard et al., 2007). The use of this statistical technique in the experiments described in this thesis is very similar, as it also employs a proxy marker of neuronal activity estimated in discrete regions of the brain.

This technique has previously been used to derive anatomical-based models to explain the interregional correlations based on activity patterns of Fos seen between various regions of interest (Jenkins et al., 2003; Poirier et al., 2008; Albasser et al., 2010b). These models involved sites known to be important for memory, including the perirhinal cortex, and were then applied to established anatomical pathways between regions of interest within and beyond the temporal lobe. By applying SEM to the Fos counts from the initial bow-tie maze study of recognition memory, two different patterns of correlated activity emerged (Albasser et al., 2010b). These patterns depended on whether the rats had explored novel or familiar objects. The optimal network model of correlated activity associated with exploring novel objects (Figure 1.10 lower) involved area Te2, parahippocampal regions (perirhinal cortex and lateral entorhinal cortex), as well as various hippocampal subfields (Albasser et al., 2010b). The best fitting SEM model associated with exploring familiar objects (Figure 1.10 upper) again involved area Te2, the perirhinal and lateral entorhinal cortices, but there was a crucial difference in the hippocampus (Figure 1.10). While novel stimuli were associated with preferential activity correlations in the direct pathway from the lateral entorhinal cortex to the dentate gyrus (and CA3), familiar stimuli were principally associated with correlated activity in the direct pathway from the lateral entorhinal cortex to CA1, i.e., the familiarity network largely bypassed the pathway to the dentate gyrus (Albasser et al.,

2010b). These differences are striking as they suggest a different mode of hippocampal interaction when learning about novel as opposed to familiar stimuli (Figure 1.10). This methodology also provides the ideal framework for addressing the question of what happens to these learning related networks if the hippocampus is removed. This will be the first experiment to be described in this thesis.

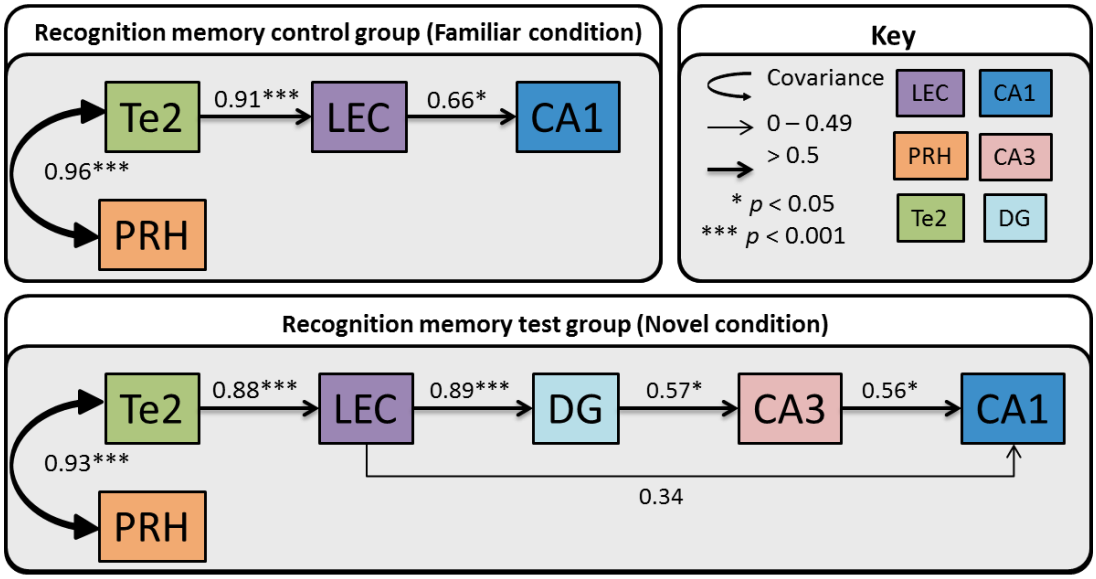

Figure 1.10. Neural networks derived for recognition memory.

Optimal interactions derived from SEM of Fos-related activity in the control familiar object condition (top panel) and novel object condition (bottom panel). The strength of the causal influence of each path is denoted both by the thickness of the arrow and by the path coefficient next to that path. Sites depicted: area Te2 (Te2), perirhinal cortex (PRH), lateral entorhinal cortex (LEC), hippocampal subfields CA1, CA3 and dentate gyrus (DG), dorsal subiculum (dSub), anterior thalamic nuclei (Ant Thal) and prelimbic cortex (PL). *p < 0.05; ***p < 0.001. Adapted from Albasser et al., 2010b.

The inference is that stimuli signalled as being familiar activate the hippocampus in a way that is qualitatively different from that seen for novel stimuli. The familiar stimulus model could be further examined by looking at a closely related form of memory, recency memory. This term describes the ability to distinguish stimuli based on their temporal properties, i.e., how long ago in the past they were last encountered. To test recency memory, it is necessary to use familiar stimuli, and so it might be predicted that the c-*fos* activity network associated with recency memory will preferentially involve direct connections from the lateral entorhinal cortex to CA1. This question will be also addressed in this thesis.

Other relevant evidence comes from a study that compared activity levels of a different immediate early gene, zif268, in the hippocampal and parahippocampal regions of rats.

The learning task, spatial working memory in a radial arm maze, was selected as it is known to depend on the hippocampus (Olton et al., 1979). In contrast to object recognition, task performance does not normally require the integrity of the perirhinal cortex (Aggleton et al., 2004). In this experiment, zif268 levels associated with either early or late learning of a radial-arm maze task (Poirier et al., 2008) were compared. The optimal network model associated with early learning (i.e., when there should be more novel information and larger gains of learning) was remarkably similar to that found for novel object recognition in the bow-tie maze. Consequently, early radial-maze learning was associated with entorhinal → dentate/CA3 interaction (Poirier et al., 2008). In contrast, late learning was more associated with direct entorhinal → CA1 interactions, while the dentate gyrus and CA fields seemed to be functionally disconnected. Together, these studies demonstrate that combining c-*fos* imaging studies with SEM is a powerful technique that can be used to explore neural network dynamics associated with different learning opportunities.

1.6 Models of hippocampal-parahippocampal interactions

The perirhinal cortex has both direct and indirect anatomical connections with the hippocampus via the entorhinal cortex (Furtak et al., 2007; Burwell & Agster, 2008). Consequently, there are several means by which these regions have the potential to impact on one another. The notion that these areas function interdependently is central to many models describing how the medial temporal lobe supports memory. However, there are several, in some cases conflicting, viewpoints on the specific nature of these systems interactions; two of which were described in Section 1.3.2. A signal from the perirhinal cortex affecting hippocampal processing is predicted by several models of medial temporal lobe interactions and some of these will be described in this section.

1.6.1 Gatekeeper hypothesis

One such hypothesis is the gatekeeper model of declarative function (Fernández & Tendolkar, 2006). In this model, Fernandez and Tendolkar (2006) propose that the rhinal cortex performs integrated processes of recognition, encoding and information transfer to the hippocampus. When a novel stimulus is encountered, many neurons of the rhinal cortex are required to process it, giving the sensation of novelty, efficient encoding of the stimulus properties and efficient transfer of information to the hippocampus. In contrast, when a familiar stimulus is encountered few rhinal neurons are required for processing and, as such, leads to a sense of familiarity, less effective

encoding of stimulus properties and a reduction in information transfer to the hippocampus (Fernández & Tendolkar, 2006). This model is supported by rodent and primate studies that have demonstrated an effect of activity suppression upon stimulus repetition (Fahy et al., 1993; Zhu et al., 1995a; Xiang & Brown, 1998; Woloszyn & Sheinberg, 2012). Particularly convincing evidence comes from human imaging studies that demonstrated perceived memory strength corresponds to a reduction in activity in the rhinal cortex upon subsequent viewing of a stimulus (Gonsalves et al., 2006; Montaldi et al., 2006). The SEM findings described above both concur with and extend these notions by identifying potential anatomical substrates reflecting changes in hippocampal activity, depending on the novelty or familiarity of the stimulus being processed. One of the main aims of this thesis is to explore further the relationship between object class (i.e., its novelty or familiarity) and activity in these regions and perhaps more informatively, how regional activity changes in concert.

1.6.2 Binding of item and context model

This model is based on the premise that there are two processing streams within the medial temporal lobe that can be dissociated based on the type of information to be encoded (Eichenbaum et al., 2007). Object feature, so-called 'what', information is initially processed by the perirhinal and subsequently the lateral entorhinal cortex. Contextual, or 'where', information is dealt with by the parahippocampal (primate homologue of rodent postrhinal) cortex and medial entorhinal cortex. These 'what' and 'where' information streams then converge on the hippocampus to be bound together to form item–context associations (Eichenbaum et al., 2007, 2012).

The model was formalised by Diana et al., (2007) as the 'binding of item and context' (BIC) model. It predicts that judgements of prior occurrence of items can be supported by the perirhinal cortex as only 'what' information, and not associated contextual information, is required for these familiarity decisions. This model further predicts that the parahippocampal cortex, in addition to the hippocampus, is required for recollective processing as these regions represent contextual information and item-context relational information respectively. Further, item familiarity is hypothesised to be reflected in an attenuated response in the perirhinal cortex as compared to the initial encounter. Depending on the circumstances, this perirhinal activation may be sufficient to reactivate the pattern of activity in the hippocampus that occurred during learning, which in turn can reactivate the contextual information in the parahippocampal cortex, resulting in recollection (Diana et al., 2007; Ranganath, 2010). Thus, this model

addresses how different types of stimuli to be processed define regional activation patterns rather than directly addressing recognition memory *per se*. The predictions derived from this model regarding recollection and familiarity are, however, consistent with dual process accounts of recognition memory. Accordingly, this model predicts that hippocampal damage will selectivity impact recollection and spare familiarity (Eichenbaum et al., 2007), as the hippocampus is proposed to provide a spatiotemporal framework within which memories for events and their contexts can be tied together in 'memory space' (Eichenbaum et al., 2012).

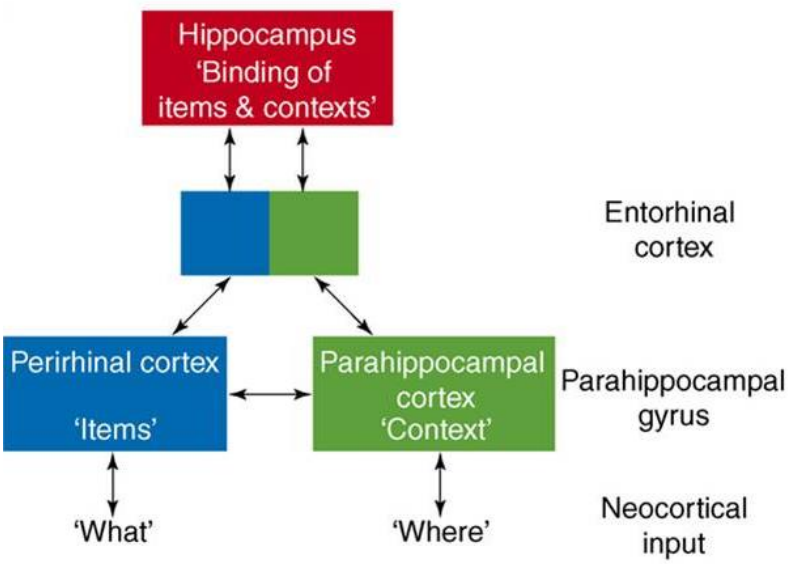

Figure 1.11. Schematic of BIC model.

Representation of the anatomical connections among, and the proposed roles of, the hippocampus, perirhinal cortex and parahippocampal cortex in episodic memory according to the BIC model. The arrow between the perirhinal cortex and parahippocampal cortex indicates the anatomic connection between the two regions. Adapted from Diana et al., 2007

More recently the BIC model has been expanded upon and this new iteration is known as the anterior temporal and posterior medial (AT-PM) framework (Ranganath & Ritchey, 2012). The idea of two processing streams was extended beyond the medial temporal lobe into two separate functional networks. The AT system is composed of the perirhinal and lateral entorhinal cortices, the temporopolar cortex, lateral orbitofrontal cortex and amygdala. This anterior system supports object perception as well as familiarity and semantic memory. The PM system includes the parahippocampal cortex, retrosplenial cortex, anterior thalamic nuclei, mammillary bodies, pre- and parasubiculum as well as components of the default mode network. This posterior

system is proposed to support scene perception in addition to episodic and recollective memory. The hippocampus is postulated to be the point of convergence between these two systems (Ranganath & Ritchey, 2012).

1.6.3 Knierim's local vs. global reference frames

This model also finds its roots in the existence of two parallel processing streams within the medial temporal lobe. The lateral entorhinal cortex processes non-spatial 'what' information and the medial entorhinal cortex processes spatial 'where' information supplied by the perirhinal and postrhinal cortices respectively. The lateral entorhinal cortex subsequently projects this information to the distal region of CA1 and proximal subiculum, while the medial entorhinal cortex forwards information to the proximal region of CA1 and distal subiculum. These separate information streams are postulated to interact in a 'side-loop' that projects to the dentate gyrus and CA3 and this is engaged when object-context association are behaviourally relevant (Knierim et al., 2006).

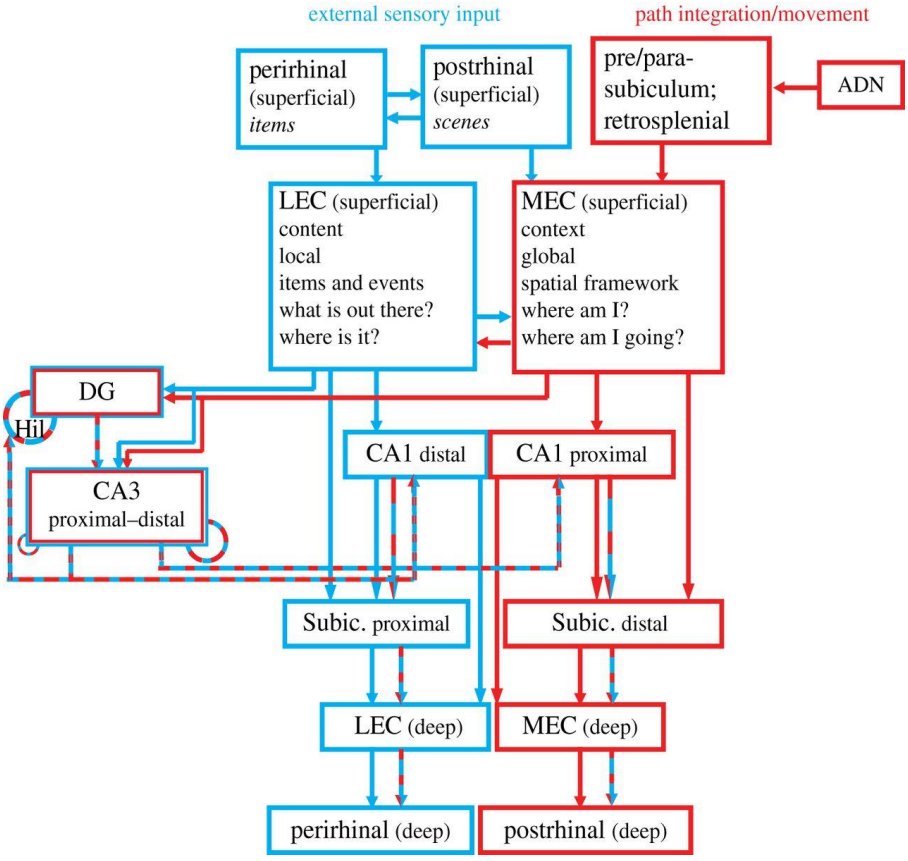

Figure 1.12. Wiring diagram proposed process of local and global reference frames.

This schematic depicts the parallel processing streams into the hippocampus proposed to underlie local reference frames (blue) and global (red) reference frames/path integration. The diagram structure emphasizes the dual processing streams that pass through the lateral entorhinal cortex and medial entorhinal cortex. Adapted from Knierim et al., 2014.

1.6.4 Perceptual mnemonic feature conjunction model

Of additional interest is a model of perirhinal cortex function known as the perceptual mnemonic feature conjunction model. This model hypothesises that the perirhinal cortex functions in perception as well as memory processing by its involvement in the ventral visual processing stream (Murray & Bussey, 1999; Bussey et al., 2005, 2007; Murray & Wise, 2012). It suggests that stimuli are encoded or represented hierarchically throughout the ventral visual stream. Individual features of stimuli are represented early in visual processing in caudal brain regions. These representations become more integrated and complex in more rostral brain regions activated later in visual processing. This information converges on the perirhinal cortex, which functions to encode complex conjunctive representations of stimuli in order to allow for object identification by resolving feature ambiguity (Murray & Bussey, 1999; Murray & Richmond, 2001; Bussey et al., 2005; Murray et al., 2007). This theory is supported by experiments that have shown that loss of the perirhinal cortex in monkeys and rats is associated with deficits in discriminating stimuli with high feature ambiguity, that is, many overlapping features, even when no delay is imposed and so theoretically cannot tax memory (Buckley et al, 2001; Bussey et al., 2002, 2003; Saksida et al, 2006; Bartko et al., 2007a,b). Similar impairments have been observed in patients with widespread damage to the medial temporal lobe but not if the damage is restricted to the hippocampus (Barense et al., 2005, Lee et al., 2005a,b).

Loss of the perirhinal cortex would, based on this hierarchical representation viewpoint, be predicted to cause judgements of prior occurrence to be based on the lower level feature-based representations of the stimuli still available earlier in the visual stream (McTighe et al., 2010). These feature-based representations would be more susceptible to interference as specific features of an object, for example its colour or shape, are likely to overlap with those of other intervening stimuli creating feature ambiguity between stimuli (Bartko et al., 2007a,b; Romberg et al., 2012). In this way, perirhinal cortex lesions are proposed to induce ‘false memories’ or incorrect identification of a novel stimulus as familiar (McTighe et al., 2010; Romberg et al., 2012). Inconsistent with this interpretation are several studies that have shown that rats with perirhinal lesions do not reduce their exploration of novel objects in the sample phase of spontaneous object recognition tasks (Ennaceur et al., 1996; Aggleton et al., 1997; Winters et al., 2004; Barker et al., 2007; Mumby et al., 2007; Bartko et al., 2007a,b; Albasser et al., 2009; McTighe et al., 2010; Barker et al., 2011; Albasser et al, 2015).

Further, there are examples of rodent, monkey and human studies that indicate that perirhinal damage can spare zero-delay discrimination of complex visual stimuli while impairing recognition memory (Buffalo et al., 1999, 2000; Shrager et al., 2006; Davies et al., 2007; Albasser et al., 2010). Thus, further investigation is required into the specific nature of the recognition deficit caused by perirhinal lesions.

1.7 Rationale for the following experiments

As can be seen from the description of the various models postulating how regions of the medial temporal lobe interact to support different forms of memory, a consensus has not been reached on the nature of these systems interactions. This is true for even the most fundamental forms of memory, including recognition memory. It is important to clarify basic forms of cognitive processing before more complex processes can be experimentally addressed. Thus, the behavioural experiments in this thesis will focus on the simple principles of novelty and familiarity.

The real advantage of the immediate-early gene imaging technique employed throughout the experiments described in this thesis is the incredibly high anatomical resolution that can be achieved. This allows for the assessment and comparison of regional neuronal activity between different behavioural conditions not only at the regional level, but also within regional subdivisions. This is important as even within a single brain region, efferent and afferent connections can vary dramatically along different axes. These topographical differences could account for discrepancies observed between lesion studies. Thus, in combination with structural equation modelling, it will allow for the assessment of functional models of the medial temporal lobe with unparalleled resolution. In addition, this type of analysis can also be carried out in rats that have received lesions, thereby allowing for the assessment of network dynamics following damage to purported components of the network. Many models imply that the perirhinal cortex has a considerable impact on hippocampal functioning, and thus would predict that removal of the perirhinal cortex would cause dysfunction in hippocampal processing. There are models that predict the opposite pattern. These were the hypotheses I set out to test.

As described in Section 1.5.2, Albasser et al., (2010b) found different modes of hippocampal-parahippocampal interactions when rats performed a recognition memory task (novel vs. familiar stimuli) or explored familiar objects. The aim of the experiment described in Chapter 3 was to replicate this dissociation and extend the findings by

including rats that had received lesions to the hippocampus. In this way, the idea of functional interdependence between the hippocampus and perirhinal cortex could be tested behaviourally, at the level of regional activation and by assessing how network dynamics are affected by loss of the hippocampus.

Based on the finding that novel or familiar stimuli alter the way in which regions of the medial temporal lobe interact, the aim of the experiment described in Chapter 4 was to vary the degree of familiarity of test objects in intact animals and assess if regional activations and interactions were altered by this associative change. This was accomplished with a recency, or temporal order, task.

Chapters 5 and 6 focus on assessing if dysfunction occurs in the hippocampus due to loss of the perirhinal cortex, first in a novel context task (Chapter 5) and subsequently in a novel object based task (Chapter 6). Again, the impact of the lesions was tested at multiple levels; behaviourally, regionally and at a systems level. Throughout all of the experiments described in this thesis, the underpinning aim was to provide as highly resolute anatomical data as possible.

2 General Methods

2.1 Overview

Each of the experiments to be described in this thesis followed a similar progression of phases (Figure 2.1). This general protocol will be described here, followed by a description of the specificities of each experiment in the respective chapters. The rats involved in the experiments described in Chapter 4 are the only ones that did not receive surgical intervention before their behavioural training. Rats of Chapter 3 received lesions to the hippocampus and those of Chapters 5 and 6 received lesions to the perirhinal cortex.

Rats performed a behavioural task followed by immunohistochemical visualisation of the protein product of the immediate early gene, c-*fos*. The number of Fos-positive cells were then quantified in various regions of interest within the brain based on the type of behavioural task. Finally, structural equation modelling was applied to the activity related Fos data.

2.2 Animals

In all experiments subjects were male, Lister Hooded rats (Rattus norvegicus; Charles River, UK or Harlan, UK). They were housed in pairs under diurnal conditions (12h light/12h dark). During behavioural testing they were food restricted so that they remained close to 85% of their free feeding body weight. Water was available *ad libitum* throughout. All experiments were performed in accordance with the UK Animals (Scientific Procedures) Act, 1986 and associated guidelines and approved by local ethical committees at Cardiff University. Where the rats were not naïve, a description of the behavioural tasks they had previously experienced will be outlined in the respective chapter.

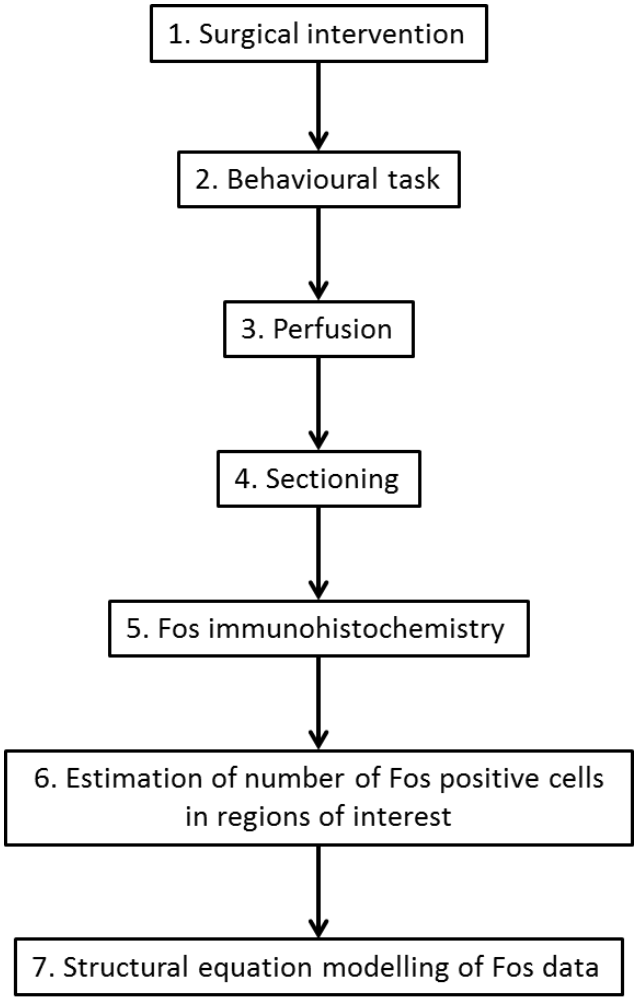

Figure 2.1. General experimental progression.

Graphic illustrating the general steps involved in each of the experiments to be described.

2.3 Object related behavioural testing

For all experiments, except that described in Chapter 5, behavioural testing took place in a bow-tie maze (Albasser et al., 2010a).

2.3.1 Bow-tie maze

The maze is made with steel walls and a wooden floor (Figure 2.2). The maze measured 120mm long, 50cm wide and 50cm tall. Each end of the maze was triangular in shape with their apices joined by a 12cm corridor. In the middle of the corridor was an opaque sliding-door that divided the maze in half. Recessed in the floor, by the back wall of each triangular area, were two food wells 3.5cm in diameter and 2cm deep. These food wells were separated by a steel divider that projected 15cm into the maze from the centre of the back wall.

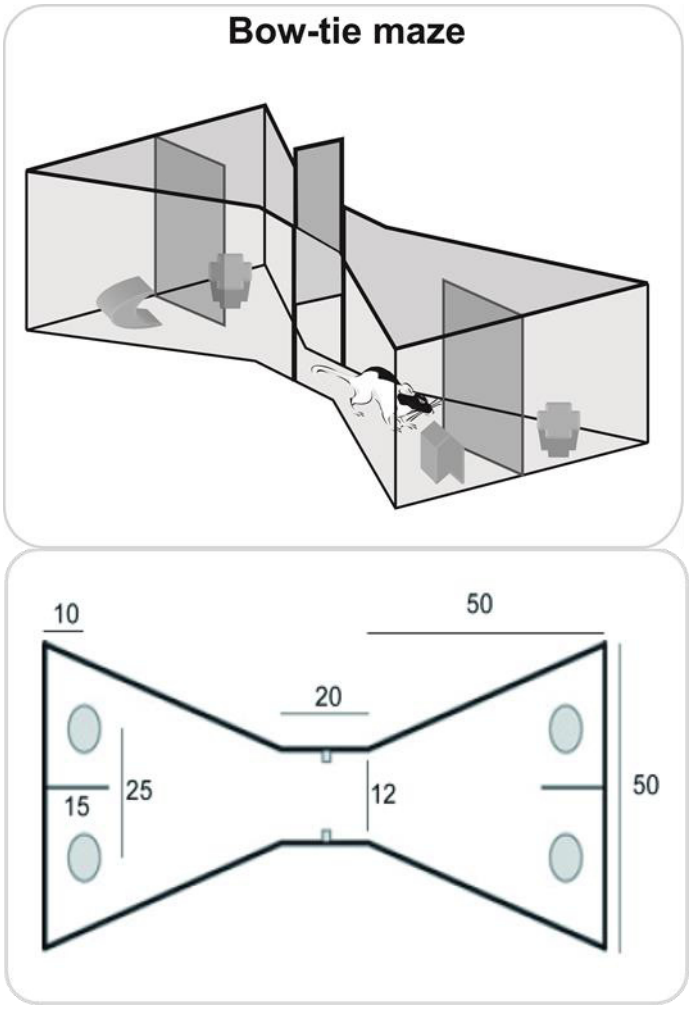

Figure 2.2. Bow-tie maze.

Upper panel is a graphic of the test apparatus used for testing object recognition and object recency memory. A sliding door in the centre divides the maze into two halves so that objects can be placed over the food wells in one half while the animal is completing the task in the other half. Upper panel adapted from Albasser et al. (2011a). Lower panel is a schematic of the bow-tie maze, with dimensions in centimetres. Lower panel adapted from Adapted from Albasser et al. (2010b).

2.3.2 Objects

When rats were tested in the bow-tie maze they were presented with different three-dimensional junk objects, which varied in colour, shape, size and texture (Figure 2.3). Any object with an obvious scent was excluded. Every object had an identical duplicate and so if an object was to be presented twice in the same session a different copy could be used to avoid the possibility of odour marking. All objects were large enough to cover a food well but light enough to be displaced by a rat. All objects were cleaned with alcohol wipes after each session.

Figure 2.3. Example object set.

Set of objects used for object recognition test in the bow-tie maze.

2.3.3 Pre-training in the bow-tie maze

This phase took seven days and by its completion all rats would run from one side of the maze to the other and displace objects covering a food well in order to access food rewards. Day one: several 45mg sucrose pellets (Noyes, Lancaster, NH, USA) were spread out over the floor of the maze to encourage exploration. Rats were placed into the maze in their home-cage pairs for 20 minutes and allowed to freely explore and consume the sucrose pellets. Day two: sucrose pellets were placed only around the food wells and each rat was placed in the maze individually for 10 minutes. Day three: initially, one sucrose pellet was placed in each of the food wells. Individual rats were placed in the maze and the food wells at opposite ends of the maze were alternately re-baited for 10 minutes to encourage the rats to move between these two end areas. Days four to seven: the sliding door that divided the maze into two separate areas was introduced. Additionally, small pairs of objects were placed to partially cover the sucrose baited food wells. Once a rat had collected the sucrose pellets from both food wells on one side of the maze the central door was lifted to allow access to the other side of the maze where further objects covered baited food wells. This process was continued with the objects covering increasingly more of the food wells until the rats would displace the objects when they completely covered the food wells. Pre-training was complete when the rats would run from one side of the maze to the other as soon as the central door was raised. The four pairs of objects used during pre-training were not used in the subsequent experiments.

2.3.4 Behavioural testing

This will be described in the respective chapters.

2.3.5 Analysis of behaviour

The test phases of all object based experiments were video-recorded and object exploration was timed by an experimenter unaware of the surgical history of the individual rats. Object exploration was defined as directing the nose at a distance <1cm from the object with the vibrissae moving, and/or touching it with the nose or paws. Behaviour that did not count as exploration included when rats sat on the object, if they used the object to rear upward with their nose pointing at the ceiling, or chewing the object. From these timings, two measures of discrimination were calculated. Index D1 is the amount of time spent exploring the novel (or relatively less familiar) object minus the time spent exploring the familiar (or relatively more familiar) object. The 'cumulative D1' is the sum of the D1 scores across all 20 trials. The second measure, D2, takes into account differences in total exploration times as D1 is divided by the total amount of exploration given to both objects (Ennaceur & Delacour, 1988). Thus, the D2 ratio can fall between -1 and +1. If the ratio is positive, the rat exhibits a preference for novel objects. The 'updated D2' is the D2 score recalculated after each trial.

2.4 Perfusion

Following completion of the test phase in all of the experiments, rats were placed in a dark holding room for 90 minutes (in experiments where training sessions had taken place, the rats had previously been placed in the same dark holding room after each training session). This interval was selected as previous studies have shown that expression of Fos, the protein product of c-*fos*, peaks between 60 and 120 minutes after the inducing event (Bisler et al., 2002; Zangenehpour & Chaudhuri, 2002). They were then given a lethal overdose of sodium pentobarbital (60mg/kg, Euthatal, Rhone Merieux) and transcardially perfused with 0.1M phosphate-buffered saline (PBS) followed by 4% paraformaldehyde in 0.1M PBS (PFA). Brains were removed from the skull, postfixed in PFA for 4 hours, and then incubated in 25% sucrose at room temperature overnight on a stirrer plate.

2.5 Sectioning and histology

The brains were sectioned in the coronal plane into 40µm sections using a freezing microtome (Leica, SM2400). A series of 1 in 4 sections was collected in PBS and the

remaining three series were collected in cryoprotectant (30% w/v sucrose, 1% w/v polyvinyl pyrrolidone and 30 % v/v ethylene glycol dissolved in PBS) and stored at -20°C until further processing was required.

The series collected in PBS were subsequently mounted onto double gelatin-subbed glass slides. Sections were allowed to air dry for at least 48 hours to ensure they had adhered to the slides and were then stained with cresyl violet, a Nissl stain. The cresyl violet stain was made by dissolving 0.5g cresyl violet and 1.211g sodium acetate in 1L distilled water (dH_2O) with 0.425ml 5M formic acid. This was stirred for 48 hours and filtered before use. The sections were first hydrated in a series of two minute washes in decreasing concentrations of alcohol, followed by two minutes in dH_2O. The sections were then stained for 2-5 minutes in the cresyl violet stain, followed by 30 seconds in dH_2O. The sections were again dehydrated in a series of increasing concentrations of alcohol, cleared in xylene and coverslipped using the mounting media, DPX (Thermo Scientific, UK).

2.6 Lesion analysis

Based on the examination of the cresyl stained series of sections using an upright bright-field microscope, the extent of the hippocampal lesion in each hemisphere (Chapter 3) was drawn onto corresponding coronal plates from a rat brain atlas (Paxinos & Watson, 2005), from bregma -2.12mm to – 6.80mm. These images were then scanned and the area of damage calculated using the image analysis software, ANALYSIS^D (Soft-Imaging Systems, Olympus).

The extent of the perirhinal cortex lesions (Chapters 5 and 6) were also examined in cresyl stained sections using an upright bright-field microscope. One hemisphere in each brain was designated to be analysed for Fos expression while the other was eliminated from the study. This was due to the relatively common presence of small amounts of cell disruption in the temporal regions of the hippocampal subfield, CA1, in one hemisphere caused by the lesions to the perirhinal cortex. A hemisphere was excluded from the study if there was any evidence of cell disruption was seen in more than one section. Brains that suffered damage to both hippocampi were completely excluded from the study. The extent of the lesions in both hemispheres were drawn onto corresponding coronal plates from the rat brain atlas (Paxinos & Watson, 2005), from bregma -2.80mm to – 6.72mm. These images were then scanned and the area of damage calculated using cellSens Dimension Desktop, version 1.12 (Olympus Corporation).

2.7 Immunohistochemistry

Another 1 in 4 series from each brain was immunohistochemically stained for the protein, Fos. This was carried out on free-floating sections. Tissue sections from one animal from each experimental group was processed concurrently in the same reaction vessel to decrease variation. The sections were washed six times in PBS to remove the cryoprotectant. Sections were then washed in 0.2% Triton-X 100 in 0.1M PBS (PBST), once in 1% H_2O_2 in PBST (to block endogenous peroxidases), then four further times in PBST. Sections were then incubated in a blocking solution of 3% normal goat serum (NGS) in PBST for one hour followed by the primary antibody solution; rabbit-anti-c-*fos* and 1% NGS diluted in PBST (see Table 2.1 for dilutions and vendors), for 48 hours at 4^0C. Sections were then washed four times in PBST, and incubated in the secondary antibody solution; biotinylated goat-anti-rabbit (1:200; Vector Laboratories) diluted in 1.5% normal goat serum in PBST for 2 hours at room temperature. Sections were washed four times in PBST. They were then incubated in avidin-biotinylated horseradish peroxidase complex in PBST (Elite kit, Vector Laboratories) for 1 hour at room temperature. Sections were washed four times in PBST, and then twice in 0.05M Tris buffer (pH 7.4). All washes were 10 minutes unless otherwise stated. Finally, diaminobenzidine (DAB Substrate Kit, Vector Laboratories) was used as the chromogen to visualise the location of immunostaining. The reaction was stopped in cold PBS. The sections were mounted onto double gelatin-subbed glass slides and allowed to air dry for at least 48 hours, dehydrated in increasing concentration of alcohol washes, cleared in xylene and coverslipped using DPX as the mounting media.

Table 2.1. Rabbit-anti-c-*fos* polyclonal antibodies.

	Dilution Factor	Company	Catalog number
Chapter 3	1:15,000	Calbiochem, EMD Millipore	PC38
Chapter 4	1:3,000	Calbiochem, EMD Millipore	Ab-5
Chapter 5	1:15,000	Calbiochem, EMD Millipore	PC38
Chapter 6	1:10,000	Synaptic Systems	226 003
Chapter 7	1:10,000	Synaptic Systems	226 003

2.8 Image capture and analysis of Fos-positive cells

For the experiments described in Chapters 3 and 4, images from each region of interest were captured from four consecutive sections (each 120µm apart) from both hemispheres of each brain. This was done using a 5x objective lens (numerical aperture

of 0.12) on a Leica DMRB microscope with an Olympus DP70 camera. As the field of view was 0.84 x 0.63mm, cortical regions required one image per section to include all cortical lamina, while for the septal hippocampus multiple images were taken and combined (Microsoft Ice, Microsoft). Using ANALYSIS^D software (Soft-Imaging Systems, Olympus Corporation), Fos-positive cells were quantified by counting the number of immunopositive nuclei (mean feret diameter of 4-20µm) stained above a grayscale threshold set 60-70 units below the peak grey value measured by a pixel intensity histogram.

For the experiment detailed in Chapter 5, images of the regions of interest were captured and analysed as described above with one main difference; images were captured from six consecutive sections from one hemisphere per animal. This was due to the elimination of hemispheres due to the presence of small amounts of damage to caudal regions of the hippocampal subfield, CA1, caused by the lesions to the perirhinal cortex. The equivalent hemisphere (left or right) was also analysed in the corresponding surgical control ('sham') animal.

Image capture for Chapter 6 was also carried out using the same Leica DMRB microscope with the 5x objective lens (numerical aperture of 0.12), however the camera was an Olympus DP73 and the associated software was cellSens Dimension, version 1.8.1 (Olympus Corporation). The field of view was 1.4 x 1.1 mm. As described for Chapter 5, images were captured from six consecutive sections from one hemisphere per rat due to the common presence of small amounts of unilateral damage to the temporal region of CA1. Using cellSens Dimensions Desktop software, the number of Fos-positive neurons were quantified by counting the immunopositive nuclei (diameter of 4-20µm, sphericity of 0.1-1.0) stained above a grayscale threshold set 50-60 units below the peak grey value measured by a pixel intensity histogram. For each region of interest within an experiment the greyscale threshold was kept constant but was altered slightly between regions of interest (i.e. for one region of interest the grayscale threshold applied to all of the images was -55 whereas for another region the threshold applied to all images was -60).

In all cases, a mean Fos count per region per brain was obtained by averaging the number of Fos-positive neurons in each image from that region.

2.9 Statistical analysis

All statistical analyses were carried out using the programme SPSS, version 20.0 (IBM Corp, Armonk, NY, USA). Initially all behavioural and Fos expression data were checked for normality using the Shapiro–Wilk test in conjunction with examination of frequency histograms. Where data transformation was necessary it is detailed in the respective chapter.

Group comparisons were made using a t-test or ANOVAs and simple effects were examined when a significant ($p \leq 0.05$) interaction was obtained. The homogeneity of variance of the between subjects variables was verified using Levene's test. Mauchly's test was employed to test for sphericity of the within subjects variables. If the variables were found to be non-spherical the Greenhouse-Gueisser epsilon was used (Howell, 2011). Bivariate correlations were calculated using the Pearson product-moment correlation coefficient for inter-regional Fos-positive cell counts. The levels of the correlations were compared between the groups using Fisher's *r*-to-*z* transformation (Zar, 2010).

The inter-regional correlation tables in each chapter show probability levels uncorrected for multiple comparisons because the individual correlations are of limited significance. Rather, the anatomical constraints on the structural equation modeling analysis and their overall fit indices help to compensate for the Type I errors inherent in the multiple correlations that comprise the model. Consequently, it is important that any model must match established patterns of connectivity between the regions of interest so that the number of potential models are constrained.

2.10 Structural equation modelling

Even though the mean number of Fos-positive neurons in a set of brain regions may appear to be unaffected by a behavioural condition or a lesion intervention, the underlying correlations between these same regions may be markedly different (e.g., Poirier et al., 2008). Thus structural equation modelling techniques were employed to assess whether the activity in one region directly affected another region and how these inter-regional relationships ("network dynamics") might be altered by the behavioural task or a lesion.

Standard regression tests if a single explanatory variable (e.g., X_1) can be used to predict the values of a single dependent variable (e.g., Y), this type of relationship is depicted in

Figure 2.4A (Protzner & McIntosh, 2006). Multiple regression estimates the effects that several independent predictor variables have on a single dependent variable (Figure 2.4B; Protzner & McIntosh, 2006), while path analysis can evaluate more complex relationships between a set of variables (Figure 2.4C). Path analysis is a structural equation modelling (SEM) technique, it uses multiple-equation regression models to assess potentially causal relationships between sets of observed variables in order to test if the relationship among these variables fits a theoretical structure. This type of analysis can help to explain how several variables are related to one another by developing a set of regression equations that best account for the mathematical relationships between them (Streiner, 2005). This set of equations is known as a model and is often represented graphically in a path diagram; an example is depicted in Figure 2.4C. In these path diagrams rectangles represent observed variables, while the circles represent the residual error associated with that observed variable (also known as disturbances). The residual errors represent the variance in the associated variable that cannot be accounted for by the inputs as set out in the model; this can include measurement error as well as any other influences that impact the values but that are not accounted for by the model (Hoyle, 2012). The residuals are not always depicted in path diagrams but are assumed to be accounted for. The arrows between the observed variables represent the relationship between those two variables and is known as a path (giving the technique its name; Streiner, 2005). This technique also makes it possible to test the potential direction of effects between variables (Schumacker & Lomax, 2010); for example, given two variables, X_1 and X_2, does X_1 influence the values of X_2 or does X_2 influence X_1. Setting out these relationships based on a hypothesis is known as model specification (Schumacker & Lomax, 2010).

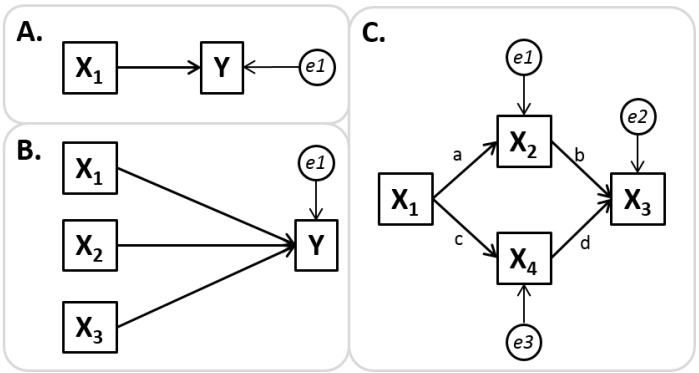

Figure 2.4. Depiction of relationships tested in regression, multiple regression and path analysis.

Schematic depictions of (A) standard regression, (B) multiple regression and (C) a set of hypothesised relationships between variables (a model) that can be tested using path analysis.

Using the example in Figure 2.4C, path analysis can be used to test whether variable X_1 has an effect on X_2 and X_4, and simultaneously if X_2 and X_4 have an effect on the values of X_3. The variable, X_1, is termed an exogenous variable as it has only outputs and no inputs while the others are endogenous variables as they have inputs set out in the model. This method can be thought of as testing if each endogenous variable within the hypothesised model can be predicted by its inputs. Exogenous variables do not have residual errors associated with them as their values are not accounted for by the model (Streiner, 2005). The relationships between the variables, (a, b, c, and d) are parameters to be estimated; these are known as path coefficients and are analogous to regression coefficients in multiple regression (Hoyle, 2012). However before a model can be estimated, the identification problem must be addressed (Schumacker & Lomax, 2010).

Models can only be tested if they are 'identified'; i.e., if there is only one possible solution. A necessary criterion for a model to be identified is that the number of parameters to be estimated are fewer than the number of distinct values in the sample variance-covariance matrix (Figure 2.5B). Again, to take the example in Figure 2.4C, there are four observed variables, thus, the dataset would consist of four sample variances (the measure of spread of data within one variable) and 6 sample covariances (the measure of how two variables change together) for a total of 10 distinct sample parameters (Figure 2.5). The model requires estimation of four path coefficients, three equation error variances and one independent variable variance, giving a total of eight parameters to be estimated. Subtracting the number of parameters to be estimated from the distinct sample parameters give the degrees of freedom associated with the model (Schumacker & Lomax, 2010).

A.

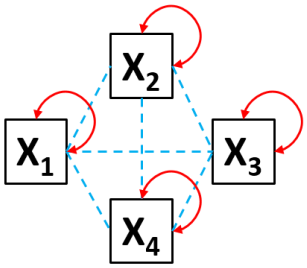

B.

	X_1	X_2	X_3	X_4
X_1	Variance of X_1			
X_2	Covariance between X_1 & X_2	Variance of X_2		
X_3	Covariance between X_1 & X_3	Covariance between X_2 & X_3	Variance of X_3	
X_4	Covariance between X_1 & X_4	Covariance between X_2 & X_4	Covariance between X_3 & X_4	Variance of X_4

Figure 2.5. Variance and covariance in a dataset.

(A) Depiction of an example data set in which the variance associated with each variable is depicted by red double headed arrows and all of the covariances between variables are shown by blue dashed lines. (B) Example variance-covariance matrix.

The next step is model estimation. The path coefficients are estimated by a series of layered multiple regression analyses. For the model in Figure 2.4C two layers of regression are required; two standard regressions are calculated to estimate if X_1 can predict X_2 and if X_1 can predict X_3. The second layer of analysis is a multiple regression where X_2 and X_3 are the predictors and X_4 is the dependent variable (Hoyle, 2012). The model depicted above can be defined by a regression lines with formulae:

$$X_2 = aX_1 + e1$$

$$X_4 = cX_1 + e3$$

$$X_3 = bX_2 + dX_4 + e2$$

The SEM software package, SPSS AMOS version 20.0 (IBM Corp, Armonk, NY, USA) was used to compute the path analyses presented in this thesis. The parameters were estimated using maximum likelihood estimation. This type of estimation is iterative; each parameter is estimated separately in each equation to meet the least squares criterion of minimised residual errors (Hoyle, 2012; Schumacker & Lomax, 2010). This estimation method aims to find values for the path coefficients that, given the model, maximise the likelihood of observed data, or in other words, minimise the difference between the observed and estimated data. Maximum likelihood estimation was chosen as method of estimation as it is recommended for use with smaller sample sizes and it allows the software to estimate missing data points and (Arbuckle, 2011).

Estimated path coefficients are commonly divided by their standard deviation in order to give standardised partial regression coefficients (Schumacker & Lomax, 2010); standardised path coefficients are presented in this thesis. Once the path coefficients have been estimated, the estimated regression equations are used to generate predicted variances and covariances of the variables. The predicted (implied) variance-covariance matrix can then be compared to the actual observed (sample) variance-covariance matrix (Figure 2.5B) in order to assess if the model (set of regression equations) could have produced the observed data set.

Path analysis estimates the way in which observed variables influence one another after a model structure has been hypothesised; it does not however, suggest a model structure (Schumacker & Lomax, 2010). For this reason, all models tested were based on well-established anatomical connections (Witter et al., 2000; Furtak et al., 2007; Van Strien et al., 2009). In these anatomical models the path coefficients can be considered to be estimates of 'effective connectivity' - the extent to which one region directly influences the other (Protzner & McIntosh, 2006). Additional assumptions of this method are: the independence of observations; that the endogenous variables (those that have inputs set out in the model) are measured on a continuous scale; that the relationships between the variables are linear; and, that the observed variables have multivariate normal distribution (Streiner, 2005; Arbuckle, 2011).

Following estimation an anatomical model was tested; each model was assessed based on how well the implied variance-covariance matrix replicates the sample variance-covariance matrices of the observed data (Schumacker & Lomax, 2010). This criterion is summarised by the χ^2 statistic. A model with good fit has a non-significant χ^2 and the ratio of χ^2 to the degrees of freedom is < 2 (Tabachnick & Fidell, 2001). If these criteria are met the implied variance-covariance matrix does not differ significantly from that of the sample. Two further goodness of fit indices are presented in this thesis; the comparative fit index (CFI) and the root mean square error of approximation (RMSEA). These were chosen as they have been shown to be most applicable for small sample sizes (Fan & Wang, 1998; Hu & Bentler, 1998).

The CFI index is based on a baseline comparison to an independence model in which there is no relationship (path) between any of the regions. This type of independence model has the worst possible fit (0) and so a higher CFI value indicates that the specified model is different from the independence model and as such has better fit; a CFI >0.9 is considered acceptable. The RMSEA index accounts for parsimony in the model as it

estimates the square root of the mean lack of fit per degree of freedom; an RMSEA <0.1 is considered acceptable (Tabachnick & Fidell, 2001). In order to ensure that the model fit statistics remained robust with small sample size each model contained at least as many cases as the number of variables to be estimated (Bollen & Long, 1992; Wothke, 1993). Additionally, the squared multiple correlation (R^2 or coefficient of determination) is presented for each endogenous brain region in the models. This value is a measure of the proportion of its variance that can be explained by its inputs within the model (Arbuckle, 2011). If the indices of fit did not reach acceptable levels then the specified model was not supported by the sample data and the model was modified. If the criteria were met then the specified model was supported by the data (Schumacker & Lomax, 2010).

Connections within the medial temporal lobe are complex and often reciprocal (Witter et al., 2000; Furtak et al., 2007; Van Strien et al., 2009). Where reciprocal projections are known to occur the paths were tested in both directions and the strongest one is presented. The aim here is to reproduce the prevailing flow of activity and it is appreciated that these models are anatomically simplistic and cannot capture the entire multifaceted interactions that occur between these sites. A direction of effect cannot be inferred between some anatomical regions as the fit of the models did not change when the path direction was reversed; this is indicated in the figures by a double headed arrow.

The data from different groups were then compared on the same network models by a stacking procedure in order to test for group differences in the path coefficients within the same overall model. For stacking, the path coefficients of all paths in the model are constrained so that they must have the same value across all groups; this is termed the structural weights model. If the model fit when the paths are unconstrained is significantly worse than when all paths are free to have different values for the different groups, as determined by a χ^2 difference test, this indicates that the strength of at least some of the paths differ among the groups (Protzner & McIntosh, 2006; Schumacker & Lomax, 2010). Subsequently, each path can be independently unconstrained and the fit compared to the structural weights model, again using a χ^2 difference test. If the fit of the model is significantly improved by unconstraining a path, it can be concluded that the strength of this path is different for the groups in question. Furthermore, Protzner and McIntosh (2006) presented findings that indicate that differences between groups are detectable and valid “regardless of absolute model fit” when the stipulated model is based on known anatomical connections.

3 Mapping Parahippocampal Systems for Recognition and Recency Memory in the Absence of the Rat Hippocampus

3.1 Introduction

Medial temporal lobe structures are vital for recognition memory, the ability to discriminate novel from familiar stimuli. Foremost in importance amongst these structures is the perirhinal cortex; evidence for its integral role in recognition memory has been provided by lesion studies in the monkey and rat (Zola-Morgan et al., 1989, Mumby & Pinel, 1994, Murray, 1996; Brown & Aggleton, 2001; Winters et al., 2008; Warburton & Brown, 2010) and neuronal recording studies in the monkey and rat (Fahy et al., 1993; Zhu et al., 1995a; Xiang & Brown, 1998). Functional heterogeneity between the hippocampus and perirhinal cortex is supported by lesion studies in which rodents successfully identify novelty in the absence of the hippocampus (Aggleton et al., 1986, Winters et al., 2004, Forwood et al., 2005, O'Brien et al., 2006; Albasser et al., 2009). Additionally, a set of studies has demonstrated that fornix lesions, which disconnect the hippocampus, differentially affect recall while sparing novelty detection when tested simultaneously in the rat (Eacott & Easton, 2007, Eacott et al., 2009; Easton & Eacott, 2010).

There remains, however, considerable uncertainty about the contributions of the hippocampus to recognition memory. While many studies (outlined above) report no apparent effect of hippocampal lesions, such lesions have been shown to sometimes impair behavioural tests of object recognition (Clark et al., 2000; Broadbent et al., 2004, 2010; Prusky et al., 2004; Cohen et al., 2013). One possible explanation for the frequent lack of evident hippocampal lesion deficits is found within those two-process models of recognition memory which assume that the perirhinal cortex is independently responsible for familiarity-based recognition (e.g., Aggleton & Brown, 1999; Norman & O'Reilly, 2003; Diana et al., 2007). This particular two-process view contrasts with other models, e.g., where interactions between perirhinal cortex and hippocampus more broadly support recognition (Wixted & Squire, 2011) or hierarchical models that emphasise the perceptual role of the perirhinal cortex (Cowell et al., 2010).

Human studies also provide contradictory evidence for the role of the hippocampus in recognition memory. Some reports provide evidence of a functional dissociation consistent with dual process models (Davachi et al., 2003; Henson et al., 2003; Ranganath et al., 2004; Diana et al., 2007; Staresina et al., 2012). Other studies support the single process view as some patients with focal hippocampal damage can have similar deficits in both forms of recognition memory (Stark et al., 2002; Manns et al., 2003). Thus, debate continues over the relationship of these putative mnemonic processes and their anatomical substrates (Aggleton and Brown, 2006; Diana et al., 2007; Wixted & Squire, 2011; Aggleton, 2012). The present study directly examined the importance of these interactions by measuring the impact of hippocampal lesions on perirhinal cortex network activity associated with recognition memory.

Expression of the immediate-early gene (IEG) c-*fos* provides a signal of neuronal activity strongly associated with recognition memory. For example, perirhinal c-*fos* activity increases when animals are passively shown novel stimuli (Zhu et al., 1995b, 1996; Wan et al., 1999, 2004). In the same studies, hippocampal c-*fos* changes were not observed. Increased perirhinal c-*fos* expression is also seen when rats actively explore and discriminate novel from familiar objects (Albasser et al., 2010b), with this perirhinal c-*fos* upregulation being required for stable recognition memory (Seoane et al., 2012). Active object exploration also reveals networks of c-*fos* activity that link parahippocampal sites with the hippocampus, patterns that vary depending on whether stimuli are novel or familiar (Albasser et al., 2010b). The functional significance of these hippocampal activations for recognition memory remains, however, unknown.

To test the involvement of the hippocampus in modifying perirhinal cortex activity, rats with excitotoxic lesions of the hippocampus and control rats with sham surgeries explored pairs of objects (one novel, one familiar) over multiple recognition trials (Novel Object condition). Two other groups (hippocampal and sham lesions) only explored objects made familiar by prior exposure over previous sessions, so testing recency memory (Familiar Object condition). The initial question was whether the hippocampal lesions affected either recognition or recency memory performance. The next question was whether the hippocampal lesions altered c-*fos* activity levels in the perirhinal cortex (areas 35, 36) and lateral entorhinal cortex. Then, using the c-*fos* activity data, networks of inter-correlated parahippocampal sites associated with either recognition memory or recency memory were derived with structural equation modelling. The impact of hippocampal lesions on these networks was then assessed.

The final question concerned the potential role of the entorhinal cortex in regulating how hippocampal subfield activity is differentially affected by novel or familiar objects.

3.2 Materials and Methods

3.2.1 Animals

Subjects were 42 male, Lister Hooded rats (Harlan). They were housed as described in general methods section 2.2. Rats were approximately 12 months old at the beginning of the c-*fos* imaging study. These animals had previously received either hippocampal lesions (n=22) or sham surgeries (n=20). They had been trained on a variety of geometric discriminations in a water maze, a spatial alternation task in a T-maze and a biconditional learning task in boxes (Albasser et al., 2013a).

3.2.2 Surgery

The rats were approximately three months old at the time of surgery. The surgeries were carried out by Dr. M. Horne. Twenty-two rats received bilateral hippocampal lesions, while 20 rats served as surgical controls. Anaesthesia was induced in all animals with a mixture of oxygen and isoflurane gas. They were then placed in a stereotaxic frame with the incisor bar set at -3.3mm to the horizontal plane. Analgesia in the form of 0.1mg/kg Metacam (Boehringer Ingelheim Vetmedica, Germany) was administered subcutaneously. To expose the skull, a midline sagittal incision was made in the scalp and the skin was retracted. A craniotomy was made above the injection sites and dura cut to expose cortex. The hippocampal lesions (n = 22) were made by injections of ibotenic acid (Biosearch Technologies, San Rafael, CA) diluted to 63mM in PBS (0.1M, pH 7.4). The ibotenic acid was administered via a 2µm Hamilton syringe (gauge 23, outside diameter 0.63 mm) connected to a microinjector (Kopf Instruments, Model 5000) set at a rate of 0.1µL/min and subsequent diffusion time of two minutes. The animals received 14 injections to each hemisphere (for co-ordinates and volumes see Table 3.1). The surgical control animals (n = 20) were treated in the same way until the dura was exposed. While nothing was infused into the brain, the dura was pierced 14 times per hemisphere with a 25-gauge Microlance needle (Becton Dickinson, Drogheda, Ireland).

Table 3.1. Stereotaxic coordinates and volume of ibotenic acid for lesions of the hippocampus.

Anteroposterior	Mediolateral	Dorsoventral	Volume (µL)
-5.4	±4.2	-3.9	0.10
-5.4	±5.0	-6.1	0.08
-5.4	±5.0	-5.3	0.08
-5.4	±5.0	-4.5	0.09
-4.7	±4.0	-7.2	0.10
-4.7	±4.0	-3.5	0.05
-4.7	±4.5	-6.5	0.05
-3.9	±2.2	-3.0	0.10
-3.9	±2.2	-1.8	0.10
-3.9	±3.5	-2.7	0.10
-3.1	±1.4	-3	0.10
-3.1	±1.4	-2.1	0.10
-3.1	±3.0	-2.7	0.10
-2.4	±1.0	-3.0	0.05

The coordinates are given as distance (mm) from bregma.

3.2.3 Apparatus

Testing took place in a bow-tie maze as described in the General Methods section (Figure 2.2).

3.2.4 Objects

A total of 147 different junk objects were used. Every object had an identical duplicate. These objects were then equally divided into seven sets of 21 pairs. All objects were large enough to cover a food well but light enough to be displaced by a rat. All objects were cleaned with alcohol wipes after each session.

3.2.5 Behavioural testing

3.2.5.1 Animal groups

The animals were divided between two behavioural conditions, creating four groups. The animals that received hippocampal lesions were assigned to either the Novel Object condition (n=11; HPC Novel) or the Familiar Object condition (n=11; HPC Familiar). Likewise, the surgical control or ‘sham’ animals were divided between the Novel Object

condition (n=10; Sham Novel) and the Familiar Object condition (n=10; Sham Familiar).

3.2.5.2 Pre-training

As described in general methods section 2.3.3.

3.2.5.3 Shared Protocol for session 1

Behavioural testing was carried out by Eman Amin. The initial session was identical for all four groups. A single 45mg sucrose pellet was placed in each food well, i.e., under every object. Session 1 consisted of 21 trials of 1 min each. At the start of the session the rat was placed on one side of the maze which contained a single object (object A; trial 0). The rat displaced the object to retrieve the single sucrose pellet (Figure 3.1). After 1 min the experimenter opened the door and the rat ran to the other side of the maze to begin trial 1, where an identical copy of the now familiar object A was presented along with a novel object (object B). The rat was allowed to freely explore these objects for 1 min. The door was again opened and the rat would run to the other side of the maze to begin trial 2, where a copy of the now familiar object (object B) and a novel object (object C) covered the two food wells (Figure 3.1). Trial 3 consisted of familiar object C and novel object D. This running recognition protocol was continued with pairs of objects (one novel, one familiar), covering the baited food wells, until 21 trials were completed. Placement of the novel object on the left or right was counterbalanced.

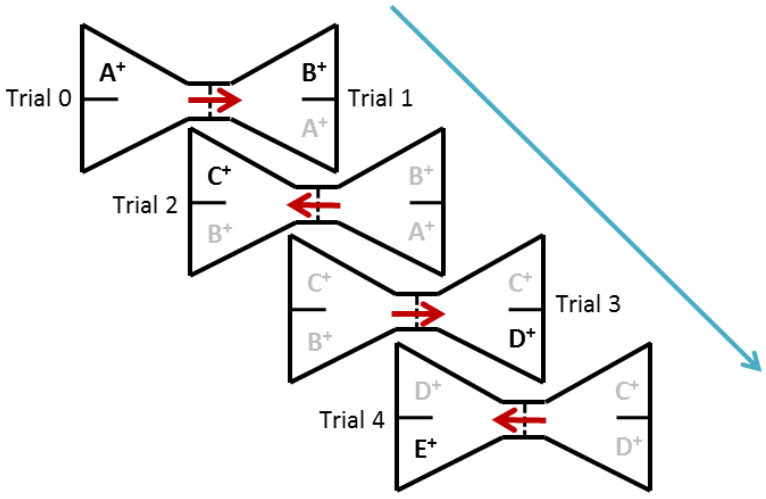

Figure 3.1. General procedure showing the order of presentation of objects.

All objects are rewarded (+). Red arrows show the directions of the rats' movements while blue arrow indicates progression through successive trials. Group Novel: black letters represents novel objects and grey letters the familiar objects.

3.2.5.4 Novel Object condition

Both the HPC Novel and Sham Novel groups received thirteen sessions that were run as described for Session 1 (Figure 3.1). Consequently, in each trial the animals were allowed to explore one novel object and one familiar object (familiar as its copy was seen in the preceding trial) as described above. All objects covered a single sucrose pellet. The first twelve training sessions were given over six consecutive days, i.e., two sessions per day. New sets of objects were used for each of the first six sessions and then used once again in Sessions 7-12. The object order and object pairings were not repeated. The final test session was on day seven. The protocol was exactly as described above, except that a novel set of twenty-one object pairs was used (Set 7). As before, each trial comprised one novel object and one object made familiar by its use on the previous trial.

3.2.5.5 Familiar Object condition

The test protocol for both familiar groups (HPC Familiar, Sham Familiar) remained the same as described for Session 1. In contrast to the Novel Object condition, the same twenty-one pairs of objects were used in all twelve training sessions, though in different orders. This same set of objects (Set 7) was then used again for the final test (Session 13). Consequently, the objects used in every session for the Familiar Object condition were the same (Set 7) as those used in just the final test session (Session 13) of the Novel Object condition. This comparison task was intended to match the sensorimotor demands of the Novel Object condition while reducing the impact of object novelty.

On completion of their respective test sessions the rats from both conditions were placed in a dark room for 90 minutes and then perfused as described in the General Methods section 2.4.

3.2.6 Analysis of behaviour

As described in general methods section 2.3.5.

3.2.7 Lesion analysis

As described in general methods section 2.6.

3.2.8 Immunohistochemistry

As described in general methods section 2.7.

3.2.9 Regions of interest

All of the regions of interest (ROI) sampled for c-*fos* analysis are depicted in Figure 3.2. The parahippocampal regions were mid and caudal levels of areas 35 and 36 in the perirhinal cortex (PRH; see Burwell, 2001); as well as area Te2, and lateral entorhinal cortex (LEC) adjacent to caudal PRH (from AP -4.80 to -5.52). Area Te2 was included as it is a key source of visual inputs to perirhinal cortex (Burwell & Amaral, 1998b; Agster & Burwell, 2009) and because of prior evidence of the importance of this area in the rat brain for visual recognition (Zhu et al., 1996; Wan et al., 1999; Ho et al., 2011). In the sham surgical groups only, additional Fos-positive cell counts were made in the septal hippocampus (dentate gyrus, CA1 and CA3; from AP -2.52 to -3.24; Strange et al., 2014). The septal hippocampus was chosen because projections from the region of LEC analysed here preferentially terminate in septal hippocampus (Ruth et al., 1988; Dolorfo & Amaral, 1998), consistent with the finding that subfields in this part of the hippocampus can be integrated into parahippocampal IEG activity models with good fit (Albasser et al., 2010b).

Reflecting the different patterns of inputs from the cortical layers of the lateral entorhinal cortex to the various hippocampal subfields, separate counts were made in layers II, III and V+VI (combined) of the entorhinal cortex. These distinctions follow the finding that neurons in LEC layer II project to the dentate gyrus and CA3 while neurons in LEC layer III project to CA1 (Steward & Scoville, 1976; Amaral, 1993; Insausti et al., 1997). There is, however, some inconsistency in the literature regarding the division between layers II and III of the LEC. Some describe layer II as comprising a cell dense superficial IIa and a deeper, slightly less dense IIb (Swanson, 1992). Others describe layer IIb as being the superficial component of layer III (Insausti et al., 1997; Dolorfo & Amaral 1998). The latter definition is used in the present study as this most closely matches the sources of the contrasting inputs to the different hippocampal subfields (Ohara et al., 2013).

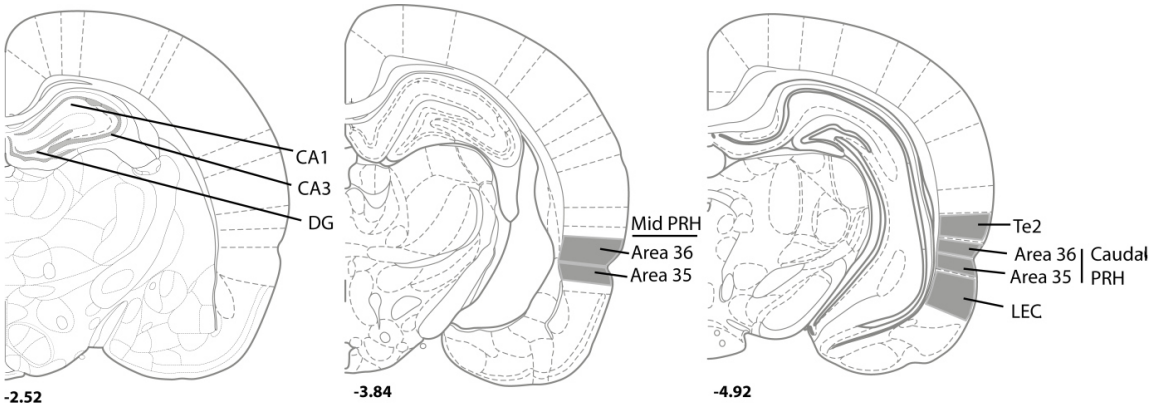

Figure 3.2. Regions of Interest.

Coronal sections depicting regions of interest: CA1, CA3 and dentate gyrus (DG) from the septal hippocampus, areas 35 and 36 for the mid and caudal perirhinal cortex, area Te2 and lateral entorhinal cortex (LEC). The numbers below refer to the approximate distance in mm from bregma. Adapted from the atlas of Paxinos & Watson (2005).

3.2.10 Image capture and analysis of c-Fos activation

As described in general methods section 2.8.

3.2.11 Statistical analysis

3.2.11.1 Behavioural data

Behavioural data ware analysed using an ANOVA with two between-subjects factors [surgical group (Sham, Hippocampal lesion) and behavioural condition (Novel Object, Familiar Object)]. Separate analyses examined cumulative D1, updated D2 and total cumulative exploration scores for the final test session as the measures are not independent. One-tailed, two-sample t-tests were calculated for the cumulative D1 and updated D2 scores after the final test trial of the test session to determine if discrimination performance was significantly above chance level (zero) for each group.

3.2.11.2 Fos data

To analyse group differences (Sham vs. Lesion; Familiar Objects vs. Novel Objects) in the numbers of c-*fos* activated cells in the parahippocampal cortices, a two between-subjects factor (Lesion type and Familiar/Novel objects) and one within-subject factor (Region of Interest) ANOVA was calculated. This analysis was carried out separately for three regional groupings: i) divisions within perirhinal cortex, ii) areas Te2 and LEC, and iii) the various cortical layers of the LEC. The Fos counts in the various hippocampal subfields (sham groups only) were compared using a one between (Familiar/Novel objects) by one within-subject (ROI) ANOVA.

Pearson product-moment correlation coefficients were calculated for the Fos-positive cell counts in the various parahippocampal sites, as well as with the D2 discrimination ratio. The D2 index was preferred as it better compensates for individual differences in overall levels of object exploration. The levels of the correlations obtained between perirhinal cortex and D2 for each of the behavioural groups were also compared between the groups using Fisher's *r*-to-*z* transformation (Zar, 2010).

3.2.12 Structural equation modelling

As described in general methods section 2.10.

3.3 Results

3.3.1 Lesion analysis

Three animals were eliminated from analysis due to inadequate lesion size; two from group HPC Novel and one from group HPC Familiar. A further animal was removed from group HPC Familiar due to extensive cortical damage. Thus, final group numbers were as follows: HPC Familiar, n = 9; HPC Novel, n = 9; Sham Familiar, n = 10; Sham Novel, n = 10.

Figure 3.3 illustrates the cases with the largest and smallest hippocampal lesions in the HPC Familiar and HPC Novel groups. Assessments of total damage to the hippocampus (excluding the subiculum) ranged from 35% to 79% in the HPC Familiar group (median = 61%) and from 29% to 73% in the HPC Novel group (median =50%). It should be noted that these percentages underestimate the amount of actual tissue loss as they are based on coronal sections and so do not take into account the additional degree of hippocampal shrinkage in the anterior-posterior plane, which was clearly evident in all cases. The overall percentage of damage to septal, intermediate, and temporal hippocampus did not distinguish the two groups ($F_{1,16} = 2.75$, $p = 0.12$), although there was proportionately more tissue loss in the septal than temporal hippocampus across both groups ($F_{2,32} = 8.65$, $p = 0.001$). The group by region interaction was close to significant ($F_{2,32} = 3.21$, $p = 0.054$) as there was a tendency for the HPC Familiar group to suffer more tissue loss in the intermediate hippocampus.

The only region to exhibit any consistent sparing in both groups was the most medial region of the septal dentate gyrus. In some cases this sparing extended laterally to encompass the most medial regions of septal CA1 and CA3. There were also typically

small amounts of sparing of dentate gyrus, CA1, and CA3 at the temporal pole of the hippocampus.

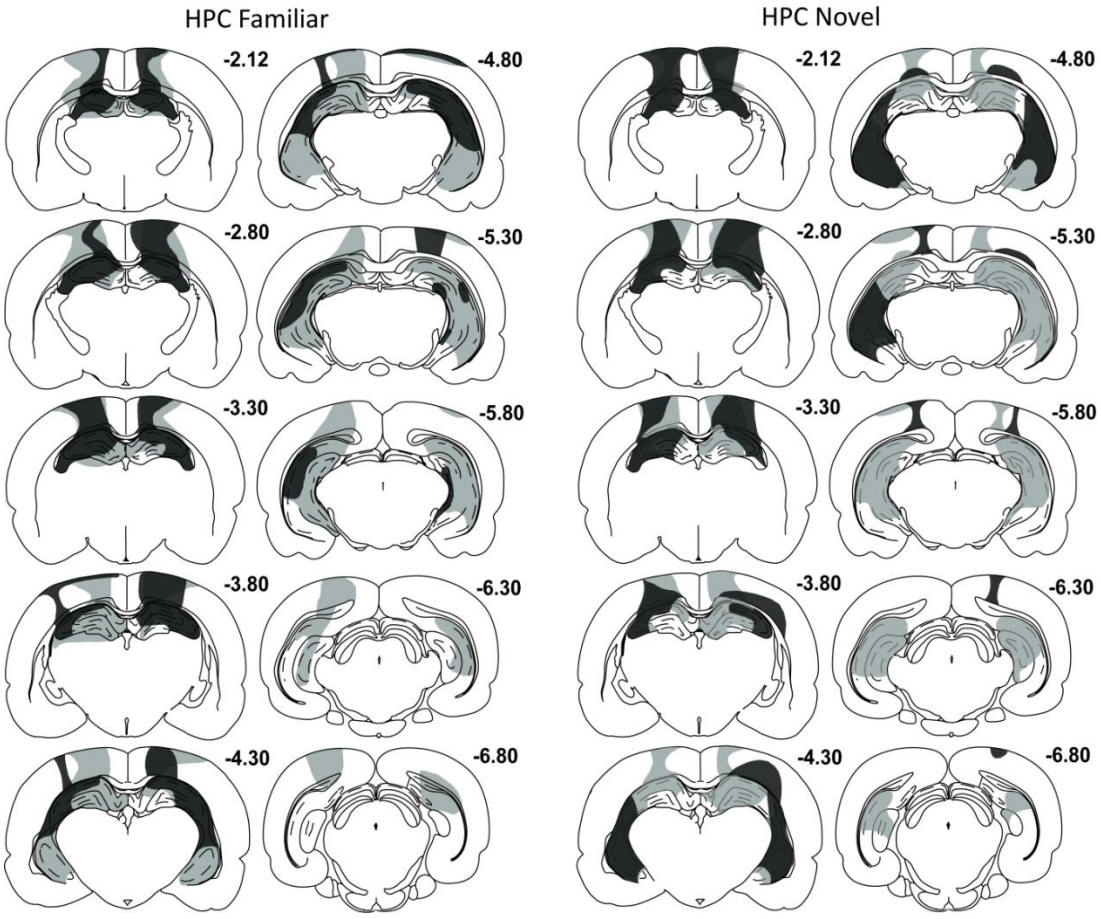

Figure 3.3. Hippocampal lesion reconstructions.

Diagrammatic reconstructions of the hippocampal lesions showing the individual cases with the largest (grey) and smallest (black) lesions for group HPC Familiar (left; n=9) and group HPC Novel (right; n=9). The numbers refer to the distance (in millimetres) from bregma (adapted from Paxinos & Watson, 2005).

In six of the HPC Novel group, tissue damage extended ventrally to cause very small amounts of thalamic damage. In two cases there was partial bilateral damage to the laterodorsal nucleus (LD), three cases suffered unilateral damage to the lateral posterior nucleus, and the final case sustained unilateral damage to both LD and the lateral posterior nucleus, but in contralateral hemispheres. In five of the HPC Familiar group cases there was a very small amount of dorsal thalamic damage; one showed unilateral LD damage, three sustained bilateral LD damage and the last case had bilateral damage to LD accompanied by unilateral anteroventral nucleus damage. All rats displayed some cell loss and thinning in cortical regions overlying the hippocampus (Figure 3.3). This

cortical involvement varied and sometimes included motor cortex, primary somatosensory area and the parietal region of posterior association cortex, and dysgranular retrosplenial cortex.

3.3.2 Behavioural testing

Analysis of the cumulative recognition scores from the final session (Figure 3.4) showed the expected higher D1 discrimination indices for the Novel Object conditions than for the Familiar Object conditions ($F_{1,34} = 5.13$, $p = 0.03$) irrespective of lesion status. There was no effect of the hippocampal lesions on these discrimination scores across the two conditions ($F < 1$) and no lesion by object type interaction ($F < 1$). All four groups performed above chance based on their cumulative D1 scores (HPC Familiar: $t_8 = 4.63$, $p = 0.002$; HPC Novel: $t_8 = 8.71$, $p \leq 0.001$; Sham Familiar: $t_9 = 3.82$, $p = 0.004$; Sham Novel: $t_9 = 7.47$ $p \leq 0.001$; Figure 3.4), showing that the rats could not only distinguish novel from familiar (Novel Object condition) but could also distinguish between an object from the previous trial and one from all previous days (Familiar Object condition).

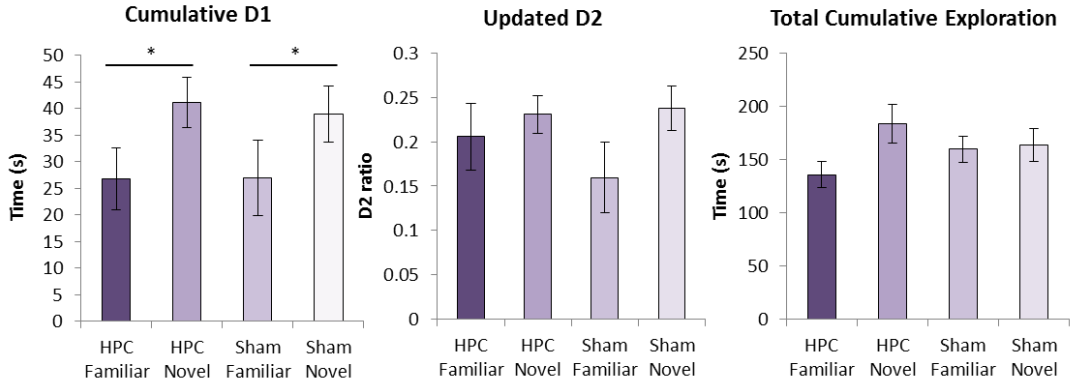

Figure 3.4. Behavioural measures from the final session of the object recognition test.

The graphs depict group performance as measured by: the cumulative D1 recognition index (left panel), the updated D2 ratio (middle panel), and cumulative exploration time for all objects (right panel). For D1 and D2, a score of zero indicates a failure to discriminate. All D1 and D2 scores are significantly above zero (one-sample t tests, all $p < 0.01$). * $p < 0.05$ Novel Objects compared to Familiar Objects. Data are presented as means ±SEM.

Analyses based on the D2 index provided a similar pattern (Figure 3.4) except that the discrimination scores failed to differ significantly between the Novel and Familiar conditions ($F_{1,34} = 3.01$, $p = 0.09$). As with D1, there was no evidence of a hippocampal lesion effect ($F < 1$), nor was there a lesion by condition interaction ($F < 1$). Once again,

all four groups performed above chance in this final session (HPC Familiar: $t_8 = 5.50$, $p \leq 0.001$; HPC Novel: $t_8 = 10.9$, $p \leq 0.001$; Sham Familiar: $t_9 = 4.03$, $p = 0.003$; Sham Novel: $t_9 = 9.59$ $p \leq 0.001$; Figure 3.4).

Total levels of object exploration in the final session were also calculated (Cumulative Exploration, Figure 3.4). This measure was not affected by lesion ($F < 1$) or test condition ($F_{1,34} = 3.09$, $p = 0.088$), nor was there an interaction between these factors ($F_{1,34} = 2.18$, $p = 0.15$). Finally, correlation coefficients were calculated to assess if there was an association between lesion size at three levels of the hippocampus (septal, intermediate and temporal) and either of the discrimination measures (D1 and D2). No significant correlations were found (all $p > 0.1$) nor was there any indication that animals with smaller lesions discriminated better in either the Novel or Familiar conditions.

3.3.3 Fos-positive cell counts

3.3.3.1 Correlations with recognition performance (D2)

The D2 recognition index correlated significantly with the Fos cell counts summed across the perirhinal cortex (areas 35 and 36 combined) for both the HPC Novel ($r = -0.70$, $p = 0.037$) and the HPC Familiar ($r = -0.81$, $p = 0.008$) groups (Table 3.2). In both cases the correlation was negative. The corresponding correlations for the remaining groups (Sham Novel: $r = -0.46$, $p = 0.18$; Sham Familiar: $r = -0.30$, $p = 0.39$) were not significant. Furthermore, comparisons made between these correlation levels were not significant, i.e., all $p > 0.05$. When mid and caudal areas 35 and 36 were considered separately, all four subareas had a significant negative correlation with D2 in group HPC Familiar (all $p < 0.05$), as did mid area 35 in group HPC Novel ($r = -0.74$, $p = 0.021$). No other ROI in the four groups showed a significant correlation between D2 and Fos-positive cell counts, nor did the D1 discrimination measure correlate significantly with any ROI.

Table 3.2. Correlations of perirhinal activity with discrmination score.

Group:		HPC Familiar	HPC Novel	Sham Familiar	Sham Novel
Combined PRH Fos	r-value	-.813**	-.696*	-0.304	-0.457
	p-value	0.008	0.037	0.393	0.184

Correlations between the Fos-positive cell counts from across all analysed perirhinal (PRH) sub-regions with the discrimination performance (updated D2) for each group. The r-values are Pearson coefficients. * $p < 0.05$, ** $p < 0.01$, for two-tailed correlations.

3.3.3.2 Perirhinal cortex – comparison of Fos counts

Comparisons across the four perirhinal sites (mid and caudal, areas 35 and 36) found no overall effect of hippocampal lesions ($F < 1$) on Fos positive cell counts (Figures 3.5, 3.6A). A hippocampal lesion effect was found, however, in the interaction with separate counts in the four areas (lesion by area $F_{3,102} = 5.29$, $p = 0.002$). Simple effects analysis showed that this interaction largely arose from the Familiar Object condition as mid perirhinal areas often contained higher Fos counts in the Sham group than the corresponding HPC group, but this difference disappeared in the caudal perirhinal cortex (Figure 3.6A). There was, in addition, an overall effect of ROI ($F_{3,102} = 27.1$, $p < 0.001$), reflecting the consistently lower levels of Fos expression in more caudal perirhinal cortex (Figure 3.6A). There was no overall effect of behavioural condition (Novel vs. Familiar Objects, $F < 1$), i.e., the Fos counts were not higher in the Novel Object groups. Likewise, there were no significant interactions with the two behavioural conditions.

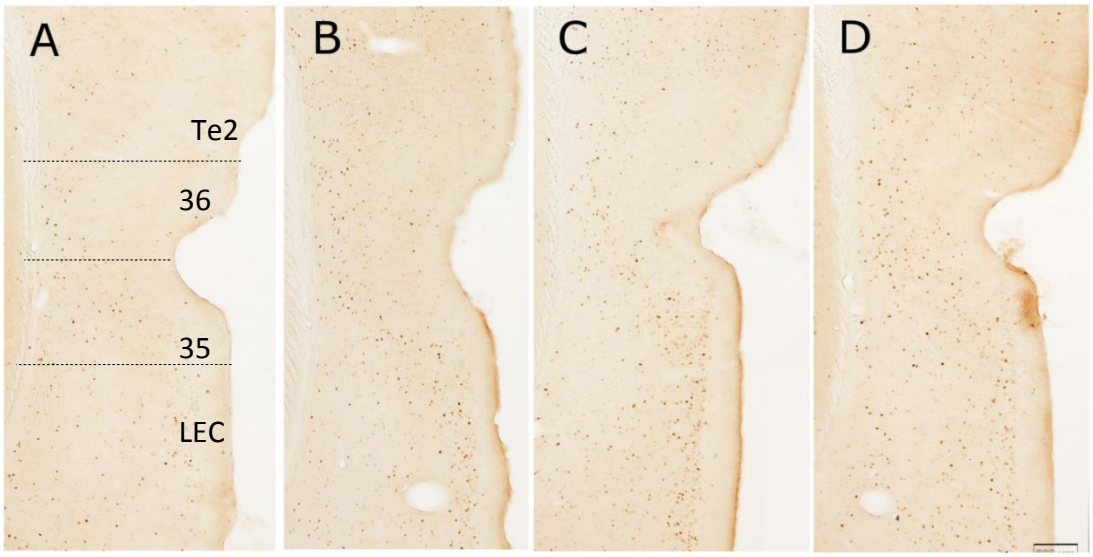

Figure 3.5. Representative photomicrographs of parahippocampal cortex.

These sections depict Fos positive cells in cortical area Te2, caudal PRH composite areas 35 and 36 and lateral entorhinal cortex (LEC) for groups HPC Familiar (A), HPC Novel (B), Sham Familiar (C) and Sham Novel (D). Scale bar: 200µm.

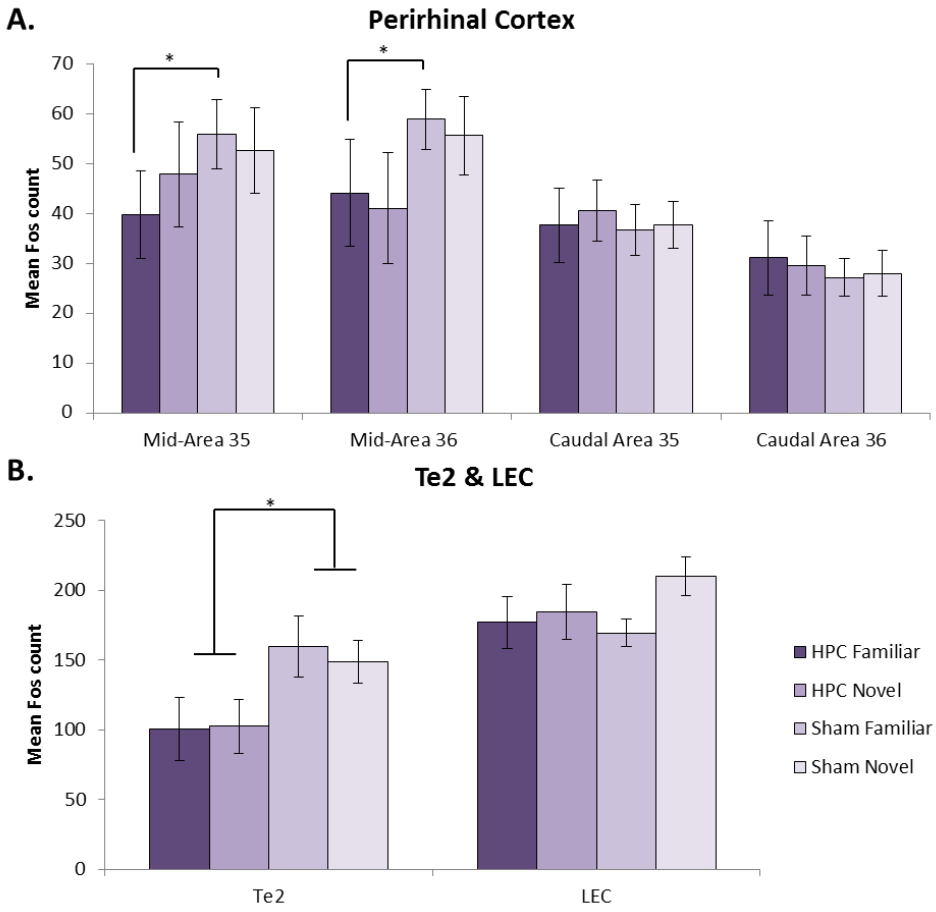

Figure 3.6. Parahippocampal Fos expression.

(A) Graph depicting mean counts of perirhinal Fos-positive cells in all four groups in areas 35 and 36 at mid- and caudal levels. (B) Graph depicting mean counts of Fos-positive cells in cortical areas adjacent to perirhinal cortex; area Te2 and lateral entorhinal cortex (LEC). * p <0.05 compared to appropriate sham condition. Data are presented as means ±SEM

3.3.3.3 Area Te2 and lateral entorhinal cortex – comparison of Fos counts

There was an overall effect of hippocampal surgery ($F_{1,34}$ = 4.32, p = 0.045) as the rats with lesions had lower Fos counts (Figures 3.5, 3.6B). The surgical group by area interaction ($F_{1,34}$ = 4.82, p = 0.035) reflected how this reduction in Fos counts after hippocampal surgery was essentially confined to area Te2 (Figure 3.6B). This Te2 reduction was only significant for the Familiar condition (simple effects $F_{1,34}$ = 5.60, p = 0.024). There was no overall difference in the Fos counts for the Novel and Familiar Object groups (F < 1) and no interaction with this factor.

Analysis of the cortical layers of LEC revealed no significant lesion effect (F < 1) or effect of behavioural condition ($F_{1,34}$ = 2.57, p = 0.12) on the numbers of Fos positive cells in layers II, III or V+VI (Figure 3.7). There was also no interaction between these factors ($F_{1,34}$ = 1.07, p = 0.31).

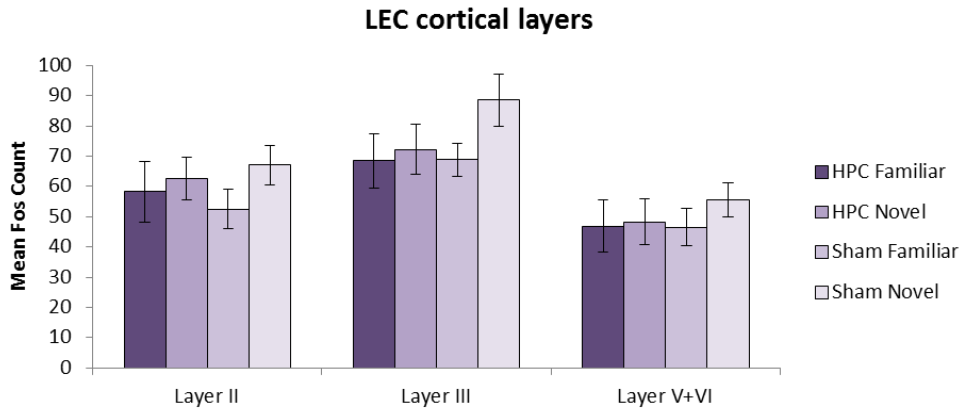

Figure 3.7. Lateral entorhinal cortex: laminar Fos expression.

Graph depicts mean counts of Fos-positive cells in all four groups in cortical layer II, III and V + VI combined. Data are presented as means ±SEM

3.3.3.4 Hippocampal subfields – comparison of Fos counts in Sham groups

No significant group differences (Novel vs. Familiar Objects) were found in the Fos counts from the septal hippocampus (dentate gyrus, CA3 and CA1, $F<1$, Figure 3.8). There was also no evidence of a group by subfield interaction ($F_{1,21} = 1.07$, $p = 0.36$).

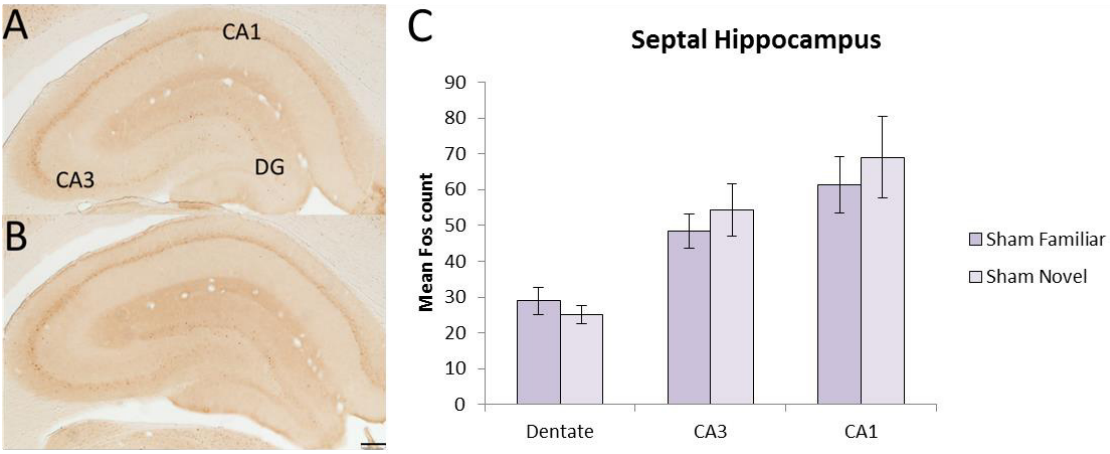

Figure 3.8. Hippocampal Fos expression.

Representative micrographs from coronal sections depict Fos positive cells in dentate gyrus (DG), CA3 and CA1 at the septal level of the hippocampus for groups Sham Familiar (A), Sham Novel (B). Scale bar: 200µm. (C) Graph depicts counts of Fos-positive cells for the two sham groups divided by subfield. Data are presented as means ±SEM

3.3.4 Structural equation modelling

The models were calculated using the correlations between the Fos counts found in the different medial temporal sites for the two groups with hippocampal lesions (Table 3.3) and the two groups with sham surgeries (Table 3.4). These tables of correlations present probability levels that are not corrected for multiple comparisons as the individual

correlations are of limited significance. More importantly, these same correlations provide the source data for the structural equation modelling, in which the fit of the overall model helps to compensate for Type 1 errors in the individual correlations that comprise the model. Because of this same concern, it is important that any model must conform to established patterns of connectivity between the regions of interest, i.e., the number of potential models is constrained.

Table 3.3. Inter-region correlations of Fos-positive cell counts in the two hippocampal lesion groups.

HPC Novel										
		Te2	Mid Area35	Mid Area36	Caudal Area35	Caudal Area36	Whole LEC	LEC Layer II	LEC Layer III	LEC Layers V+VI
Te2	r-value		.636	.607	**0.707***	**0.684***	**0.698***	.019	**.818****	**.937*****
	p-value		.066	.083	**.033**	**.042**	**.036**	.960	**.007**	**<0.001**
Mid Area35	r-value	**0.818****		**0.923*****	**0.824****	**0.669***	.659	.214	.638	**.816****
	p-value	**.007**		**<0.001**	**.006**	**.049**	.054	.580	.065	**.007**
Mid Area36	r-value	.661	**0.963*****		**0.848****	**0.785***	.461	-.012	.482	**.731***
	p-value	.052	**<0.001**		**.004**	**.012**	.212	.975	.189	**.025**
Caudal Area 35	r-value	**0.758***	**0.943*****	**0.949*****		**0.930*****	.627	.191	.639	**.766***
	p-value	**.018**	**<0.001**	**<0.001**		**<0.001**	.071	.623	.064	**.016**
Caudal Area 36	r-value	**0.774***	**0.886****	**0.882****	**0.972*****		.477	.072	.521	**.671***
	p-value	**.014**	**.001**	**.002**	**<0.001**		.194	.853	.150	**.048**
Whole LEC	r-value	.533	.338	.264	.289	.446				
	p-value	.140	.373	.492	.451	.229				
LEC Layer II	r-value	.023	-.326	-.394	-.336	-.129			.550	.233
	p-value	.953	.391	.294	.377	.740			.125	.546
LEC Layer III	r-value	.540	.279	.184	.252	.421		**.709***		**.910****
	p-value	.134	.468	.636	.514	.260		**.032**		**.001**
LEC Layers	r-value	**.739***	**.788***	**.706***	**.761***	**.786***		-.010	.497	
	p-value	**.023**	**.012**	**.033**	**.017**	**.012**		.980	.173	
HPC Familiar										

The top right diagonal matrix (darker grey) relates to data from HPC Novel object group while the bottom left diagonal matrix (lighter grey) relates to data from HPC Familiar object group. The *r*-values are Pearson coefficients. Significant correlations are in bold. * $p < 0.05$, ** $p < 0.01$, *** $p < 0.001$, for two-tailed correlations (uncorrected for multiple comparisons – see main text). Sites included: area Te2, area 35 and area 36 of the perirhinal cortex, and lateral entorhinal cortex (LEC; both as a whole and divided into cortical layers II, III and V+VI).

Table 3.4. Inter-region correlations of Fos-positive cell counts in the two sham lesion groups.

		Sham Novel											
		Te2	Mid Area35	Mid Area36	Caudal Area35	Caudal Area36	Whole LEC	LEC Layer II	LEC Layer III	LEC Layer V+VI	DG	CA3	CA1
Te2	r-value		.617	**0.822****	.358	.600	-.079	-.529	-.108	**.662***	.121	**.639***	.598
	p-value		.058	**.004**	.310	.067	.827	.116	.767	**.037**	.739	**.046**	.068
Mid Area35	r-value	.306		**0.687***	**0.756***	.392	.476	-.266	.449	**.884****	.545	**0.748***	.619
	p-value	.390		**.028**	**.011**	.263	.165	.457	.193	**.001**	.104	**.013**	.056
Mid Area36	r-value	.013	**0.77****		.589	**0.82****	-.061	**-.677***	-.054	**.757***	.338	**0.761***	**0.775****
	p-value	.972	**.009**		.073	**.004**	.867	**.032**	.883	**.011**	.340	**.011**	**.008**
Caudal Area 35	r-value	.587	**0.686***	.384		**0.641***	.334	-.416	.360	**.775****	**0.661***	**0.801****	**0.767****
	p-value	.074	**.029**	.274		**.046**	.346	.232	.307	**.008**	**.037**	**.005**	**.010**
Caudal Area 36	r-value	.618	.564	.438	**0.917*****		-.231	**-.723***	-.167	.551	.122	.571	**0.669***
	p-value	.057	.090	.205	**<0.001**		.521	**.018**	.644	.099	.737	.084	**.034**
Whole LEC	r-value	.270	.142	-.117	-.064	-.072					.411	.214	.145
	p-value	.451	.696	.747	.861	.843					.238	.553	.689
LEC Layer II	r-value	-.342	**-.720***	-.621	**-.740***	**-.742***			.551	-.591	-.197	-.465	-.486
	p-value	.334	**.019**	.055	**.015**	**.014**			.099	.072	.585	.175	.155
LEC Layer III	r-value	.280	.216	-.154	-.057	-.111		.222		.228	.387	.181	.115
	p-value	.433	.548	.672	.875	.760		.537		.526	.270	.617	.751
LEC Layers	r-value	.570	**.782****	.539	**.689***	**.714***		**-.683***	.443		.578	**.782****	**.706***
	p-value	.086	**.007**	.108	**.027**	**.020**		**.029**	.200		.080	**.008**	**.023**
DG	r-value	.242	.237	.401	.027	.032	-.132	-.255	-.081	.083		**0.789****	**0.713***
	p-value	.501	.510	.251	.941	.929	.716	.476	.823	.820		**.007**	**.021**
CA3	r-value	.553	.509	.531	.360	.371	.291	-.347	.272	.536	**0.769****		**0.957*****
	p-value	.097	.133	.115	.307	.291	.414	.326	.446	.110	**.009**		**<0.001**
CA1	r-value	.297	.468	**0.636***	.298	.343	.306	-.288	.178	.524	**0.664***	**0.901*****	
	p-value	.405	.173	**.048**	.402	.332	.390	.420	.623	.120	**.036**	**<0.001**	
		Sham Familiar											

The top right diagonal matrix (darker grey) displays data from the Sham Novel object group while the bottom left diagonal matrix (lighter grey) displays data from the Sham Familiar object group. The r-values are the Pearson coefficients. Significant correlations are in bold. * $p < 0.05$, ** $p < 0.01$, *** $p < 0.001$, for two-tailed correlations (uncorrected for multiple comparisons – see main text). Sites included: area Te2, area 35 and area 36 of the perirhinal cortex, lateral entorhinal cortex (LEC; both as a whole and divided into cortical layers II, III and V+VI), and hippocampal subfields CA1, CA3 and dentate gyrus (DG).

3.3.4.1 Parahippocampal models

Separate models with acceptable fit could be derived from all four groups (Figure 3.9). It was striking that the same structural model was optimal for all four groups, whether the hippocampus was intact or not, and whether the rats explored novel or familiar objects. The only difference concerned the strengths of particular path coefficients. Starting from area Te2, two pathways ran in parallel to area 35; one pathway via area 36 and the other via the lateral entorhinal cortex (HPC Familiar: $\chi^2_2 = 1.3$, $p = 0.51$; CFI = 1.0; RMSEA = 0.0; HPC Novel: $\chi^2_2 = 0.04$, $p = 0.98$; CFI = 1.0; RMSEA = 0.0; Sham Familiar: $\chi^2_2 = 1.0$, $p = 0.61$; CFI = 1.0; RMSEA = 0.0; Sham Novel: $\chi^2_2 = 0.60$, $p = 0.73$; CFI = 1.0; RMSEA = 0.0; Figure 3.9). In all four groups, the link from area 36 to area 35 had significant path coefficients.

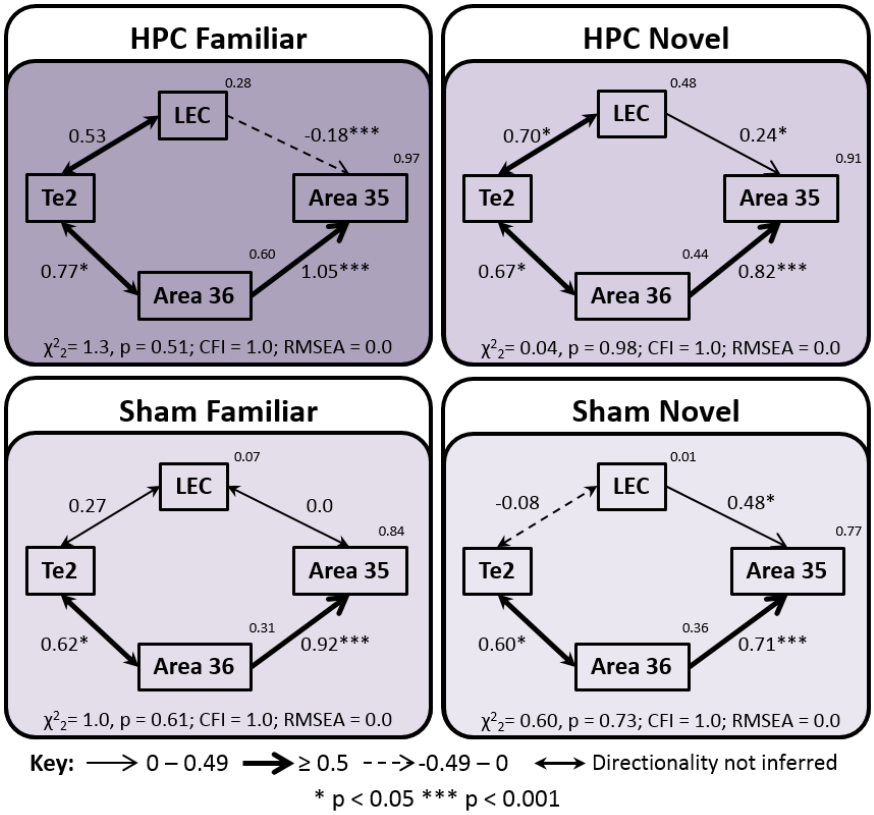

Figure 3.9. Parahippocampal models for all groups separately.

The four models show the optimal parahippocampal interactions derived from structural equation modelling for all groups separately; HPC Familiar (top left), HPC Novel (top right), Sham Familiar (bottom left) and Sham Novel (bottom right). The fit is noted beside each model (CFI, comparative fit index; RMSEA, root mean square error of approximation). The strength of the causal influence of each path is denoted both by the thickness of the arrow and by the path coefficient next to that path. The number above each region is the proportion of its variance that can be explained by its inputs. Sites depicted: area Te2, area 35 and area 36 of the perirhinal cortex, and lateral entorhinal cortex (LEC). * $p < 0.05$; *** $p < 0.001$.

When the data from all four groups were combined, the same optimal model emerged but with even higher levels of fit (χ^2_2= 0.2, p = 0.93; CFI = 1.0; RMSEA = 0.0; Figure 3.10). This model, for each group individually, as well as incorporating all four groups was also tested with the path directions reversed. This modification generated poorer fitting models when paths from area 36 to area 35 and LEC to area 35 were reversed whereas in the case of the paths between Te2 and area 36 and Te2 and LEC path direction did not affect model fit.

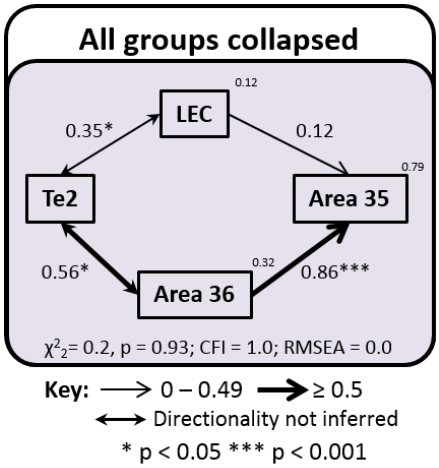

Figure 3.10. Parahippocampal model for all groups collapsed.

Optimal parahippocampal for all groups collapsed into a single data set. Model fit is noted beside the model (CFI, comparative fit index; RMSEA, root mean square error of approximation). The strength of the causal influence of each path is denoted both by the thickness of the arrow and by the number next to that path. The number above each region is the proportion of its variance that can be explained by its inputs. Sites depicted: area Te2, area 35 and area 36 of the perirhinal cortex and lateral entorhinal cortex (LEC). * $p < 0.05$; *** $p < 0.001$.

Although the data from all four groups fit the same model, the path strengths between the cortical regions differ (Figure 3.9). The four groups were, therefore, stacked on the same model in order to compare these differing path strengths. The structural weights of each of the paths were constrained such that they had to have the same value in all of the groups, i.e., setting the models for each of the groups to be identical. This procedure produced a model of poorer fit than the model in which the structural weights of all paths were free to vary between the groups ($\chi^2_{12\ Diff} = 24.5$, $p = 0.018$), indicating at least one of the paths differed between the groups. In order to find this path, the structural weights of each path were unconstrained individually. The group difference lay in the path from lateral entorhinal cortex to area 35 as it was only when this path was unconstrained, in isolation, that there was a significant increase in model fit when compared to the completely constrained model ($\chi^2_{3\ Diff} = 11.9$, $p = 0.009$).

Examination of Figure 3.9 suggests that this significant difference within the same model structure reflects the lower path coefficients for lateral entorhinal to area 35 in the two Familiar Object groups. This difference was tested formally in a series of stacking procedures. These procedures confirmed that Novel Object versus Familiar Object comparison, rather than Sham lesion versus Hippocampus lesion, was associated with the change in path coefficients. This analysis initially involved collapsing and stacking the groups across the two between-subjects' factors, lesion type and object type.

Figure 3.11 upper panels illustrate the separate model fits when the groups were collapsed within each lesion type (Sham or Hippocampal lesions), i.e., ignoring the behavioural condition. Both the 'hippocampal' and 'sham' models were well-fitting, and when the two groups were stacked on the same model in which all path coefficients were free to vary, the fit was not significantly better than the completely constrained model ($\chi^2_{4\ Diff} = 9.06$, $p = 0.06$) nor was the model improved by allowing the path from lateral entorhinal cortex to area 35 to vary between groups ($\chi^2_{1\ Diff} = 2.11$, $p = 0.15$). Thus, it can be concluded that the group difference found in the path coefficients for this pathway between LEC and area 35 is not driven by hippocampal damage. It should be noted that if the path between Te2 and the lateral entorhinal cortex is unconstrained the model fit is improved by a small but significant amount ($\chi^2_{1\ Diff} = 4.53$, $p = 0.03$).

Finally, the groups were collapsed within the Novel Object or Familiar Object conditions (Figure 3.11 Lower), i.e., ignoring the surgical condition. Once again, both models had good fit. Allowing all the path coefficients to differ between groups significantly improved fit over the completely constrained model ($\chi^2_{4\ Diff} = 11.86$, $p = 0.018$), indicating that there is a network difference between the animals exploring novel objects and those that explored familiar ones. Again, paths were unconstrained individually and this network difference was found in the path coefficients between lateral entorhinal cortex and area 35 ($\chi^2_{1\ Diff} = 7.11$, $p = 0.007$), which was positive and significant for the Novel Object conditions but negative and non-significant for the Familiar Object conditions (Figure 3.11 Lower). In order to ensure this effect was not due to an interaction between lesion type and object type, the groups HPC Novel and Sham Novel (Figure 3.9; top right and bottom right respectively) were also stacked but no significant differences were found ($\chi^2_{4\ Diff} = 5.29$, $p = 0.30$). Similarly, the groups HPC Familiar and Sham Familiar (Figure 3.9; top left and bottom left respectively) were stacked and again there were no differences between these groups on the model ($\chi^2_{4\ Diff} = 5.61$, $p = 0.23$). Thus, it can be concluded that the difference in this path strength reflects the exploration of different object types (Novel or Familiar Objects).

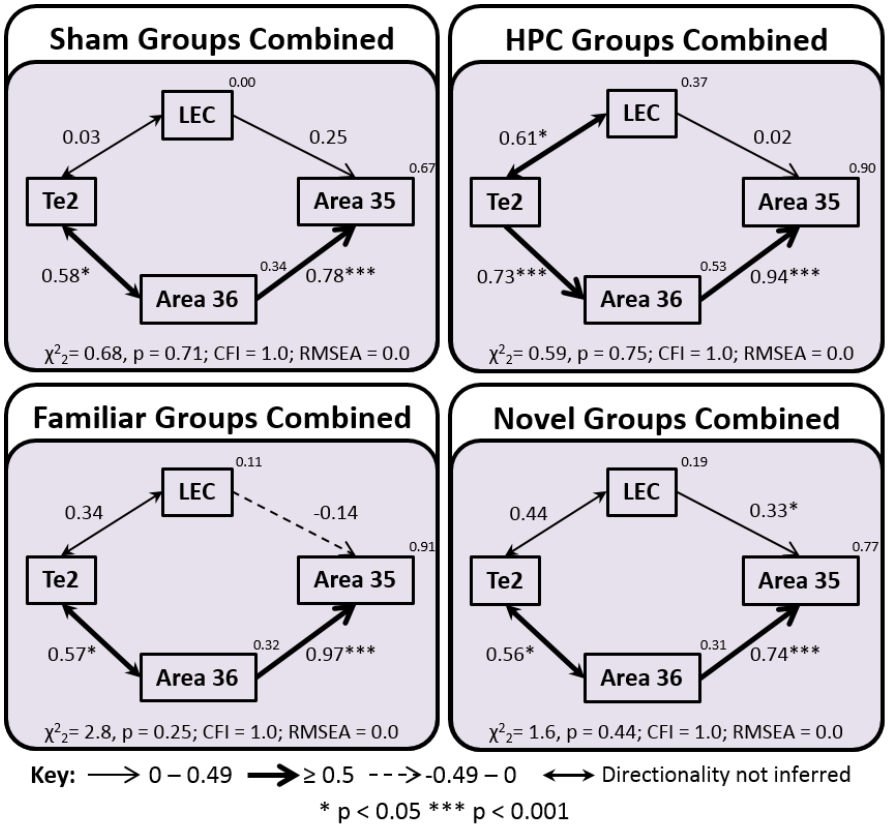

Figure 3.11. Parahippocampal models when the groups are combined.

The groups were combined according to their surgical status (Upper panels) and by their behaviour status (Lower panels). The upper panels depict the optimal parahippocampal interactions derived from structural equation modelling for both sham surgical groups (upper left) and both hippocampal lesion groups (upper right), i.e., irrespective of behaviour. The lower panels depict the optimal parahippocampal interactions for groups combined according to their behavioural condition (both familiar groups, lower left; both novel groups, lower right), i.e., irrespective of surgery. Model fit is noted beside each model (CFI, comparative fit index; RMSEA, root mean square error of approximation). The strength of the causal influence of each path is denoted both by the thickness of the arrow and by the path coefficient next to that path. The number above each region is the proportion of its variance that can be explained by its inputs. Sites depicted: area Te2, area 35 and area 36 of the perirhinal cortex and lateral entorhinal cortex (LEC). * $p < 0.05$; *** $p < 0.001$.

3.3.4.2 Hippocampal-Parahippocampal models (Sham animals only)

Network models that included the septal hippocampal subfields were calculated for the Sham Familiar and Sham Novel groups. The septal hippocampus was selected as previous research has found that this hippocampal region gives the best fitting models for Fos expression associated with recognition memory (Albasser et al., 2010b). Due to the addition of more regions to the models, areas 35 and 36 were collapsed to a single region (PRH) in order to retain sufficient degrees of freedom for parameters to be estimated.

The optimal models for groups Sham Familiar and Sham Novel are depicted in Figure 3.12A and D respectively. Once again, differences between the Familiar and Novel conditions appear. The optimal model for group Sham Familiar involved a path between Te2 and lateral entorhinal cortex and another path from Te2, via perirhinal cortex, to lateral entorhinal cortex, which in turn projects directly to the CA1 subfield. The resulting model had good fit (χ^2_2 = 1.3, p = 0.52; CFI = 1.0; RMSEA = 0.0; Figure 3.12A) although only the path from Te2 to PRH was significant. For group Sham Novel the best fit was provided by a simple linear model that began with a path between the perirhinal cortex and lateral entorhinal cortex, and from there onto dentate gyrus, then to CA3 and, thence, to CA1 (Figure 3.12D). The fit for this model was, however, relatively poor (χ^2_6 = 11.1, p = 0.085; CFI = 0.84; RMSEA = 0.31).

The models for the Novel and Familiar conditions that incorporated the hippocampus were recalculated with additional correlation data (Figure 3.12B, E). This was possible because the two sham groups from the present study were a direct replication of a study from the same laboratory using identical protocols and apparatus (Albasser et al., 2010b). While the fine details of the Familiar and Novel network models derived by Albasser et al. (2010b) differ slightly from those in the present study within the parahippocampal cortices (although all involve Te2, caudal PRH and LEC), the patterns of projections to the hippocampus bear a striking resemblance. The correlational c-*fos* data from Albasser et al. (2010b) were accordingly added to the present data to derive models with greater power (Figure 3.12B, E).

The optimal Familiar condition model for the combined data sets remained the same as that derived for group Sham Familiar in the present study (Figure 3.12B). This model not only retained its high fit (χ^2_2 = 0.6, p = 0.75; CFI = 1.0; RMSEA = 0.0) but all path coefficients gained significance. The optimal Novel condition model for the combined data sets (Figure 3.12E) was, however, different to that described for just group Sham

Novel (which did not have high fit, see Figure 3.12D). Now the fit for the combined model was good (χ^2_5 = 7.4, p = 0.19; CFI = 0.97; RMSEA = 0.16) and all of the path coefficients gained significance (Figure 3.12E). While the parahippocampal components of the Combined Novel and Combined Familiar groups appear very similar (Figure 3.12B, E), obvious differences occur in the pathways from the lateral entorhinal cortex. For novel stimuli, the lateral entorhinal cortex projects first to CA3 and then to CA1 in the best fitting model. For familiar stimuli, the pathway from the lateral entorhinal cortex leads just to CA1 in the best fitting model.

Layer II of the LEC is known to project to the dentate gyrus and CA3, while layer III projects to CA1 (Steward & Scoville, 1976). Accordingly, the subsequent SEM analyses carried out on these combined models replaced the Fos counts from the whole of the lateral entorhinal cortex with either layer II or III counts, while all other aspects of each model remained the same (Figure 3.12C, F). Based on the anatomical projections it might be expected that layer III, but not layer II, of the LEC would provide a model of good fit for the Familiar groups as it is the principal source of the inputs to CA1. This was found to be the case (Figure 3.12C). Replacing all of LEC with just layer III created a Familiar model of high fit (χ^2_2 = 0.55, p = 0.76; CFI = 1.0; RMSEA = 0.0) in which all path coefficients retained their significance ($p < 0.05$); whereas, using just layer II generated a Familiar model of poor fit (χ^2_2 = 4.58, p = 0.10; CFI = 0.89; RMSEA = 0.26). For the Novel groups the converse would be predicted. However, it was found that including layer II or layer III generated Novel condition models of acceptable fit (Figure 3.12F): layer II (χ^2_5 = 7.68, p = 0.18; CFI = 0.97; RMSEA = 0.17) and layer III (χ^2_5 = 6.69, p = 0.25; CFI = 0.97; RMSEA = 0.13).

The remaining laminae (V and VI) of the lateral entorhinal cortex are also of interest as they are the primary targets for the efferents from the hippocampus and subiculum (Van Strien et al., 2009), as well as the source of projections beyond the temporal lobe to sites such as prefrontal cortex (Insausti et al., 1997). Hence, in the final SEM analyses, Fos counts obtained from combined layers V and VI of the LEC were added to the models in the place of counts from the whole lateral entorhinal cortex (i.e., for the novel condition this analysis was based on the model depicted in Figure 3.12E and for the familiar condition the analysis was based in the model depicted in Figure 3.12B). Interestingly, this generated a model of good fit for the novel group (χ^2_5 = 2.22, p = 0.81; CFI = 1.0; RMSEA = 0.0) but one of poor fit for the familiar group (χ^2_2 = 5.86, p = 0.053; CFI = 0.80; RMSEA = 0.32).

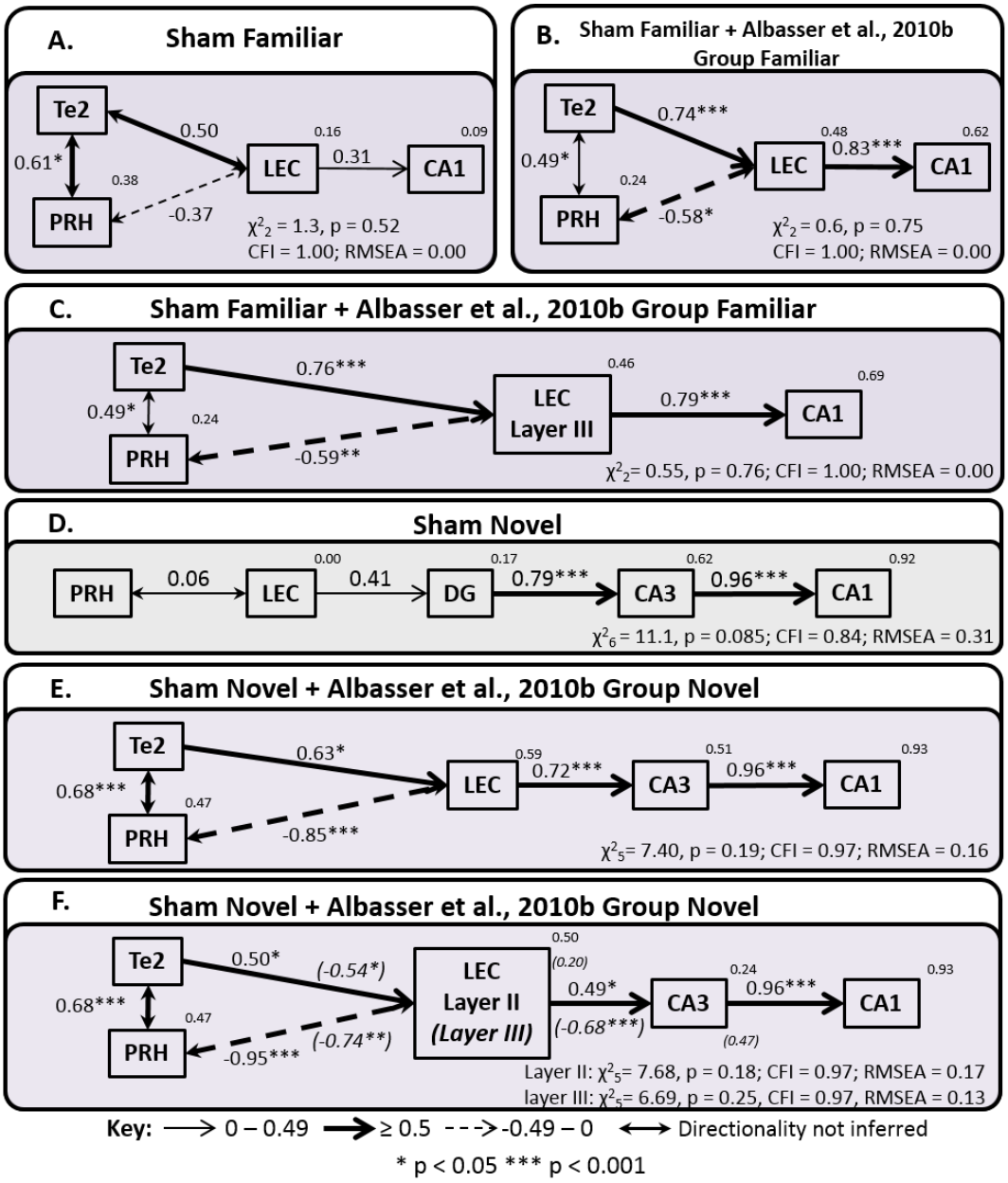

Figure 3.12. Optimal parahippocampal – hippocampal interactions.

The first three panels depict models for the Familiar condition (A-C), the bottom three panels (D-F) depict models for the Novel condition. **A**. Optimal model for group Sham Familiar using the present data. **B**. Optimal model when group Sham Familiar is collapsed with Group Familiar from Albasser *et al*., (2010b). **C**. Depicts the same model as B, but the LEC data are now just taken from cortical layer III. **D**. Optimal model for the group Sham Novel using the present data. **E**. Optimal model when group Sham Novel is collapsed with Group Novel from Albasser et al., (2010b). **F**. Depicts the same model as E, but the LEC data are now just taken from cortical layer II or from layer III (the italicised path coefficients in brackets relate to layer III). The model fit is provided at the bottom of each panel (CFI, comparative fit index; RMSEA, root mean square error of approximation) and models with unacceptable fit are represented with a pale grey background. The strength of the causal influence of each path is denoted both by the thickness of the arrow and by the path coefficient next to that path. The number above each region is the proportion of its variance that can be explained by its inputs. Sites depicted: area Te2, area 35 and area 36 of the perirhinal cortex, lateral entorhinal cortex (LEC) and hippocampal subfields CA1, CA3 and dentate gyrus (DG). * $p < 0.05$; *** $p < 0.001$.

3.4 Discussion

Despite their many interconnections, it has been proposed by some that the perirhinal cortex can support recognition memory independent of the hippocampus (e.g., Aggleton & Brown, 1999; Norman & O'Reilly, 2003; Diana et al., 2007). To assess this structural independence prediction, the present study examined the impact of hippocampal lesions on perirhinal cortex activity linked to recognition memory, as measured by c-*fos* expression. To induce c-*fos* expression, rats with either hippocampal lesions or sham surgeries actively explored pairs of objects, one novel and one familiar (Novel Object condition) in the bow-tie maze; a task that is impaired by lesions to the perirhinal cortex (Albasser et al., 2011a,b). The expression of c-*fos* in the perirhinal cortex, along with area Te2 and various hippocampal subfields, has previously been found to be sensitive to this behavioural manipulation in normal rats (Albasser et al., 2010b). Additional information was provided by a Familiar Object condition, which involved pairs of objects presented at different times in the past, so taxing recency memory (Albasser et al., 2010b). Again, there was a group with hippocampal lesions and a group with sham surgeries. All four groups in the present study successfully discriminated between the stimuli in their respective Novel Object and Familiar Object conditions.

Differences in the overall levels of c-*fos* expression were not observed between the Novel and Familiar Object conditions (but see Albasser et al., 2010b). Rather, the two behavioural conditions led to different patterns of inter-correlated c-*fos* activity. At the same time, significant correlations were found between recognition and recency performance and perirhinal Fos counts, these correlations are consistent with c-*fos* activation being closely linked to recognition memory performance (Seoane et al., 2012). As these perirhinal correlations were significant only in rats with hippocampal lesions, it is possible that the surgeries led to some form of cortical compensation (Cohen et al., 2013). Against this view is the finding that these perirhinal correlations did not differ significantly between the surgical and sham groups, nor did the hippocampal fields show evidence of a significant correlation with object discrimination in the two control groups. Whichever view is correct, the present data still support the notion that the perirhinal cortex can effectively function independent of the hippocampus to support recognition memory, while recognising its normal interactions with the hippocampus (Warburton & Brown, 2010).

Irrespective of surgical status, structural equation modelling revealed that discriminating novel objects (recognition memory) was associated with particular activity patterns

linking area Te2, the perirhinal cortex, and lateral entorhinal cortex. In the Novel Object surgical control rats, further correlated pathways linked lateral entorhinal cortex to hippocampal area CA3 and, thence, to CA1 (Figure 3.12; these same pathways could not be explored in those rats with hippocampal lesions). Discriminating between familiar objects (recency memory) was also associated with a similar parahippocampal network involving area Te2, perirhinal cortex, and lateral entorhinal cortex. For the Familiar Object surgical controls, the correlated pathway from lateral entorhinal cortex to the hippocampus went directly to CA1, i.e., not to CA3 as in the Novel Object condition (Figure 3.12).

In the present study, the very short retention delays helped to ensure successful object recognition and object recency discriminations by the surgical control groups. This same feature may also explain the lack of any hippocampal lesion effect on recognition or recency memory performance, though it is only for recency memory that consistent hippocampal lesion deficits are typically reported (Agster et al., 2002; Fortin et al., 2002; Forwood et al., 2005; Hoge & Kesner, 2007; Barker & Warburton, 2011; Albasser et al., 2012). It would seem, therefore, that the parahippocampal cortex can solve simple recency problems, a view supported both by the correlations between perirhinal Fos counts and recency performance, and by the ability of perirhinal units to signal recency differences (Zhu et al., 1995a; Xiang & Brown, 1998). The impact of the hippocampal lesions on c-*fos* activity levels was restricted to this same recency memory condition, with decreases in mid perirhinal cortex and area Te2. This decrease in perirhinal c-*fos* activity could reflect a disruption of the close cooperation between the perirhinal cortex and hippocampus that is thought to underlie recency memory (Warburton & Brown, 2010; Barker & Warburton, 2011).

The perirhinal Fos counts correlated negatively with the performance index D2 for both recognition and recency memory in the hippocampal lesioned groups. The negative sign may seem surprising given that presenting exclusively novel stimuli increases perirhinal Fos counts (Zhu et al., 1995b, 1996; Wan et al., 1999, 2004). A likely explanation stems from the fact that recognition memory tests involve the presentation of both novel and familiar stimuli for discrimination. Electrophysiological studies have shown that repeated, i.e., familiar, stimuli are associated with a drop in perirhinal activity, which is thought to provide a familiarity signal (Zhu et al., 1995a; Xiang & Brown, 1998; Brown & Aggleton, 2001). The implication is that effective recognition performance relates most to the fall in activity on stimulus repetition, rather than the initial level of activity

associated with novel stimuli *per se*. For this reason, low perirhinal activity may be the hallmark of effective recognition (Montaldi et al., 2006). The same logic could also apply to recency discriminations based on relative familiarity (Zhu et al., 1995a; Xiang & Brown, 1998).

The initial network analyses, which were largely confined to the parahippocampal region, found that the model with best fit had the same overall structure for all four groups (Figure 3.9), i.e., it was not affected by hippocampal surgery. Starting from area Te2, two pathways ran in parallel to area 36 and to the lateral entorhinal cortex, each then projecting to area 35 (Figure 3.9). In all four groups, the link from area 36 to area 35 had significant path coefficients, echoing the prevailing connectivity (Burwell & Amaral, 1998b). However, stacking the models revealed that the pathway from lateral entorhinal cortex to area 35 had stronger effective connectivity in the Novel Object condition. A combined model based on all four groups was also tested. When the path directions were reversed poorer fitting models emerged, except in the cases of the paths between Te2 and area 36 and between Te2 and LEC, where path direction did not affect model fit. These results may reflect the dense reciprocal connections between Te2 and area 36 (Furtak et al., 2007), and moderate reciprocal connections between Te2 and LEC (Burwell & Amaral, 1998b; Agster & Burwell, 2009).

The final network analyses used just the surgical control animals as the goal was to link parahippocampal with hippocampal activity. The best fitting models occurred when the present Fos data were combined with those from a previous study (Albasser et al., 2010b), which used identical protocols in intact rats. Novel stimuli (recognition) were associated with correlated pathways from the lateral entorhinal cortex to hippocampal field CA3 (perforant pathway), while familiar stimuli (recency) were associated with correlated pathways from the lateral entorhinal cortex to CA1 (temporoammonic pathway). The latter findings extend those studies that have specifically implicated the CA1 subfield in temporal discriminations and also help to explain the apparent dissociation with CA3 (Gilbert et al., 2001; Amin et al., 2006; Hoge & Kesner, 2007; Kesner et al., 2010). The activation contrast between the perforant and temporoammonic pathways has been noted in other IEG studies comparing novel with more familiar stimuli (Poirier et al., 2008; Albasser et al., 2010b), though these previous studies had less power. In these earlier IEG studies, the best fit for novel stimuli involved the perforant pathway from entorhinal cortex to the dentate gyrus and, thence, to CA3 (Poirier et al., 2008; Albasser et al., 2010b). In the present study, the dentate

gyrus was not included in the best novel stimulus model, though there were significant positive correlations between dentate gyrus and CA3 c-*fos* activity (p=0.007). Additional examination of this novel/familiar pathway dissociation showed that layer III, but not layer II, c-*fos* activity in the lateral entorhinal cortex produced a model of high fit for the Familiar Object condition. This finding matches the connectivity as layer III projects to CA1 while layer II projects to the dentate gyrus and CA3 (Steward & Scoville, 1976). More unexpectedly, both layer II and layer III generated models of acceptable fit for the Novel Object condition.

The different hippocampal subfield interactions for the Novel Object (CA3) and Familiar Object (CA1) conditions (Figure 3.12) imply that the hippocampus can help distinguish novel from familiar stimuli (i.e., support object recognition). There are, however, several caveats. Not only did the hippocampal lesions leave parahippocampal c-*fos* activity levels unaffected for novel stimuli, consistent with spared novelty/familiarity information, but many hippocampal lesion studies have failed to find changes in object recognition memory performance (for reviews see Mumby, 2001; Winters et al., 2008; Brown et al., 2010). An alternative explanation for this differential hippocampal signal stems from the fact that when a rat explores an object it does more than register its novelty or familiarity. The rat will spontaneously learn associated information, including its spatial and temporal properties, along with its context (Poucet, 1989; Dix & Aggleton, 1999; Hannesson et al., 2004). The extent of this new associative learning should be greatest for novel stimuli (Wagner, 1981). Lesion studies have repeatedly shown that this additional associative learning requires the hippocampus (Save et al., 1992; Barker & Warburton, 2011) so, potentially, explaining the altered pattern of IEG activity in that structure. This spatial and temporal information related to the object would then be available to support recollective-based recognition (Fortin et al., 2004; Diana et al., 2007; Easton & Eacott, 2010).

If this analysis is correct it would be predicted that output routes from the hippocampus would emerge, reflecting this new associative information. One output that was considered is from the hippocampus to the entorhinal cortex. The large proportion of hippocampal efferents terminate in the deep layers of lateral entorhinal cortex (Van Strien et al., 2009), so providing the rationale to focus on just these layers. It was found that in the novel object condition, Fos counts in combined cortical layers V and VI of the lateral entorhinal cortex of the sham animals correlated significantly with Fos counts in hippocampal subfields CA1 and CA3, whereas these correlations were not significant in

the familiar object condition (Table 3.3). The resulting structural equation modelling provided models with good fit for the Novel but not the Familiar conditions. While this preliminary analysis suggests a potential feedback loop in the case of Novel stimuli, these hippocampal pathways were seemingly not critical for the c-*fos* responses to novel stimuli in perirhinal cortex.

The additional hippocampal learning need not, however, aid familiarity-based recognition memory as that is context free (Barker & Warburton, 2011b). In this account, the perirhinal cortex is required for object-based information, including familiarity, while the hippocampus supports additional associative learning, in conjunction with the parahippocampal region (Diana et al., 2007; Barker & Warburton, 2011b). This description closely maps onto dual process models of recognition, which often assume two, largely independent information streams (Yonelinas, 2002; Norman & O'Reilly, 2003). The present findings also concur with the further assumption that this independence reflects different anatomical substrates (Aggleton & Brown, 1999; Diana et al., 2007; Vann et al., 2009), with the perirhinal cortex, in particular, responsible for familiarity-based recognition, while the hippocampus is responsible for recollective-based recognition (Brown & Aggleton, 2001; Aggleton et al., 2005; Eichenbaum et al., 2007; Rudebeck et al., 2009). Specifically, the models of parahippocampal-hippocampal interactions presented here map on to the 'what' pathway of the binding of item and context model (Diana et al, 2007).

3.4.1 Summary

To summarise the findings of this study, rats with hippocampal lesions successfully discriminated novel from familiar objects while others discriminated the relative recency of objects. Further, interactions in the parahippocampal region were unaffected by loss of the hippocampus for these types of memory, indicating that the perirhinal cortex can process object memories independently from the hippocampus. Models of interactions between the parahippocampal cortex and the hippocampus indicate a differential mode of hippocampal engagement when animals explore novel compared to familiar objects. Familiar objects engaged the pathway from lateral entorhinal cortex layer III to CA1 while novel objects engaged the pathway from lateral entorhinal cortex, layers II or III to CA3 and then to CA1. Additionally, when rats were discriminating novel from familiar objects there was a stronger effective connection between area 35 of the perirhinal cortex and the lateral entorhinal cortex providing a possible route by which novelty information from the perirhinal cortex could generate the switch between the pathways.

4 Contrasting networks for recognition memory and recency memory revealed by immediate-early gene imaging in the rat

4.1 Introduction

Recency memory, or temporal order memory, is the ability to discriminate objects with varying degrees of familiarity based on the relative distance in time since they were last encountered. It has been demonstrated that lesions to the perirhinal cortex in rats consistently cause impairments in both object recognition and object recency memory (Mumby & Pinel, 1994; Ennaceur et al., 1996; Brown & Aggleton, 2001; Barker & Warburton, 2011a,b; Winters et al., 2008). The perirhinal cortex does not however complete these tasks in isolation and there is evidence that recognition memory and recency memory partly depend on different neural pathways. Evidence for this comes from lesion studies; damage to the hippocampus or medial prefrontal cortex are consistently implicated in object recency memory but not recognition memory (Mumby, 2001; Fortin et al., 2002; Kesner et al., 2002; Hannesson et al., 2004a,b; Forwood et al., 2005; Barker et al., 2007; Hoge & Kesner, 2007; Barker & Warburton, 2011a,b; DeVito & Eichenbaum, 2011; Albasser et al., 2012).

Immediate-early gene (IEG) imaging can be used as an indirect measure of neural activity (Herdegen, 1996; Chaudhuri, 1997; Tischmeyer & Grimm, 1999; Guzowski et al., 2005). Further evidence for divergent neural networks that underpin recognition and recency memory comes from IEG imaging experiments. Utilising the expression of the IEG, c-*fos*, rats engaged in novel object recognition or recency memory tasks have been shown to display different patterns of integrated neuronal activity across medial temporal lobe regions. Structural equation modelling on c-*fos* data generated from animals engaged in a recency discrimination task revealed that this test recruited the pathway from lateral entorhinal cortex (principally layer III) to CA1 in the hippocampus (Chapter 3, Albasser et al., 2010b). The fundamental difference between the optimal network model derived for the novel as compared to the familiar object based task was the involvement of hippocampal subfield CA3 in the novel object discrimination task (Chapter 3, Albasser et al., 2010b). The present study sought, therefore, to examine if

the pattern of functional connectivity observed during the familiar object based task described in Chapter 3 can be generalised to other forms of familiar object based tasks; particularly when the temporal properties of the test stimuli are more specifically manipulated.

Behavioural tests of object recency memory in rodents typically involve a paradigm in which there is a discrete intervening event (Mitchell & Laicacona 1998; Ennaceur, 2010). In such tests, the animal is introduced to an identical pair of objects (A+A) and then removed from the test apparatus. When the animal is returned to the apparatus it is exposed to a second pair of identical objects (B+B), again followed by removal from the test arena. Subsequent testing involves presentation of objects A and B together for the first time to allow for selection between them (e.g., Mitchell & Laicacona 1998; Hannesson et al., 2004a,b; Barker et al., 2007; Albasser et al., 2012). Rats with intact recency memory will spend more time exploring the more novel object, i.e., that seen least recently (Ennaceur & Delacour, 1988; Mitchell & Laicacona 1998; Albasser at al., 2012). This form of recency testing, in which the stimulus presentations are separated by distinctive events, is sometimes known as between-block recency; the imposition of an additional episode or experience may aid in separating the two items to be distinguished based on their temporal properties (Templer & Hampton, 2013). This protocol can be compared with within-block recency; the ability to select between stimuli previously presented in a single, continuous series, i.e., without any specific intervening event (e.g., Shaw & Aggleton, 1993; Agster et al., 2002; Fortin et al., 2002). Reflecting the majority of published studies on object recency by rodents, the present study focussed on recency discriminations when the objects are separated by time as well as by a distinct event (being removed from the apparatus).

Rather than give each rat a single recency memory test, which may not be sufficient to produce a measurable difference in c-*fos* expression, the rats received 20 recency trials in a test session prior to histological analysis (Experiment 2). Consequently, each rat in the Recency Test condition first explored 20 pairs of objects, where the objects in each pair were identical but differed from those in all of the other pairs (first sample phase). After a delay of 90 minutes in a dark room, the second sample phase consisted of another 20 duplicate pairs of objects, which differed from those in all of the other sample trials (see Table 4.1). Each trial in the subsequent Recency Test consisted of pairs of non-identical objects, one from the first sample phase, the other from the second sample phase. The bow-tie maze (Albsasser et al., 2010a,b) was used for all behavioural

testing as this apparatus makes it possible to deliver multiple consecutive trials without the need to handle the rat.

A similar behavioural design was used for the Recency Control condition in Experiment 2. The goal was to match the sensorimotor demands of the experimental group but make the recency discrimination impossible to solve. For this reason the rats in each condition had to be equally familiar with the objects to be discriminated. The first and second sample phases were identical to those described above for the Recency Test group (see Table 4.1). The final test phase in the Recency Control condition also involved the same objects that were used for the Recency Test and, once again, each trial contained two different objects (Table 4.1). But for this group the object pairings were selected to make their temporal properties almost indistinguishable. Consequently, each object pair in the Recency Control condition consisted of two items from adjacent trials in the same sample phase. Thus, while objects to be discriminated in the Recency Test condition were separated by 110 minutes, those in the Recency Control were separated by less than a minute (in practice this was just a few seconds). In all other respects, this control protocol matched the recency memory condition (Table 4.1).

Following either the recency or the control procedures, Fos, the protein product of c-*fos,* was visualised by immunohistochemistry and quantified across multiple brain sites. Structural equation modelling was applied to the resulting Fos-related activity data to test anatomically-plausible patterns of functional connectivity.

In the rodent, several regions beyond the medial temporal lobe have been implicated in recency memory processing. As mentioned above, these sites include medial prefrontal cortex but nuclei of the anterior and midline thalamus have also been shown to contribute to recency memory (Mitchell & Laiacona, 1998; Hannesson et al., 2004a,b; Wolff et al., 2006; Cross et al., 2013; Dumont & Aggleton, 2013). Additionally, informative data have come from crossed lesion studies; in this experimental paradigm a lesion is made in a brain region in one hemisphere while a different region is damaged in the contralateral hemisphere. Behavioural deficits observed following this type of intervention are interpreted as signifying not only that those regions are required for successful completion of the task but also specifically that interaction between the two regions in question is an essential task requirement. Separate crossed lesion studies have demonstrated that successful recency memory requires a functional connection between the perirhinal and medial prefrontal cortices as well as between the medial dorsal thalamic nucleus and the medial prefrontal cortex (Hannesson et al., 2004b; Barker et

al., 2007; Barker & Warburton, 2011a; Cross et al., 2013). Together, this implies that these regions form at least part of an integrated neural network that is required for recency discriminations but not for the judgement of prior occurrence. There is also evidence that lesions to the anterior thalamic nuclei principally disrupt recency memory which does not involve an intervening event (Wolf et al., 2006; Dumont et al., 2013); thus one may predict their differential involvement across the experimental conditions in this experiment. Indeed, these regions are all implicated in Aggleton's parahippocampal–prefrontal network for discriminating the familiarity and recency of occurrence of objects (Aggleton, 2012). Based on these data, in addition to verifying the previously derived network model for familiar object processing derived in Chapter 3, a subsequent aim was to extend and optimise the model to incorporate regions outside of the medial temporal lobe.

Prior to recency testing, all rats were initially examined for their ability to recognise objects after the same retention delays as those proposed for the recency memory problem (Experiment 1; Recognition control). Had the rats not been able to retain familiarity information in this recognition control test, then the subsequent recency task (Experiment 2) could also effectively be seen as just a recognition test; i.e., novel (forgotten sample) vs. familiar.

4.2 Materials and methods

4.2.1 Animals

Subjects comprised 18 naïve, male, Lister Hooded rats (Harlan, Bicester, UK). They were housed as described in General Methods section 2.2. The rats were approximately 10 weeks old at the start of the study and weighed 277-355g.

4.2.2 Apparatus

Testing took place in a bow-tie maze as described in the General Methods section 2.3.1 (Figure 2.2).

4.2.3 Objects

Each experiment used separate collections of pairs of three-dimensional junk objects made of plastic, glass or ceramics. Experiment 1 used 100 objects while Experiment 2 used 80 objects (see Table 4.1).

4.2.4 Behavioural Testing

4.2.4.1 Pre-training

As described in the General Methods section 2.3.3.

4.2.4.2 General testing protocol

Both Experiments 1 and 2 involved two sample phases and one test phase (Table 4.1). The two protocols only differed in the final test phase. In both cases, each of the three phases contained 20 trials, each of one minute duration. Each phase was separated by 90 minutes. At the beginning of the first sample phase each rat was placed in one end of the maze, which was empty. The experimenter then lifted the central door so that the rat could run to the other side of the maze to begin Trial 1, where a pair of identical novel objects (A1 and A2) covered the two sucrose wells, each containing a single sucrose pellet. The rat was allowed to retrieve the food pellets and freely explore the objects during the one minute trial. The sliding door was then lifted so that the rat could run to the other side of the maze to begin Trial 2, where another duplicate pair of novel objects (B1 and B2) covered the two food wells. This sample phase protocol continued with pairs of identical novel objects, covering baited food wells, until 20 trials were completed. Rats were then placed in a dark, quiet holding room, for 90 minutes, until the beginning of the next phase when they were returned to the bow-tie maze (Table 4.1).

The second sample phase was identical to that described above, except that new duplicate pairs of objects were used on each of the 20 trials; thus, 40 pairs of novel objects were seen by the rats on completion of the second sample phase. The rats were returned to the dark holding room for a further 90 minutes before the test phases for Experiments 1 and 2 began.

4.2.4.3 Experiment 1 (Recognition control)

Following the two sample phases described above, each trial in the test phase consisted of a pair of dissimilar objects over the two food wells. One object was familiar (from the first sample phase) while the other object was novel (Table 4.1). This test phase comprised 20 consecutive trials of one minute each. As a consequence, recognition of the familiar object from the first sample phase involved a retention delay of 220 minutes. All objects (both novel and familiar) were baited with a single sucrose pellet and the position of the novel object (left or right) was counterbalanced.

Table 4.1. Schematic showing the sequence of object presentations in different phases of experiment.

Behavioural Design																				
Trials	**1**	**2**	**3**	**4**	**5**	**6**	**7**	**8**	**9**	**10**	**11**	**12**	**13**	**14**	**15**	**16**	**17**	**18**	**19**	**20**
1st Sample phase	**A**	**B**	**C**	**D**	**E**	**F**	**G**	**H**	**I**	**J**	**K**	**L**	**M**	**N**	**O**	**P**	**Q**	**R**	**S**	**T**
	A	**B**	**C**	**D**	**E**	**F**	**G**	**H**	**I**	**J**	**K**	**L**	**M**	**N**	**O**	**P**	**Q**	**R**	**S**	**T**
2nd Sample phase	**a**	**b**	**c**	**d**	**e**	**f**	**g**	**h**	**i**	**j**	**k**	**l**	**m**	**n**	**o**	**p**	**q**	**r**	**s**	**t**
	a	**b**	**c**	**d**	**e**	**f**	**g**	**h**	**i**	**j**	**k**	**l**	**m**	**n**	**o**	**p**	**q**	**r**	**s**	**t**
Recognition Control (Exp. 1)	A	B	C	D	E	F	G	H	I	J	K	L	M	N	O	P	Q	R	S	T
	α	β	γ	δ	ε	ζ	η	θ	ι	ξ	κ	Λ	μ	ν	ο	π	ς	ρ	σ	τ
Recency Test (Exp. 2)	A	B	C	D	E	F	G	H	I	J	K	L	M	N	O	P	Q	R	S	T
	a	b	c	d	e	f	g	h	i	j	k	L	m	n	o	p	q	r	s	t
Recency Control (Exp. 2)	A	a	C	c	E	e	G	g	I	i	K	k	M	m	O	o	Q	q	S	s
	B	b	D	d	F	f	H	h	J	j	L	l	N	n	P	p	R	r	T	t

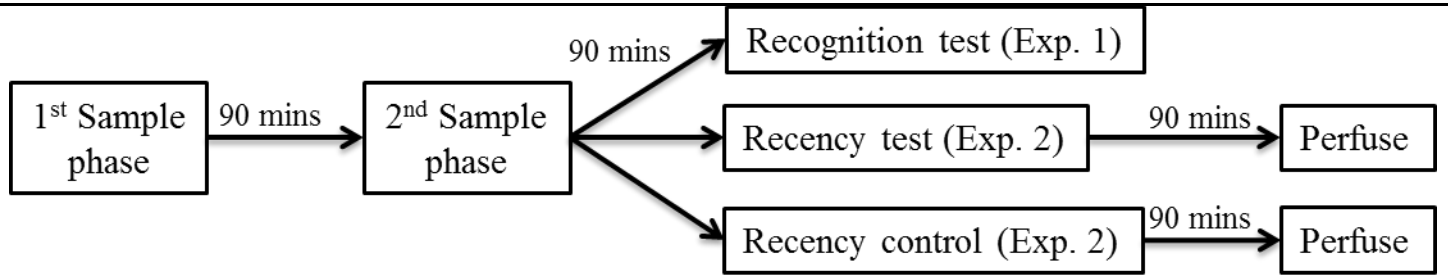

Different objects are represented by different letters and by changes in case (upper or lower). Bold characters represent the first presentation of an object (i.e., when novel). The structure of the first two phases for Experiments 1 and 2 were identical. For the recognition memory test (Exp. 1) each test trial comprised one familiar and one novel object. For the recency conditions (Exp. 2) each test trial comprised two familiar objects from different times in the past.

4.2.4.4 Experiment 2 (Recency memory c-*fos*)

Pairs of rats from the same cage were randomly divided between two behavioural protocols (Recency Test and Recency Control). Testing began at least five days after completion of Experiment 1.

4.2.4.5 Recency Test group

The two sample phases for the nine rats were exactly as described in the general protocol with new objects pairs (see Table 4.1). In the test phase, rats were now presented with two different, familiar objects; one object seen in the first (earlier) sample phase and a more recent object seen in the second sample phase (see Table 4.1). The test phase began 90 minutes after completion of sample phase 2. The pairs of objects were matched so that the object from trial 1 of sample phase 1 was paired with the object from trial 1 of sample phase 2, and so on (see Table 4.1). This meant that the objects from the two sample phases were separated by 110 minutes (Table 4.1). The test phase consisted of 20 trials, each of one minute. All objects were baited with a single sucrose pellet. Placement of the more recent object to the left or right side was counterbalanced. At test, items from the first sample phase were explored 220 minutes after their initial sample, i.e., the same retention interval as used in Experiment 1. On completion of the final test phase, the rats were placed in a dark room for 90 minutes and then perfused as described in the General Methods section 2.4.

4.2.4.6 Recency Control group

The two sample phases for the nine rats were identical to those for the Recency Test group (Table 4.1). In the third phase, the rats were again presented with non-identical pairs of objects that were seen previously in the sample phases. This time, the pairs of objects were taken from successive trials in the same phase. For example, in trial 1 of the third phase, the objects presented were from trial 1 and trial 2 of the first sample phase, while in trial 2 the objects presented were from trial 1 and trial 2 of the second sample phase (Table 4.1). The object pairings in the final test phase not only ensured that the order in which individual objects occurred was as closely matched as possible to that used in the Recency Test (Table 4.1), but also ensured that the recency differences were particularly small as they were between objects that occurred in consecutive trials. Although each sample trial lasted one minute, because the rats ran directly from the end of one sample trial to the next sample trial, the interval between successive objects was, in practice, often just a few seconds. The test phase again consisted of 20 trials of one

minute each. All objects were baited with a single sucrose pellet. Placement of the more recent object on the left or right was counterbalanced. On completion of the test session, the rats were placed in a dark room for 90 minutes and then perfused as described in the General Methods section 2.4.

4.2.5 Analysis of behaviour

As described in General Methods section 2.3.5.

4.2.6 Immunohistochemistry

As described in General Methods section 2.7.

4.2.7 Regions of interest

The multiple regions of interest are illustrated in Figure 4.1. Two brain atlases (Swanson, 1992; Paxinos & Watson, 2005) helped to verify the locations of brain areas, unless otherwise specified. The anterior – posterior (AP) coordinates (mm from bregma) in the descriptions below and in Figure 4.1 are from Paxinos & Watson (2005). The regional categories below reflect the groupings subsequently used in the statistical analyses of Fos counts.

4.2.7.1 Perirhinal cortex

The perirhinal cortex (PRH) nomenclature and borders were taken from Burwell (2001). Separate counts were made in the rostral (from AP -2.76 to -3.84), mid (AP-3.84 to 4.80) and caudal (from AP -4.80 to -5.52) perirhinal cortex. The PRH was also subdivided into areas 35 (ventral) and 36 (dorsal), making a total of six areas within this regional category.

4.2.7.2 Parahippocampal cortex

Separate cells counts were taken from the lateral and medial entorhinal cortices (LEC and MEC respectively) from sections near AP -4.92 to -5.52. In addition, cell counts were taken from the visual association area Te2, which is dorsal to area 36. This cortical area is interconnected with the postrhinal, perirhinal and lateral entorhinal cortices, and has previously been implicated in visual novelty detection (Wan et al., 1999; Zhu et al., 1996; Albasser et al., 2010b; Ho et al., 2011). Fos counts were also made in the postrhinal cortex (POR; AP -7.08 to -8.04); the boundaries were based on Burwell (2001). Much of the postrhinal cortex corresponds to the area labelled as the ectorhinal cortex by Paxinos and Watson (2005).

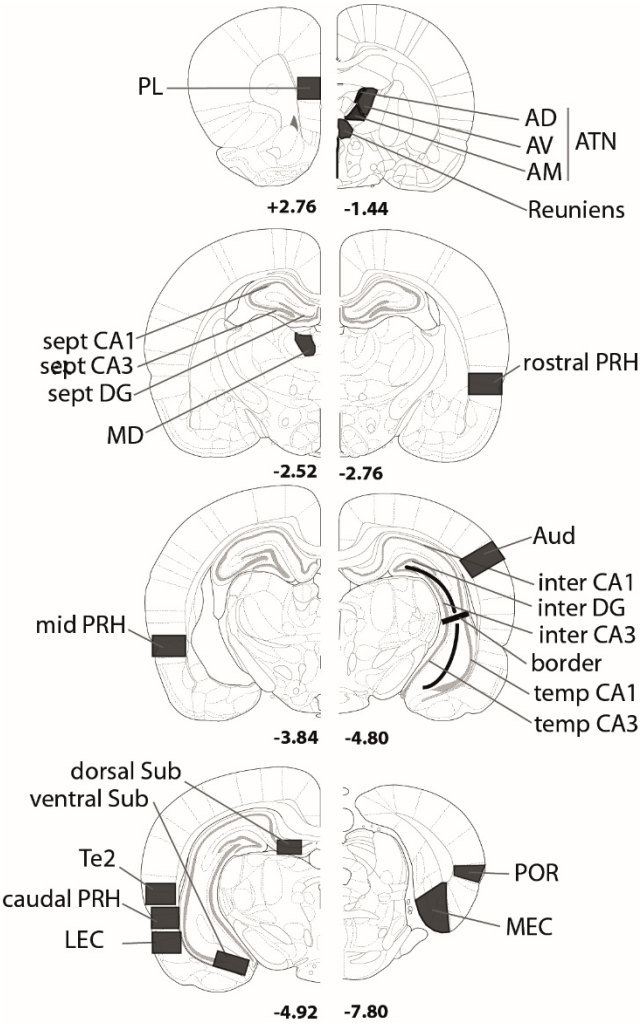

Figure 4.1. Regions of interest for c-*fos* analyses.

Sites included: AD, anterodorsal thalamic nucleus; AM, anteromedial thalamic nucleus; ATN, anterior thalamic nuclei; Aud, primary auditory cortex; AV, anteroventral thalamic nucleus; CA fields, intermediate (inter), septal (sept) and temporal (temp); DG, dentate gyrus; dorsal Sub, dorsal subiculum; LEC, lateral entorhinal cortex; MD, medial dorsal thalamic nucleus; MEC, medial entorhinal cortex; PL, prelimbic cortex; PRH, perirhinal cortex, caudal, mid and rostral levels; POR, postrhinal cortex; Reuniens, nucleus reuniens of thalamus; Te2, area Te2; ventral Sub, ventral subiculum. The numbers below refer to the approximate distance in mm from bregma. Adapted from the atlas of Paxinos & Watson (2005).

4.2.7.3 Hippocampal formation

Hippocampal subfields (dentate gyrus, CA1, and CA3) were subdivided into their septal (dorsal), intermediate, and temporal (ventral) divisions (Bast, 2007; Strange et al., 2014). The septal hippocampus counts (dentate gyrus, CA3 and CA1) were obtained from sections at AP -2.52 to -3.24 while those for the intermediate hippocampus (dentate gyrus, CA1, CA3) came from AP -4.80 to -5.52. The border between the intermediate

and temporal hippocampus corresponds to -5.0 mm dorsoventral from bregma (Paxinos & Watson, 2005). Within the temporal (ventral) hippocampus, counts were made in CA1 and CA3 fields (at the same AP as the intermediate hippocampus). Additional cell counts were taken in both the dorsal and ventral subiculum (from around AP -5.16).

4.2.7.4 Prelimbic cortex and limbic thalamus

Fos-positive neuronal cell counts were made within the prelimbic (PL) region of the medal prefrontal cortex from AP +3.72 to +2.76. Cell counts were also made in five thalamic nuclei that are directly interconnected with either the hippocampus or prefrontal cortex. These were the anterodorsal (AD), anteromedial (AM), anteroventral (AV), medial dorsal (MD) nuclei, and nucleus reuniens (see Figure 4.1).

4.2.7.5 Auditory cortex

Counts of Fos-positive cells were made in the auditory cortex (Aud) from AP -4.80 to -5.52 to provide an area where a null result might be expected if the behavioural tasks are well matched.

4.2.8 Image capture and analysis of *c-fos* activation

As described in General Methods section 2.8.

4.2.9 Statistical analysis

4.2.9.1 Behavioural data

For Experiment 1, the final cumulative D1 and updated D2 scores were compared using two-sample t-tests (two-tailed) for the groups of rats that would subsequently comprise the separate behavioural groups in Experiment 2. One-sample t-tests (one-tailed), were then applied to the cumulative D1 and updated D2 scores to determine if the indices of performance were significantly above chance level (zero) for the two groups of rats. The same analyses were applied to the behavioural data from Experiment 2, with the addition that total cumulative levels of exploration were also compared between the two recency groups (two-tailed, two-sample t-test). Additional paired sample t-tests (two-tailed) were calculated on the behavioural measures for the Recency Control group to compare between trials involving objects from the first sample phase and those from the second sample phase (Table 4.1).

4.2.9.2 Fos data

Initial comparisons used the raw counts of Fos-positive cells in the regions of interest to make direct comparisons between the two recency groups. Furthermore, sub-regions within the various regions of interest (e.g., within the hippocampal formation and parahippocampal region) were first brought together in groups and then analysed with a one between-subjects factor (recency condition) and one within-subjects factor (ROI) ANOVA. This regional grouping procedure reduced the numbers of comparisons and so helps to protect against Type I errors. These groupings are described in the Regions of Interest section 4.2.7. Further, as perirhinal cortex was analysed at three levels along its rostral-caudal extent, this was taken into account when analysing Fos expression; a one between-subjects factor (recency condition) and two within-subjects factor (rostral-caudal level and ROI) ANOVA was calculated. Finally, Fos counts in auditory cortex were compared between the behavioural conditions with a two-sample t-test (two-tailed).

The Fos counts for all individual areas were also correlated (Pearson product moment coefficient) with all of the other areas, as well as with the behavioural indices of performance (D1, D2, total exploration), for each of the two groups. In view of the large number of individual areas counted (27 in total), some sites were again combined prior to these correlations to reduce the total numbers of comparisons. Examples include the three anterior thalamic nuclei, the subfield counts across different parts of the hippocampal AP axis (septal, temporal, intermediate), the dorsal and ventral subiculum, and areas 35 and 36.

4.2.10 Structural equation modelling

As described in General Methods section 2.10.

4.3 Results

4.3.1 Experiment 1 (Recognition control)

Comparisons between the two sets of rats that would subsequently form the Recency test group and the Recency control group showed that there were no significant differences for either the cumulative D1 ($t_{16} = 0.37$, $p = 0.72$) or final, updated D2 ($t_{16} = 0.11$, $p = 0.92$). Importantly, both groups of rats displayed a clear preference for novel over familiar objects in the test phase (Figure 4.2 lower panels). Consequently the future Recency Test group was above chance for both discrimination measures (D1: $t_8 =$

4.87, $p < 0.001$; D2: $t_8 = 8.25$, $p < 0.001$). Likewise, the same discrimination measures for the future Recency Control group were above chance (D1: $t_8 = 6.06$, $p < 0.001$; D2: $t_8 = 5.84$, $p < 0.001$).

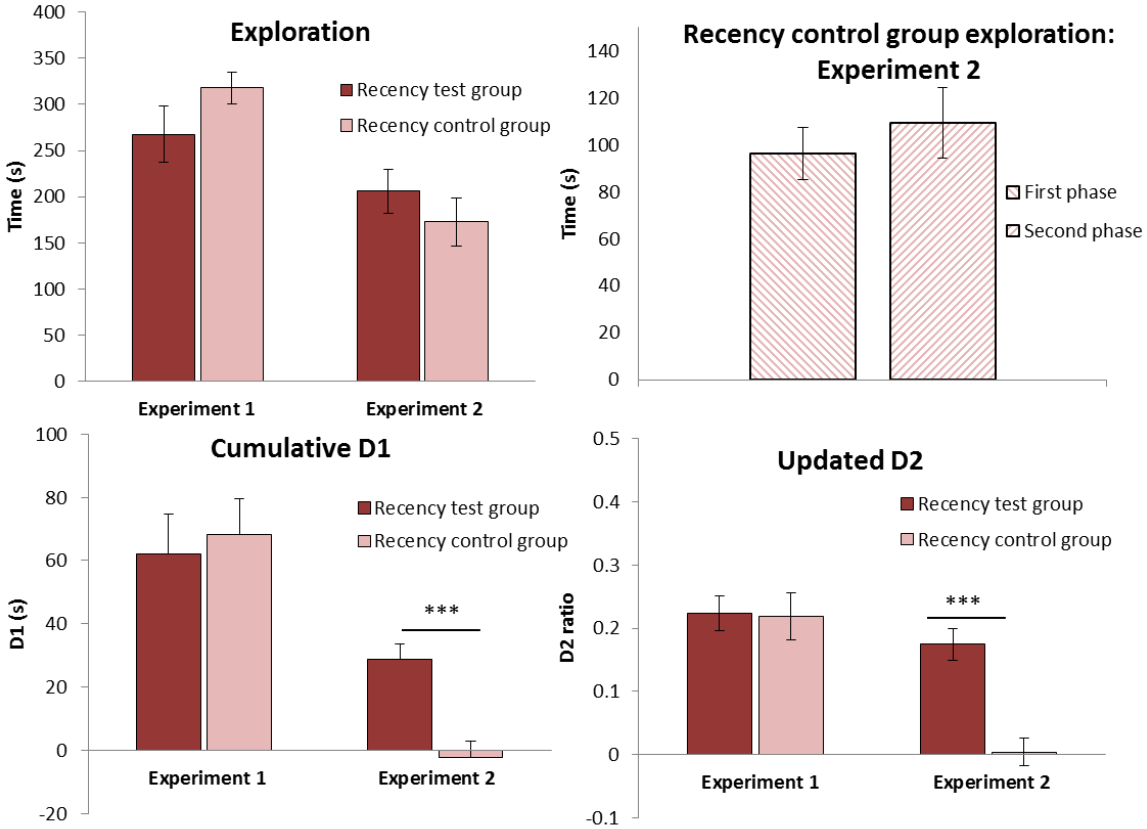

Figure 4.2. Experiment 1 and 2: Behavioural measures of object recognition and recency memory.

The top left graph shows the mean total time rats spent exploring all objects in the test phase of Experiments 1 and 2. The top right graph illustrates the exploration time of the Recency Control group in the test session of Experiment 2 divided into exploration of objects first seen in sample phase 1 and objects first seen in sample phase 2. The bottom left graph depicts the difference in time spent exploring novel objects minus time spent exploring familiar objects (Exp. 1) or time spent exploring less recent objects minus time spent exploring recent objects (Exp. 2) across the 20 trials (cumulative D1). The bottom right graph represents the same data as the bottom left graph but the discrimination scores are expressed as the Updated D2 ratios (D1/exploration). All graphs show the mean performance ± standard error of the mean. Note, that for Experiment 1 the group names refer to how the rats were subsequently allocated for Experiment 2. *** $p < 0.001$

4.3.2 Experiment 2 (Recency memory c-*fos*)

4.3.2.1 Behaviour

As expected, the Recency Test group had superior recency discrimination scores to those of the Recency Controls, as measured by both the cumulative D1 ($t_{16} = 4.17$, $p = 0.001$)

and updated D2 ($t_{16} = 4.77$, $p \leq 0.001$) scores (Figure 4.2 lower panels). The Recency Test group successfully discriminated objects in the first sample phase from those in the more recent, second sample phase (D1: $t_8 = 5.67$, $p < 0.001$; D2: $t_8 = 6.42$, $p < 0.001$). In contrast, the Recency Control group failed to discriminate between objects that were temporally adjacent in the same series (D1: $t_8 = 0.40$, $p = 0.35$; D2: $t_8 = 0.17$, $p = 0.44$). Finally, there was no group difference in total exploration times (Figure 4.2, upper left panel; $t_8 = 0.82$, $p= 0.43$).

In view of their status, it is important to test whether the Recency Control group showed any differential behaviour reflecting the temporal properties of the stimuli. Using data from the test phase only, it was possible to separate the final series of trials into those involving objects from the first sample phase (odd numbered trials) and those from the second sample phase (even numbered trials). No difference was found in total exploration (Figure 4.2, upper right panel; $t_8 = 1.51$, $p = 0.17$). Likewise, in neither subset of trials could the control rats discriminate the objects based on their relative recency, nor did the recognition score (D2) differ for these two subsets of trials ($t_8 = 0.31$, $p = 0.77$).

4.3.2.2 Fos activation: group differences and correlation data

The counts of Fos-positive cells in the two behavioural conditions rarely differed in the various regions of interest (Figure 4.3). Attention, therefore, focused on two sets of correlations. The first set of correlations concerned an area's Fos count and the behavioural performance (D1, D2, total exploration) of each group (Table 4.2).

One concern is that the multiple correlations will increase the risk of Type 1 errors. For this reason it is notable that in the Recency Test group, of the 20 sites examined (Table 4.2), the Fos counts significantly correlated ($p < 0.05$) with D2 scores in 10 sites and with D1 in 11 sites. Far fewer sites in the Recency Control group had Fos counts that correlated with either D2 or D1 (maximum of two), though these correlations in the control group are more difficult to interpret given that the recency memory scores in this group were close to zero. It is, therefore, particularly interesting that the opposite group pattern was seen for total exploration levels. None of the 20 sites had Fos counts that correlated with total exploration in the Recency Test group, but there was a significant correlation in seven sites for the Recency Control group.

The second set of correlations concerns the inter-area Fos counts within each of the two groups (Table 4.2). These show probability levels uncorrected for multiple comparisons

as the individual correlations are of limited informative value. More importantly, these same correlations provide the source data for the structural equation modelling, where the fit of the overall model helps to compensate for Type 1 errors in the individual correlations that comprise the model. In view of this same issue, it is important that any model must match established patterns of connectivity between the regions of interest, i.e., potential models are constrained.

In an attempt to further address the possibility of Type 1 errors by decreasing the numbers of correlations and to help reduce variance, the subfield Fos counts for the septal, intermediate and temporal sub-regions of the hippocampus were combined, as were counts from the three anterior thalamic nuclei. Additionally, it was these combined regional counts that were utilised in the subsequent structural equation modelling analyses. Thus, a total of 20 analysed regions remained but 23 are included in Table 4.2. Due to the assumed importance of the perirhinal cortex in object based tasks, the separate Fos data for areas 35 and 36 were included to investigate their relationship with the behavioural measures. Combined counts at each of the three analysed rostral-caudal levels of perirhinal cortex were also included as these data were used in the subsequent structural equation modelling analyses.

Table 4.2. Experiment 2: Inter-area correlations of c-*fos* counts and behavioural measures

		Recency Test group																												
		Exploration	D1	D2	Rostral Area35	Rostral Area36	Rostral PRH	Mid Area35	Mid Area36	Mid PRH	Caudal Area35	Caudal Area36	Caudal PRH	Te2	LEC	MEC	POR	CA1	CA3	DG	Dorsal Sub	Ventral Sub	PL	MD	ATN	Reuniens	Aud		
Exploration	r-value		.612	-.213	.373	.252	.313	.551	.202	.387	.244	.003	.122	.103	.179	.210	.124	-.070	.154	-.081	.088	.078	.271	.465	.112	.280	-.305	r-value	Exploration
	p-value		.080	.582	.322	.513	.413	.124	.603	.303	.526	.994	.754	.792	.645	.588	.751	.857	.692	.837	.821	.842	.480	.208	.774	.466	.425	p-value	
D1	r-value	**-.676***		.617	**.764***	**.671***	**.720***	**.798***	**.691***	**.775***	**.800****	**.724***	**.780***	.657	**.718***	**.774***	.574	.574	**.668***	.394	.663	**.779***	.484	.334	.378	**.717***	.485	r-value	D1
	p-value	**.045**		.077	**.017**	**.048**	**.029**	**.010**	**.039**	**.014**	**.010**	**.027**	**.013**	.054	**.029**	**.014**	.106	.106	**.049**	.294	.052	**.013**	.187	.379	.316	**.030**	.186	p-value	
D2	r-value	-.655	**.933*****		.553	.532	.545	.467	.653	.588	**.788***	**.882****	**.858****	**.773***	**.758***	**.715***	**.677***	**.790***	**.677***	.597	.553	**.880****	.290	.019	.310	.650	**.879****	r-value	D2
	p-value	.056	**<0.001**		.123	.141	.129	.205	.056	.096	**.012**	**.002**	**.003**	**.014**	**.018**	**.030**	**.045**	**.011**	**.045**	.090	.122	**.002**	.449	.961	.417	.058	**.002**	p-value	
Rostral	r-value	.103	-.182	.012		**.976*****	**.994*****	**.874****	**.960*****	**.959*****	.623	**.712***	**.686***	**.793***	**.689***	.629	.302	.417	.623	.228	.614	.606	**.820****	.556	.485	**.813****	**.700***	r-value	Rostral
Area35	p-value	.793	.639	.975		**<0.001**	**<0.001**	**.002**	**<0.001**	**<0.001**	.073	**.031**	**.041**	**.011**	**.040**	.070	.430	.264	.073	.556	.079	.084	**.007**	.120	.185	**.008**	**.036**	p-value	Area35
Rostral	r-value	.351	-.656	-.484	**.677***		**.994*****	**.825****	**.931*****	**.918*****	.506	**.676***	.610	**.757***	.595	.631	.270	.363	.591	.175	.641	.584	**.896****	.535	.507	**.768***	**.757***	r-value	Rostral
Area36	p-value	.355	.055	.187	**.045**		**<0.001**	**.006**	**<0.001**	**<0.001**	.165	**.046**	.081	**.018**	.091	.068	.483	.337	.094	.653	.063	.098	**.001**	.137	.163	**.016**	**.018**	p-value	Area36
Rostral PRH	r-value	.251	-.464	-.265	**.911****	**.920*****		**.854****	**.951*****	**.943*****	.566	**.698***	.651	**.779***	.645	.634	.287	.391	.610	.202	.632	.598	**.864****	.549	.500	**.795***	**.734***	r-value	Rostral PRH
	p-value	.515	.208	.491	**.001**	**<0.001**		**.003**	**<0.001**	**<0.001**	.112	**.037**	.058	**.013**	.061	.067	.454	.298	.081	.603	.068	.089	**.003**	.126	.171	**.010**	**.024**	p-value	
Mid Area35	r-value	.382	.023	.135	**.760***	.288	.566		**.835****	**.955*****	.585	.563	.588	**.823****	.569	.482	.499	.334	**.688***	.262	.446	.591	**.757***	.516	.657	**.893****	.531	r-value	Mid Area35
	p-value	.311	.954	.728	**.017**	.452	.112		**.005**	**<0.001**	.098	.115	.096	**.006**	.110	.189	.171	.380	**.041**	.496	.229	.094	**.018**	.155	.055	**.001**	.141	p-value	
Mid Area36	r-value	.634	-.296	-.165	**.728***	.425	.625	**.904****		**.961*****	**.701***	**.804****	**.774***	**.849****	**.675***	.528	.309	.415	.589	.221	.578	.602	**.723***	.381	.456	**.813****	**.787***	r-value	Mid Area36
	p-value	.067	.440	.672	**.026**	.254	.072	**.001**		**<0.001**	**.035**	**.009**	**.014**	**.004**	**.046**	.144	.419	.267	.095	.568	.103	.086	**.028**	.312	.217	**.008**	**.012**	p-value	
Mid PRH	r-value	.528	-.150	-.024	**.762***	.370	.612	**.973*****	**.979*****		**.673***	**.717***	**.714***	**.873****	.651	.528	.419	.392	.665	.251	.536	.623	**.772***	.466	.578	**.889****	**.692***	r-value	Mid PRH
	p-value	.144	.701	.950	**.017**	.327	.080	**<0.001**	**<0.001**		**.047**	**.030**	**.031**	**.002**	.057	.144	.262	.297	.051	.514	.137	.073	**.015**	.207	.103	**.001**	**.039**	p-value	
Caudal	r-value	**.716***	-.475	-.434	.546	.492	.566	.663	**.858****	**.785***		**.900****	**.973*****	**.732***	**.765***	.586	.606	.646	.576	.454	.529	**.781***	.229	.011	.127	.658	.580	r-value	Caudal
Area35	p-value	**.030**	.197	.244	.128	.178	.112	.052	**.003**	**.012**		**.001**	**<0.001**	**.025**	**.016**	.097	.083	.060	.105	.219	.143	**.013**	.554	.978	.744	.054	.101	p-value	Area35
Caudal	r-value	.584	-.491	-.486	.342	.282	.340	.407	**.683***	.567	**.897****		**.976*****	**.732***	**.675***	**.689***	.504	.577	.510	.308	**.678***	**.791***	.400	-.033	.148	.611	**.839****	r-value	Caudal
Area36	p-value	.099	.179	.184	.367	.463	.371	.277	**.043**	.111	**.001**		**<0.001**	**.025**	**.046**	**.040**	.166	.104	.161	.421	**.045**	**.011**	.286	.933	.703	.080	**.005**	p-value	Area36
Caudal PRH	r-value	.661	-.497	-.475	.446	.387	.454	.537	**.783***	**.684***	**.969*****	**.978*****		**.751***	**.737***	.656	.568	.626	.556	.388	.622	**.807****	.326	-.012	.142	.651	**.733***	r-value	Caudal PRH
	p-value	.052	.174	.197	.228	.303	.219	.136	**.013**	**.042**	**<0.001**	**<0.001**		**.020**	**.023**	.055	.111	.071	.120	.302	.074	**.009**	.392	.975	.716	.058	**.025**	p-value	
Te2	r-value	.345	-.132	-.021	**.700***	.158	.461	**.799****	**.819****	**.830****	.633	.558	.608		**.787***	.529	**.701***	.662	**.845****	.592	.421	**.796***	.649	.394	.601	**.964*****	**.766***	r-value	Te2
	p-value	.363	.734	.958	**.036**	.684	.212	**.010**	**.007**	**.006**	.068	.118	.083		**.012**	.144	**.035**	.052	**.004**	.093	.259	**.010**	.058	.294	.087	**<0.001**	**.016**	p-value	
LEC	r-value	.654	-.097	-.131	.186	-.130	.026	**.733***	**.715***	**.742***	.599	.476	.546	.633		**.705***	.586	**.897****	**.819****	**.771***	.452	**.806****	.379	.495	.360	**.776***	.589	r-value	LEC
	p-value	.056	.804	.737	.632	.739	.946	**.025**	**.030**	**.022**	.088	.196	.128	.067		**.034**	.097	**.001**	**.007**	**.015**	.222	**.009**	.314	.176	.341	**.014**	.095	p-value	
MEC	r-value	.317	.191	.308	.396	-.086	.162	**.735***	**.740***	**.756***	.641	.586	.627	**.701***	.662		.582	**.682***	.594	.440	.636	**.833****	.520	.393	.175	.512	.656	r-value	MEC
	p-value	.406	.622	.419	.292	.827	.676	**.024**	**.023**	**.018**	.063	.097	.071	**.035**	.052		.100	**.043**	.092	.236	.065	**.005**	.151	.295	.652	.158	.055	p-value	
POR	r-value	**.688***	-.191	-.130	.209	-.010	.106	**.671***	**.771***	**.742***	**.740***	**.692***	**.733***	.586	**.875****	**.835****		**.678***	**.736***	**.679***	.212	**.841****	.318	.181	.335	**.671***	.456	r-value	POR
	p-value	**.040**	.623	.738	.590	.981	.787	**.048**	**.015**	**.022**	**.023**	**.039**	**.025**	.097	**.002**	**.005**		**.045**	**.024**	**.044**	.584	**.005**	.404	.641	.378	**.048**	.218	p-value	
CA1	r-value	.583	.004	-.080	-.073	-.393	-.259	.516	.570	.559	.504	.524	.529	.510	**.917****	.664	**.859****		**.851****	**.932*****	.497	**.862****	.193	.254	.398	.648	.558	r-value	CA1
	p-value	.100	.991	.837	.852	.295	.501	.155	.109	.118	.167	.147	.143	.161	**.001**	.051	**.003**		**.004**	**<0.001**	.174	**.003**	.620	.509	.289	.059	.118	p-value	
CA3	r-value	.535	-.249	-.267	.460	.110	.306	.661	**.787***	**.746***	.610	.572	.605	**.712***	.665	.436	.552	.659		**.863****	.530	**.852****	.528	.435	**.760***	**.907****	.575	r-value	CA3
	p-value	.138	.519	.488	.213	.779	.423	.053	**.012**	**.021**	.081	.108	.084	**.031**	.050	.240	.123	.053		**.003**	.143	**.004**	.144	.242	**.017**	**.001**	.105	p-value	
DG	r-value	.616	-.085	-.188	-.029	-.228	-.143	.463	.602	.550	.570	.599	.601	.372	**.778***	.548	**.772***	**.906****	**.769***		.304	**.727***	.103	.257	.512	.623	.344	r-value	DG
	p-value	.078	.827	.629	.940	.555	.713	.209	.086	.125	.109	.089	.087	.324	**.014**	.126	**.015**	**.001**	**.015**		.427	**.027**	.792	.505	.159	.073	.365	p-value	
Dorsal Sub	r-value	.264	-.189	-.264	.271	-.115	.080	.323	.411	.379	.286	.350	.329	**.699***	.414	.161	.178	.438	**.767***	.396		.657	.439	-.057	.426	.458	.613	r-value	Dorsal Sub
	p-value	.493	.627	.492	.481	.768	.838	.396	.272	.315	.456	.356	.387	**.036**	.268	.680	.646	.238	**.016**	.291		.055	.237	.885	.252	.215	.079	p-value	
Ventral Sub	r-value	**.688***	-.169	-.099	.488	.242	.395	**.783***	**.848****	**.838*****	**.817****	.593	**.713***	**.757***	**.740***	**.768***	**.752***	.609	.575	.519	.378		.465	.198	.426	**.766***	**.736***	r-value	Ventral Sub
	p-value	**.040**	.664	.799	.183	.530	.292	**.013**	**.004**	**.005**	**.007**	.092	**.031**	**.018**	**.023**	**.016**	**.019**	.082	.105	.152	.315		.207	.610	.253	**.016**	**.024**	p-value	
PL	r-value	**.691***	-.273	-.194	.345	.048	.210	.622	**.805****	**.737***	**.748***	**.716***	**.750***	**.820****	**.727***	**.770***	**.796***	**.734***	**.706***	.647	.595	**.871****		.638	.507	**.693***	.583	r-value	PL
	p-value	**.039**	.478	.618	.364	.903	.587	.073	**.009**	**.024**	**.021**	**.030**	**.020**	**.007**	**.027**	**.015**	**.010**	**.024**	**.033**	.060	.091	**.002**		.065	.163	**.038**	.099	p-value	
MD	r-value	**.909****	**-.755***	**-.702***	.392	.513	.496	.489	**.761***	.649	**.867****	**.772***	**.836****	.591	.592	.389	.651	.484	.631	.512	.448	**.754***	**.782***		.324	.500	.116	r-value	MD
	p-value	**.001**	**.019**	**.035**	.297	.158	.175	.182	**.017**	.059	**.002**	**.015**	**.005**	.094	.093	.300	.058	.186	.069	.158	.226	**.019**	**.013**		.395	.171	.766	p-value	
ATN	r-value	**.906****	**-.719***	-.594	.418	.500	.503	.523	**.787***	**.679***	**.775***	.655	**.729***	.619	.585	.420	.656	.472	.638	.483	.436	**.754***	**.813****	**.961*****		**.732***	.393	r-value	ATN
	p-value	**.001**	**.029**	.092	.262	.170	.168	.148	**.012**	**.044**	**.014**	.055	**.026**	.076	.098	.260	.055	.200	.064	.187	.241	**.019**	**.008**	**<0.001**		**.025**	.295	p-value	
Reuniens	r-value	**.676***	-.267	-.325	.345	.022	.196	**.671***	**.789***	**.752***	**.716***	.655	**.701***	**.775***	**.826****	.550	**.694***	**.801****	**.915****	**.790***	**.778***	**.768***	**.850****	**.755***	**.721***		.641	r-value	Reuniens
	p-value	**.045**	.487	.393	.364	.955	.614	**.048**	**.012**	**.020**	**.030**	.055	**.035**	**.014**	**.006**	.125	**.038**	**.009**	**.001**	**.011**	**.014**	**.016**	**.004**	**.019**	**.028**		.063	p-value	
Aud	r-value	.000	-.043	.061	.510	.063	.306	.357	.350	.362	.199	.182	.195	**.781***	.150	.303	.046	.059	.338	-.139	**.711***	.439	.537	.289	.337	.419		r-value	Aud
	p-value	1.000	.912	.877	.161	.872	.423	.346	.355	.338	.609	.639	.616	**.013**	.700	.428	.907	.880	.373	.721	**.032**	.237	.136	.452	.376	.262		p-value	
		Recency Control group																		Recency Control group									

The top right diagonal matrix (darker grey) relates to data from the Recency Test group while to bottom left diagonal matrix (lighter grey) relates to data from the Recency Control group. Significant correlations (uncorrected) are in bold. *p<0.05, **p<0.01, ***p<0.001. Abbreviations: see Figure 4.1.

4.3.2.2.1 Perirhinal cortex

Comparisons involving the six sub-regions of perirhinal cortex found no significant difference in the numbers of Fos-positive cells between the Recency Test and Control groups ($F < 1$; Figures. 4.3A, 4.4). There was no differential effect on the rostral mid or caudal level of perirhinal cortex ($F < 1$) nor a difference between areas 35 or 36 ($F_{1,16} = 3.14$, $p = 0.095$). Additionally, none of the interactions were significant ($F < 1$).

For the Recency Test group, there were significant correlations between the Fos counts and the D1 index in rostral areas 35 and 36 (area 35: $r = 0.76$, $p = 0.017$; area 36: $r = 0.67$, $p = 0.048$) but no significant correlations were found with D2 ($p > 0.1$). Similarly, mid area 35 and 36 correlated with D1 (area 35: $r = 0.80$, $p = 0.01$; area 36: $r = 0.69$, $p = 0.039$), but again no significant correlations with D2 (area 35: $p = 0.21$; area 36: $p = 0.056$). However, a more consistent effect was seen in caudal 35 and 36 where c-*fos* counts significantly correlated with D1 (area 35: $r = 0.80$, $p = 0.01$; area 36: $r = 0.72$, $p = 0.027$) and with D2 (area 35: $r = 0.79$, $p = 0.012$; area 36: $r = 0.88$, $p = 0.002$). No comparable D1 or D2 correlations were found for the Recency Control group. The only significant correlation in this group was between caudal area 35 and total exploration ($r = 0.72$, $p = 0.03$).

4.3.2.2.2 Parahippocampal cortices

Among these areas there was no evidence that the total counts of Fos-positive neurons differed between the Recency Test and Control groups ($F < 1$), nor was there a region of interest by group interaction ($F < 1$; Figure 4.3B).

There were significant correlations between discrimination performance by the Recency Test rats and their Fos counts in the lateral entorhinal cortex (D1: $r = 0.72$, $p = 0.029$; D2: $r = 0.76$, $p = 0.018$) and in the medial entorhinal cortex (D1: $r = 0.77$, $p = 0.014$; D2: $r = 0.72$, $p = 0.03$). In the postrhinal cortex, a significant correlation was also found with D2 ($r = 0.68$, $p = 0.045$). Finally, the Recency Test group also had a significant correlation between Fos protein counts in area Te2 and the updated D2 ratio ($r = 0.77$, $p = 0.014$). The Recency Control group presented a very different picture as none of the parahippocampal cortical areas correlated with the discrimination parameters D1 or D2 (presumably reflecting the very low D1 and D2 scores). This group did, however, show a significant correlation between the Fos counts in postrhinal cortex and total exploration ($r = 0.69$, $p = 0.04$).

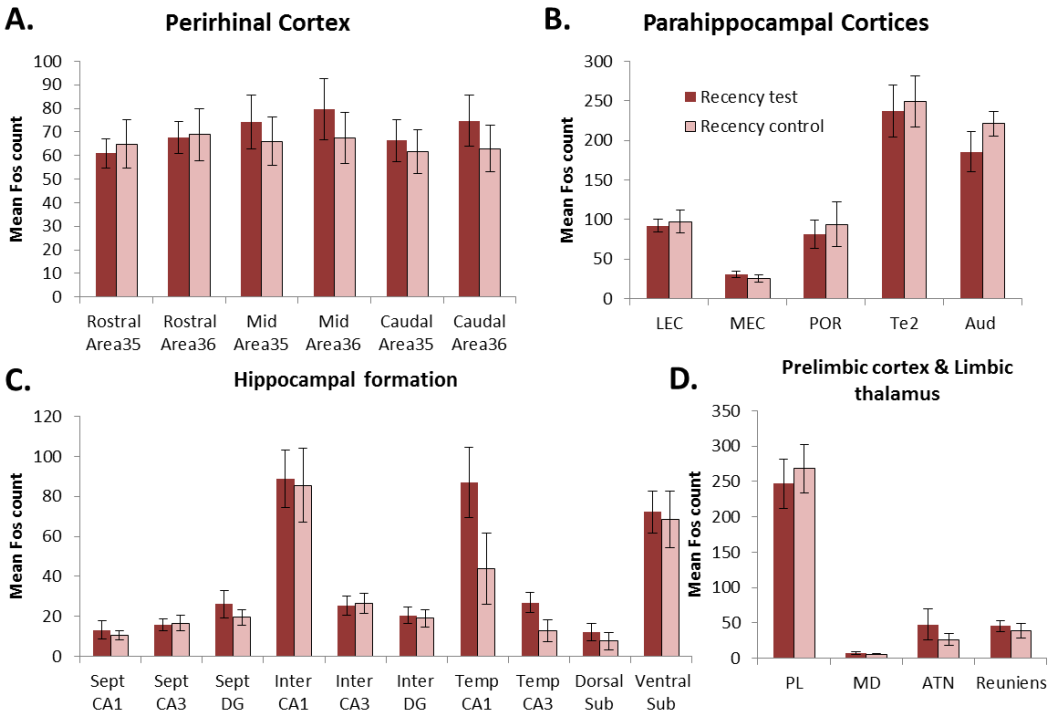

Figure 4.3. Counts of Fos-positive cells in regions of interest following the two behavioural conditions in Experiment 2.

Darker bars represent the Recency Test group while the lighter bars represent the Recency Control group. Abbreviations: ATN, anterior thalamic nuclei; Aud, primary auditory cortex; CA fields, intermediate (inter), septal (sept) and temporal (temp); DG, dentate gyrus, intermediate (inter) and septal (sept); dorsal Sub, dorsal subiculum; LEC, lateral entorhinal cortex; MEC, medial entorhinal cortex; MD, medial dorsal thalamic nucleus; PL, prelimbic cortex; POR, postrhinal cortex; Reuniens, nucleus reuniens of thalamus; Te2, area Te2; ventral Sub, ventral subiculum. Data are presented as group mean ± SEM.

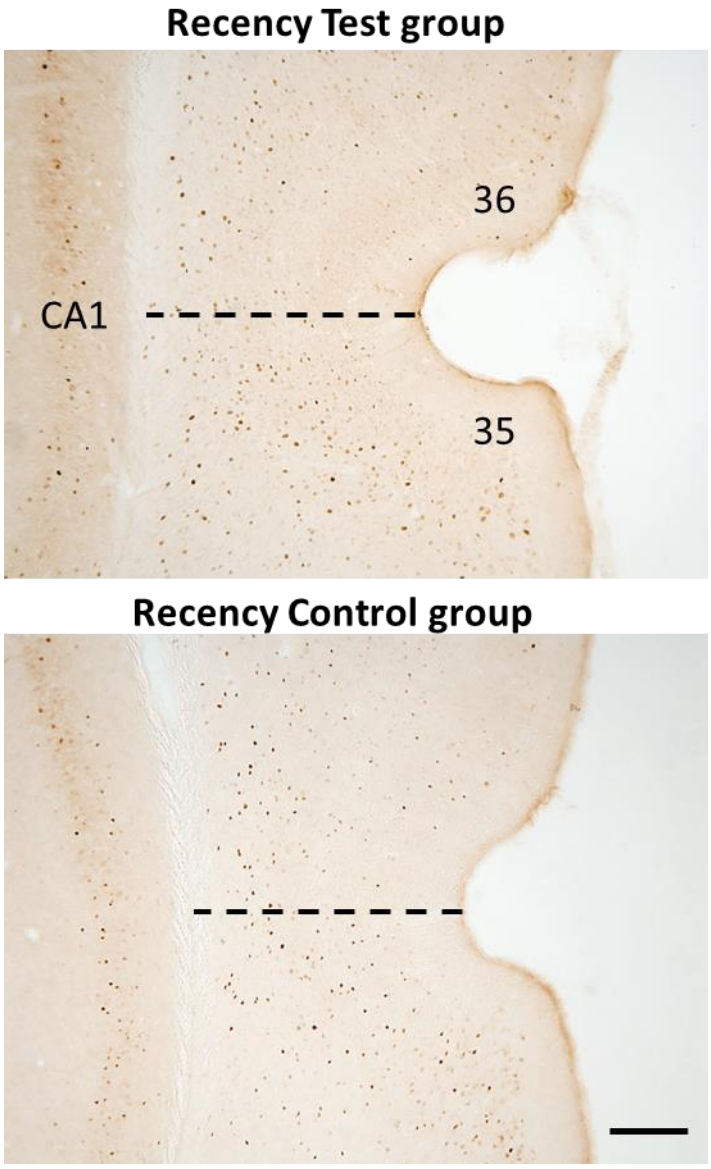

Figure 4.4. Representative photomicrographs of perirhinal cortex.

Photomicrographs depict Fos-positive cells in the perirhinal cortex (coronal section) from rats in the Recency Test (top panel) and Recency Control (bottom panel) groups. The areas shown are caudal perirhinal cortex (area 35 and 36) and hippocampal field CA1. Scale bar 200 µm.

4.3.2.2.3 Hippocampal formation

No significant differences were found in the total number of Fos-positive cells between the two behavioural groups in septal or intermediate CA1, CA3 or dentate gyrus, or temporal CA1 and CA3 ($F < 1$), nor was there an interaction between region and group ($F < 1$; Figure 4.3C).

For the Recency Test group, significant positive correlations were found between D2 and CA1 Fos counts ($r = 0.79$, $p = 0.011$) but not D1 ($r = 0.57$, $p = 0.106$). Both

discrimination indices correlated with Fos counts in CA3 (D1: r = 0.67, p = 0.049; D2: r = 0.68, p = 0.045). In the same group, neither D1 nor D2 correlated significantly with the dentate gyrus counts (D1: r = 0.39, p = 0.29; D2: r = 0.60, p = 0.09). The Recency Control group failed to show any significant correlation between discrimination behaviour and Fos counts. (Note that the correlation data here refer to the subfield counts summed across the septal, intermediate and temporal hippocampus).

There was also no evidence of a Fos count difference between the two behavioural groups ($F < 1$) in either division of the subiculum (dorsal or ventral), nor was there an interaction between the behavioural groups and the regions of interest ($F < 1$; Figure 4.3C).

In the Recency Test group, the ventral subiculum Fos counts showed significant correlations with both D1 (r = 0.78, p = 0.013) and D2 (r = 0.88, p = 0.002). There was also a borderline significant correlation between D1 and the dorsal subiculum Fos counts (r = 0.66, p = 0.052) but not for the D2 index (r = 0.55, p = 0.12). In contrast, analyses using the Recency Control data found no significant correlations for either the ventral and dorsal subiculum with D1 or D2 (all $p > 0.05$).

4.3.2.2.4 Prelimbic cortex and limbic thalamus

As described above, the Fos counts for the three anterior thalamic nuclei were first combined as their individual counts were typically very low. Thus, the regions of interest to be compared were the anterior thalamic nuclei (ATN), the medial dorsal thalamic nucleus (MD), nucleus reuniens of the thalamus as well as the prelimbic cortex (Figure 4.3D). The counts of Fos-positive cells did not differ between the two behavioural groups ($F < 1$) and there was no interaction ($F < 1$).

The Fos count in the nucleus reuniens correlated significantly with D1 (r = 0.72, p = 0.03) in the Recency Test group; no other significant correlations were found between the behavioural measures (D1 and D2) and the Fos counts in the other limbic regions of interest in the Recency Test group. There was a significant negative correlation in the Recency Control group between MD counts and both the D1 (r = -0.76, p = 0.019) and the updated D2 (r = -0.70, p = 0.035) discrimination indices. In addition, the MD counts in this group significantly correlated with exploration (r = 0.91, p = 0.001). Also, in the Recency Control group the ATN Fos counts correlated significantly with D1 (r = -0.72, p = 0.029) and total exploration (r = 0.91, p = 0.001), but not with the updated D2 (r = 0.59, p = 0.092). Finally, the Fos counts in nucleus reuniens and the prelimbic cortex

correlated significantly with total exploration (r = 0.70, p = 0.045; r = 0.69, p = 0.039 respectively) in the Recency Control group (D1 and D2: p > 0.4).

4.3.2.2.5 Auditory cortex

No differences were found between the two groups in this area (t_{16} = 1.21, p = 0.24; Figure 4.3). There was, however, a positive correlation between Fos expression and the D2 ratio in the Recency Test group (r = 0.88, p = 0.002). No significant correlations were found between behaviour and region of interest in the Recency Control group.

4.3.3 Structural equation modelling

4.3.3.1 Testing previously derived model of familiar object processing

The first network model to be tested was that previously derived for familiar object processing (Chapter 3). This network was composed of parallel projections between area Te2 and both perirhinal and lateral entorhinal cortices. Perirhinal cortex also connected with lateral entorhinal cortex which then projected directly to the septal region of CA1. Fos data derived from both the Recency Test (Figure 4.5A) and Recency Control (Figure 4.5B) groups were tested on this network model. Overall, this model was found to attain a good level of fit for both behavioural groups (Recency Test: χ^2_2 = 2.21, p = 0.33; CFI = 0.99; RMSEA = 0.11; Recency Control: χ^2_2 = 0.16, p = 0.92; CFI = 1.0; RMSEA = 0.0). Additionally, when the Fos data obtained from the current Recency Test group were stacked against Fos data generated by the Sham Familiar group in Chapter 3 on the same network model there was no difference between the groups ($\chi^2_{4\ Diff}$ = 4.37, p= 0.36). In contrast, when the data from the current Recency Test group were tested on the optimal network model derived for novel object processing (Figure 3.12E) in the Sham Novel group in Chapter 3 the indices of fit were found to be outside of acceptable levels (χ^2_5 = 6.96, p = 0.22; CFI = 0.93; RMSEA = 0.22). Furthermore, when the current Recency Test group was stacked against data from the Sham Novel group in Chapter 3, on the novel object network model, a significant difference was detected between the groups ($\chi^2_{5\ Diff}$ = 12.6, p = 0.004). Thus it can be concluded that the relationships between these regions differ when rats are discriminating novel as compared to familiar objects.

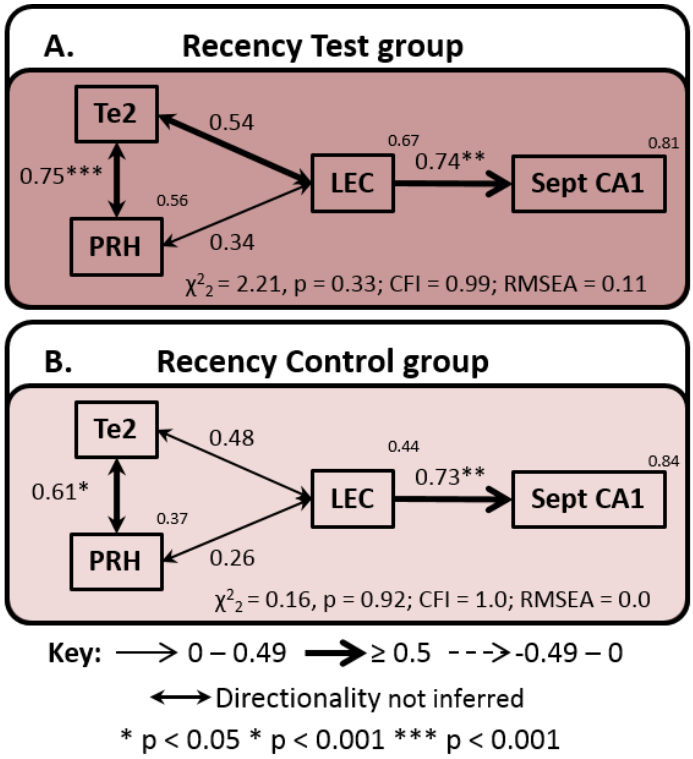

Figure 4.5. Model of familiar object processing

Depiction of data from the current Recency Test (A) and Recency control (B) groups tested on the network model previously derived for familiar object processing (Experiment 2). The model fit is provided at the bottom of each panel (CFI, comparative fit index; RMSEA, root mean square error of approximation). The strength of the causal influence of each path is denoted both by the thickness of the arrow and by the path coefficient next to that path. The number above each region is the proportion of its variance that can be explained by its inputs. Sites depicted: area Te2 (Te2); subfield CA1 from the septal region of the hippocampus (Sept CA1); lateral entorhinal cortex (LEC); prelimbic cortex (PL); perirhinal cortex (PRH). * $p < 0.05$ ** $p < 0.01$; *** $p < 0.001$.

4.3.3.2 Extended models for recency conditions

The next models to be tested were intended to extend this existing model of familiar object processing to include regions beyond the medial temporal lobe that have been shown to be involved in recency memory (Mitchell & Laiacona, 1998; Hannesson et al., 2004a,b; Wolff et al., 2006; Cross et al., 2013; Dumont & Aggleton, 2013). The Fos counts from areas 35 and 36 of the perirhinal cortex were combined, but the rostral, mid, and caudal perirhinal regions remained separate as previous studies have identified the particular significance of caudal perirhinal cortex for visual recognition (Albasser et al., 2009, 2010b; Chapter 3). Within the hippocampus, the septal, intermediate and temporal parts of CA1, CA3 and dentate gyrus were combined prior to testing for network models as preliminary analyses based on the separate results from each division (septal, intermediate or temporal) failed to create acceptable models. The counts from the three

anterior thalamic nuclei were summed as the individual scores were low. Only the dorsal subiculum was used to create models as it has been demonstrated that it is the dorsal subiculum that principally projects to the anterior thalamic nuclei (Wright et al., 2013).

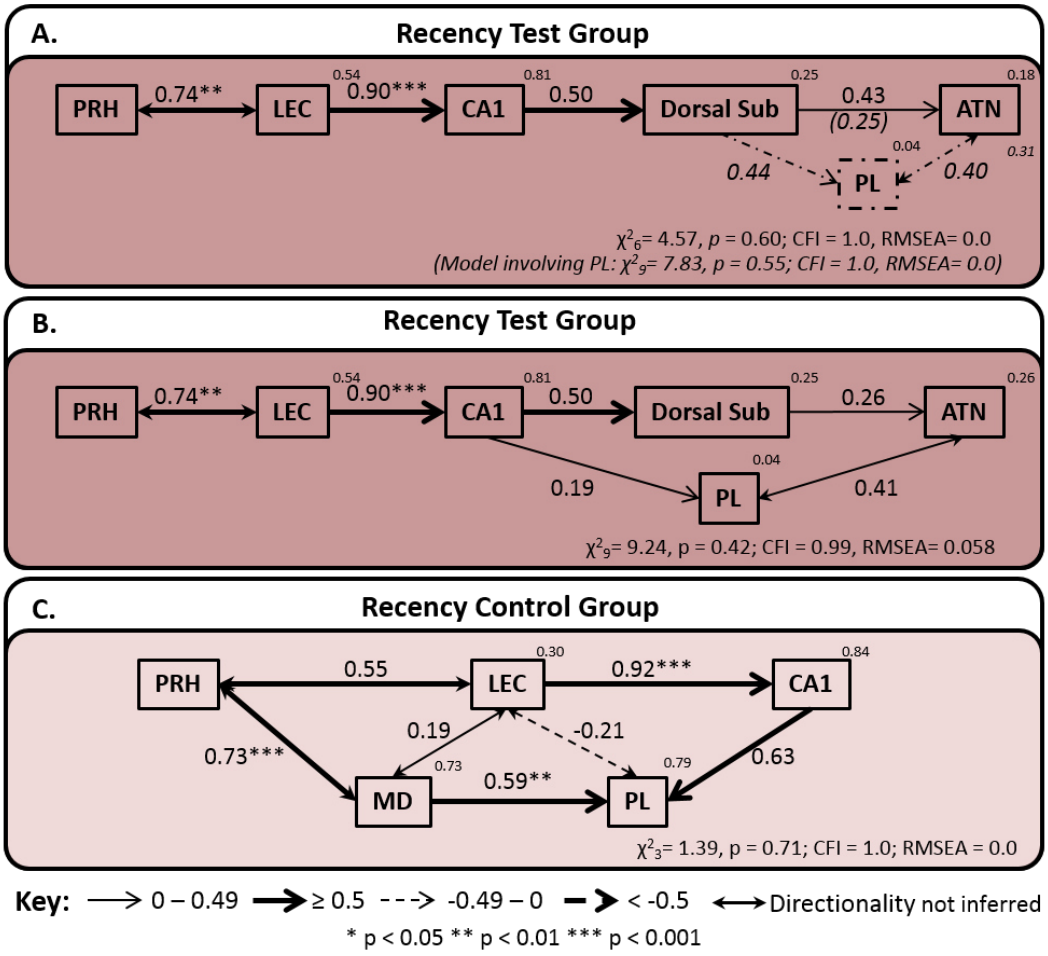

Figure 4.6. Optimal models for recency conditions.

Schematics of the network models with best fit for the Recency Test (A, B) and Recency control (C) groups (Experiment 2). The model fit is provided at the bottom of each panel (CFI, comparative fit index; RMSEA, root mean square error of approximation). The strength of the causal influence of each path is denoted both by the thickness of the arrow and by the path coefficient next to that path. Note, the dashed pathways involving the prelimbic cortex (PL) have been added to the first Recency Test model as these provide a further model with good fit. The number in brackets is the path coefficient when the prelimbic cortex is added to the Recency Test model and the additional fit indices in italics are related to this model. The number above each region is the proportion of its variance that can be explained by its inputs. Sites depicted: anterior thalamic nuclei (ATN); dorsal subiculum (Dorsal Sub); hippocampal subfield CA1; lateral entorhinal cortex (LEC); medial dorsal thalamic nucleus (MD); prelimbic cortex (PL); perirhinal cortex (PRH). ** $p < 0.01$; *** $p < 0.001$.

4.3.3.2.1 Recency Test group

It was possible to generate three very closely related models with good fit (Figure 4.5A, B), the only difference being whether prelimbic cortex was added to the network, and if so, where. The first network was a serial model involving a connection between caudal perirhinal cortex and lateral entorhinal cortex and then successive projections to CA1, dorsal subiculum, and the anterior thalamic nuclei (χ^2_6 = 4.57, p = 0.60; CFI = 1.0; RMSEA = 0.0; Figure 4.5A). The second model involved additional projections from the dorsal subiculum to the prelimbic cortex and between the prelimbic cortex to the anterior thalamic nuclei (χ^2_9 = 7.83, p = 0.55; CFI = 1.0; RMSEA = 0.0; Figure 4.5A). A third acceptable model again involved projections between perirhinal cortex and lateral entorhinal cortex, thence onto CA1, with CA1 projecting to both prelimbic cortex and the dorsal subiculum, with dorsal subiculum subsequently projecting to the anterior thalamic nuclei and an addition connection between prelimbic cortex and the anterior thalamic nuclei (χ^2_9 = 9.24, p = 0.42; CFI = 0.99; RMSEA = 0.06). In all three models, there were significant pathways from caudal perirhinal cortex to lateral entorhinal cortex (p = 0.002) and from lateral entorhinal to CA1 (p < 0.001). Also, as noted above, there were significant correlations between D1 and D2 with Fos counts in the perirhinal cortex, lateral entorhinal cortex, CA1 and CA3. None of the acceptable models for the Recency Test group involved the entorhinal projections to either dentate gyrus or CA3.

4.3.3.2.2 Recency Control group

Only one acceptable model involving parahippocampal and hippocampal regions could be derived (Figure 4.5C). Like the Recency Test group, the model for the Recency Control group again included caudal perirhinal cortex, the lateral entorhinal cortex and CA1, but in addition the model incorporated the prelimbic cortex and the medial dorsal thalamic nucleus (MD). The resulting network created a model with good fit (χ^2_3 = 1.39, p = 0.71; CFI = 1.0; RMSEA = 0.0). Three of the pathways involved in the models were significant; caudal perirhinal cortex to MD (p < 0.001), lateral entorhinal cortex to CA1 (p < 0.001) and the pathway from MD to the prelimbic cortex (p = 0.003).

4.3.3.2.3 Comparison between the models for Recency Test and Recency Control groups

Several acceptable models were generated for the Recency Test group; the comparisons to follow will be based on the network model depicted in Figure 4.6A that includes prelimbic cortex. This decision is based on the very good level of fit, as well as the inclusion of the prelimbic cortex in the model as this was hypothesised during study design.

Initially data from the Recency Control group were tested on the model derived for the Recency Test group (Figure 4.7A); this was found to have poor fit ($\chi^2_9 = 12.5$, $p = 0.19$; CFI = 0.88; RMSEA = 0.22). In the reverse comparison, the Fos data obtained from the Recency Test group were then tested on the optimal model for the Recency Control group (Figure 4.7B); the fit of this model was extremely poor ($\chi^2_3 = 15.0$, $p = 0.002$; CFI = 0.66; RMSEA = 0.71).

A stacking procedure was then undertaken between the Recency Test and Recency Control groups. Initially the data from these groups were stacked on the optimal model for the Recency Test group (Figure 4.7A); the structural weights of each of the paths were constrained such that they had to have the same value in both groups, i.e., setting the corresponding pathways in each of the groups to be identical. There was no significant difference between the model in which the structural weights of the paths were constrained to be the same and the model in which they were free to vary ($\chi^2_{6\ Diff} = 9.16$, $p = 0.16$). This is not necessarily surprising considering both groups are exploring objects that are familiar due to a single previous exposure and the pathways from perirhinal cortex to lateral entorhinal cortex and then to CA1 are a component of both optimal models. However, the groups do differ from one another as the optimal models for each group are different (Figure 4.6). Furthermore, when the same stacking procedure is carried out based on the optimal model for the Recency Control group (Figure 4.7B) a significant difference was found between the model in which the structural weights are free to vary and the model in which they are constrained to be the same ($\chi^2_{7\ Diff} = 19.4$, $p = 0.007$). This illustrates that the Fos data from the Recency Test group does not fit the Recency Control group model. When the pathways were unconstrained individually the only one to significantly improve the fit of the model was that between the perirhinal cortex and MD ($\chi^2_{1\ Diff} = 12.4$, $p = 0.0004$; all other paths: $\chi^2_{1\ Diff} < 2$, $p > 0.13$).

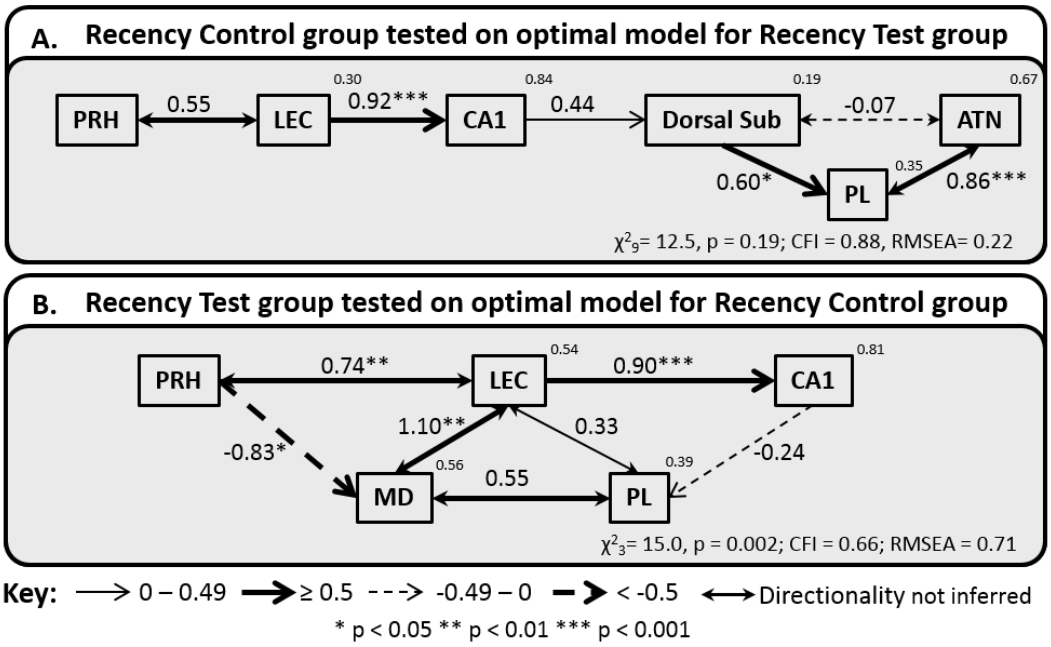

Figure 4.7. Poor fitting models of Recency data tested on the optimal model for the other group.

Schematics of the network models for the Recency Control group tested on the optimal model for the Recency Test group (A) and Recency Test group tested on the optimal model for the Recency Control group (B) (Experiment 2). The model fit is provided at the bottom of each panel (CFI, comparative fit index; RMSEA, root mean square error of approximation) and models with unacceptable fit are represented with a pale grey background. The strength of the causal influence of each path is denoted both by the thickness of the arrow and by the path coefficient next to that path. The number above each region is the proportion of its variance that can be explained by its inputs. Sites depicted: anterior thalamic nuclei (ATN); dorsal subiculum (Dorsal Sub); hippocampal subfield CA1; lateral entorhinal cortex (LEC); medial dorsal thalamic nucleus (MD); prelimbic cortex (PL); perirhinal cortex (PRH). * $p < 0.05$;** $p < 0.01$; *** $p < 0.001$.

4.4 Discussion

The present experiment used the expression of c-*fos* to map neuronal activity associated with object recency memory in rats. By applying structural equation modelling to the counts of Fos-positive cells, models have previously been derived that interlink medial temporal activity associated with recognition memory (Albasser et al., 2010b; Chapter 3). The present study sought to confirm and extend these investigations by deriving activity models for recency memory, i.e., temporal order memory.

The Recency Test group in Experiment 2 was able to discriminate between familiar objects separated by an interval of 110 minutes. In contrast, the Recency Control rats were given pairs of familiar objects that were separated by, at most, one minute (but often in practice, only seconds). In this way, it was possible to very closely match the

sensorimotor experiences of the two groups. The Recency Control group showed no evidence of being able to discriminate between the test objects. Thus, although the control rats were given a recency problem, the behavioural evidence indicated that the rats in this condition treated the objects as though they were temporally indistinguishable.

An important assumption is that in Experiment 2 the Recency Test group relied on recency memory. It has been suggested that in this type of recency task, that employs two discrete sample phases, greater exploration time dedicated to the object from the first sample phase may actually reflect the fact that the rat had forgotten that it previously encountered this object (Ennaceur, 2010). This would essentially mean that the task was an object recognition task. In order to address this possibility, all rats were first tested on their ability to distinguish novel from familiar objects (Experiment 1). This initial experiment used the same retention delays for the familiar objects as those subsequently used for the recency memory tests in Experiment 2. The ability of the rats to recognise novel objects, when compared with familiar objects encountered 110 minutes previously in sample phase 1 of Experiment 1, confirmed that they could retain familiarity information over the time intervals subsequently used in the recency tests. This finding is important as it shows that the recency tests did involve the rats discriminating between two familiar objects. A caveat is that it cannot be proven that this assumption applies to each individual trial as the results from Experiment 1 reflect cumulative data from multiple trials, while the objects, by necessity, were different from those in Experiment 1.

Performance in the Recency Test condition, as measured by the discrimination measures, cumulative D1 and updated D2, correlated with the Fos-positive cell counts in several regions of interest; most notably within the parahippocampal cortex and hippocampus. Significant positive correlations with recency performance were found for both areas 35 and 36 along the rostral-caudal extent of the perirhinal cortex. Other positive correlations between recency discrimination performance and Fos counts were found in area Te2 and lateral entorhinal cortex. There is a danger of Type 1 errors due to multiple comparisons based on the relatively low numbers of rats in the Recency Test group and the total numbers of correlations. There was, however, a strong clustering of significant correlations in the regions that have been associated with recency memory in previous studies. For example, the link between recency memory performance and activity in the perirhinal cortex builds on considerable evidence highlighting the role of

this area in processing complex visual information, including information to help resolve both visual recognition and visual recency problems (Fahy, 1993; Brown & Xiang, 1998; Brown & Aggleton, 2001; Hannesson et al., 2004a; Winters et al., 2008; Barker et al., 2007; Barker & Warburton, 2011a). Moreover, these correlations were strongest and most consistent in the caudal region of perirhinal cortex. This fits with the mounting evidence that the caudal region of perirhinal cortex has a greater role in visual object processing than more rostral levels (Zhu et al., 1995; Wan et al., 1999, 2004; Warburton et al., 2003, 2005; Albasser et al., 2009, 2010b; Chapter 3). The correlations presented here extend this object processing association to include the visual association area, Te2, and the entorhinal cortex; regions that are both strongly interconnected with the perirhinal cortex (Burwell & Amaral, 1998b; Furtak et al., 2007). Area Te2 has previously been implicated in object recognition memory, with evidence from lesion studies (Ho et al, 2011) and c-*fos* expression studies (Zhu et al., 1995b, 1996, 1997; Wan et al., 1999, 2004; Albasser et al., 2010b). The present, additional links with recency memory also builds on previous electrophysiological evidence that Te2 cells can signal temporal order differences (Zhu et al., 1995a). Additionally, significant correlations were observed between the recency memory performance in the Recency Test group and the Fos-positive cell counts in CA1, CA3 and subiculum. This regional pattern parallels existing literature on hippocampal lesion studies. These have not only shown the importance of the hippocampus for object recency memory (Barker et al., 2007; Barker & Warburton, 2011a), including when tested in the bow-tie maze (Albasser et al., 2012), but have also shown that this hippocampal involvement depends on the perirhinal cortex (Warburton & Brown, 2010; Barker & Warburton, 2011b). Further, neuronal recording studies have implicated the hippocampus in encoding the passage of time (Manns et al., 2007; Kraus et al., 2013).

There were no differences found between the two behavioural conditions in the number of Fos-positive cells in any of the analysed regions of interest. This may reflect how well matched the sensorimotor demands of the groups were. There are studies that have demonstrated a similar overall lack of absolute regional differences, while the underlying correlations between the same regions were different (Poirier et al., 2008; Chapter 3). These patterns of correlations were explored with structural equation modelling.

The first network model to be tested was the optimal model derived for group Sham Familiar in Chapter 3. This model begins with the visual association area, Te2, which

projects to both the caudal region of the perirhinal cortex and adjacent lateral entorhinal cortex. The perirhinal cortex also converges on lateral entorhinal cortex, which projects directly to CA1 in the septal region of the hippocampus. This network model was found to have good fit for both behavioural conditions in the current experiment. Furthermore, when data from the current Recency Test group were directly compared on this network model with data from group Sham Familiar in Chapter 3, no differences were found between them. In the experiment described in Chapter 3, the Sham Familiar rats were simultaneously shown a highly familiar object (last seen in the previous trial) and an object that is less recent but still highly familiar (seen in all 12 previous sessions). The same protocol was also used for 'Group Familiar' in Albasser et al., 2010b. Consequently, these familiarity conditions involved recency judgements; albeit less temporally controlled. It is, therefore, striking that in four behavioural conditions involving familiar objects (Recency Test, Recency Control, group 'Sham Familiar' from Chapter 3 and 'Group Familiar' from Albasser et al., 2010b), the optimal network model involved direct lateral entorhinal cortex to CA1 interactions but not lateral entorhinal to dentate gyrus or CA3 interactions. The same patterns are echoed in a *zif*268 study of spatial learning, as familiar spatial problems preferentially engaged entorhinal cortex to CA1 pathways, while more novel spatial problems engaged pathways from entorhinal cortex to the dentate gyrus and CA3 (Poirier et al., 2008).

Further to this, when the present Recency Test group was tested on the best fitting model associated with the discrimination of novel stimuli, i.e., recognition memory, that was derived for group 'Sham Novel' in the experiment outlined in Chapter 3, the fit was inadequate. For object recognition memory, the optimal network had parallel pathways from area Te2 to the lateral entorhinal cortex and the perirhinal cortex, the perirhinal pathway then converged on the lateral entorhinal cortex (Figure 3.12E). Subsequently the lateral entorhinal cortex projected to CA3 and then on to CA1. The lack of fit of the present recency data to that model was confirmed by the result of the stacking procedure that directly compared Fos data from the current Recency Test group with data from the Sham Novel group in Chapter 3 on the network of novel object recognition (Figure 3.12E). The dataset for each group were found to be significantly different from one another. The optimal network model derived for 'Group Novel' in Albasser et al., 2010b, which also performed a novel object recognition task, involved parallel pathways from the lateral entorhinal cortex; one to the dentate gyrus and another to CA1. The dentate gyrus pathway next involved CA3, which then converged on CA1. Thus, it appears that the presence of novelty led to different patterns of hippocampal

engagement, involving greater parahippocampal interaction with dentate gyrus and/or CA3.

Following these initial SEM analyses, the subsequent aim of this study was to extend the network models to include regions beyond the medial temporal lobe but known to interact with medial temporal lobe structures to support associative memory (Aggleton, 2012). The individual septotemporal levels (septal, intermediate and temporal) of CA1, CA3 and dentate gyrus were collapsed as this allowed for simplification of the models to be tested, as, for example, previous models have been based in the septal region of the hippocampus but the temporal level of CA1 preferentially projects to prelimbic cortex (Conde et al., 1995). Additionally, preliminary investigations based on the separate results from each hippocampal level failed to generate models of acceptable fit.

Perhaps unsurprisingly, based on the fact that the data from both groups fit the same familiar object processing model, the optimal c-*fos* network models derived specifically for the Recency Test and Recency Control conditions individually were quite similar. Based on the preceding analyses this is hypothesised to reflect the fact that both conditions involved objects that were familiar. Both networks involved pathways from the caudal perirhinal cortex to lateral entorhinal cortex and, thence, to CA1. The dorsal subiculum was used to create models as it has been demonstrated that it is the dorsal rather than the ventral subiculum or CA subfields of the hippocampus that principally project to the anterior thalamic nuclei (Swanson & Cowen, 1975; Sikes et al., 1977; Wright et al., 2013). Neither the dentate gyrus nor CA3 could be incorporated into models with acceptable fit. The two networks did, however, differ as the main Recency Test model was linear while the Recency Control model had parallel pathways from the perirhinal cortex (Figure 4.6). As a consequence, the Recency Control model contained fewer degrees of freedom, so limiting its ability to pick out the key pathways.

The network models for both behavioural groups involved the prelimbic cortex, as well as limbic thalamic nuclei. Prelimbic cortex has repeatedly been implicated in recency memory (Hannesson et al., 2004a,b; DeVito & Eichenbaum, 2011; Cross et al., 2013). Additionally, it is known to project to the anterior thalamic nuclei, specifically to the anteromedial nucleus. Also, there are direct projections from CA1 and the subiculum to prelimbic cortex (Conde et al., 1995; Vertes, 2004), further supporting the models derived for the Recency Test group. In support of the Recency Control model, the medial prefrontal cortex is also known to be densely reciprocally connected to the medial dorsal thalamic nucleus (Groenewegen, 1988) and there is disconnection

evidence that these areas operate in conjunction to support recency discriminations (Cross et al., 2013). Further, the medial dorsal thalamic nucleus is known to receive projections from the deep layers of lateral entorhinal cortex (Groenewegen, 1988).

Lesion studies have implicated the anterior thalamic nuclei in some forms of recency memory (Mitchell & Dalrymple-Alford, 2005; Wolff et al., 2006; Dumont & Aggleton, 2013). In the present study, the anterior thalamic nuclei were incorporated in the best fitting models for the Recency Test group while the medial dorsal nucleus was incorporated in the Recency Control model. The implication is that the anterior thalamic nuclei and medial dorsal nuclei have subtly different roles concerning familiar objects; this is conceivable based on their very different properties. In particular, the anterior thalamic nuclei have been repeatedly implicated in episodic memory (Aggleton & Brown, 1999, 2006; Carlesimo et al., 2011), and it could be argued that tests of recency memory which involve intervening events, as well the passage of time *per se*, place added demands on episodic memory (see Eacott & Easton, 2010). In doing so, one would predict a particular link between the subiculum and anterior thalamic nuclei for such recency problems as seen here. An inconsistency is that these anterior thalamic lesion studies found deficits in tests of recency memory that involved comparing stimuli that were encountered in a single sequence, rather than when an intervening event was introduced between stimulus presentations (Wolff et al., 2006; Dumont & Aggleton, 2013). Thus, the opposite pattern to the one presented here may have been expected; i.e. anterior thalamic involvement in the Recency Control rather than the Recency Test model. However, there were additional differences between those studies and the present one. Wolff et al., (2006) employed a different stimulus type (odours). Dumont and Aggleton (2013) used fewer objects with shorter retention delays. Furthermore, in a single lesion study it was demonstrated that lesions of the anterior thalamic nuclei cause a deficit in a recency memory task that involved a delay while a lesion to the posteromedial thalamus, which included the medial dorsal nucleus, did not (Mitchell & Dalrymple-Alford, 2005). Thus, further work is required to elucidate the precise nature of the role that these thalamic nuclei play in recency memory. The present models do, however, provide support for the parahippocampal–prefrontal network for discriminating the familiarity and recency of occurrence of objects (Aggleton, 2012).

4.4.1 Summary

In summary, tasks involving familiar stimuli (recency memory) result in networks of activation that differ appreciably from those networks associated with novel stimuli

(recognition memory). Although all of the networks involve the hippocampus, lesion evidence shows that this structure is often not required for successful novelty detection (Mumby, 2001; Winters et al., 2004; Forwood et al., 2005; Brown et al., 2010), although it is consistently required for recency memory (Agster et al., 2002; Fortin et al., 2002; Barker et al., 2007; Barker & Warburton, 2011a,b; but see Chapter 3). Furthermore, recency memory appears especially linked with the CA1 field, with supporting evidence from both lesion studies (Gilbert et al., 2001; Hoge & Kesner, 2007; Kesner et al., 2010) and the present c-*fos* analyses. The implication is that object novelty is initially detected upstream from the hippocampus and this information then moderates modes of hippocampal processing. This change in the hippocampal processing of novel stimuli could then result in better learning of stimulus attributes, via activity in the dentate gyrus and CA3. This enhanced attribute information can then aid recognition judgments as the associated information may increase the confidence of novel versus familiar discriminations (Eichenbaum et al., 2010). At the same time, the novelty signal itself is often sufficient to guide object recognition and so does not require the integrity of the hippocampus.

5 Mapping activity patterns for encoding a novel context following removal of the perirhinal cortex in rats

5.1 Introduction

The hippocampus is central to processing spatial aspects of memory; this has been demonstrated across many experimental paradigms including electrophysiological recording studies, lesion studies and disconnection studies (O'Keefe & Dostrovsky 1971; Morris et al., 1982; Moser et al., 1993; O'Keefe & Burgess, 1996; Gaffan & Eacott, 1997; Broadbent et al., 2004; Warburton & Brown, 2010; Albasser et al., 2013). The perirhinal cortex is vitally involved in successful recognition memory (Suzuki et al., 1993; Mumby & Pinel, 1994; Xiang & Brown, 1998; Barker et al., 2007); the ability to discriminate novel from familiar stimuli (Mandler, 1980; Brown & Aggleton, 2001). The contribution of the perirhinal cortex to spatial memory is more contentious. Many lesion studies have demonstrated that perirhinal cortex is not required for explicit tests of spatial memory (Aggleton et al., 1997; Ennaceur & Aggleton, 1997; Glen & Mumby 1998; Machin et al., 2002). Indeed, these processes have been doubly dissociated in a single study; hippocampal lesions were shown to cause a deficit in a spatial task but not a recognition memory task, while, perirhinal lesions induced the opposite pattern of results (Winters et al., 2004). However, there are also perirhinal lesion studies that tax spatial memory and report deficits (Wiig & Bilkey, 1994a,b; Liu & Bilkey, 1998a,b, 2001; reviewed in Aggleton et al, 2004). Thus, descriptions of an overarching medial temporal lobe memory system, in which all of the components have similar functional properties and inter-dependence, persist (Squire & Zola-Morgan, 1991; Wixted & Squire, 2011).

One component of spatial processing is contextual learning; the hippocampus is known to be involved in learning about the context in which an event occurred. This has been demonstrated using the contextual fear conditioning paradigm. This involves placing a rat in a novel context, known as the unconditioned stimulus. Subsequently, an aversive

stimulus is delivered, most commonly a mild electric shock to the foot, which is known as the unconditioned stimulus. When a normal rat is later returned to the conditioned context it will express 'threat detection memory' by freezing (Philips & LeDoux, 1992). Hippocampal lesions impair contextual learning in this paradigm and this impairment presents itself as a reduction in freezing behaviour when the rat it returned to the conditioned context (Philips & LeDoux, 1992; Chen et al., 1996; Good & Honey, 1997; Maren & Fanselow, 1997; Richmond et al., 1999; Sachetti et al., 1999; Lee & Kesner, 2004). This effect is thought to be based on the role of the hippocampus in contextual learning as hippocampal lesions disrupt contextual memory in similar appetitive tasks (Honey & Good, 1993; Good & Bannerman, 1997) as well as tests of spontaneous explorations of a familiar object in a novel context or location (Mumby et al., 2002; Good et al., 2007). Although it should be noted that there is some evidence that only the integration of all three parameters (object, location and context) require the hippocampus (Langston & Wood, 2010).

If the perirhinal cortex and hippocampus are functionally interdependent then perirhinal lesions would be expected to cause hippocampal dysfunction in a hippocampal dependent task as hippocampal activity should be high and so would potentially be more susceptible to perturbation. However, if these two regions function in an independent manner then perirhinal lesions would not affect intrinsic hippocampal activity. This experimental design was intended to complement the study described in Chapter 3. In that experiment, the interdependence of the hippocampus and perirhinal cortex was examined following a behavioural task known to be dependent on the perirhinal cortex. In the present experiment the objective was to examine if excitotoxic lesions to the perirhinal cortex cause activity dysfunction within the hippocampus or alterations to its intrinsic interactions following exposure to a novel context, a task known to engage the hippocampus.

An associated aim was to examine the activity of other regions associated with spatial or contextual memory processing in the medial temporal lobe. Of particular interest were the postrhinal cortex and medial entorhinal cortex. These two cortical regions, along with the hippocampus, constitute the 'where' pathway as set out by the binding of item and context model and other similar models of medial temporal lobe regional interactions (Diana et al., 2007; Eichenbaum et al., 2007; depicted in Figure 1.11). A large proportion of the evidence for this 'where' network is derived from studies that implicate these regions in spatial processing activity in isolation, for example, in

traditional lesion studies. Thus, a further aim of the present study was to examine the functional interactions between these regions in the intact brain. This allowed for activity in the 'where' pathway be explicitly tested in relation to novel context exploration, with the additional possibility of anatomically refining the proposed interaction between the postrhinal cortex, medial entorhinal cortex and hippocampus.

The perirhinal cortex has reciprocal connections with both the medial entorhinal and postrhinal cortices (Burwell & Amaral, 1998a,b) and thus, a further possibility is that previously observed perirhinal induced deficits in spatial learning may be due to deafferentation of these regions. This could include perturbations in their interactions with each other or with the hippocampus. Comparisons of cortical interactions between the surgical control and perirhinal lesion rats also allow for testing of this possibility.

Expression of the immediate-early gene (IEG) c-*fos* was again employed as a proxy marker of neuronal activity. This IEG was chosen due to its sensitivity to novelty; its activity is reliably increased in the perirhinal cortex when rats are passively shown novel stimuli (Zhu et al., 1995b, 1996; Wan et al., 1999). Perirhinal and hippocampal Fos up-regulation is seen when rats actively explore objects in order to discriminate novel from familiar (Albasser et al., 2010). This perirhinal upregulation is required for stable recognition memory (Seoane et al., 2012). Critically, expression of c-*fos* has also been shown to be sensitive to spatial novelty (Wan et al., 1999; Vann et al., 2000; Jenkins et al., 2002, 2004; Sheth et al., 2008) and has been used to assess the neuronal activity associated with spatial memory (Tischmeyer & Grimm, 1999; Jenkins et al., 2003). It has also been demonstrated that c-*fos* expression in the hippocampus is essential for encoding spatial memories (He et al., 2002). Importantly, it has been shown that c-*fos* expression in the perirhinal cortex and hippocampus is sensitive to the effect of contextual novelty as well as to explicit tests of spatial memory (Zhu et al., 1997). Additionally, increased Fos expression in the perirhinal cortex has been associated with contextual fear conditioning (Albrechet-Souza et al., 2011). It has also been demonstrated that memory engrams in the hippocampus related to a specific context can be reactivated in a different context, when the genetic manipulation is placed under control of the c-*fos* promotor (Liu et al., 2012; Ramirez et al., 2013). This further implicates the expression of c-*fos* in this type of contextual processing.

Network models of c-*fos* activity associated with object recognition link parahippocampal sites to the hippocampus with altered patterns depending on whether the stimuli are novel or familiar (Albasser et al., 2010b; Chapter 3). Additionally,

another study that employed an IEG-imaging paradigm examined network models within the hippocampus following an 'early' or 'late' spatial learning task (Poirier at al., 2008). Although this study exploited expression of the IEG, Zif268, similar patterns of intra-hippocampal interactions were seen. Medial temporal lobe processing of novel stimuli (objects or spatial cues) was associated with activation of the perforant pathway, whereas processing of familiar stimuli was found to rely more heavily on the direct connection between the entorhinal cortex and CA1; the temporoammonic pathway (Poirier at al., 2008; Albasser et al., 2010b; Chapter 3). Thus, a further aim of the study was to explore if these patterns can be generalised to early contextual learning; i.e. are there general patterns of correlated activity associated with learning about novelty in the environment.

To test the importance of the perirhinal cortex on hippocampal activity, a group of rats with excitotoxic lesions to the perirhinal cortex and another group with sham surgeries were exposed to a novel context. Two other groups (perirhinal and sham lesions) were exposed to their home-cage and so served as baseline controls for Fos expression. The initial goal of the study was to assess if perirhinal lesions altered c-*fos* activity levels in the hippocampus and entorhinal cortex.

Then, using the c-*fos* activity data, specific networks of inter-correlated regions previously associated with learning about novelty were assessed using structural equation modelling. Following this, optimal models for exposure to a novel context were derived and the impact of perirhinal lesions on these networks was assessed.

5.2 Materials and Methods

5.2.1 Animals

Subjects were 56 male, Lister Hooded rats (Harlan). They were housed as described in General Methods section 2.2. These rats were from two cohorts of animals; JAR166 and JAR169. Rats in JAR166 (n = 29) were approximately 11 months old at the beginning the c-*fos* imaging study. Eighteen of these rats had previously received lesions to the perirhinal cortex while 11 served as their surgical controls. Rats from cohort JAR169 (n = 27) were approximately 7 months old at the beginning the present experiment. Of these rats, 15 had received lesions to the perirhinal cortex while 12 received sham surgeries. Prior to the current experiment both cohorts received object recognition memory tasks in the bow-tie maze; JAR166 were tested twice while JAR169 were tested three times. Additionally, both cohorts received a single object recognition test in an

open field paradigm. Rats were not behaviourally tested for at least two week before the current experiment.

5.2.2 Surgery

The rats were approximately three months old at the time of surgery. The surgeries were carried out by Dr. C. Olarte Sanchez. The same procedure was followed for both cohorts of animals. In total, 33 rats received bilateral perirhinal cortex lesions, while 23 rats served as surgical controls. All rats weighed between 285g and 300g at the time of surgery. Anaesthesia was induced in all animals using a mixture of oxygen and isoflurane gas, before placing them in a stereotaxic frame (David Kopf Instruments, Tujunga, CA, USA), with the incisor bar set at +5.0 mm to the horizontal plane. A midline sagittal incision was made in the scalp and the skin was retracted to expose the skull. A craniotomy was made above the injection sites. The PRH lesions were made by injecting a solution of N-methyl-d-aspartate (NMDA; Sigma, Poole, UK) diluted to 0.09M in PBS (0.1M, pH 7.4) using a 1µm Hamilton syringe (gauge 26s, outside diameter 0.47 mm) held with a micro-injector (Kopf Instruments, Model 5000). Bilateral injections of NMDA were made at a rate of 0.10 µL/min, with a subsequent diffusion time of four minutes. The animals received three injections in each hemisphere (for co-ordinates and volumes see Table 5.1). Rats in the surgical control group received identical treatment, except that the dura was perforated with a 25-gauge Microlance 3 needle (Becton Dickinson, Drogheda, Ireland) and no fluid was infused into the brain.

Table 5.1. Stereotaxic coordinates for lesions of the PRH.

Anteroposterior	Mediolateral	Dorsoventral	Volume (µL)
-1.8	±5.9	-9.3	0.225
-3.4	±6.1	-9.6	0.225
-5.0	±6.2	-9.0	0.225

5.2.3 Apparatus – Activity boxes

The rats were tested in a novel environment which monitored their locomotor activity. A 3 x 6 activity test cage rack was located in a novel room. The 18 activity test cages (Paul Fray, Cambridge, UK) had dimensions of 56 cm × 39 cm × 19 cm and contained two photobeams placed 20cm apart, positioned 18 cm from the short walls (Figure 5.1).

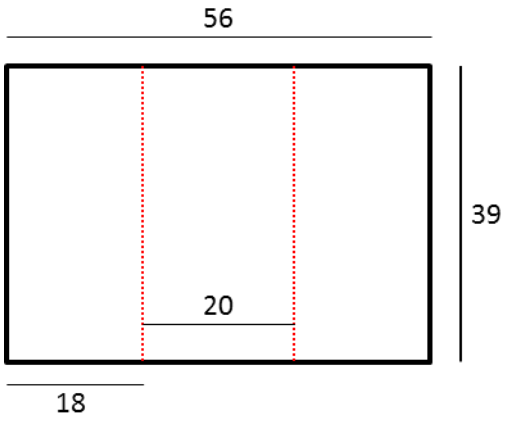

Figure 5.1 Schematic of activity box.

Schematic of activity box from above with dimensions in centimetres.

5.2.4 Behavioural testing

The animals were divided between two behavioural conditions creating four groups. The animals that received perirhinal lesions were assigned to either a novel context condition (PRH Novel, n = 18; nine from JAR166, nine from JAR169) or a home-cage control condition (PRH Baseline, n = 15; eight from JAR166, seven from JAR169) to serve as a baseline comparison for subsequent Fos immunohistochemistry. Likewise, the surgical control or 'sham' animals were divided between a novel context condition (Sham novel, n = 11; four from JAR166, seven from JAR169) and a comparative baseline control condition (Sham baseline, n = 12; seven from JAR166, five from JAR169).

Behavioural testing was carried out by Eman Amin. The rats from JAR166 were tested in the activity boxes eight months after surgery while rats from JAR169 were tested four months after surgery. Each rat was taken into the room and placed individually inside an activity test cage. The box was illuminated and the locomotor activity of the rat was recorded for 20 min. The number of total beam breaks that took place over the 20 minutes was recorded. These data were then divided into two categories; 'same beam' (a single beam being repeatedly broken) as well as 'beam crossovers' (both the front and back beams broken sequentially). On completion of their exposure to the novel context, the rats were placed in a dark room for 90 minutes and then perfused as described in the General Methods section 2.4.

5.2.5 Lesion analysis

As described in General Methods section 2.6.

5.2.6 Immunohistochemistry

Brain sections were stored at -20°C in cryoprotectant until all rats had completed their respective behavioural protocol. The sections were then immunohistochemically stained with one rat from each of the four behavioural groups in the same reaction vessel. The protocol was as described in General Methods section 2.7.

5.2.7 Regions of interest

The multiple regions of interest are illustrated in Figure 5.2. Two brain atlases (Paxinos & Watson, 2005; Swanson, 1992) helped to verify the locations of brain areas, unless otherwise specified. The anterior – posterior (AP) coordinates (mm from bregma) given in the descriptions below and in Figure 5.2 are from Paxinos & Watson (2005). The regions below reflect the groupings subsequently used in the statistical analyses of Fos counts.

5.2.7.1 Hippocampal formation

Hippocampal subfields (dentate gyrus, CA1, and CA3) were subdivided into their septal (dorsal), intermediate, and temporal (ventral) divisions (Bast, 2007; Strange et al., 2014). The septal hippocampus counts (dentate gyrus, CA3 and CA1) were obtained from sections from AP -2.52 to -3.24, while those for the intermediate hippocampus (dentate gyrus, CA1, CA3) came from sections from AP -4.80 to -5.52. The border between the intermediate and temporal hippocampus corresponds to -5.0 mm ventral from bregma (Paxinos & Watson, 2005). Within the temporal hippocampus, counts were made in CA1 and CA3 fields (at the same AP as the intermediate hippocampus). Additional cell counts were taken in both the dorsal and ventral subiculum (from around AP -5.16).

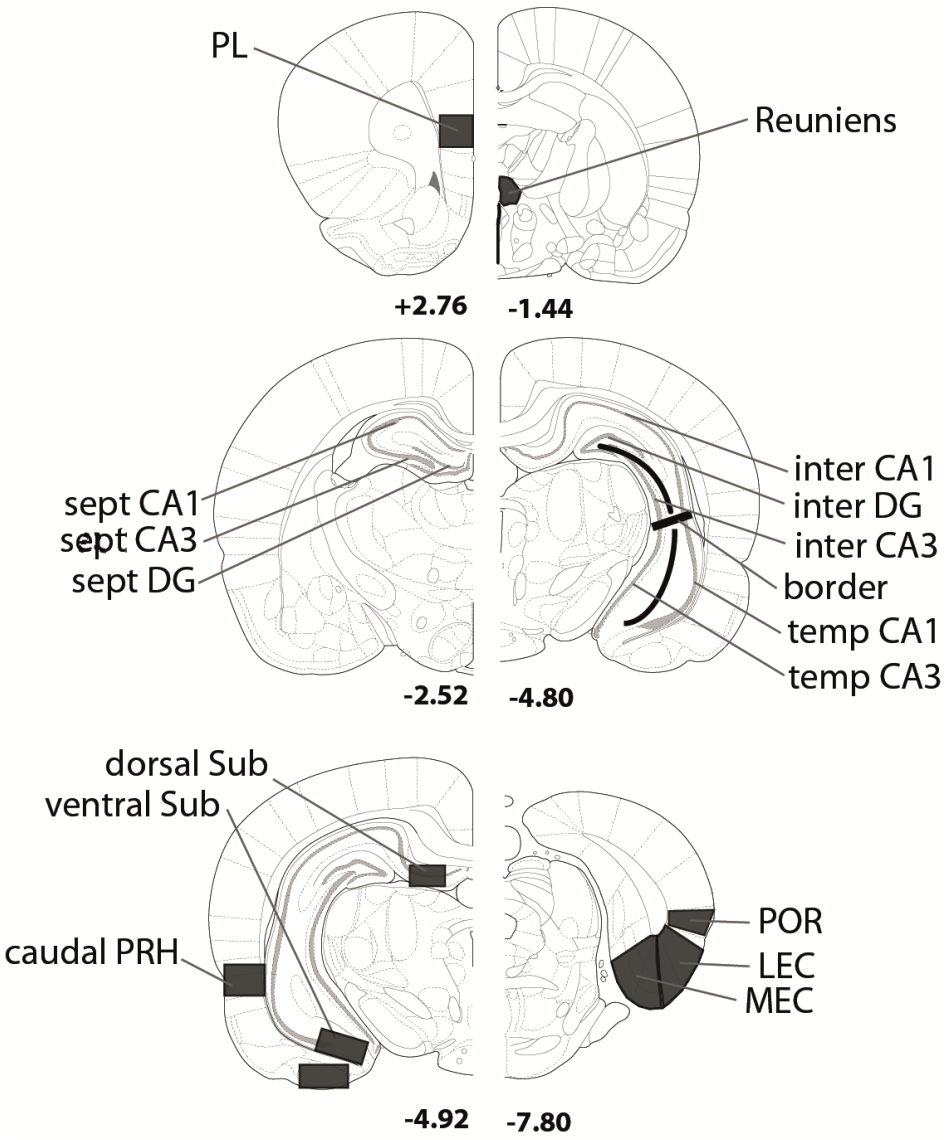

Figure 5.2. Regions of interest for c-*fos* analyses

Sites included: CA fields - intermediate (inter), septal (sept) and temporal (temp); DG, dentate gyrus; dorsal Sub, dorsal subiculum; LEC, lateral entorhinal cortex; MEC, medial entorhinal cortex; PL, prelimbic cortex; PRH, perirhinal cortex; POR, postrhinal cortex; Reuniens, nucleus reuniens of thalamus; ventral Sub, ventral subiculum. The numbers below refer to the approximate distance in mm from bregma. Adapted from the atlas of Paxinos & Watson (2005).

5.2.7.2 Rhinal cortices

Separate cell counts were taken from the lateral and medial entorhinal cortices (LEC and MEC respectively) from sections AP -7.08 to -8.04. Fos counts were also made in the postrhinal cortex (at the same AP level); the boundaries were based on Burwell & Amaral (1998b).

5.2.7.3 Frontal cortex and thalamus

Fos-positive cell counts were made within the prelimbic cortex (PL) from AP +3.72 to +2.76 and nucleus reuniens from AP -1.44 to -2.28.

5.2.7.4 Perirhinal cortex

In the sham surgical groups only, additional Fos-positive cell counts were made at caudal (from AP -4.80 to -5.52) levels of areas 35 and 36 in the perirhinal cortex (PRH; see Burwell, 2001). The caudal region was chosen based on previous demonstrations that this region is particularly involved in the processing of novel visual stimuli (Albasser et al., 2009, 2010b; Chapter 3, 4).

5.2.8 Image capture and analysis of c-*fos* activation

As described in General Methods section 2.8.

5.2.9 Statistical analysis

5.2.9.1 Behavioural data

Behavioural data were only generated for the animals placed in the activity boxes ('Peri Novel' and 'Sham Novel') as the baseline control groups ('Peri Baseline' and 'Sham Baseline') remained in their home-cages. These were compared by an ANOVA with one between-subject factor (surgical condition) and one within-subject factor ('same beam' or 'beam crossovers').

5.2.9.2 Fos data

To analyse group differences (sham vs. lesion; baseline vs. novel context) in the numbers of c-*fos* activated cells in the regions of interest, a two between-subjects factor (surgical condition and Baseline/Novel context) and one within-subject factor (Region of Interest; ROI) ANOVA was calculated. This analysis was carried out separately for three regional groupings: i) divisions within the hippocampal formation, ii) medial and lateral entorhinal cortex as well as postrhinal cortex, and iii) prelimbic cortex and nucleus reuniens of the thalamus. The aim of this regional grouping procedure was to reduce the likelihood of Type 1 errors by reducing the number of comparisons. The Fos counts in the perirhinal cortex (sham groups only) were compared using a one between (Baseline/Novel context) by one within-subject factor (ROI) ANOVA. Where an interaction was found to be significant, the simple effects were examined.

Examination of the distribution of the Fos data revealed that Fos counts from novel groups were normally distributed. However, counts obtained from both baseline control

groups ('Peri Baseline' and 'Sham Baseline') were non-normal. This was confirmed formally by the Shapiro-Wilk test. The Fos counts in all regions of interest in the baseline groups displayed moderately positively-skewed distributions and their means were proportional to their variance. Thus, the data were transformed using a square-root transformation (Howell, 2011) for those analyses that involved only these groups. The ANOVAs described above were calculated based on the raw Fos counts for all groups as a comparison between raw Fos counts for two groups and transformed data for the other two groups would be difficult to interpret. Also, an ANOVA is relatively robust to violations of the normality assumption when group sample sizes are equal (Howell, 2011). The data are displayed as mean Fos counts ± standard error of the mean.

Pearson product-moment correlation coefficients were calculated for the raw Fos-positive cell counts in the various sites, as well as with the activity of animals in the Novel Context condition. In the baseline control groups, Pearson product-moment correlation coefficients were calculated based on the transformed data as these data were subsequently used for the structural equation modelling analyses. The levels of the correlations obtained between regions were also compared between the perirhinal and sham lesion groups using Fisher's *r*-to-*z* transformation (Zar, 2010).

5.2.10 Structural equation modelling

As described in General Methods section 2.10.

5.3 Results

5.3.1 Lesion analysis

In most cases, the lesions encompassed the whole rostral-caudal extent of the perirhinal cortex with very small amounts of tissue sparing. The attempt to make complete perirhinal cortex lesions inevitably led to some extra-perirhinal damage. This was typically observed in the most ventral region of area Te2, and the most dorsal region of the piriform and lateral entorhinal cortices, the cortical areas adjacent to the perirhinal cortex (Figure 5.3). Subcortical damage was observed in some cases in the CA1 subfield of the hippocampus, but only at the temporal level (Figure 5.3). A hemisphere was removed from analysis if gliosis was seen in two or more consecutive sections of the temporal region of CA1. Due to the prevalence of this extra-perirhinal damage seven animals were excluded from group Peri Novel (six from JAR166, one from JAR169) and three animals were excluded from Peri Baseline (all from JAR166). Following the exclusion of these animals, the group numbers were as follows: Peri Novel, n = 11;

Sham Novel, n = 11; Peri Baseline, n = 12; Sham Baseline, n = 12. Overall perirhinal damage ranged from 64.3% to 100%. The largest and smallest lesions were quantified separately for the animals from each cohort in the two behavioural conditions (Figure 5.3; Table 5.2).

Of these remaining animals, only one hemisphere was analysed per brain for Fos-positive cells; six left hemispheres and five right hemispheres were analysed in group Peri Novel, while three left hemispheres and nine right hemispheres were analysed in group Peri Baseline. The corresponding hemispheres were analysed in the matched surgical controls.

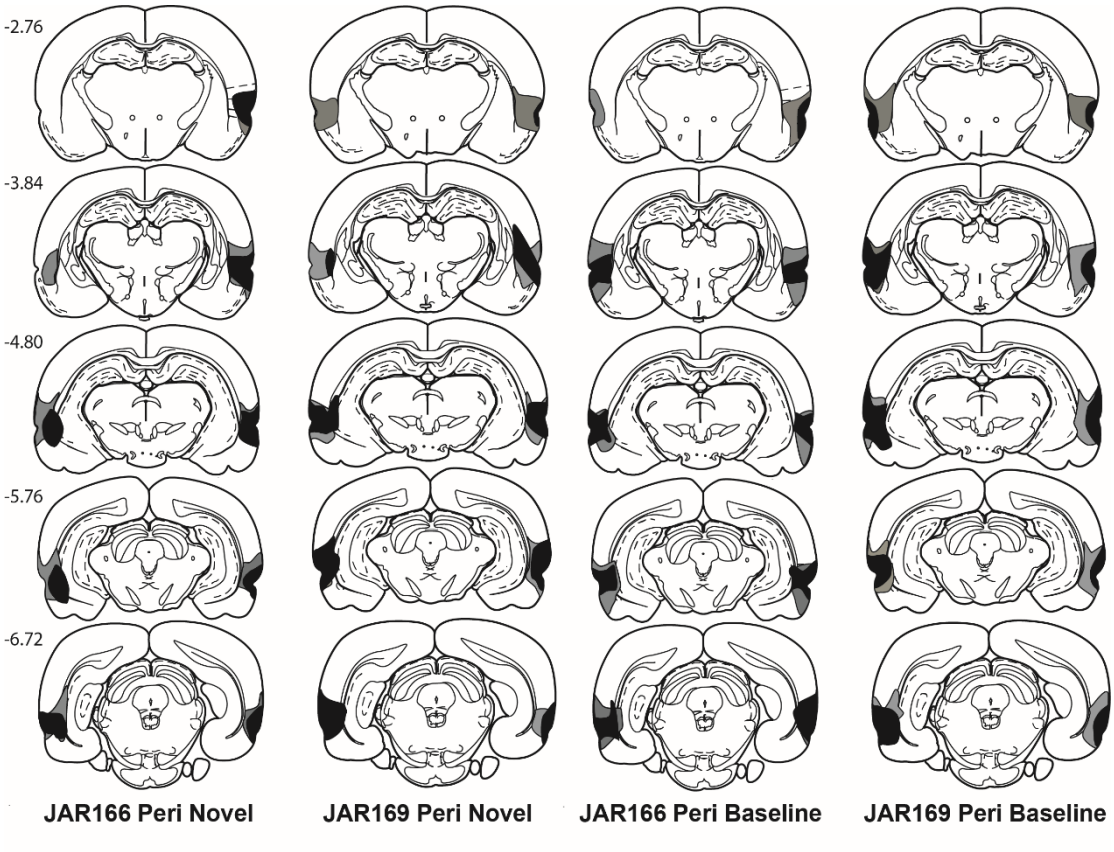

Figure 5.3. Perirhinal lesion reconstructions.

Diagrammatic reconstructions of the perirhinal cortex lesions showing the individual cases with the largest (grey) and smallest (black) lesions for rats from cohort JAR166 and JAR169 in groups Peri Novel and Peri Baseline. The numbers refer to the distance (in millimetres) from bregma (adapted from Paxinos & Watson, 2005).

Table 5.2. Range of damage to perirhinal cortex each cohort in both behavioural conditions.

	Peri Novel		Peri Baseline	
	Smallest	Largest	Smallest	Largest
JAR166	64.3%	80.6%	81.0%	92.7%
JAR169	76.7%	93.4%	71.3%	100.0%

5.3.2 Behavioural testing

Analysis on the two components of total beam breaks ('same beam' or 'beam crossovers') revealed that there was no overall effect of the presence of a perirhinal cortex lesion ($F_{1,18} = 1.36$, $p = 0.26$; Figure 5.4). This lack of effect was uniform as the interaction between lesion and type of beam break was also non-significant ($F_{1,18} = 3.21$, $p = 0.09$).

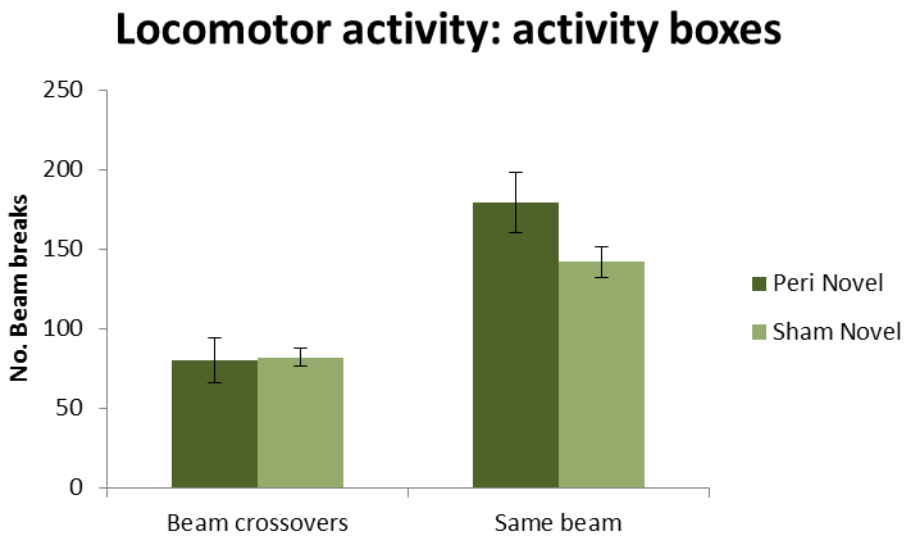

Figure 5.4. Behavioural measures.

Graphs illustrate the locomotor activity measures from the activity box for groups Peri Novel and Sham Novel. Data are presented as means ±SEM.

5.3.3 Fos-positive cell counts

5.3.3.1 Hippocampal subfields – comparison of Fos counts

Three levels along the rostral-caudal axis of the hippocampus were examined (septal, intermediate and temporal; division based on Bast et al., 2009). At the septal and intermediate levels, three subfields were assessed [CA1, CA3 and dentate gyrus (DG)] and at the temporal level of the hippocampus two subfields were assessed (CA1 and

CA3) as DG is not present at this level. Additionally, counts were made in dorsal and ventral subiculum.

While perirhinal cortex lesions had no apparent effect on the number of Fos-positive neurons in the hippocampal formation, being placed in a novel context dramatically increased hippocampal Fos expression (Figure 5.5, 5.6). A significant Mauchly's test ($p \leq 0.001$) indicated that the assumption of sphericity of the within-subject variable (ROI) was violated and so corrected degrees of freedom are presented below (as described in General Methods section 2.9). Formally comparing Fos-positive cell counts across the ten hippocampal subfields found no overall effect of perirhinal lesions ($F_{1,42} = 1.43$, $p = 0.24$). The Fos counts in the animals placed in a novel context were consistently higher than the Fos counts of animals that were exposed to their highly familiar home-cage context ($F_{1,42} = 166$, $p \leq 0.001$). Additionally, there was an overall effect of subfield ($F_{2.8,116} = 101$, $p \leq 0.001$); reflecting the differing levels of Fos expression in each of the subfields (Figure 5.5, 5.6). There was, however, no lesion by context interaction ($F < 1$) nor was the lesion by subfield interaction significant ($F_{2.8,116} = 1.12$, $p = 0.34$). There was a significant context by subfield interaction ($F_{2.8,116} = 48.2$, $p \leq 0.001$); simple effects revealed that all ten subfields had higher Fos-positive cell counts when exposed to a novel context than when compared to baseline, but the magnitude of this difference differed among the subfields (All $F_{1, 42} > 27$, $p \leq 0.001$; Figure 5.5, 5.6). Finally, the three-way interaction was not significant ($F < 1$).

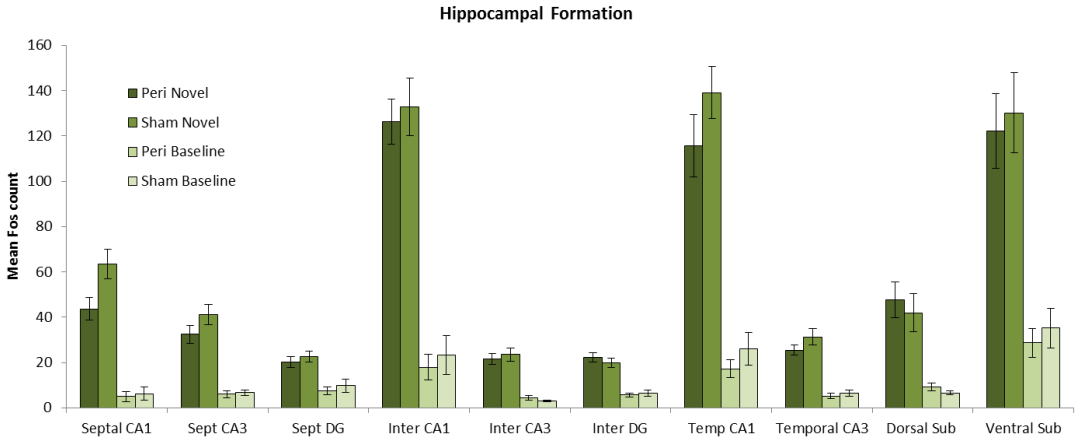

Figure 5.5. Mean Fos-positive cell counts per group in the hippocampal formation.

Sites analysed: CA fields – intermediate (inter), septal (sept) and temporal (temp); dentate gyrus (DG); subiculum (Sub). Exposure to a novel context reliable increased Fos-related activity in all regions analysed ($p < 0.001$). Data are presented as means ±SEM.

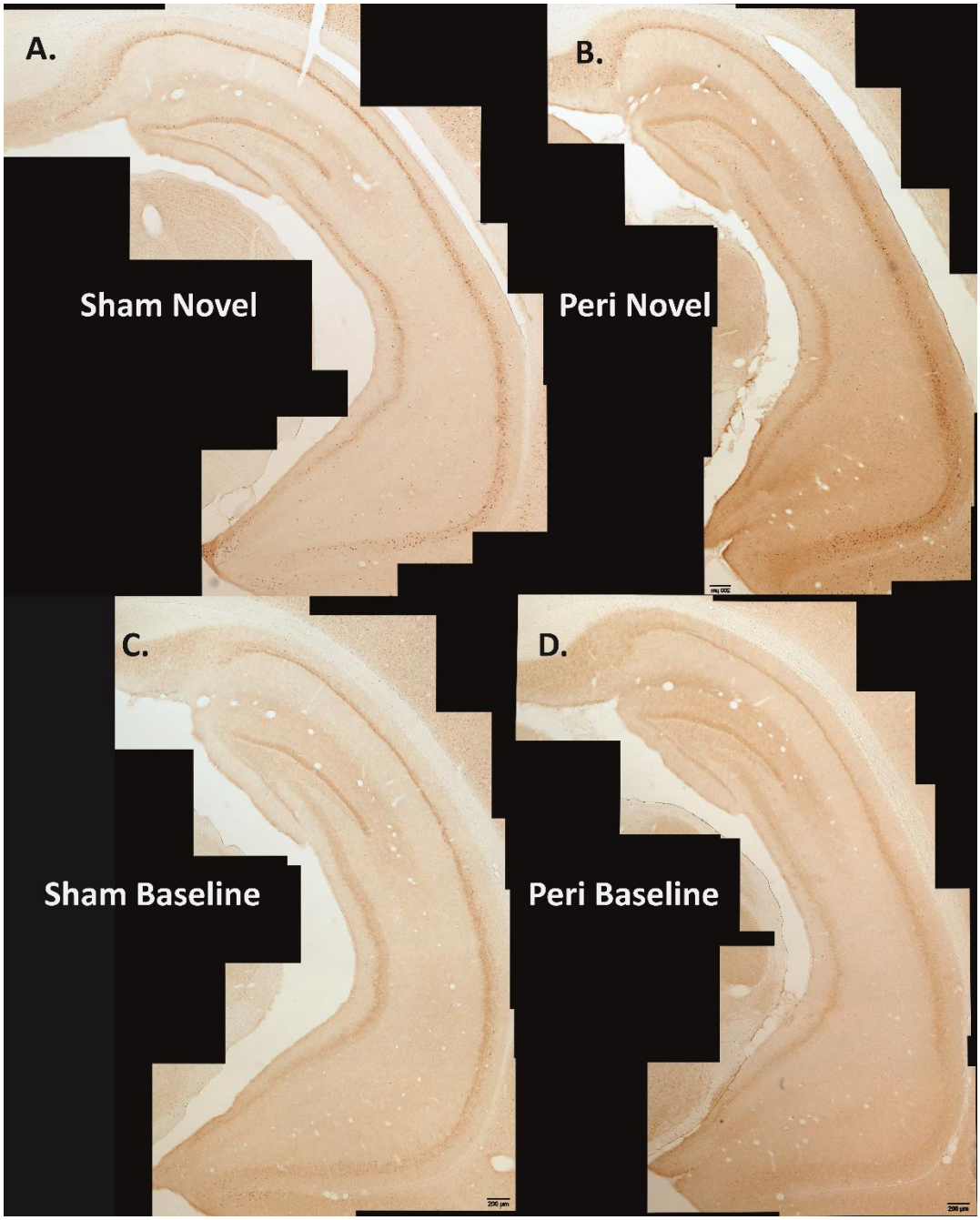

Figure 5.6. Hippocampal Fos expression.

Representative photomicrographs from coronal section depict Fos-positive cells in intermediate and temporal levels of the hippocampus in groups (A) Sham Novel, (B) Peri Novel, (C) Sham Baseline and (D) Peri Baseline. Scale bar: 200 µm.

5.3.3.2 Medial and lateral entorhinal cortex and postrhinal cortex – comparison of Fos counts

As in the hippocampus, the assumption of sphericity was also violated in the rhinal cortex and so corrected degrees of freedom are presented. In the three regions of the rhinal cortex analysed here, Fos-positive cell counts in rats with lesions to the perirhinal

cortex were consistently lower than their surgical controls (Figure 5.7). This was reflected by a significant effect of lesion ($F_{1,40} = 5.41$, $p = 0.025$). As observed in the hippocampal formation, novel context exploration produced higher Fos counts in MEC, LEC and postrhinal cortex than exposure to the highly familiar home-cage ($F_{1,40} = 113$, $p \leq 0.001$; Figure 5.7). There was also an overall effect of region ($F_{1.2,49} = 224$, $p \leq 0.001$) as each of these regions had differing Fos-positive cell counts. The region by lesion interaction was significant, indicating that the various regions of the rhinal cortex were differentially affected by the presence of a perirhinal cortex lesion ($F_{1.2,49} = 6.00$, $p = 0.013$); simple effects analysis revealed that this difference was driven by higher Fos counts in the LEC of sham animals when compared to animals with perirhinal lesions ($F_{1,40} = 6.56$, $p = 0.014$; Figure 5.7). This lesion effect did not extend to the MEC or postrhinal cortex ($F_{1,40} = 3.44$, $p = 0.071$; $F_{1,40} = 1.59$, $p = 0.21$ respectively). Additionally, the context differentially affected the three regions of the rhinal cortex ($F_{1.2,49} = 114$, $p \leq 0.001$); simple effects revealed that MEC, LEC and postrhinal cortex all had higher Fos-positive cell counts when exposed to a novel context compared to baseline but the magnitude of this difference differed among these regions (MEC: $F_{1,40} = 65.9$, $p \leq 0.001$; LEC: $F_{1,40} = 131$, $p \leq 0.001$; POR: $F_{1,40} = 46.8$, $p \leq 0.001$; Figure 5.7). Finally, the three-way interaction was non-significant ($F_{2,80} = 1.61$, $p = 0.21$).

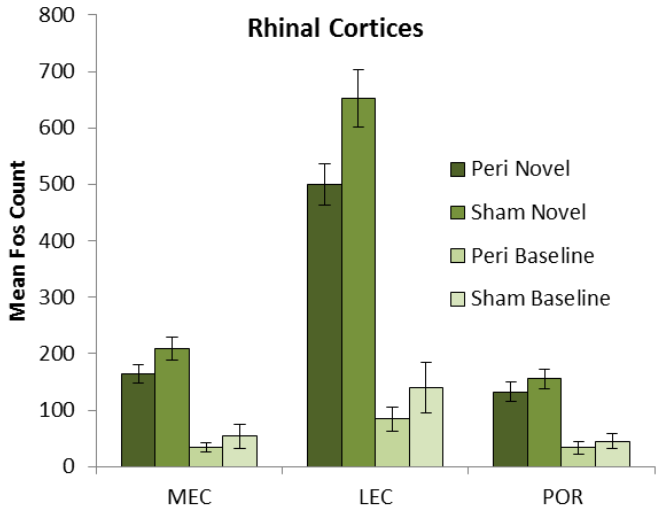

Figure 5.7. Mean Fos-positive cell counts per group in the rhinal cortices.

Sites analysed: lateral entorhinal cortex (LEC); medial entorhinal cortex (MEC); postrhinal cortex (POR). Exposure to a novel context reliable increased Fos-related activity in all regions analysed ($p < 0.001$). Data are presented as means ±SEM.

5.3.3.3 Prelimbic cortex and nucleus reuniens of the thalamus – comparison of Fos counts

Lesions to the perirhinal cortex did not affect Fos-related activity in the prelimbic cortex or nucleus reuniens of the thalamus but, as with all other regions described, exposure to a novel context increased the numbers of Fos-positive cells (Figure 5.8).

In these regions, the overall effect of lesions in the perirhinal cortex was not significant ($F_{1,42} = 2.01$, $p = 0.16$). The effect of exploring a novel context compared to a familiar home-cage caused a significant increase in the number of Fos-positive cells in both prelimbic cortex and nucleus reuniens ($F_{1,42} = 64.3$, $p \leq 0.001$; Figure 5.8). There was also an overall effect of region ($F_{1,42} = 78.1$, $p \leq 0.001$) as Fos counts were different between these two regions. There was no lesion by context interaction ($F_{1,42} = 2.15$, $p = 0.15$), nor was the region by lesion interaction significant ($F < 1$). Consistent with all of the other regional groupings, the context by region interaction was significant ($F_{1,42} = 21.7$, $p \leq 0.001$); higher Fos-positive cell counts were observed when rats were exposed to a novel context but the extent of the difference differed between these regions (PL: $F_{1,42} = 47.5$, $p \leq 0.001$; Reuniens: $F_{1,42} = 52.1$, $p \leq 0.001$; Figure 5.8). Finally, the three-way interaction was not significant ($F < 1$).

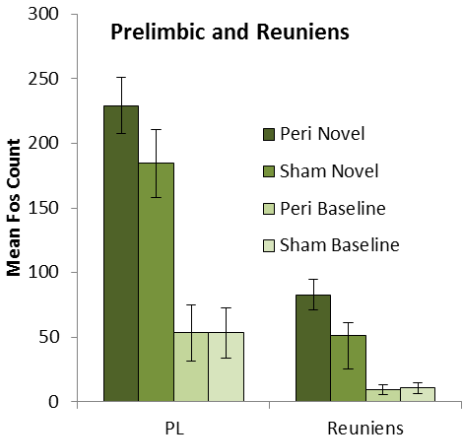

Figure 5.8. . Mean Fos-positive cell counts per group in the prelimbic cortex and nucleus reuniens.

Sites analysed: prelimbic cortex (PL); nucleus reuniens of the thalamus (Reuniens). Exposure to a novel context reliably increased Fos-related activity in all regions analysed ($p < 0.001$). Data are presented as means ±SEM.

5.3.3.4 Perirhinal cortex – comparison of Fos counts in shams groups

The pattern observed in all other regions was repeated in the perirhinal cortex. In Areas 35 and 36 of the surgical control groups (groups Sham Novel and Sham Baseline) there was a significant condition difference; higher Fos counts were associated with the novel

context ($F_{1,21} = 41.7$, $p \leq 0.001$; Figure 5.9). Overall, the Fos counts in Area 35 were no different to those in Area 36 ($F < 1$). The context did however affect the two areas differently ($F_{1,21} = 9.84$, $p = 0.005$); simple effects analysis revealed that context novelty significantly influenced both regions, but increased Fos counts in Area 35 to a greater extent (Area 35: $F_{1,21} = 44.2$, $p \leq 0.001$; Area 36: $F_{1,21} = 25.5$, $p \leq 0.001$; Figure 5.9).

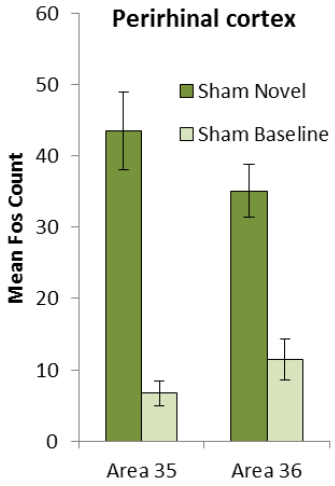

Figure 5.9. Mean Fos-positive cell counts in the perirhinal cortex in the Sham groups.

Sites analysed: Areas 35 and 36 of the perirhinal cortex. Exposure to a novel context reliable increased Fos-related activity in all regions analysed ($p < 0.001$). Data are presented as means ±SEM.

5.3.4 Correlation tables

Two sets of Pearson product moment correlation coefficients were calculated for groups Sham Novel and Peri Novel. The first set was between the behavioural measures from the activity box and the number of Fos-positive neurons in the various regions of interest (Table 5.3; first two rows/columns). In both of these animal groups only one region reached significance; intermediate CA3 in group Sham Novel, and temporal CA3 in group Peri Novel. Fos counts in both of these regions correlated with the number times a single beam was repeatedly broken (same beam breaks). Due to the large numbers of correlations calculated, combined with the fact that these correlations only just reached the level of significance, it seems unlikely that these isolated correlations are meaningful. Thus, this indicates that activity in the analysed brain regions was not merely driven by motor activity of the animals in either group.

The second set of Pearson product moment correlation coefficients calculated for the two groups exposed to the novel context were inter-regional correlations of the raw Fos counts (remainder of Table 5.3). This was to give an indication of how the activity of the

different brain regions co-varied. These inter-regional correlations were also calculated for the baseline groups (Table 5.4), however these correlations are based on square-root transformations of the Fos counts rather than the raw Fos counts as the raw counts in these groups were not normally distributed (Howell, 2011).

These tables of correlations present probability levels that are not corrected for multiple comparisons as the individual correlations are of limited significance. More importantly, these correlations provide the source data for the structural equation modelling, in which the fit of the overall model helps to compensate for Type 1 errors in the individual correlations that comprise the model. Because of this, it is important that any model must conform to known patterns of anatomical connectivity between the regions of interest; this constrains the number of potential models. It is still of note that in both of the groups in the novel condition, approximately one-quarter of the possible correlations reached significance level. Whereas for both of the baseline groups approximately three-quarters of the possible correlations reached significance level.

Table 5.3. Behavioural and inter-region correlations of Fos-positive cell counts in the two Novel groups.

		Sham Novel																					
		Beam Cross overs	Same Beam	Septal CA1	Septal CA3	Septal DG	Inter CA1	Inter CA3	Inter DG	Temp CA1	Temp CA3	Dorsal Sub	Ventral Sub	PL	MEC	LEC	POR	Reuniens	Caudal area 35	Caudal area 36	Caudal PRH		
Beam Crossovers	r-value		0.311	0.586	0.017	0.226	0.267	0.371	-0.085	0.335	0.513	-0.027	0.399	0.033	0.008	-0.355	0.333	0.317	0.403	0.077	0.296	r-value	Beam Crossovers
	p-value		0.382	0.075	0.962	0.530	0.456	0.291	0.816	0.345	0.129	0.942	0.253	0.927	0.983	0.314	0.347	0.372	0.248	0.833	0.407	p-value	
Same Beam	r-value	0.530		0.033	0.161	0.028	0.538	**.754***	0.347	0.398	0.165	0.174	0.096	0.606	0.184	-0.069	-0.099	0.271	-0.357	-0.314	-0.369	r-value	Same Beam
	p-value	0.093		0.927	0.657	0.938	0.108	**0.012**	0.326	0.255	0.649	0.631	0.792	0.063	0.611	0.850	0.786	0.450	0.312	0.377	0.294	p-value	
Septal CA1	r-value	0.010	0.139		0.427	0.181	**.656***	0.456	0.220	**.623***	0.450	0.197	**.712***	0.434	**.717***	0.572	**.728***	0.328	**.709***	0.527	**.663***	r-value	Septal CA1
	p-value	0.977	0.683		0.190	0.593	**0.028**	0.158	0.515	**0.041**	0.165	0.562	**0.014**	0.183	**0.013**	0.066	**0.011**	0.325	**0.014**	0.096	**0.026**	p-value	
Septal CA3	r-value	-0.354	0.075	**.850****		0.184	**.708***	0.457	0.306	**.716***	-0.098	0.025	0.481	0.441	0.472	0.565	0.571	0.328	0.410	0.276	0.398	r-value	Septal CA3
	p-value	0.285	0.828	**0.001**		0.588	**0.015**	0.157	0.360	**0.013**	0.774	0.942	0.134	0.175	0.143	0.070	0.067	0.325	0.211	0.411	0.225	p-value	
Septal DG	r-value	0.235	0.477	0.418	0.251		0.215	-0.051	.626*	-0.085	0.491	**.706***	0.027	-0.429	-0.091	0.070	0.326	**.664***	0.145	0.522	0.375	r-value	Septal DG
	p-value	0.487	0.138	0.201	0.457		0.525	0.882	0.040	0.803	0.125	**0.015**	0.937	0.188	0.790	0.839	0.327	**0.026**	0.671	0.100	0.256	p-value	
Inter CA1	r-value	0.116	0.422	**.832****	**.816****	0.276		0.457	0.473	**.909*****	0.333	0.424	**.618***	**.626***	**.749****	**.742****	0.571	0.509	0.522	0.601	**.616***	r-value	Inter CA1
	p-value	0.735	0.196	**0.001**	**0.002**	0.411		0.158	0.142	**<0.001**	0.317	0.194	**0.043**	**0.039**	**0.008**	**0.009**	0.067	0.109	0.099	0.050	**0.044**	p-value	
Inter CA3	r-value	-0.005	0.474	0.053	0.170	0.232	0.012		0.225	0.452	0.067	-0.112	0.398	**.699***	0.436	0.274	0.362	0.138	-0.003	-0.176	-0.102	r-value	Inter CA3
	p-value	0.988	0.140	0.877	0.618	0.492	0.972		0.506	0.162	0.846	0.743	0.226	**0.017**	0.180	0.414	0.274	0.686	0.993	0.605	0.766	p-value	
Inter DG	r-value	0.459	0.400	**.627***	0.462	0.471	**.622***	0.321		0.188	0.291	**.800****	0.222	0.194	0.367	0.319	0.052	0.322	0.116	0.589	0.383	r-value	Inter DG
	p-value	0.155	0.223	**0.039**	0.152	0.144	**0.041**	0.336		0.580	0.385	**0.003**	0.511	0.567	0.267	0.340	0.878	0.334	0.734	0.056	0.246	p-value	
Temporal CA1	r-value	-0.074	0.015	**.810****	**.873*****	0.109	**.855****	-0.142	0.588		0.263	0.054	**.768****	**.712***	**.717***	**.668***	0.443	0.325	**.632***	0.466	**.606***	r-value	Temporal CA1
	p-value	0.828	0.965	**0.003**	**<0.001**	0.750	**0.001**	0.676	0.057		0.435	0.875	**0.006**	**0.014**	**0.013**	**0.025**	0.173	0.329	**0.037**	0.148	**0.048**	p-value	
Temporal CA3	r-value	0.392	**.629***	0.171	0.123	0.415	0.136	**.814****	0.500	-0.016		0.442	0.578	0.054	0.283	0.230	0.092	**.710***	0.565	0.507	0.579	r-value	Temporal CA3
	p-value	0.233	**0.038**	0.616	0.718	0.204	0.689	**0.002**	0.118	0.962		0.173	0.063	0.874	0.400	0.496	0.787	**0.014**	0.070	0.111	0.062	p-value	
Dorsal Sub	r-value	0.150	0.126	**.793****	**.626***	0.447	**.748****	-0.160	**.705***	**.705***	-0.004		-0.024	-0.079	0.285	0.315	0.162	0.526	0.108	**.647***	0.406	r-value	Dorsal Sub
	p-value	0.659	0.713	**0.004**	**0.040**	0.168	**0.008**	0.638	**0.015**	**0.015**	0.990		0.944	0.817	0.396	0.345	0.635	0.096	0.751	**0.031**	0.215	p-value	
Ventral Sub	r-value	-0.147	-0.189	-0.311	-0.195	0.306	-0.420	0.213	0.277	-0.231	0.149	0.000		0.575	**.656***	0.520	0.246	0.311	**.835****	0.508	**.731***	r-value	Ventral Sub
	p-value	0.667	0.578	0.351	0.565	0.359	0.199	0.529	0.410	0.494	0.662	1.000		0.064	**0.028**	0.101	0.467	0.351	**0.001**	0.111	**0.011**	p-value	
PL	r-value	0.357	0.429	0.409	0.337	**.604***	0.484	0.302	**.824****	0.339	0.407	**.722***	0.406		**.718***	0.505	0.120	0.038	0.219	-0.012	0.103	r-value	PL
	p-value	0.281	0.187	0.211	0.311	**0.049**	0.132	0.366	**0.002**	0.308	0.215	**0.012**	0.215		**0.013**	0.113	0.725	0.911	0.518	0.971	0.762	p-value	
MEC	r-value	-0.014	0.012	-0.070	-0.075	0.216	-0.316	**.624***	0.363	-0.220	**.629***	0.008	**.667***	0.335		**.888*****	0.435	0.231	**.618***	0.497	0.588	r-value	MEC
	p-value	0.968	0.973	0.839	0.826	0.523	0.343	**0.040**	0.273	0.515	**0.038**	0.982	**0.025**	0.314		**<0.001**	0.181	0.495	**0.043**	0.120	0.057	p-value	
LEC	r-value	0.433	0.224	0.136	0.022	0.082	0.095	0.422	0.515	0.068	**.634***	0.339	0.245	0.574	**.695***		0.565	0.389	0.555	0.533	0.572	r-value	LEC
	p-value	0.183	0.507	0.690	0.948	0.812	0.780	0.197	0.105	0.842	**0.036**	0.308	0.468	0.065	**0.018**		0.070	0.237	0.076	0.091	0.066	p-value	
POR	r-value	-0.160	0.104	0.522	0.464	0.576	0.304	0.439	**.752****	0.292	0.333	0.528	0.513	**.614***	0.526	0.220		0.421	0.352	0.314	0.359	r-value	POR
	p-value	0.639	0.761	0.100	0.151	0.064	0.363	0.177	**0.008**	0.384	0.317	0.095	0.107	**0.045**	0.097	0.515		0.197	0.289	0.346	0.279	p-value	
Reuniens	r-value	-0.326	0.217	0.550	**.693***	0.193	0.477	0.520	0.533	0.503	0.405	0.459	0.113	0.359	0.494	0.388	0.595		0.356	0.340	0.391	r-value	Reuniens
	p-value	0.327	0.521	0.080	**0.018**	0.570	0.138	0.101	0.092	0.115	0.216	0.155	0.740	0.278	0.122	0.238	0.054		0.283	0.306	0.234	p-value	
Caudal area 35	r-value										Correlations absent due to perirhinal lesion surgeries									.679*	**.920*****	r-value	Caudal area 35
	p-value																			0.022	**<0.001**	p-value	
Caudal area 36	r-value																				**.909*****	r-value	Caudal area 36
	p-value																				**<0.001**	p-value	
Caudal PRH	r-value																					r-value	Caudal PRH
	p-value																					p-value	
		Peri Novel																					

The top right diagonal matrix (darker grey) displays correlation data from the Sham Novel object group while the bottom left diagonal matrix displays correlation data from the Peri Novel group (lighter grey). The r-values are Pearson correlation coefficients. * $p < 0.05$, ** $p < 0.01$, *** $p < 0.001$, for two-tailed correlations (uncorrected for multiple comparisons – see main text). Sites included: area 35 and area 36 of the perirhinal cortex (PRH); CA fields - intermediate (inter), septal and temporal (temp); dentate gyrus (DG); lateral entorhinal cortex (LEC); medial entorhinal cortex (MEC); nucleus reuniens of the thalamus (Reuniens); prelimbic cortex (PL); postrhinal cortex (POR); subiculum (Sub).

Table 5.4. Inter-region correlations of Fos-positive cell counts in the two Baseline groups.

Sham Baseline Control (SqRt transforrmed)																					
		Septal CA1	Septal CA3	Septal DG	Inter CA1	Inter CA3	Inter DG	Temp CA1	Temp CA3	Dorsal Sub	Ventral Sub	PL	MEC	LEC	POR	Reuniens	Caudal area 35	Caudal area 36	Caudal PRH		
Septal CA1	r-value		.721**	.780**	.949***	0.344	.772**	.853***	.595*	.626*	.859***	.883***	.952***	.906***	.789**	.909***	.793**	.715**	.767**	r-value	Septal CA1
	p-value		0.008	0.003	<0.001	0.274	0.003	<0.001	0.041	0.029	<0.001	<0.001	<0.001	<0.001	0.002	<0.001	0.002	0.009	0.004	p-value	
Septal CA3	r-value	.597*		.625*	.711**	0.553	.747**	.726**	0.170	0.377	.711**	.619*	.689*	.725*	0.573	.701*	.702*	0.574	.643*	r-value	Septal CA3
	p-value	0.040		0.030	0.010	0.062	0.005	0.007	0.596	0.226	0.009	0.032	0.019	0.012	0.051	0.011	0.011	0.051	0.024	p-value	
Septal DG	r-value	.712**	0.056		.583*	-0.002	.709**	0.547	0.309	0.471	.645*	.632*	.712*	.634*	0.373	.679*	0.412	0.367	0.391	r-value	Septal DG
	p-value	0.009	0.863		0.046	0.996	0.010	0.066	0.328	0.122	0.024	0.028	0.014	0.036	0.232	0.015	0.183	0.240	0.209	p-value	
Inter CA1	r-value	.903***	.676*	0.525		0.489	.754**	.893***	.634*	.590*	.897***	.876***	.968***	.954***	.901***	.934***	.903***	.798**	.867***	r-value	Inter CA1
	p-value	<0.001	0.016	0.079		0.107	0.005	<0.001	0.027	0.044	<0.001	<0.001	<0.001	<0.001	<0.001	<0.001	<0.001	0.002	<0.001	p-value	
Inter CA3	r-value	.772**	0.566	0.543	.812**		0.425	0.543	0.361	0.534	0.512	0.300	0.396	0.474	.676*	0.402	.593*	0.390	0.493	r-value	Inter CA3
	p-value	0.003	0.055	0.068	0.001		0.169	0.068	0.248	0.074	0.089	0.344	0.227	0.141	0.016	0.196	0.042	0.210	0.103	p-value	
Inter DG	r-value	.807**	0.301	.851***	.774**	.781**		.892***	0.543	0.548	.880***	.886***	.808**	.788**	.748**	.769**	.814**	.766**	.809**	r-value	Inter DG
	p-value	0.002	0.342	<0.001	0.003	0.003		<0.001	0.068	0.065	<0.001	<0.001	0.003	0.004	0.005	0.003	0.001	0.004	0.001	p-value	
Temporal CA1	r-value	.761**	.641*	0.328	.935***	.810**	.651*		.595*	.677*	.901***	.940***	.951***	.943***	.896***	.821***	.906***	.866***	.912***	r-value	Temporal CA1
	p-value	0.004	0.025	0.297	<0.001	0.001	0.022		0.041	0.016	<0.001	<0.001	<0.001	<0.001	<0.001	<0.001	<0.001	<0.001	<0.001	p-value	
Temporal CA3	r-value	.770**	0.216	.664*	.795**	.804**	.873***	.748**		0.574	0.561	.677*	0.597	0.558	.737**	.640*	.595*	.716**	.696*	r-value	Temporal CA3
	p-value	0.003	0.499	0.019	0.002	0.002	<0.001	0.005		0.051	0.058	0.016	0.053	0.074	0.006	0.025	0.041	0.009	0.012	p-value	
Dorsal Sub	r-value	0.557	0.452	0.530	0.543	.662*	.604*	0.543	0.490		.580*	0.569	0.597	0.530	.707*	.590*	0.494	0.415	0.463	r-value	Dorsal Sub
	p-value	0.060	0.141	0.077	0.068	0.019	0.037	0.068	0.106		0.048	0.054	0.052	0.094	0.010	0.044	0.103	0.180	0.129	p-value	
Ventral Sub	r-value	.892***	0.574	0.496	.836**	.693*	.711**	.757**	.722**	0.408		.868***	.920***	.919***	.838**	.900***	.893***	.731**	.819**	r-value	Ventral Sub
	p-value	<0.001	0.051	0.101	0.001	0.013	0.010	0.004	0.008	0.188		<0.001	<0.001	<0.001	0.001	<0.001	<0.001	0.007	0.001	p-value	
PL	r-value	.724**	0.534	0.298	.873***	.586*	.631*	.808**	.752**	0.410	.737**		.937***	.897***	.806**	.834**	.859***	.868***	.891***	r-value	PL
	p-value	0.008	0.074	0.346	<0.001	0.045	0.028	0.001	0.005	0.186	0.006		<0.001	<0.001	0.002	0.001	<0.001	<0.001	<0.001	p-value	
MEC	r-value	.865**	0.542	.664*	.843**	.940***	.829**	.790**	.796**	.751**	.791**	.623*		.985***	.878***	.883***	.886***	.812**	.869**	r-value	MEC
	p-value	0.001	0.085	0.026	0.001	<0.001	0.002	0.004	0.003	0.008	0.004	0.041		<0.001	<0.001	<0.001	<0.001	0.002	0.001	p-value	
LEC	r-value	.855**	.680*	0.489	.938***	.896***	.758**	.959***	.757**	.683*	.759**	.754**	.872***		.878***	.859**	.895***	.829**	.884***	r-value	LEC
	p-value	0.001	0.021	0.127	<0.001	<0.001	0.007	<0.001	0.007	0.021	0.007	0.007	<0.001		<0.001	0.001	<0.001	0.002	<0.001	p-value	
POR	r-value	.832**	0.479	0.530	.876***	.791**	.772**	.854**	.917***	0.566	.748**	.843**	.775**	.843**		.799**	.873***	.808**	.866***	r-value	POR
	p-value	0.001	0.136	0.094	<0.001	0.004	0.005	0.001	<0.001	0.070	0.008	0.001	0.005	0.001		0.002	<0.001	0.001	<0.001	p-value	
Reuniens	r-value	.643*	0.494	0.212	.704*	0.390	0.455	.633*	.632*	0.150	.628*	.833**	0.359	0.571	.817**		.868***	.746**	.819**	r-value	Reuniens
	p-value	0.024	0.103	0.509	0.011	0.210	0.137	0.027	0.028	0.642	0.029	0.001	0.278	0.066	0.002		<0.001	0.005	0.001	p-value	
Caudal area 35	r-value																	.849***	.941***	r-value	Caudal area 35
	p-value																	<0.001	<0.001	p-value	
Caudal area 36	r-value																		.978***	r-value	Caudal area 36
	p-value																		<0.001	p-value	
Caudal PRH	r-value																			r-value	Caudal PRH
	p-value																			p-value	
Peri Baseline Control (SqRt transforrmed)																					

Correlations absent due to perirhinal lesion surgeries

The top right diagonal matrix displays correlation data from the Sham Baseline group while to bottom left diagonal matrix displays correlation data from the Peri Baseline group. The r-values are the Pearson correlation coefficients. * $p < 0.05$, ** $p < 0.01$, *** $p < 0.001$, for two-tailed correlations (uncorrected for multiple comparisons – see main text). Sites included: Sites included: area 35 and area 36 (a36) of the perirhinal cortex (PRH); CA fields - intermediate (inter), septal and temporal (temp); dentate gyrus (DG); lateral entorhinal cortex (LEC); medial entorhinal cortex (MEC); nucleus reuniens of the thalamus (Reuniens); prelimbic cortex (PL); postrhinal cortex (POR); subiculum (Sub).

5.3.5 Structural equation modelling

5.3.5.1 Comparison of early learning network models

The structural equation modelling analyses presented here provide estimates of how well the observed activity data map on to known anatomical pathways. The path coefficients within the models provide quantitative estimates of neural coupling between different brain regions associated with exploration of a novel environment. The first networks to be tested were those derived in previous studies that addressed learning about different types of novel stimuli; one network from a study of object recognition memory (Chapter 3) and the other from a study of early spatial cue learning (Poirier et al., 2008). The idea was to test if the same anatomical pathways are engaged when rats learn about novel stimuli.

The intention was to estimate regional activity in the same brain regions in both the lesion and sham groups. Because of this, cortical area Te2 was not analysed in the current experiment as damage was often observed in this region in the perirhinal lesion rats. For the same reason, a more caudal region of the LEC was analysed here than that reported in the previous experiments (Chapter 3 & 4). Consequently, the precise optimal network model for novel object recognition memory, derived in Chapter 3 (Figure 3.12E), could not be tested. However, the common portion of the network could be tested; a simple linear model from the perirhinal cortex to LEC, then to septal CA3 and subsequently on to septal CA1 was tested for the Fos-related activity data generated by the group, Sham Novel (Figure 5.10A). The activity data did not fit this model (χ^2_4 = 5.06, p = 0.17; CFI = 0.77; RMSEA = 0.26; Figure 5.10A). A subset of this model was tested for the data from group Peri Novel, without the inclusion of the perirhinal cortex, and this was found to have acceptable fit (χ^2_1 = 0.51, p = 0.48; CFI = 1.0; RMSEA = 0.0). Examination of this model for Peri Novel (Figure 5.10B) reveals that it seems to be driven by a highly significant effective connection between septal CA3 and CA1; LEC has little effect on CA3. Thus, it was concluded that learning about novel objects or novel environments does not activate the same patterns of regional activity in the rodent medial temporal lobe.

Poirier et al., (2008) derived an optimal network model for early spatial cue learning (using Zif268 expression); this network is illustrated in Figure 5.10C, D. Again, the entire network could not be precisely reproduced as the previous network involved retrosplenial cortex which was not analysed in the current study. Nonetheless, the principal part of the model could be tested and, interestingly, the activity data from

group Sham Novel was found to have acceptable fit (χ^2_1 = 1.18, p = 0.28; CFI = 0.97; RMSEA = 0.13; Figure 5.10C) while the Fos-related activity data generated by group Peri Novel did not (χ^2_1 = 1.91, p = 0.17; CFI = 0.91; RMSEA = 0.30; Figure 5.10D). This suggests two preliminary findings. First, that the anatomical network associated with learning about a novel environment can be generalised across environments, even when they have very different features. Second, that perirhinal lesions seem to affect this network.

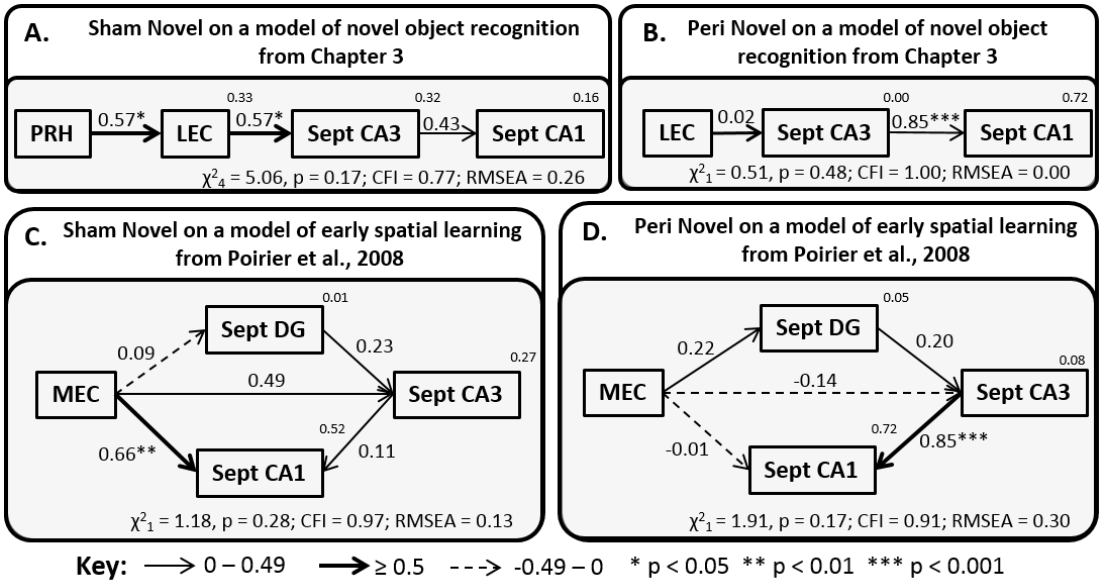

Figure 5.10. Tests of network models derived in previous studies of novelty learning.

(A) Data from Sham Novel tested on a network model previously derived for novel object recognition. (B) Data from Peri Novel tested on a network model previously derived for novel object recognition. (C) Data from Sham Novel tested on a network model previously derived for early spatial cue learning. (D) Data from Peri Novel tested on a network model previously derived for early spatial cue learning. Model fit is noted at the bottom of each model (CFI, comparative fit index; RMSEA, root mean square error of approximation). The strength of the causal influence of each path is denoted both by the thickness of the arrow and by the path coefficient next to that path. The number above each region is the proportion of its variance that can be explained by its inputs. Sites depicted: lateral entorhinal cortex (LEC), medial entorhinal cortex (MEC) and septal (sept) hippocampal subfields CA1, CA3 and dentate gyrus (DG). * p < 0.05; ** p <0.01; *** p < 0.001.

5.3.5.2 Preliminary analyses

Given that the network model of early spatial learning for group Sham Novel described above has only one degree of freedom (Figure 5.10C) this model has limited explanatory power. However this model does give an indication of the integrated patterns of hippocampal activity when rats explore a novel environment and so these relationships were further explored with more extensive network models. In addition, network models that fit the patterns of activity for all behavioural groups were sought and so the next aim

was to create a reference model, as described in Poirier et al (2008). This is a basic network model that activity data from all behavioural groups will fit that can subsequently be modified to create optimal models for each group. The reference network was determined by first collapsing Fos-positive cell counts for hippocampal subfields CA1, CA3 and DG across the rostral-caudal extent of the hippocampus in order to limit the possible number of models.

The reference network model (structure depicted in Figure 5.11) was initially tested on data pooled from all animals (n = 46). The optimal network model derived for these data involved parallel connections between MEC and LEC and from MEC to DG, CA3, CA1. The intrinsic hippocampal connections between DG and CA3 and from CA3 to CA1 were also present in this functional model. Additionally, LEC was connected to DG and CA1. The Fos-related activity data fit this network model well ($\chi^2_2 = 2.56$, $p = 0.28$; CFI = 0.99; RMSEA = 0.079) and the path coefficients for all pathways in the model were significant except that from MEC to DG.

This reference network was then tested for Fos data from each of the groups individually (Figure 5.11). This network model had good fit for three of the four groups; the exception being group Peri Baseline (Figure 5.11D); the RMSEA was quite high suggesting that a simpler model is required for this group. Examination of the path strengths of the network models for each of the groups suggests differences between the groups. This was tested directly by stacking the data from the four groups on the reference model. The strength of each of the paths was constrained such that they had to have the same value in all of the groups, i.e., setting the models for the groups to be identical. This procedure produced a model of poorer fit than the model in which the path strengths of all paths were free to vary between the groups ($\chi^2_{24\ \mathrm{Diff}} = 59.9$, $p < 0.001$). Even when the three groups for which the model had good fit were stacked in the same manner (excluding Peri Baseline), there was a significant difference between them ($\chi^2_{16\ \mathrm{Diff}} = 37.2$, $p = 0.002$). This indicates that the difference observed in the four-group comparison was not simply driven by an ill-fitting model for group Peri Baseline. All of this suggests that while the overall qualitative structure may be the same for three of the groups (as the network model has good fit), the effective functional connectivity between regions that compose the network are different between the groups.

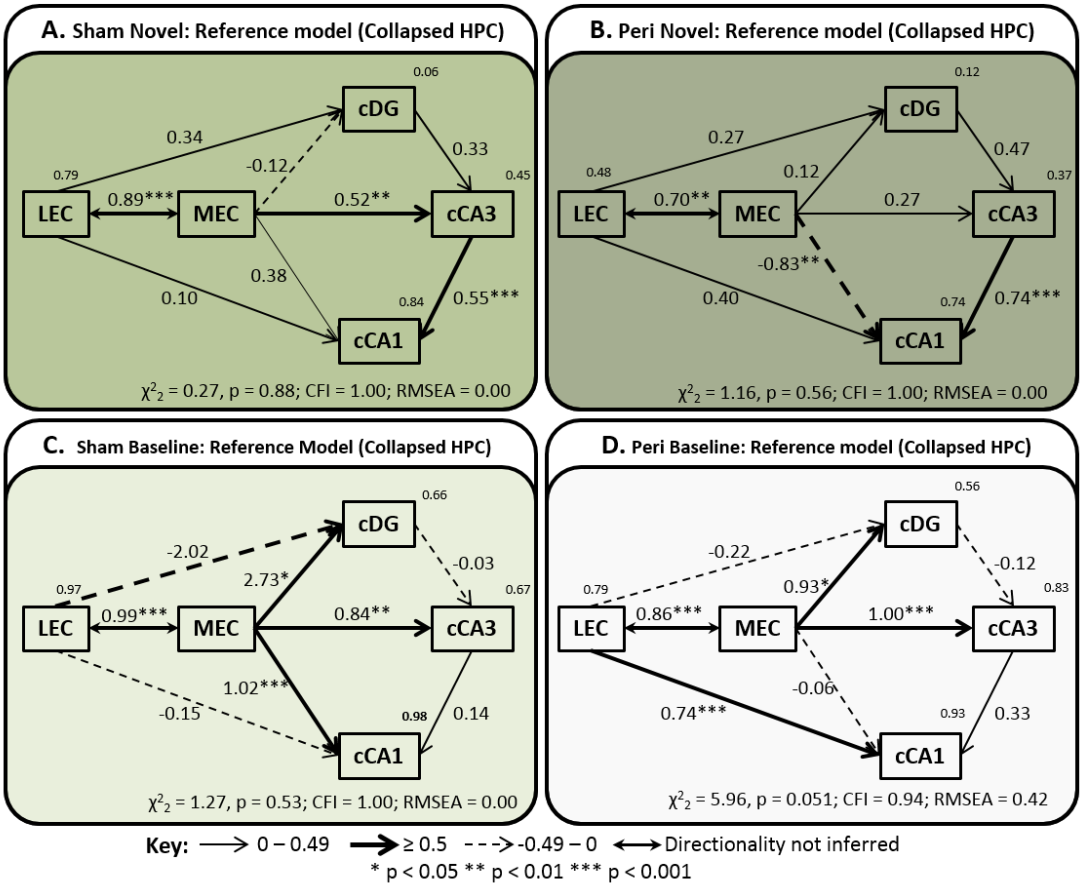

Figure 5.11. Reference model for parahippocampal – hippocampal interactions.

These models were derived from structural equation modelling based on Fos data collapsed over the rostral-caudal extent of the hippocampus. Reference model for groups Sham Novel (A), Peri Novel (B), Sham Baseline (C) and Peri Baseline (D). Model fit is noted at the bottom of each model (CFI, comparative fit index; RMSEA, root mean square error of approximation) and models with unacceptable fit are represented with a pale grey background. The strength of the causal influence of each path is denoted both by the thickness of the arrow and by the path coefficient next to that path. The number above each region is the proportion of its variance that can be explained by its inputs. Sites depicted: lateral entorhinal cortex (LEC), medial entorhinal cortex (MEC) and collapsed (c) hippocampal subfields CA1, CA3 and dentate gyrus (DG). * $p < 0.05$; ** $p < 0.01$; *** $p < 0.001$.

5.3.5.3 Optimal models for groups exposed to a novel context

The reference model was subsequently used as a starting point to individually fit models of higher spatial resolution for the groups exposed to the novel context. In order to do this, the hippocampal Fos counts were divided back into septal, intermediate and temporal levels. This provided the potential for a very large number of network models and so in order to constrain this number only hippocampal subfields from the same septotemporal level were included in a model. Successive connections along the tri-synaptic loop are known to extend someway along the septotemporal axis of the hippocampus; however, this is not complete (Amaral, 1993; Amaral & Lavanex, 2007). For instance, mossy fibres from the septal region of the dentate gyrus do not project to

the entire septotemporal length of CA3. It was decided to limit these connections to those from the same septotemporal level to avoid addition of implausible connections and to limit the number of possible models. As a consequence, models that involved, for example, only intermediate hippocampal subfields were tested. This reduced the possibility of type I errors. Fos-positive counts were not obtained for temporal dentate gyrus as it was not present at the level at which the temporal hippocampus was analysed. Thus, when the temporal CA fields were tested in a model, the collapsed counts from septal and intermediate dentate gyrus were used as a proxy for temporal dentate gyrus. An additional constraint was that models would only be accepted if they had more than two degrees of freedom due to the limited explanatory power of models with low degrees of freedom. Finally, a maximum of six nodes could be included in each model in order to ensure model fit statistics remained robust given the sample size (Bollen & Long, 1992; Wothke, 1993).

Initially, the reference model was tested for each group individually for the three separate levels of the hippocampus. At each level, modifications were made to the reference model, such as adding additional regions or removing weak pathways. No well-fitting models for either group Sham Novel or group Peri Novel could be derived using hippocampal subfields from the septal level that conformed to the criteria listed above.

The first well-fitting model to be derived for group Sham Novel was based on the intermediate hippocampal subfields (Figure 5.12A). The structure of the model was very similar to that of the reference model, excluding the path from LEC to intermediate dentate gyrus and an additional region was included, the postrhinal cortex, connected to MEC. The activity data fit this network model well ($\chi^2_7 = 7.12$, $p = 0.42$; CFI = 0.99; RMSEA = 0.041). Only six regions could be included in each model, thus if postrhinal cortex was removed from the model and subiculum was added, via a pathway from intermediate CA1 (Figure 5.12A), this also produced a model of good fit ($\chi^2_7 = 5.68$, $p = 0.58$; CFI = 1.0; RMSEA = 0.0). Neither of these network models had acceptable levels of fit for any of the other groups (Figure 5.12B-D). In order to assess differences in the way novelty-related information was processed, the data from group Sham Novel and Sham Baseline were stacked on this network model in order to formally compare the path coefficients between the two behavioural conditions. Overall, the model in which the path coefficients were all free to vary had significantly better fit than the structural weights model in which all path coefficients were constrained to be the same for both

groups ($\chi^2_{8\ Diff}$ = 16.4, p = 0.036). When each of the paths were subsequently allowed to vary individually, only freeing the paths from MEC to LEC ($\chi^2_{1\ Diff}$ = 4.34, p = 0.04) and from MEC to dentate gyrus ($\chi^2_{1\ Diff}$ = 7.30, p = 0.008) significantly improved fit (all other paths: $\chi^2_{1\ Diff}$ < 2.3, p > 0.13).

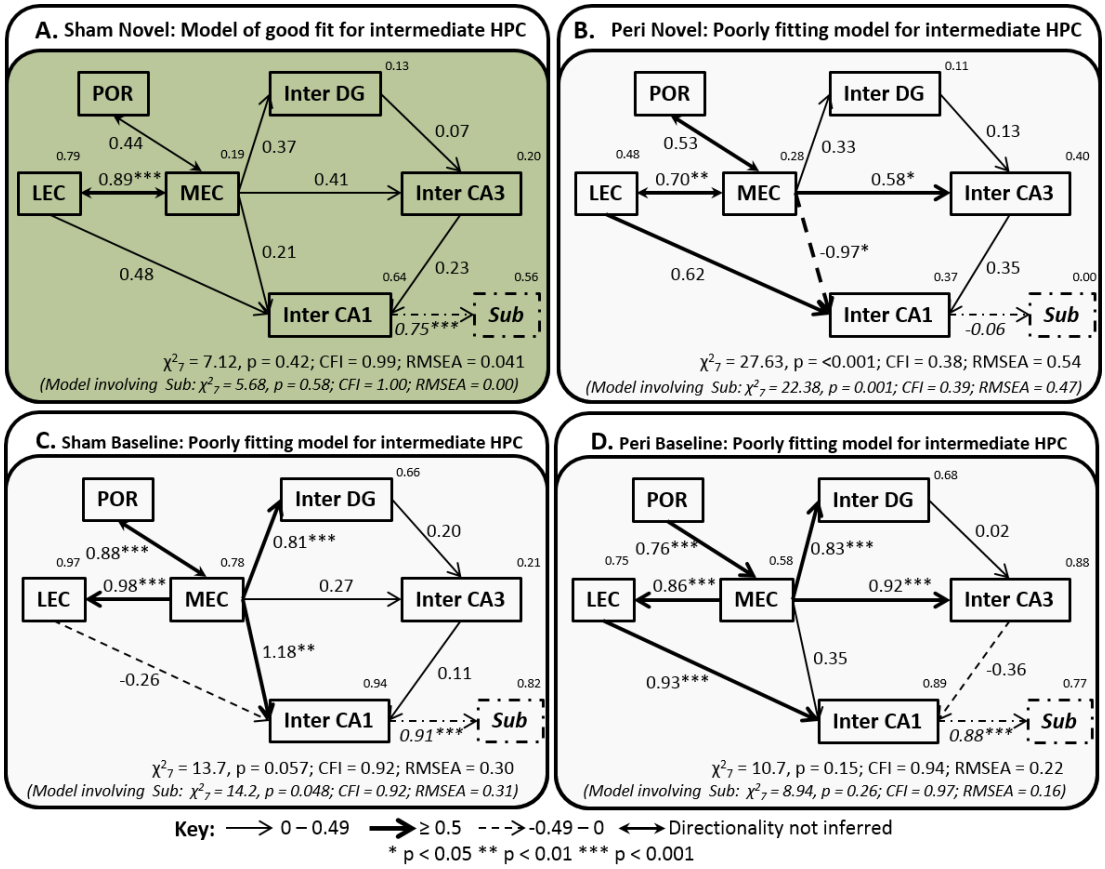

Figure 5.12. Model of good fit for of parahippocampal – intermediate hippocampal interactions for group Sham Novel.

(A) Network model of good fit for activity data from group Sham Novel. (B) Illustrates the same network model for group Peri Novel but it has poor fit. (C) The same model for group Sham Baseline which also has poor fit. (D) The same poorly fitting model for group Peri Baseline. Model fit is noted at the bottom of each model (CFI, comparative fit index; RMSEA, root mean square error of approximation) and models with unacceptable fit are represented with a pale grey background. The strength of the causal influence of each path is denoted both by the thickness of the arrow and by the path coefficient next to that path. The number above each region is the proportion of its variance that can be explained by its inputs. Sites depicted: lateral entorhinal cortex (LEC), medial entorhinal cortex (MEC), postrhinal cortex (POR), intermediate (inter) hippocampal subfields CA1, CA3 and dentate gyrus (DG) and subiculum. Note that the dashed pathway involving Sub was added as this provided a further model with good fit; the additional fit indices in italics are related to this model. * p < 0.05; ** p <0.01; *** p < 0.001.

Another well-fitting model involving the intermediate hippocampus could be derived for group Sham Novel (χ^2_4 = 4.04, p = 0.40; CFI = 0.99; RMSEA = 0.03l; Figure 5.13A). The interactions between MEC and the hippocampal sub-regions remained the same as

the previously described model but the parahippocampal connections were simplified to one pathway between postrhinal cortex and MEC. Again, this network model did not have acceptable levels of fit for any of the other behavioural groups (Figure 5.13B-D). The groups Sham Novel and Sham Baseline were also stacked on this model. The only path that caused a significant improvement in model fit over the structural weights model when it was unconstrained was the pathway from MEC to dentate gyrus ($\chi^2_{1\ Diff} = 7.31$, $p = 0.007$).

No network models connecting the subfields at the intermediate level of the hippocampus could be derived with acceptable fit for group Peri Novel. Consequently, although non-ideal, models involving collapsed septal and intermediate dentate gyrus along with temporal CA1 and CA3 were explored. Again, the models were initially based on the reference model and subsequently modified. The pathways connecting LEC to dentate gyrus and temporal CA1 were eliminated, as was the path from MEC to CA1 (Figure 5.14B), producing a model of acceptable fit for group Peri Novel ($\chi^2_5 = 5.22$, $p = 0.39$; CFI = 0.98; RMSEA = 0.07) but not for the other groups (Figure 5.14A, C, D).

It should be noted that none of the network models derived for the groups exposed to a novel context had acceptable levels of fit in the equivalent baseline group. This suggests that the models are meaningful and not simply driven by spurious correlations associated with baseline Fos expression.

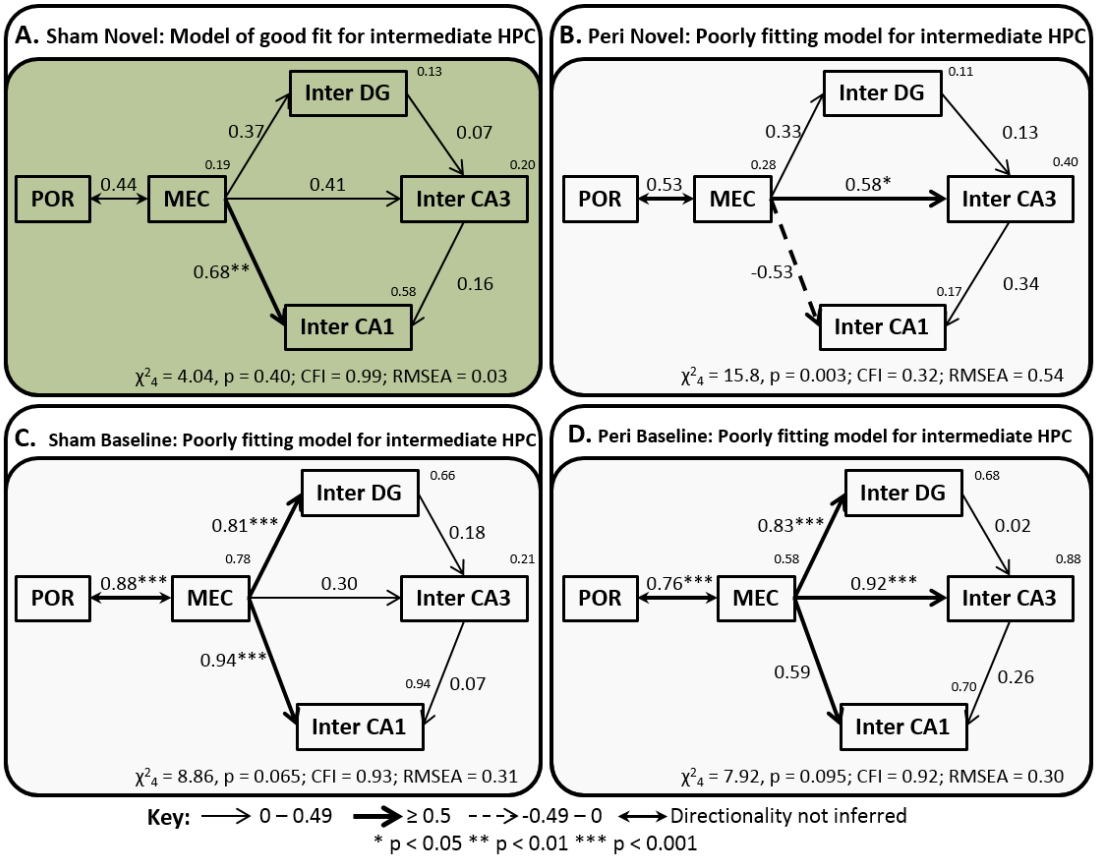

Figure 5.13. Alternative model of parahippocampal – intermediate hippocampal interactions for group Sham Novel.

Simplified model of parahippocampal – intermediate hippocampal interactions for group Sham Novel. (A) Network model of high fit for group Sham Novel. (B) Illustrates the same network model for group Peri Novel but it has poor fit. (C) The same model for group Sham Baseline also has poor fit. (D) The same poorly fitting model for group Peri Baseline. Model fit is noted at the bottom of each model (CFI, comparative fit index; RMSEA, root mean square error of approximation). The strength of the causal influence of each path is denoted both by the thickness of the arrow and by the path coefficient next to that path. The number above each region is the proportion of its variance that can be explained by its inputs. Sites depicted: postrhinal cortex (POR), medial entorhinal cortex (MEC) and intermediate (inter) hippocampal subfields CA1, CA3 and dentate gyrus (DG). * $p < 0.05$; ** $p < 0.01$; *** $p < 0.001$.

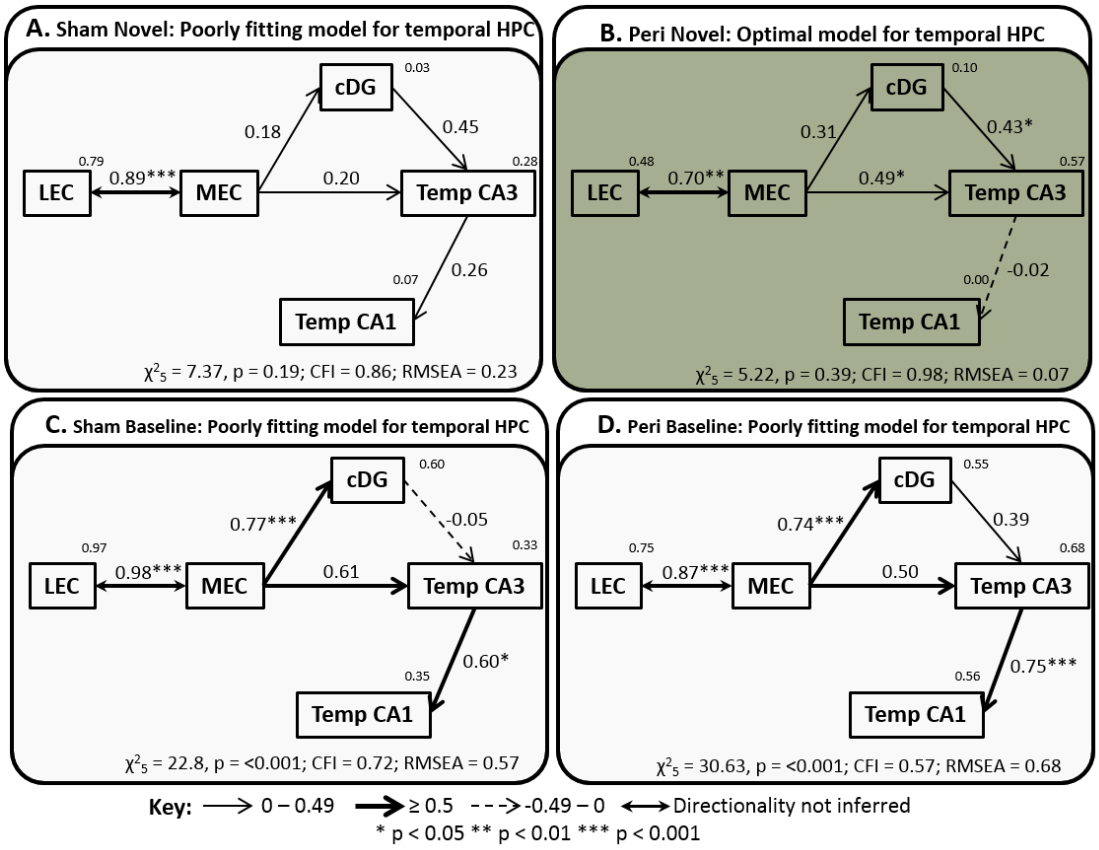

Figure 5.14. Optimal model of parahippocampal – temporal hippocampal interactions for group Peri Novel.

(A) Network model for group Sham Novel with poor fit. (B) Illustrates the optimal network model for group Peri Novel. (C) The same model for group Sham Baseline also has poor fit. (D) The same poorly fitting model for group Peri Baseline. Model fit is noted at the bottom of each model (CFI, comparative fit index; RMSEA, root mean square error of approximation). The strength of the causal influence of each path is denoted both by the thickness of the arrow and by the path coefficient next to that path. The number above each region is the proportion of its variance that can be explained by its inputs. Sites depicted: lateral entorhinal cortex (LEC), medial entorhinal cortex (MEC), temporal (temp) hippocampal subfields CA1, CA3 and collapsed (c) dentate gyrus (DG). * $p < 0.05$; ** $p < 0.01$; *** $p < 0.001$.

5.3.5.4 Effect of perirhinal cortex lesions

In order to assess the effect of lesions to the perirhinal cortex on incidental contextual learning, the data from the two novel groups were stacked on the three optimal models described above (two for Sham Novel and one for Peri Novel). Initially the two groups were stacked on the network model depicted in Figure 5.12; the unconstrained model was not significantly better than the model in which all path coefficients were constrained to be the same across the two groups (structural weights model; $\chi^2_{8\ Diff} = 8.86$, $p = 0.36$). This indicated that the groups did not differ; however, as the model had poor fit for group Peri Novel, further examination was required. To probe for differences, each of the pathways were individually unconstrained and compared to the

structural weights model. The only path that significantly improved fit when it was free to vary was that between MEC and intermediate CA1 ($\chi^2_{1\ Diff} = 7.11$, $p = 0.008$). Of potential interest is the fact that allowing the paths from LEC to CA1 and from MEC to DG to differ between the groups came close to significantly improving fit over the structural weights model ($\chi^2_{1\ Diff} = 3.66$, $p = 0.055$ for both paths; all other paths $\chi^2_{1\ Diff} < 1.6$, $p > 0.23$).

The same procedure was carried out for the network model outlined in Figure 5.13 and exactly the same pattern of results emerged; the completely unconstrained model was not significantly different from the structural weights model ($\chi^2_{6\ Diff} = 8.25$, $p = 0.22$) and when each of the pathways were examined individually only freeing the path between MEC and the intermediate CA1 significantly improved the model fit ($\chi^2_{1\ Diff} = 7.83$, $p = 0.005$; all other paths $\chi^2_{1\ Diff} < 1.5$, $p > 0.23$). Furthermore, in group Sham Novel, the correlation between Fos counts in MEC and intermediate CA1 was strong and positive ($r = 0.75$, $p = 0.008$) whereas in group Peri Novel this correlation was negative and non-significant ($r = -0.32$, $p = 0.34$). Formal comparison of these correlations using Fisher's *r*-to-*z* transformation revealed these correlations were significantly different ($z = 2.6$, $p = 0.009$).

Finally, the optimal model derived for group Peri Novel (Figure 5.14) was tested in the same way. Again, the model in which all path coefficients were free to have different values between the groups was not significantly different from the completely constrained, structural weights, model ($\chi^2_{5\ Diff} = 2.62$, $p = 0.22$). Upon further investigation, individually unconstraining each of the pathways did not significantly improve on the structural weights model (for all paths $\chi^2_{1\ Diff} < 1.2$, $p > 0.27$). This is not necessarily surprising as the path that caused the differences in the previous stacking procedures was not present in this model. Additionally, the pattern of correlations seen between MEC and intermediate CA1 was repeated at the temporal level; the correlation between Fos counts in MEC and temporal CA1 was strong and positive ($r = 0.72$ $p = 0.013$) whereas in group Peri Novel this correlation was negative and non-significant ($r = -0.22$, $p = 0.52$). Again, these correlations were significantly different ($z = 2.25$, $p = 0.024$).

Taken together, these results indicated that lesions to the perirhinal cortex caused alterations in the effective functional connection between the entorhinal cortex and CA1 at intermediate and temporal levels when animals were exploring a novel context.

5.4 Discussion

The first aim of the current study was to assess the impact of lesions to the perirhinal cortex on the hippocampus when rats explore a novel context. The second aim was to explore the possibility that based on Fos expression, there are common networks of activity in the medial temporal lobe associated with processing of multimodal novel stimuli. The third aim was to test if novel context exposure was associated with neuronal activity in the 'where' pathway postulated by the binding of item and context model (Diana et al., 2007). In order to address these aims, a group of rats with excitotoxic lesions in the perirhinal cortex and their surgical controls were exposed to a completely novel environment, an activity box in a novel room, in order to induce c-*fos* expression. Two other groups (perirhinal and sham lesions) were exposed only to their home-cages and so served as baseline controls for Fos expression. The implications of the results of the experiment are first discussed followed by the discussion of some technical considerations and limitations.

5.4.1 Theoretical implications

5.4.1.1 The effect of perirhinal lesions

Perirhinal lesions did not cause any differences in the amount of locomotion in a novel context. Following exposure to this novel context, Fos expression was examined and as expected this exposure significantly increased Fos-positive cell counts across the brain when compared to baseline controls (Zhu et al, 1997; VanElzakker et al., 2008). As outlined above, the initial goal of the study was to assess if perirhinal lesions altered the levels of this novelty related c-*fos* activity. There was no evidence of a lesion effect in any examined subfields of the hippocampus, the prelimbic cortex or the nucleus reuniens of the thalamus. A lesion effect was observed, however, in the entorhinal cortex, specifically the lateral entorhinal cortex. It is likely that this reduction in Fos-related activity is due to the loss of the dense input from perirhinal cortex to the lateral entorhinal cortex (Burwell & Amaral, 1998b). Thus, initial indications were that lesions to the perirhinal cortex did not affect overall hippocampal activity related to exposure to a novel context, but did affect activity in one of the main cortical input regions to the hippocampus (Van Strien et al., 2009). Although overall hippocampal Fos counts were ostensibly unaffected by the current perirhinal lesions, the relationships between the hippocampal subfields may have been altered (Poirier et al., 2008; Chapter 3, 4). In order to explore the concept of altered network dynamics, structural equation modelling

was undertaken on the Fos-related activity data to look for evidence of dysfunction in the intrinsic hippocampal networks.

Exploring network dynamics using structural equation modelling allows for the comparison of specific pathway coefficients between lesion groups, thus the connections between regions downstream of the lesion site can be directly compared. If perirhinal cortex lesions directly cause spatial memory impairments, it could manifest as widespread disruption of all pathways. On the other hand, if the consequence of a perirhinal lesion is to remove a signal that would normally be present (as was indicated by the absolute reduction in Fos-related activity in the lateral entorhinal cortex) the network changes could be seen on a smaller scale. The network alterations could present themselves in the connections between regions of the rhinal cortex, in the connections between the rhinal cortex and the hippocampus, or in the intrinsic connections of the hippocampus.

The reference model (Figure 5.11) had good fit for the activity data from both groups Sham Novel and Peri Novel. However, the fact that none of the more anatomically specific models generated good measures of fit for both group Sham Novel and group Peri Novel indicated that the perirhinal lesions do indeed alter contextual processing. In spite of this, examination of the path strengths of the intrinsic hippocampal connections shows that they were typically similar across both group Sham Novel and group Peri Novel, while there were often differences in the strength of the connections between the cortex and the hippocampus. Direct comparisons between the network models for groups Sham Novel and group Peri Novel revealed that the intrinsic connections between the rhinal cortices and the intrinsic hippocampal connections were unaffected. Instead, changes were identified in the pathway from medial entorhinal cortex to intermediate or temporal CA1. In the Sham Novel group, the path between these two regions was positive, whereas in the Peri Novel group it was negative. It has been suggested that path coefficients can be interpreted in the same way as correlation coefficients; a negative coefficient indicates that increased activity in one region results in a proportional activity decrease in the region to which it is connected (McIntosh & Gonzalez-Lima, 1991). The result of the dysfunction in the connection between medial entorhinal cortex and CA1 was reinforced by the need to remove this path in order to obtain a model of acceptable fit for group Peri Novel. This pathway defect was further compounded by the finding that the inter-regional correlation between the medial entorhinal cortex and CA1 was significantly different between the groups. Together this

indicates that perirhinal cortex lesions did not cause intrinsic hippocampal dysfunction, rather, that the disruption occurs in a processing step before the hippocampus. The results also point to the ability of the hippocampus to maintain intrinsic activity patterns, despite these parahippocampal changes.

Many studies that have investigated the impact of perirhinal lesions failed to find deficits on spatial tasks that are sensitive to hippocampal function (reviewed in Aggleton et al., 2004). This finding is consistent with the pattern of results presented here. There are, however, some studies that report subtle behavioural deficits in spatial tasks due to lesions of the perirhinal cortex (Wiig & Bilkey, 1994a,b; Liu & Bilkey, 1998a,b, 2001). The data described above indicate that these deficits are not due to perturbations in a single memory system based around the hippocampus. While it remains a possibility that these impairments could be due to integral involvement of the perirhinal cortex in spatial processing the results presented here indicate that deficits are due to secondary dysfunction caused by deafferentation of the surrounding cortical areas. The present lesion differences in overall activity levels in the lateral entorhinal cortex, and in the connection between medial entorhinal cortex and CA1 suggest that the spatial deficits observed following perirhinal cortex lesions are due to downstream effects of the perirhinal lesion on the entorhinal cortex and its subsequent interaction with the hippocampus. The possibility remains that this lesion effect is due to a loss of the direct connections between the perirhinal cortex and medial entorhinal cortex. Alternatively the lesion effect could be due to the loss of the more numerous indirect connections between the perirhinal cortex and medial entorhinal cortex via lateral entorhinal cortex and postrhinal cortex (Burwell & Amaral, 1998b; Burwell, 2000). The absolute reduction in Fos expression in the lateral entorhinal cortex would suggest the latter.

An alternative explanation of the lesion effects observed previously in spatial learning and one that is compatible with the results presented here comes from the suggestion that the perirhinal cortex is involved in perception of contextual stimuli (Kent & Brown, 2012). This suggestion was based around the perceptual-mnemonic feature conjugation model of perirhinal cortex function. In addition to its role in facilitating item-based memory, the perirhinal cortex has been implicated in perceptual processing (Murray & Bussey, 1999; Bussey et al., 2005, 2007; Murray & Wise, 2012). This model conceptually places the perirhinal cortex at the end of the ventral visual processing stream. Wherein, contiguous components (or features) of an item are represented as a whole, rather than the individual component parts that are represented in areas earlier in

the visual processing stream (Murray & Bussey, 1999; Murray et al., 2007). Kent and Brown (2012) suggest this role in perception may extend beyond item processing to the perception of contextual surroundings. Weight is added to this perspective by the findings that, although perirhinal lesions impair contextual fear conditioning and fear conditioning to complex auditory cues (Corodimas & LeDoux, 1995; Sachetti et al., 1999; Bucci et al., 2000, 2002; Lindquist et al., 2004, Kholodar-Smith et al., 2008a,b), they are also known to leave fear conditioning to continuous tones unimpaired (Bucci et al., 2000; Lindquist et al., 2004; Kholodar-Smith et al., 2008b). Additionally, increased Fos expression in the perirhinal cortex has been associated with contextual fear conditioning but not cued fear conditioning (Albrechet-Souza et al., 2011). If the perirhinal cortex functions in affective learning by associating the conditioned and unconditioned stimuli, lesions could be expected to impair learning in this cued fear conditioning paradigm. Thus, the perirhinal cortex may be involved in perception of contexts, but this activity is not required to maintain intrinsic hippocampal interactions.

5.4.1.2 Novelty processing network

The second aim of the current study was to use structural equation modelling methods to assess if there are specific neural networks within the medial temporal lobe that are involved in general multimodal novelty processing. Initially, novelty related data from the current study was tested on the network models derived in a study of object recognition memory (Chapter 3), and another, derived in a test of novel spatial cue learning (Poirier et al., 2008).

The optimal network model for novel object recognition memory derived in Chapter 3 involved a path directly from Te2 to LEC and another path from Te2, via perirhinal cortex, to LEC, which in turn project to septal CA3 and from there to septal CA1. Area Te2 and perirhinal cortex were not analysed in the perirhinal lesion groups of the present study and so only the common portion of the network could be tested; a simple linear model from LEC to septal CA3 and, thence, to septal CA1. This model had acceptable fit for group Peri Novel; however, examination of the path strengths (Figure 5.10B) revealed that it seems to be driven by a highly significant effective connection between septal CA3 and CA1, but LEC appeared to have little effect on CA3. This, combined with the fact that the model has only one degree of freedom and thus, relatively low explanatory power led to the rejection of this as a viable model. Further, when the perirhinal cortex was added at the start of the model and tested on the activity data from group Sham Novel, it had poor fit (Figure 5.10A).

Poirier et al. (2008) derived an optimal network model for novel spatial cue learning. It involved parallel connections from MEC to septal levels of DG, CA3 and CA1. These regions were also interconnected and CA1 was further connected to the retrosplenial cortex. Again, the entire network could not be precisely reproduced as the retrosplenial cortex was not analysed in the current study. Nonetheless, the predominant part of the model could be tested and this network model fit the activity data from group Sham Novel, although the model only had one degree of freedom. The same network model had poor levels of fit for group Peri Novel but examination of these models (Figure 5.10C, D) reveals the same pattern as that described above; the most striking difference between the surgical conditions is the path between MEC and CA1.

Although these hypothesised models did not adhere to the criteria outline in Section 5.3.5.3, the Poirier et al. (2008) network model (Figure 5.10C, D) showed potential for fitting the current novelty data and so new models of acceptable fit to the activity data were derived based around this general network structure. Initially a reference model was created based on collapsing the data for all four current animal groups, and collapsing Fos counts for CA1, CA3 and DG across the septotemporal axis of the hippocampus, in order to limit the possible number of models. The fact that this network model fitted the activity data suggests that this context based task elicits a generalised pattern of activation across the septotemporal axis of the hippocampus. It further suggests that the principal hippocampal anatomical connectivity, that is the trisynaptic loop, underpins the effective functional connectivity in these animals (Burwell, 2000; Aggleton, 2012); this is perhaps not surprising as half of the animals involved in this analysis – the baseline, home-cage control groups - were not in a position to learn anything novel. It was, therefore, striking that the same network model had very high levels of fit for three out of the four behavioural groups. Thus, it was subsequently used as a basis for the development of more regionally specific optimal group models.

Often the dorsal hippocampus is associated with spatial memory (Moser et al., 1993; Bannerman et al., 2004). The term dorsal hippocampus encompasses both the septal and intermediate levels of the delineation used here (Bast et al., 2009). The septal hippocampus did not produce models of acceptable fit for any of the groups; however, the intermediate level was implicated in two network models that had good fit for the activity data from group Sham Novel (Figures 5.12, 5.13). Perhaps relevant to the present results is the fact that the intermediate, and not the septal, hippocampus has been shown to be particularly important in place learning (Bast et al., 2009). Although the

contribution of rhinal cortex structures differed between the two well-fitting models for group Sham Novel, the qualitative structure of the connections projecting from the medial entorhinal cortex to hippocampal subfields and the intrinsic hippocampal connections remained constant across them. This same structure is also seen in the model of early spatial cue learning from Poirier et al. (2008), however, their model involved the septal level of the hippocampus rather than the intermediate level. Thus, although the network models for novel context learning and novel cue-based spatial learning are not identical, they seem to share common features.

Previous studies comparing novelty with familiarity processing using a similar IEG-imaging paradigm found another common feature. Novelty processing was associated with higher functional connectivity from entorhinal cortex along the tri-synaptic circuit of the hippocampus whereas familiarity processing involved a greater effective connection between the entorhinal cortex and CA1 (Poirier et al., 2008; Albasser et al., 2010b; Chapters 3, 4). This result was not repeated in the present study. Stacking the activity data from the Sham Novel and Sham Baseline groups, on the models derived for group Sham Novel, revealed that the main difference between the groups was a greater effective connection between medial entorhinal cortex and dentate gyrus in the baseline activity data, i.e. the group experiencing familiar stimuli. This is almost the opposite pattern to that expected. This may indicate that the previously observed pattern of novelty/familiarity driven hippocampal engagement does not extend to contextual processing. However, the result may be because the comparison between exposure to a novel activity box (in a novel room) and home-cage controls was not the appropriate comparison for the present experiment in relation to the previous studies. In the preceding protocols, the familiar stimuli were made familiar by a maximum of twelve previous exposures, whereas the present baseline animals were exposed to their home-cage almost continuously for several months. In another study that explored Fos expression, it was found that exposure of rats to an entirely novel context was associated with increased Fos expression when compared to rats that had previously been exposed to the context five times. Both groups had several times the Fos expression of the home-cage controls (VanElzakker et al., 2008). Thus it is clear that Fos expression related to the home-cage is not equivalent to Fos expression related to a stimulus made familiar by repeated, but limited, exposures. Additionally, for the Sham Baseline group, when the lateral entorhinal cortex was included in the model, medial entorhinal cortex has a very strong effective connection with intermediate CA1 (Figure 5.12C) that is not present for group Sham Novel (Figure 5.12A). Thus, the proposed pattern of hippocampal

activation when comparing novel and familiar stimuli may still occur for contextual information under more controlled circumstances.

5.4.1.3 Testing the 'where' pathway

The model depicted in Figure 5.13 essentially captures the canonical view of spatial processing; it maps on to the 'where' pathway of the binding of item and context (BIC) model (Diana et al., 2007; Ranganath, 2010). During novel context exploration, the postrhinal cortex recruits the medial entorhinal cortex which subsequently engages the three subfields of the hippocampus; the dentate gyrus, CA3 and CA1. Indeed, this model anatomically refines the BIC model as it indicates that when rats are learning about a novel context the medial entorhinal cortex recruits the intermediate level of the hippocampus by both the temporoammonic and perforant pathways. Although MEC cortical layers were not separated in the current experiment, this result echoes that of novel object recognition in Chapter 3. In that study, either LEC cortical layers II or III (associated with the perforant and temporoammonic pathways, respectively), were associated with novel object discrimination.

This result complements those of Chapters 3 and 4 in providing evidence to support the BIC model. The 'what' pathway involving the perirhinal cortex to LEC and onto the hippocampus is involved in object processing, while the postrhinal cortex to MEC and the hippocampus is engaged during context processing.

This object-context pathway dichotomy also maps onto Knierim's local vs. global reference frames model (Knierim et al., 2006, 2014). However, this model places greater emphasis on crosstalk between the two pathways. Interestingly, there is gathering evidence, particularly from single unit recordings in the rat, that LEC also plays a role in spatial processing, albeit to a lesser extent than its role in object processing, and typically in relation to item locations (Deshmukh et al., 2012; Hunsaker et al., 2013; Neunuebel et al., 2013; Knierim et al., 2014). The more complex model depicted in Figure 5.12 supports this notion.

5.4.2 Technical considerations

A potential limitation of the present study is that it involved two separate cohorts of animals that were tested at different times. The rats of cohort JAR166 were four months older than cohort JAR169 and consequently had the perirhinal lesions for four months longer. In order to address this limitation, an effort was made to balance rats from the different cohorts evenly between the four behavioural groups. However, due to the

prevalence of extra-perirhinal damage in cohort JAR166 it was necessary to exclude a relatively larger number of rats from this cohort, leaving this group slightly under represented in the final analyses. Further, the lesion size of the rats in cohort JAR166 that remained in group Peri Novel appeared smaller than that of the other groups. It is, however, worth noting that this perirhinal sparing was observed at the rostral level of the perirhinal cortex, while the mid and caudal perirhinal levels had seemingly comparable lesions to those in the other groups. Notably, the mid and caudal perirhinal levels have more numerous connections with the hippocampus (Furtak et al., 2007).

Aside from these differences, the training history of both cohorts was very similar. Both groups of animals were approximately three months old and experimentally naïve at the time of surgery. Further, both cohorts had been trained on object recognition tasks in an open field and the bow-tie maze, before being rested for approximately two weeks then beginning the current test. Thus, learning opportunities prior to the present experiment were very similar for the groups of animals. Additionally, the immunohistochemical staining for Fos was undertaken simultaneously for animals from both cohorts to reduce variance associated with this protocol. Based on these similarities, along with the fact that both cohorts of rats were represented in every behavioural group, it was presumed that group comparisons were appropriate.

Another possible caveat of the present study is the absence of a behavioural measure associated with contextual learning. The paradigm was chosen as this single exposure to a novel context is similar to the single exposure to novel objects that rats in the novel object condition received in the experiment described in Chapter 3. Additionally, contextual processing is known to engage the hippocampus (Honey & Good, 1993; Good & Bannerman, 1997; Mumby et al., 2002), and exposure to a novel context has been shown to increase hippocampal Fos expression (VanElzakker et al., 2008). However, the present results could be interpreted more readily if it were known if the lesions elicited a behavioural deficit. Of potential relevance are object-based studies that indicate that the perirhinal cortex is not involved in contextual processing (Eacott & Norman, 2004; Norman & Eacott, 2005). In addition, perirhinal lesions do not disrupt passive place learning in the water maze, a task similar to the one administered here as in the sample phase the rat is simply placed on the platform and learns about its position incidentally (unpublished observations).

5.4.3 Summary

To summarise the results of this experiment, in a task known to engage the hippocampus, hippocampal activity (as measured by Fos expression) remained unperturbed by lesions to the perirhinal cortex, indicating that hippocampal activity can be maintained in the absence of the perirhinal cortex, even when hippocampal Fos activity is high and so should be more sensitive to dysfunction. This finding again points to the functional independence of these two structures. Instead, perirhinal lesions affected activity and connections of the other rhinal cortices.

In addition, activity related to novel context processing did not fit previously derived network models of parahippocampal-hippocampal interactions for different types of novelty processing, although the common feature of the engagement of several hippocampal subfields was observed.

Finally, the network models of novel context processing derived here map onto two models that postulate how regions of the medial temporal lobe interact to support different forms of memory. These are the binding of item and context model (Diana et al., 2007) and the local vs. global reference frames model (Knierim et al., 2014).

6 Mapping medial temporal interactions in response to novel objects: The impact of perirhinal cortex lesions in rats

6.1 Introduction

Expression of c-*fos* has revealed different patterns of integrated neuronal activity across medial temporal lobe sites when rats are engaged in novel object recognition or recency memory tasks. Using structural equation modelling on c-*fos* data generated from animals engaged in an object recognition task, it has been demonstrated that this task recruited the pathway from lateral entorhinal cortex (cortical layer II or III) to hippocampal field CA3 and, thence, to CA1. Familiar stimuli in a recency task recruited the direct pathway from lateral entorhinal cortex (principally layer III) to CA1 (Albasser et al., 2010b; Chapter 3, Chapter 4). Additionally, using structural equation modelling, it was demonstrated that the functional connectivity in the parahippocampal cortex related to recognition or recency memory was not disrupted by lesions to the hippocampus (Chapter 3).

There are many models that postulate how mnemonic processing is achieved by regions of the medial temporal lobe; one such example describes the rhinal cortex (the perirhinal and entorhinal cortices) as the 'gatekeeper' of the declarative memory system (Fernández & Tendolkar, 2006). In that model it is assumed that a novel item will increase rhinal processing, leading both to a feeling that the item is unknown and enhanced transfer to the hippocampus for further encoding. Conversely, the more familiar an item is, the less perirhinal processing it requires and the less vigorously it will be encoded in memory (Fernández & Tendolkar, 2006). Another example of a mnemonic processing model is the binding item and context model (Diana et al., 2007; Eichenbaum et al., 2007). In this model, it is postulated that the perirhinal cortex engages in 'item' processing while parahippocampal cortex (the primate homologue of rodent postrhinal cortex) is involved in processing 'context'. These two cortical regions convey information to the lateral and medial entorhinal cortices respectively, which subsequently relay this information to the hippocampus where it is bound together (Diana et al., 2007). These functional models along with others (Aggleton & Brown,

1999, 2001, 2006; Bussey & Saksida, 2007; Neunuebel et al., 2013; Knierim et al., 2014) imply that the perirhinal cortex has a significant impact on hippocampal processing. Thus, it could be supposed that removal of the perirhinal cortex would cause dysfunction in hippocampal processing. The first aim of Experiment 1 was to examine the functional impact, on the hippocampus (using c-*fos* expression), of removal of the perirhinal cortex during a novel object recognition task. The next aim was to determine the extent to which the previously derived learning–related networks in the hippocampus depend on integrity of the perirhinal cortex. Experiment 1 involved a 20 trial test of object recognition memory, run in a similar manner to that of Chapter 3, in a group of rats that had lesions in the perirhinal cortex and their surgical controls. If the novel/familiar pathway differences observed previously (Albasser et al., 2010b; Chapter 3) depend on perirhinal signals of novelty, then perirhinal lesions should bias c-*fos* activity away from the 'novel' entorhinal layer II - CA3 pathway to the 'familiar' entorhinal layer III - CA1 pathway. In addition, the inclusion of surgical control rats presented an opportunity to corroborate and anatomically refine the previously derived novelty-related network model.

In the novel object based experiments, described in this thesis thus far, rats were presented with discrimination trials; as such they were always confronted with one novel and one familiar object. An earlier set of c-*fos* imaging studies involved presenting novel visual stimuli to one eye while simultaneously presenting familiar stimuli to the other eye (Zhu et al., 1995b, 1996; Wan et al., 1999, 2004). Absolute increases in c-*fos* expression were seen in the perirhinal cortex and area Te2 of the hemisphere associated with novel stimuli when compared to that associated with familiar stimuli. Features of this experimental design meant that this increased activity was not associated with network activity. Thus, it remained unclear if the networks of activity observed up to this point were generated by the rats actively discriminating between a novel and a familiar object or simply by the presence of novel stimuli in the environment. To address this question a second experiment was carried out. Experiment 2 was designed to match Experiment 1 as closely as possible with one main difference; in each trial the rats were presented with two different novel objects. This experiment involved a second cohort of rats with perirhinal lesions, along with their surgical controls.

In addition to assessing the behavioural stimuli that served to generate the previously derived functional network models, we also aimed to extend these network models to include regions beyond the medial temporal lobe but that are known to be functionally

connected. The medial prefrontal cortex is one such area that is required to interact with the perirhinal cortex to support object associative learning (Barker et al., 2007; Warburton & Brown, 2010). Additionally, it is known to be involved in cognitive tasks (Vertes et al., 2006; Heidbreder & Groenewegen, 2003). There are direct projections from the temporal region of CA1 to prelimbic cortex with return projections via the nucleus reuniens of the thalamus and retrosplenical cortex (Conde et al., 1995; Vertes et al, 2007; Prasad & Chudasama, 2013). In Experiment 1, rats were given a choice between classes of objects (novel or familiar) and so cognitive control presumably is at play when engaging in the task. The rats in Experiment 2 were presented with pairs of novel objects, and as such, did not have to make object class judgements. These pairs of novel objects were, however, dissimilar and so they must still make decisions about which objects to explore first, whether to return to a previously explored object, etc. Differences in prelimbic activity or functional connectivity could be anticipated between the groups based on the different task demands.

There is substantial evidence that lesions to the perirhinal cortex disrupt successful object recognition memory in both primates and rodents (Zola-Morgan et al., 1989, Mumby & Pinel, 1994, Murray, 1996; Brown & Aggleton, 2001; Winters et al., 2008; Albasser et al., 2009; Warburton & Brown, 2010). What remains more contentious in the literature, is the nature of this disruption. The perceptual mnemonic feature conjunction model hypothesises that the perirhinal cortex functions in perception, as well as memory, by its involvement in the ventral visual processing stream (Bussey et al., 2005). The model proposes that stimuli are represented hierarchically throughout the ventral visual stream. Individual features of stimuli are represented early in visual processing in caudal brain regions. These representations become more integrated and complex in rostral brain regions until it converges on the perirhinal cortex, which functions to encode complex conjunctive representations of stimuli in order to allow for object identification (Murray & Bussey, 1999; Murray & Richmond, 2001; Bussey et al., 2005; Murray et al., 2007). This hierarchical representation viewpoint predicts that, upon loss of the perirhinal cortex, judgements of prior occurrence would have to be based on the lower level feature-based representations of the stimuli (McTighe et al., 2010). These feature-based representations would be more susceptible to interference, as specific features of an object, for example its colour or shape, are likely to overlap with those of other intervening stimuli creating feature ambiguity between stimuli (Bartko et al., 2007a, b; Romberg et al., 2012). Thus, damage to the perirhinal cortex is predicted to cause novel objects to be perceived as familiar and, as a consequence, rats with

perirhinal lesions would be expected to spend less time exploring novel objects than intact rats. It follows that this deficit should be more profound with increasing numbers of stimuli due to greater proactive interference.

Evidence for the feature conjugation model came from a study in which rats with perirhinal lesions and their surgical controls were presented with a single pair of identical sample objects (McTighe et al., 2010). During the retention interval the rats were either returned to their home-cage or placed in a visually restricted, low-interference, environment. During the subsequent test phase the rats were presented with either the same pair or a different pair of identical objects. Rats with lesions explored the novel objects significantly less than the intact rats, but only when they had been held in their lit home-cage. When they were visually deprived during the retention interval, their subsequent exploration levels of the novel objects were restored to normal levels. This was interpreted as evidence of false-memories in the rats with perirhinal lesions, as they treated novel objects as familiar when interference could occur, but when interference was prevented, the rats performance was normal (McTighe et al., 2010). Another study carried out in mice found analogous results (Romberg et al., 2012).

Contrary to the results described above, other studies that presented pairs of novel objects to rats with perirhinal lesions found that their total exploration times were no different from their surgical controls (Albasser et al., 2011a, 2015). Additionally, in the studies reporting evidence for 'false memories', all rodents displayed normal levels of exploration in the sample phase, indicating accurate novelty detection (McTighe et al., 2010; Romberg et al., 2012). This was attributed to the memory trace of the sample objects being strong enough to cause subsequent interference during the test phase, but only when the animals were kept in their lit home-cage during the retention interval (Romberg et al., 2012). This implies that the combination of a single presentation of objects followed by time spent in a highly familiar, but non-sensory deprived environment, is sufficient to cause significant interference.

In order to further probe this susceptibility to interference, the rats in Experiment 2 were presented with 20 pairs of dissimilar novel objects. This was done to maximise the number of different features to which they were exposed. If perirhinal lesions cause novel objects to be perceived as familiar, these rats should explore all objects less than their surgical controls. Additionally, this reduction in exploration should become more profound as the number of trials increases due to increasing proactive interference.

6.2 Materials and Methods

6.2.1 Animals

6.2.1.1 Experiment 1 – Novel-Familiar object discrimination

Subjects were 29 male, Lister Hooded rats (Harlan). They were housed as described in General Methods section 2.2. These animals were pre-trained in the bow-tie maze (as described in General Methods section 2.3.3) and then given a single 10 trial novel object recognition test. Following this, they received either perirhinal cortex lesions (n = 17) or sham surgeries (n = 12). After recovery from the surgeries, they were tested a further seven times in the bow-tie maze on novel object recognition tasks with various delays between the sample and test phases. Following this, their spatial memory was tested in an active and passive placement water-maze experiment. Finally, they took part in the current c-*fos* imaging study when they were approximately 12 months old.

6.2.1.2 Experiment 2 – Novel-Novel object exploration

Subjects were 31 male, Lister Hooded rats (Harlan). They were housed as described in General Methods section 2.2. These animals had previously received either perirhinal cortex lesions (n = 18) or sham surgeries (n = 13). Following recovery from surgery they were pre-trained in the bow-tie maze (as described in General Methods section 2.3.3). They were then tested in the bow-tie maze twice; once on a novel object recognition task with long retention intervals and once on a recency task. Rats were approximately 11 months old at the beginning of the present c-*fos* imaging study.

6.2.2 Surgery

The rats in both experiments were approximately three months old at the time of surgery. The surgeries were carried out by Dr. C. Olarte Sanchez using the same protocol for both cohorts of animals. The rats in Experiment 1 weighed between 290g and 350g, while in Experiment 2 the rats weighed between 290g and 340g at the time of surgery. Anaesthesia was induced in all animals using a mixture of oxygen and isoflurane gas, before placing them in a stereotaxic frame (David Kopf Instruments, Tujunga, CA, USA), with the incisor bar set at +5.0 mm to the horizontal plane. A midline sagittal incision was made in the scalp and the skin was retracted to expose the skull. A craniotomy was made above the injection sites. The lesions were made by injecting a solution of N-methyl-d-aspartate (NMDA; Sigma, Poole, UK) diluted to 0.09M in PBS (0.1M, pH 7.4) using a 1µm Hamilton syringe (gauge 26s, outside

diameter 0.47 mm) held with a micro-injector (Kopf Instruments, Model 5000). Bilateral injections of NMDA were made at a rate of 0.10 µL / min, with a subsequent diffusion time of four minutes. The animals received three injections in each hemisphere (for co-ordinates and volumes see Table 6.1). Rats in the surgical control (Sham) groups received identical treatment, except that the dura was perforated with the same Hamilton syringe but no fluid was infused into the brain. Following completion of the surgery, 5 ml of glucose saline was administered subcutaneously to all rats and they were allowed to recover in a heated box until they regained consciousness.

Table 6.1. Stereotaxic coordinates and infusion volumes for lesions of the PRH.

Anteroposterior	Mediolateral	Dorsoventral	Volume (µL)
-1.8	±5.9	-9.3	0.22
-3.4	±6.2	-9.5	0.20
-5.0	±6.3	-8.9	0.20

6.2.3 Apparatus

Testing for both Experiments 1 and 2 took place in a bow-tie maze described in the General Methods section (Figure 2.2).

6.2.4 Objects

All stimuli used in these experiments were three-dimensional plastic, glass or ceramic 'junk' objects. Each object was large enough to cover a food well but light enough to be displaced by a rat. All objects were cleaned with 70% ethanol wipes after each session.

Experiment 1 – Novel-Familiar object discrimination

Experiment 1 utilised 20 different objects, each with an identical duplicate.

Experiment 2 – Novel-Novel object exploration

Experiment 2 utilised 40 different objects.

6.2.5 Behavioural testing

6.2.5.1 Pre-training and re-habituation to bow-tie maze

Both cohorts of rats had been previously pre-trained in the bow-tie maze, as described in the General Methods section 2.2.3. The rats were then tested on different behavioural

tasks (as outlined above). Neither cohort had been tested in the bow-tie maze for at least 3 months prior to the beginning of the present experiments. Due to the previous training in the bow-tie maze, only a single re-habituation session was carried out. This re-habituation session involved three pairs of objects and followed the pre-training protocol described for days 4-7 in the General Methods section 2.2.3. Re-habituation was complete when the rats would run from one side of the maze to the other when the door was raised. This took 7-10 minutes for each rat.

6.2.5.2 Animal groups

Experiment 1 – Novel-Familiar object discrimination

The rats with perirhinal lesions and their surgical controls were tested using the same behavioural protocol creating two groups; Peri Discrimination (n = 17) and Sham Discrimination (n = 12).

Experiment 2 – Novel-Novel object exploration

Again, all rats in this experiment were tested using the same behavioural protocol creating two groups; Peri Novel (n = 18) and Sham Novel (n = 13).

6.2.5.3 Experiment 1 – Novel-Familiar object discrimination

Animals were placed in a dark room for 30 minutes before testing began. The behavioural procedure to induce Fos expression was carried out in a single test session which consisted of 20 trials with one minute per trial. This test session was identical to session 1 described in Chapter 3 (Section 3.2.5.3 "Shared protocol for session 1"). The procedure is summarised in Figure 6.1; notably each trial consists of a novel object presented with a familiar object that is familiar because it was encountered on the previous trial.

6.2.5.4 Experiment 2 – Novel-Novel object exploration test

The aim of Experiment 2 was to match the behavioural procedure in Experiment 1 as closely as possible, while removing the discrimination component. As such, these rats were also placed in a dark room for 30 minutes before testing began and the single test session consisted of 20 trials with one minute per trial. The principal difference between the novel-familiar discrimination and novel-novel exploration conditions was that in

each trial of the novel condition the animals were presented with two different novel objects (Figure 6.1).

On completion of their respective test sessions, the rats from both Experiments 1 and 2 were returned to the same dark room for 90 minutes and then perfused as described in the General Methods section 2.4.

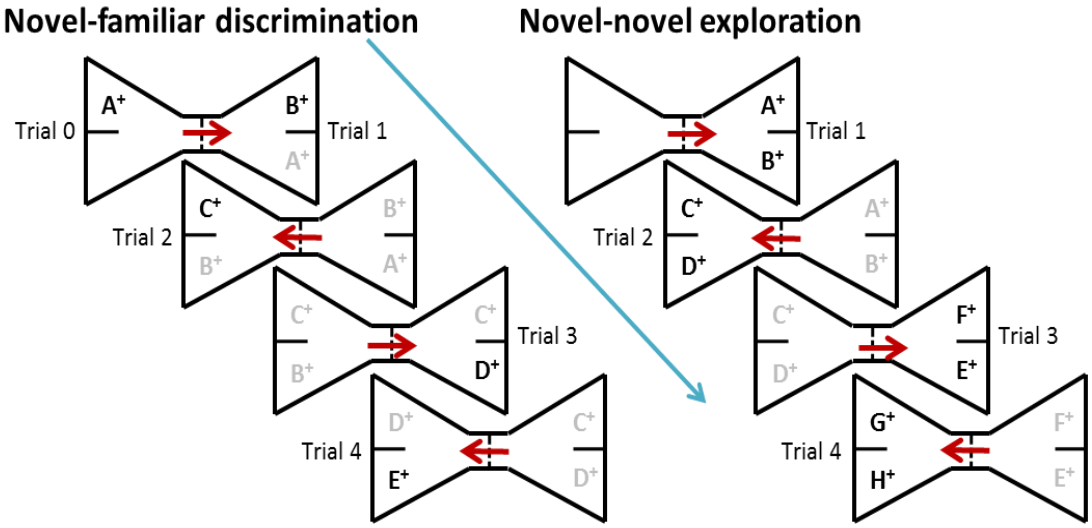

Figure 6.1. General procedure showing the order of presentation of objects in novel-familiar discrimination and novel-novel exploration behavioural conditions.

All objects are rewarded (+). Red arrows show the directions of the rats' movements while the blue arrow indicates progression through trials. Black letters denote novel objects while grey letters denote familiar objects.

6.2.6 Analysis of behaviour

The behavioural measures were calculated as described in General Methods section 2.3.5 for animals in the novel-familiar discrimination condition. For the animals in the novel-novel exploration condition, the only measure that could be calculated was total cumulative exploration.

Following the behavioural analyses the methods used and protocols followed were exactly the same for both Experiments 1 and 2.

6.2.7 Lesion analysis

As described in General Methods section 2.7.

6.2.8 Immunohistochemistry

As described in General Methods section 2.8.

6.2.9 Regions of interest

All of the regions of interest (ROI) sampled for c-*fos* analysis are depicted in Figure 6.2. Two brain atlases (Swanson, 1992; Paxinos & Watson, 2005) helped to verify the locations of brain areas, unless otherwise specified. The anterior – posterior (AP) coordinates (mm from bregma) in the descriptions below and in Figure 6.2 are from Paxinos & Watson (2005) except the perirhinal cortex borders which are from Burwell (2001). The regional groupings below reflect the groupings used subsequently in the statistical analyses of Fos counts.

6.2.9.1 Auditory and motor cortex

Counts of Fos-positive cells were made in the surgical control groups in the primary auditory cortex (Aud; from AP -4.80 to -5.52) and the primary motor cortex (from AP -1.00 to -1.60), to provide areas where a null result might be expected if the behavioural tasks are well matched. These regions were not analysed in the lesion groups as the effects of perirhinal lesions (a multi-sensory area) on auditory or motor cortex, to the best of my knowledge, is unknown.

6.2.9.2 Parahippocampal cortex in surgical controls

In the sham surgical groups only, Fos-positive cell counts could be made at the caudal level of areas 35 (ventral) and 36 (dorsal) of the perirhinal cortex (PRH; see Burwell, 2001), as well as area Te2, and lateral entorhinal cortex (LEC) adjacent to caudal PRH from AP -4.80 to -5.52. This region of LEC, here termed rostral LEC (rLEC) is also referred to as the dorsal intermediate entorhinal (DIE) field (Insausti et al., 1997). As described in Chapter 3, neurons in LEC cortical layer II preferentially project to the dentate gyrus and CA3 while neurons in LEC layer III project to CA1 (Figure 6.3; Steward & Scoville, 1976; Amaral, 1993). Moreover, the hippocampus predominantly outputs to the deeper layers of the entorhinal cortex (Figure 6.3; Tamamaki & Nojyo, 1995). Based on these differential connections, separate counts were made in layers II, III and V+VI (combined) of the rLEC, based on the cytoarchitecture of the DIE subdivision described in Insausti et al., (1997). The postrhinal cortex (POR) was also analysed for Fos-positive neurons from sections corresponding to AP -7.08 to -8.04. The borders were based on Burwell (2001), which corresponds to the caudal part of the area labelled as the ectorhinal cortex by Paxinos and Watson (2005). These regions were not analysed in the lesion groups due to the presence of extra perirhinal damage in a number of cases (detailed below).

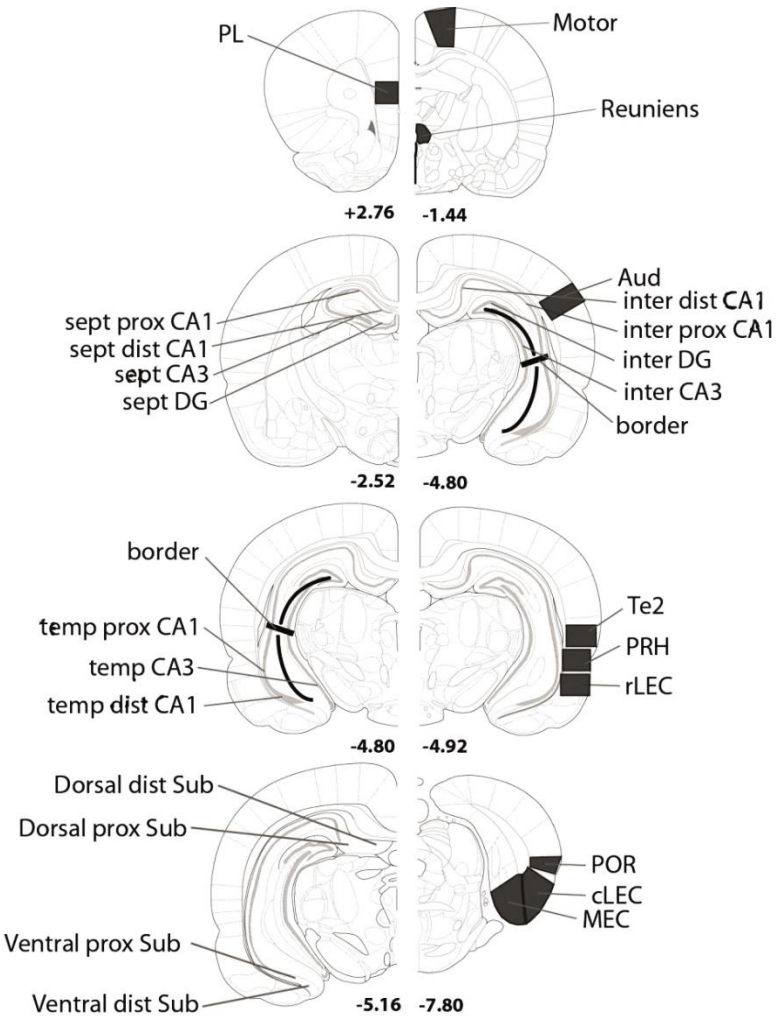

Figure 6.2. Regions of interest for c-*fos* analyses

Sites analysed: Aud, primary auditory cortex; CA3 at intermediate (inter), septal (sept) and temporal (temp) levels; distal (dist) and proximal (prox) CA1; DG, dentate gyrus; dorsal dist sub, dorsal distal subiculum; dorsal prox sub, dorsal proximal subiculum; LEC, lateral entorhinal cortex at caudal (c) rostral (r) levels; MEC, medial entorhinal cortex; PL, prelimbic cortex; PRH, perirhinal cortex; POR, postrhinal cortex; Reuniens, nucleus reuniens of thalamus; Te2, area Te2; ventral dist sub, ventral distal subiculum; ventral prox sub, ventral proximal subiculum. The numbers below refer to the approximate distance in mm from bregma. Panel -4.80 is repeated to allow for clear demonstration of all analysed regions. Adapted from the atlas of Paxinos & Watson (2005).

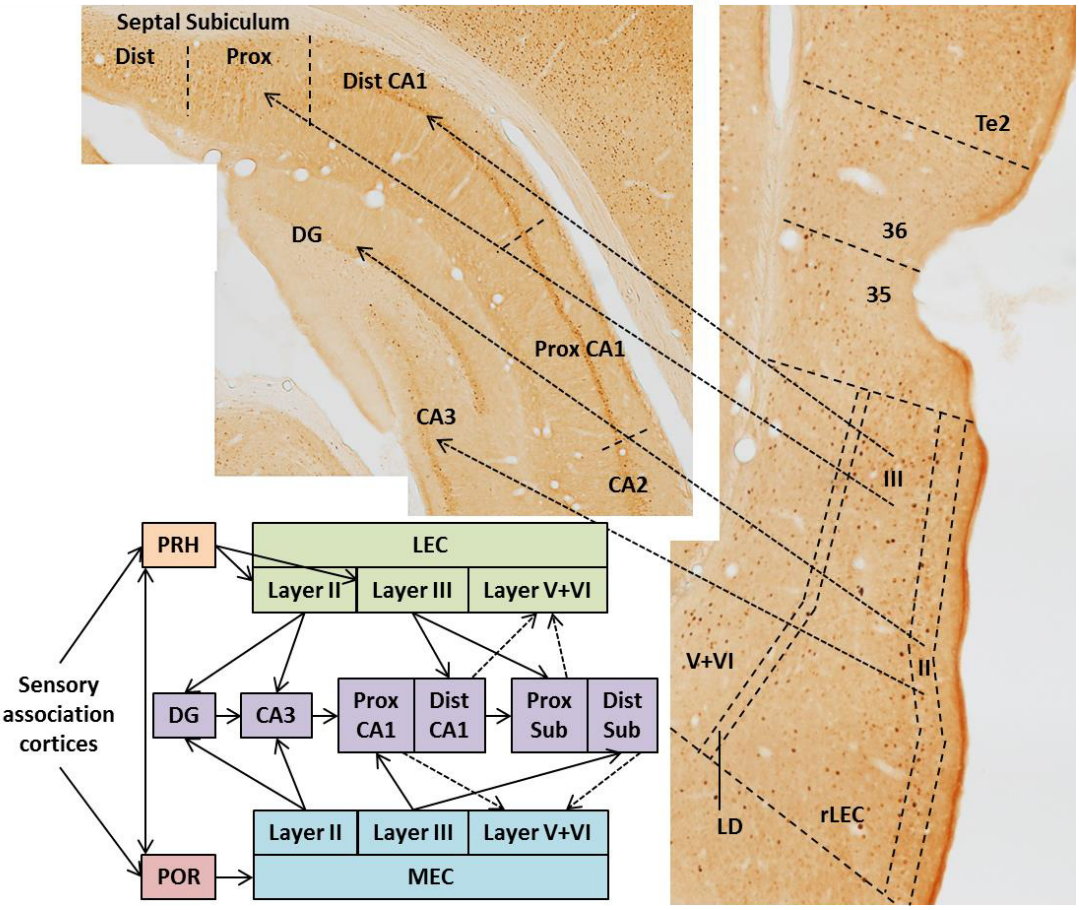

Figure 6.3. Simplified pattern of afferent inputs from the parahippocampal region to the hippocampal formation.

The photomicrographs show coronal sections stained for Fos-positive cells from a rat in Sham Novel-Familiar group. The areas shown on micrograph are area Te2, caudal perirhinal cortex and lateral entorhinal cortex with cortical layers delineated. For simplicity the schematic does not include the direct connections linking PRH (and POR) with CA1/subiculum or LEC with MEC. Abbreviations: Dist, distal; DG, dentate gyrus; II, cortical layer II; III, cortical layer III; LD, lamina dessicans; MEC, medial entorhinal cortex; POR, postrhinal; Prox, proximal; rLEC, rostral lateral entorhinal cortex; Te2, area Te2; V+VI, cortical layers V and VI combined; 35, area 35 of caudal perirhinal cortex; 36, area 36 of caudal perirhinal cortex.

6.2.9.3 Caudal entorhinal cortex

Cell counts were taken from the medial entorhinal cortex (MEC) as well as a more caudal region of LEC (cLEC) from AP -7.08 to -8.04; the boundaries based on Burwell and Amaral (1998). As described for rLEC, based on the differential laminar inputs to the hippocampus, separate counts were made in layers II, III and V+VI (combined) of the cLEC. The laminar divisions were based on the cytoarchitecture of the dorsal lateral entorhinal field described in Insausti et al. (1997).

6.2.9.4 Prelimbic cortex and thalamus

Fos-positive cell counts were made within the prelimbic cortex (PL) region (from AP +4.20 to +2.76). Cell counts were also made in the nucleus reuniens of the thalamus (from AP -1.44 to -2.52).

6.2.9.5 Hippocampal Formation

Hippocampal subfields (dentate gyrus, CA1, and CA3) were divided into their septal (dorsal), intermediate, and temporal (ventral) divisions (Bast, 2007; Strange et al., 2014). The CA1 subfield was further subdivided into its proximal and distal (relative to DG) regions. The septal hippocampus counts (dentate gyrus, CA3 and CA1) were obtained from AP -2.52 to 3.24, while those for the intermediate hippocampus (dentate gyrus, CA1, CA3) came from sections near AP -4.80 to -5.52. The border between the intermediate and temporal hippocampus corresponds to -5.0 dorsoventral from bregma (Paxinos & Watson, 2005). Within the temporal (ventral) hippocampus, counts were made in the CA1 and CA3 fields at approximately AP -4.80 to -5.52. Additional cell counts were taken in both the dorsal and ventral subiculum (from around AP -5.16); as with CA1, the subicular divisions were further subdivided into proximal and distal regions. This additional proximal-distal dimension was added due to the differential projections of the entorhinal cortex; LEC has a stronger projection to distal CA1 and proximal subiculum (i.e. inputs terminate around the border between CA1 and subiculum) while MEC preferentially projects to proximal CA1 and distal subiculum (Amaral, 1993; Witter, 1993).

6.2.10 Image capture and analysis of c-*fos* activation

As described in General Methods section 2.9.

6.2.11 Statistical analysis

6.2.11.1 Behavioural data

Initially, the behavioural data for Experiments 1 and 2 were analysed separately, comparing the lesion groups with their surgical controls. For Experiment 1, to compare groups Peri Discrimination and Sham Discrimination, a two-sample t-test (two-tailed) was calculated for total cumulative exploration while two-sample t-tests (one-tailed) were employed to compare cumulative D1 and updated D2 scores. These measures were analysed separately as they are not independent. One-sample t-tests (one-tailed) were also calculated on the cumulative D1 and updated D2 scores after the final test trial of

the test session to determine if discrimination performance was significantly above chance level (zero) for each group. Mean explorations times were further analysed by separating them by object class (novel or familiar) and then dividing this into four blocks of five consecutive trials. As the novel and familiar exploration times were obtained from the same trials these data cannot be considered to be independent and so exploration times for the object classes were analysed by separate ANOVAs with one between-subjects factor (lesion type) and one within-subjects factor (block).

For Experiment 2, the mean exploration times were grouped into four blocks of five consecutive trials, which were compared between the groups Peri Novel and Sham Novel by an ANOVA with one between-subjects factor (lesion type) and one within-subjects factor (block).

In addition, the total cumulative exploration for all four animal groups was compared using an ANOVA with two between-subjects factors [Lesion type (Sham, perirhinal lesion) and behavioural condition (Discrimination, Novel)].

Finally, the mean amount of exploration time each rat dedicated to novel objects was calculated. For the novel-familiar discrimination condition this was done by dividing the total amount of exploration dedicated just to novel objects by 20, while for rats in the novel-novel exploration condition, total cumulative exploration was divided by 40. Mean novel object exploration was also compared using an ANOVA with two between-subjects factors as described for total cumulative exploration.

6.2.11.2 Fos data

Initially, regional Fos counts were compared separately for Experiments 1 and 2. These comparisons involved separate ANOVAs based on the regional groupings described above. For each ANOVA, lesion was included as the between subject factor and ROI as the within subject factor.

Subsequently, the Fos counts in the control areas (sham groups only) were compared between Experiments 1 and 2 using a one between-subject (behavioural condition) by one within-subject (ROI) ANOVA. The same type of analysis was carried out to compare the number of Fos-positive cells in the rostral parahippocampal cortex and separately for the cortical layers of rLEC between the behavioural conditions. Following this, the number of c-*fos* activated cells in the extra-hippocampal regions of interest common to all animal groups was compared. This was accomplished by calculating ANOVAs with two between-subject factors (lesion type and behavioural

condition) and one within-subject factor (ROI). This type of analysis was carried out separately for three regional groupings: i) caudal entorhinal cortex, ii) cLEC cortical layers, iii) prelimbic cortex and nucleus reuniens of the thalamus.

Within the hippocampal formation, the subfields were divided and analysed differentially based on their anatomical connections; thus, comparisons were made in each of the subfields individually. The effect of behavioural condition and lesion status on the number of Fos-positive cells in CA1 and the subiculum were compared by calculating separate ANOVAs with two between-subject factors (lesion type and behavioural condition) and two within-subject factors (proximal-distal dimension and septotemporal level). The CA3 and dentate gyrus subfields were analysed by two between-subject factor (lesion type and behavioural condition) and one within-subject factor (septotemporal level) ANOVAs. These grouping procedures were carried out to reduce the number of comparisons and, thereby, reduce the likelihood of Type 1 errors. Where an interaction was found to be significant, the simple effects were examined.

Inter-regional Pearson product-moment correlation coefficients were calculated for the Fos-positive cell counts in all sites. The levels of the correlations obtained between prelimbic cortex and perirhinal cortex were also compared between the groups using Fisher's *r*-to-*z* transformation (Zar, 2010).

6.2.12 Structural equation modelling

As described in General Methods section 2.11.

6.3 Results

6.3.1 Lesion analysis

Experiment 1 – Novel-Familiar object discrimination

This experiment was carried out with animal cohort JAR172. Five rats with perirhinal lesions were rejected due to loss of hippocampal tissue in more than one section. Thus, final group sizes were Perirhinal Novel-Familiar, n=12 and Sham Novel-Familiar, n=12. Perirhinal damage ranged from 53.7% to 97.6% (mean 73.7%). Additionally, none of the behavioural measures significantly correlated with lesion size (total exploration: r = 0.50, p = 0.096; cumulative D1: r = 0.05, p = 0.86; updated D2: r = -0.14, p = 0.68) indicating that smaller lesions did not lead to sparing of behaviour. A total of five left hemispheres and seven right hemispheres were analysed in both groups. The lesions

typically involved almost the full anterior-posterior extent of areas 35 and 36 (Figure 6.4). A frequent feature was the encroachment of the lesion into the most dorsal parts of the piriform cortex and LEC (Figure 6.4), i.e., those cortices adjacent to area 35.

Experiment 2 – Novel-Novel object exploration

This experiment was carried out with animal cohort JAR177. Nine rats with perirhinal lesions were rejected due to damage involving the hippocampus. One surgical control rat was eliminated due to the presence of idiopathic damage to the left frontotemporal cortex. Final group sizes were, therefore, Perirhinal Novel, n = 9 and Sham Novel, n = 12. A total of two left hemispheres and seven right hemispheres were analysed in both groups, as well as an additional three left hemispheres in the Sham control group. Perirhinal damage ranged from 63.9% to 98.3% (mean 82.8%) and did not significantly correlate with exploration times ($r = -0.39$, $p = 0.31$). The appearance of the lesions in Cohort 177 matched those in Cohort 172 (Figure 6.4), with no overall difference in perirhinal tissue loss ($t_{19} = 1.68$, $p = 0.11$).

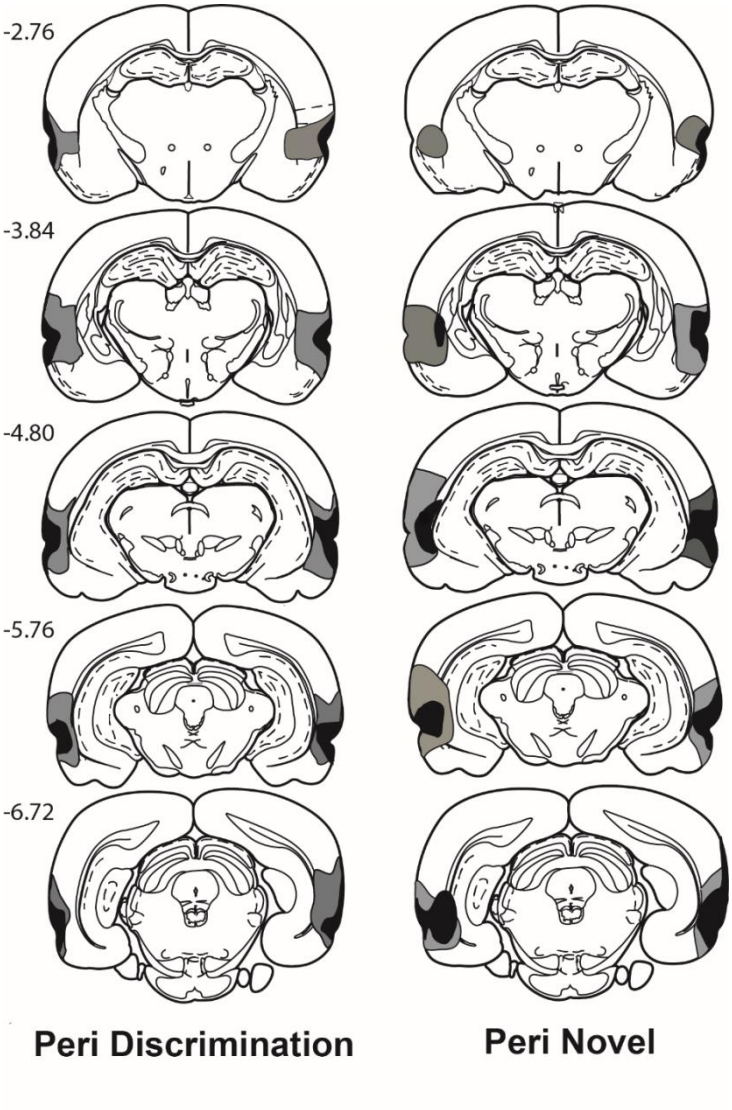

Figure 6.4. Perirhinal lesion reconstructions.

Diagrammatic reconstructions of the perirhinal cortex lesions showing the individual cases with the largest (grey) and smallest (black) lesions for group Peri Discrimination (left; n=12) and group Peri Novel (right; n=9). The numbers refer to the distance (in millimetres) from bregma (adapted from Paxinos & Watson, 2005).

6.3.2 Behavioural testing

6.3.2.1 Experiment 1- Novel-Familiar object discrimination

Comparisons between the groups Peri Discrimination and Sham Discrimination revealed that lesions to the perirhinal cortex did not alter the total amount of time rats spent exploring all objects ($t_{22} = 0.34$, $p = 0.73$; Figure 6.5 upper left panel). Further to this, both groups discriminated above chance levels based on both the cumulative D1 scores (Peri Discrimination: $t_{11} = 5.20$, $p < 0.001$; Sham Discrimination: $t_{11} = 14.8$, $p < 0.0001$; Figure 6.5 lower left panel) and updated D2 ratio (Peri Discrimination: $t_{11} = 6.11$, $p <$

0.0001; Sham Discrimination: t_{11} = 15.4, p < 0.0001; Figure 6.5 lower right panel). However, perirhinal lesions significantly reduced the efficiency of discrimination as measured by both cumulative D1 (t_{22} = 2.26, p = 0.017; Figure 6.5 lower left panel) and updated D2 (t_{22} = 2.38, p = 0.014; Figure 6.5 lower right panel). Taken together, these results demonstrate that removal of the perirhinal cortex significantly reduced the rats' ability to discriminate object novelty but do not entirely prevent it at these very short retention intervals (< 1 minute).

Additional analyses were carried out on the exploration data; these were divided into four blocks of five trials each to investigate changes in total exploration over the course of the test session separately for novel and familiar objects (Figure 6.5, middle panel). The lesion status did not affect the amount of exploration dedicated to novel objects (F < 1) nor did the amount of exploration towards novel objects change over the course of the test session ($F_{3,66}$ = 1.17, p = 0.33). There was however, a lesion by trial position interaction ($F_{3,66}$ = 4.70, p = 0.005); this was as the rats in the Sham Discrimination group displayed higher levels of exploration to novel objects in trials 6-10 than group Peri Discrimination. There were no lesion differences seen in the other blocks of trials. A similar analysis revealed no overall differences between the two groups on the amount of familiar object exploration (F < 1). Exploration of familiar objects changed as the test session progressed ($F_{3,66}$ = 4.82, p = 0.004) but this was not differentially affected by perirhinal lesions ($F_{3,66}$ = 1.24, p = 0.30). The change in exploration with trial progression is due to the reduced levels of exploration of familiar objects in trials 16-20 compared to the preceding blocks.

6.3.2.2 Experiment 2- Novel-Novel object exploration

Perirhinal lesions did not affect the total amount of time rats spent exploring novel objects, as there was no difference between groups Peri Novel and Sham Novel on total amount of object exploration ($F_{1,19}$ = 1.50, p = 0.24). The exploration data were separated into four blocks of five trials each to investigate changes in exploration over the course of the test session (Figure 6.5, upper right panel). This analysis revealed a significant effect of block ($F_{3,57}$ = 5.68, p = 0.002). Examination of the upper right panel of Figure 6.5 illustrates that the effect of block is due to the greater exploration in the first block of trials but this was not modified by perirhinal lesions ($F_{3,57}$ = 2.16, p = 0.10). Thus, exploration levels for the two groups were highly comparable.

6.3.2.3 Total cumulative exploration time comparison between conditions

Comparisons across the experiments revealed that rats presented with two novel objects spent significantly more time exploring those objects than rats presented with one novel and one familiar object in each trial ($F_{1,41}$ = 18.4, $p < 0.001$). Interestingly, this increased exploration was not affected by perirhinal lesions ($F < 1$) and there was no interaction between behavioural condition and lesion ($F_{1,41}$ = 1.67, p = 0.20).

Further, the mean amount of exploration each rat devoted to novel objects was calculated and compared between the groups (not depicted). The pattern of these results matched that described for total cumulative exploration; on average rats in the novel-novel exploration condition spent more time exploring each individual novel object than the rats in the novel-familiar discrimination condition ($F_{1,41}$ = 6.23, p = 0.017). The perirhinal lesions did not cause differences ($F < 1$), nor was the interaction significant ($F_{1,41}$ = 2.47, p = 0.12). This indicates that when a novel object is placed in competition with a familiar one, the amount of exploration dedicated to the novel object is reduced.

6.3.3 Fos-positive cell counts

Initially, the regional Fos-positive cell counts obtained from each experiment were compared separately to investigate the regional effects of lesions to the perirhinal cortex on each of the behavioural conditions. Surprisingly, no significant differences were found between groups Peri Discrimination and Sham Discrimination in any of the regional Fos counts (Table 6.2). Furthermore, the only significant difference between groups Peri Novel and Sham Novel was in the subiculum; the perirhinal lesions differentially affected Fos counts in the proximal and distal regions of the subiculum ($F_{1,19}$ = 5.55, p = 0.029). Examination of the simple effects revealed that in the surgical control rats the distal region had higher Fos counts than the proximal region of the subiculum ($F_{1,19}$ = 34.5, $p < 0.001$). This difference was not observed in rats with perirhinal lesions ($F_{1,19}$ = 3.90, p = 0.063); indicating the perirhinal lesions reduced Fos expression in distal subiculum. No other significant lesion effects or interactions were obtained (Table 6.2).

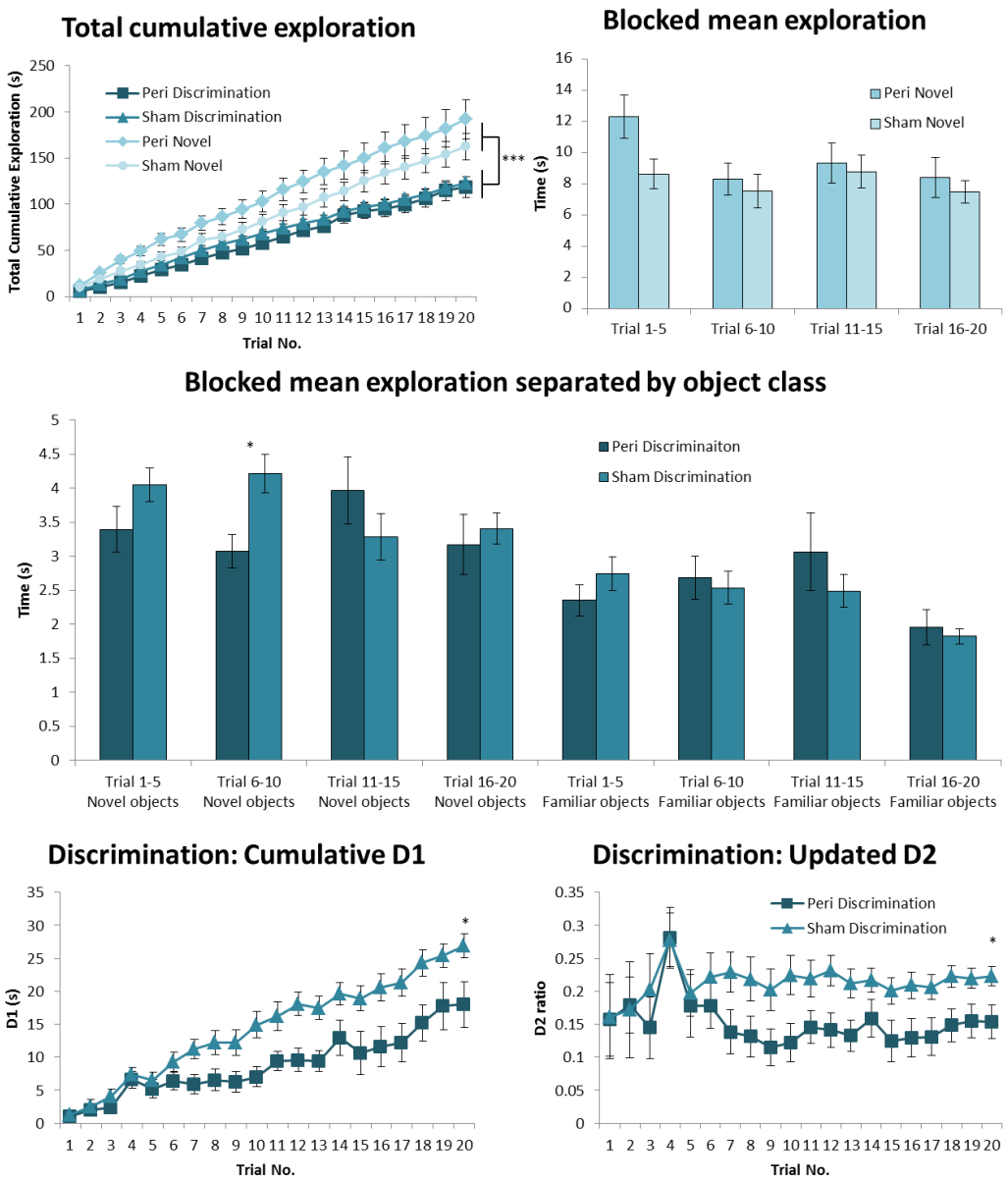

Figure 6.5. Behavioural measures for Experiments 1 and 2.

The upper left panel depicts the cumulative exploration times across the 20 test trials for all four groups. The upper right panel illustrates mean total exploration times of rats in Experiment 2 (novel-novel exploration) blocked into four sets of five consecutive trials. The middle panel shows the separate exploration levels for the novel and familiar objects in Trials 1–20, grouped into four blocks of 5 trials of rats in the novel-familiar discrimination condition. The lower panels depict discrimination performance in Experiment 1 – novel-familiar discrimination condition: cumulative D1 (lower left panel) and updated D2 ratio (lower right panel) across 20 trials. All discrimination scores are significantly above zero (one-sample t tests, all $p < 0.001$). * $p < 0.05$ Data are presented as means ±SEM.

Table 6.2. Statistics when Fos-positive cell counts analysed separately for Experiments 1 and 2.

	Peri Discrimination vs. Sham Discrimination			Peri Novel vs. Sham Novel		
	F-value	**df**	**p-value**	**F-value**	**df**	**p-value**
Caudal entorhinal cortex						
Lesion effect	1.78	1,22	0.20	0.0002	1, 19	0.99
Lesion*Region effect	1.02	1,22	0.32	0.55	1, 19	0.47
cLEC cortical layers						
Lesion effect	1.77	1,22	0.20	0.073	1, 19	0.79
Lesion*Region effect	2.25	2,44	0.12	2.97	2, 38	0.064
PL + reuniens						
Lesion effect	0.098	1,22	0.76	0.007	1,19	0.93
Lesion*Region effect	0.058	1,22	0.81	0.130	1,19	0.72
CA1						
Lesion effect	0.031	1,22	0.86	0.327	1,19	0.57
Lesion*level effect	1.16	2,44	0.32	0.358	2,38	0.70
Lesion*proximal-distal effect	0.891	1,22	0.36	0.903	1,19	0.35
Lesion*level*proximal-distal effect	0.428	2,44	0.65	0.701	2,38	0.50
CA3						
Lesion effect	0.008	1,22	0.93	4.28	1,19	0.052
Lesion*level effect	1.50	2,44	0.23	0.076	2,38	0.93
DG						
Lesion effect	0.047	1,22	0.83	3.09	1,19	0.10
Lesion*level effect	1.33	1,22	0.26	0.217	1,19	0.65
Subiculum						
Lesion effect	0.099	1,22	0.76	2.08	1,19	0.17
Lesion*dorsal-ventral effect	0.049	1,22	0.83	0.248	1,19	0.62
Lesion*proximal-distal effect	0.231	1,22	0.64	**5.55**	**1,19**	**0.029***
Lesion*proximal-distal*dorsal-ventral	0.004	1,22	0.95	0.033	1,19	0.86

6.3.3.1 Auditory and motor cortex – comparison of Fos counts in Sham groups

Prior to contrasting rats from Experiments 1 and 2, it was necessary to determine if their baseline Fos counts were comparable, as would be predicted if the two behavioural tasks were appropriately matched. Fos counts in the auditory cortex and motor cortex revealed no group difference in the two sets of sham controls ($F_{1,22}$ = 0.12, p = 0.73; Figure 6.6 upper panel), nor was there a significant region by condition interaction ($F_{1,22}$ = 2.29, p = 0.15). These two sites would not be expected to interact with the behavioural conditions. Accordingly, the behavioural conditions were considered to be sufficiently

matched, allowing for subsequent regional analyses of Fos expression to compare the two behavioural conditions.

6.3.3.2 Rostral parahippocampal cortex – comparison of Fos counts in Sham groups

Discriminating novel from familiar objects as compared to exploring only novel objects did not cause an overall difference in the number of Fos-positive neurons in the rostral parahippocampal cortex of surgical control rats ($F_{1,22} = 2.31$, $p = 0.14$; Figure 6.6 middle panel, Figure 6.7). A significant region by behavioural condition interaction was found ($F_{4,88} = 6.55$, $p < 0.001$) which reflected higher Fos expression in the rostral LEC of the Sham Discrimination group than the Sham Novel group ($F_{1,22} = 10.1$, $p = 0.004$).

Neurons in the superficial cortical layers of the LEC preferentially project to the hippocampus, while the deeper layers predominantly receive hippocampal output (Steward & Scoville, 1976; Amaral, 1993; Tamamaki & Nojyo, 1995). Based on this knowledge and the result above, the number of Fos-positive cells were separated between cortical layers II, III and V+VI (combined), and then compared between the behavioural conditions in order to assess if novel-familiar object discrimination caused a general or pathway specific increase in activity (Figure 6.6 lower panel). This analysis revealed a main effect of the behavioural condition ($F_{1,22} = 9.51$, $p = 0.005$) as well as a significant behavioural condition by layer interaction ($F_{2,44} = 9.87$, $p < 0.001$). Examination of the simple effects indicated that this interaction reflected higher Fos expression associated with the novel-familiar discrimination condition in hippocampal input cortical layer II ($F_{1,22} = 23.3$, $p < 0.001$) and layer III ($F_{1,22} = 5.96$, $p = 0.023$) but not the deeper cortical layers ($F < 1$).

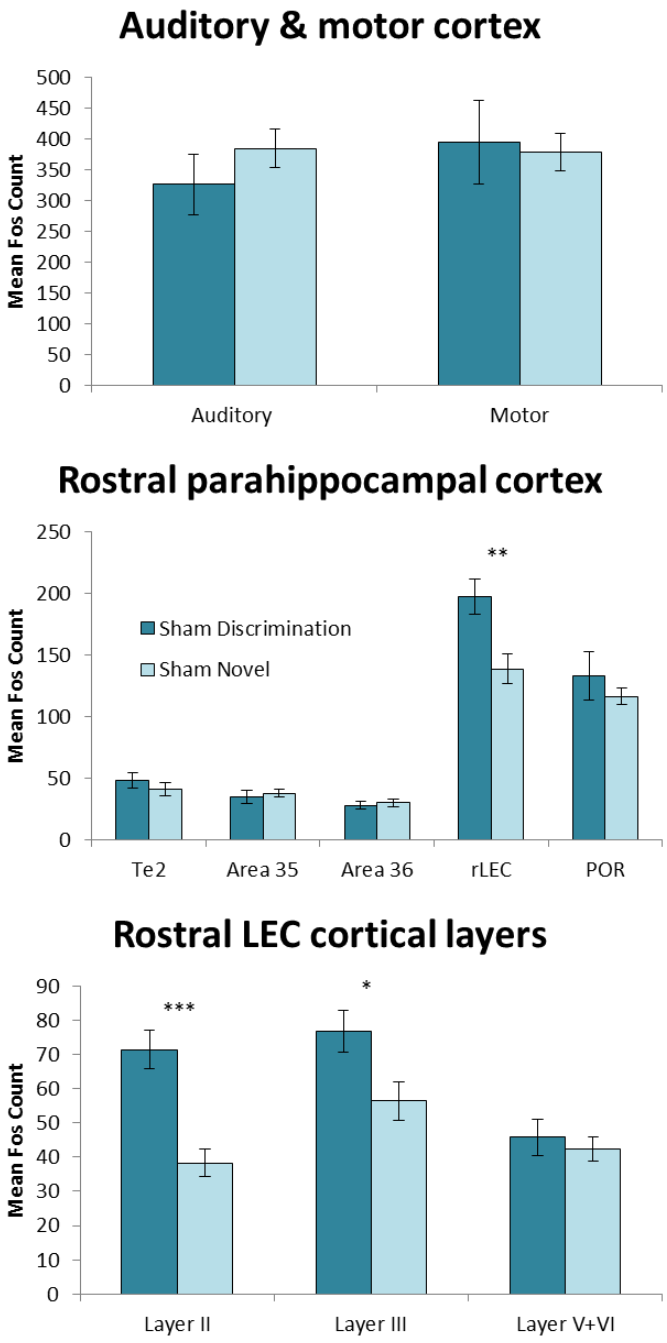

Figure 6.6. Mean counts of Fos-positive cells in groups Sham Discrimination and Sham Novel.

Graphs depicting mean counts of Fos-positive cells in the two groups of surgical control rats in the primary auditory and motor cortex cortex (upper panel), the rostral parahippocampal cortex and postrhinal cortex (POR) (middle panel) and individual cortical layers of rostral lateral entorhinal cortex (lower panel). Data are presented as means ±SEM. * $p < 0.05$, ** $p < 0.01$, *** $p < 0.001$.

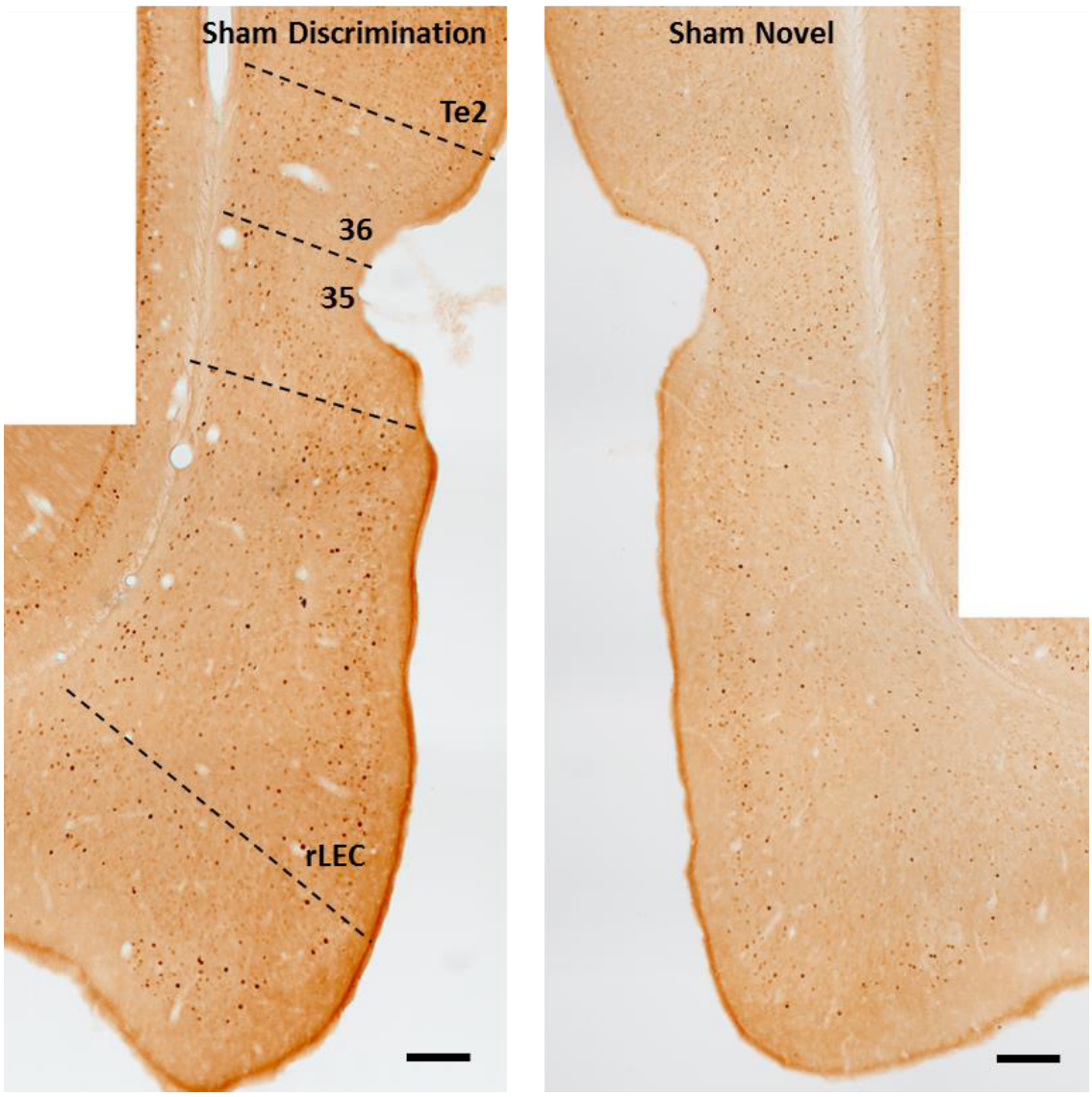

Figure 6.7. Representative photomicrographs of rostral parahippocampal cortex.

These sections depict Fos-positive cells in cortical area Te2, caudal PRH composite areas 35 and 36 and rostral lateral entorhinal cortex (rLEC) for groups, Sham Discrimination (left panel) and Sham Novel (right panel). Scale bar: 200µm.

6.3.3.3 Caudal entorhinal cortex – comparison of Fos counts

Analysis of a more caudal region of the entorhinal cortex allowed for the impact of perirhinal lesions on the medial and lateral entorhinal regions to be compared between the two behavioural conditions. There was no overall effect of perirhinal lesions on Fos-positive cell counts at the caudal level of the entorhinal cortex ($F_{1,41} = 1.22$, $p = 0.28$), nor did the lesions differentially affect the two behavioural conditions ($F_{1,41} = 1.17$, $p = 0.27$). There was, however, a significant main effect of the behavioural condition ($F_{1,41} = 4.22$, $p = 0.046$), as higher Fos counts were seen in both regions following discrimination, regardless of surgery (Figure 6.8 upper panel). This main effect was

observed equally across the entorhinal cortex as neither the behavioural condition, nor the perirhinal cortex lesions displayed a significant regional interaction ($F < 1$), nor was the three way interaction significant ($F_{1,41} = 1.46$, $p = 0.23$).

In order to investigate this result further, as described above, the number of Fos-positive cells in cortical layers II, III and V+VI (combined) in this caudal region of LEC were analysed. The laminar activity was compared to evaluate if the lamina difference in rostral LEC for the two behavioural conditions (see above) generalised to the caudal LEC (Figure 6.8 middle panel). This analysis revealed no overall effect of the behavioural condition on the caudal LEC cortical layers ($F_{1,41} = 2.87$, $p = 0.098$). Again there was no effect of perirhinal lesions ($F < 1$), nor was there a significant behavioural condition by lesion interaction ($F_{1,41} = 1.47$, $p = 0.23$). Interestingly, the cortical layers were differently modified by the behavioural condition ($F_{2,82} = 4.04$, $p = 0.021$) as rats in the novel-familiar discrimination condition had significantly higher Fos counts in hippocampal input cortical layer II ($F_{1,41} = 5.43$, $p = 0.025$) and layer III ($F_{1,41} = 5.65$, $p = 0.022$) but not the deeper cortical layers ($F < 1$) associated with hippocampal output. Again, this suggests that active discrimination leads to greater activity in hippocampal input layers compared to novel object exploration. Finally, the layer by lesion interaction was also significant ($F_{2,82} = 4.52$, $p = 0.014$). Simple effects demonstrated that cortical layer III was differentially affected by lesions to the perirhinal cortex; the lesions caused a reduction in the number of Fos-positive cells in layer III ($F_{1,41} = 4.42$, $p = 0.042$) but not layer II or V+VI ($F < 1$ for both comparisons) regardless of the behavioural condition.

6.3.3.4 Prelimbic cortex and thalamus – comparison of Fos counts

Fos-positive cell counts in the prelimbic cortex and nucleus reuniens of the thalamus were not affected by the behavioural task ($F_{1,41} = 2.74$, $p = 0.11$; Figure 6.8 lower panel) or lesions status ($F < 1$), nor was the interaction significant ($F < 1$). Similarly, neither the behavioural task nor the perirhinal cortex lesions differentially affected these two regions ($F < 1$ for all interaction terms).

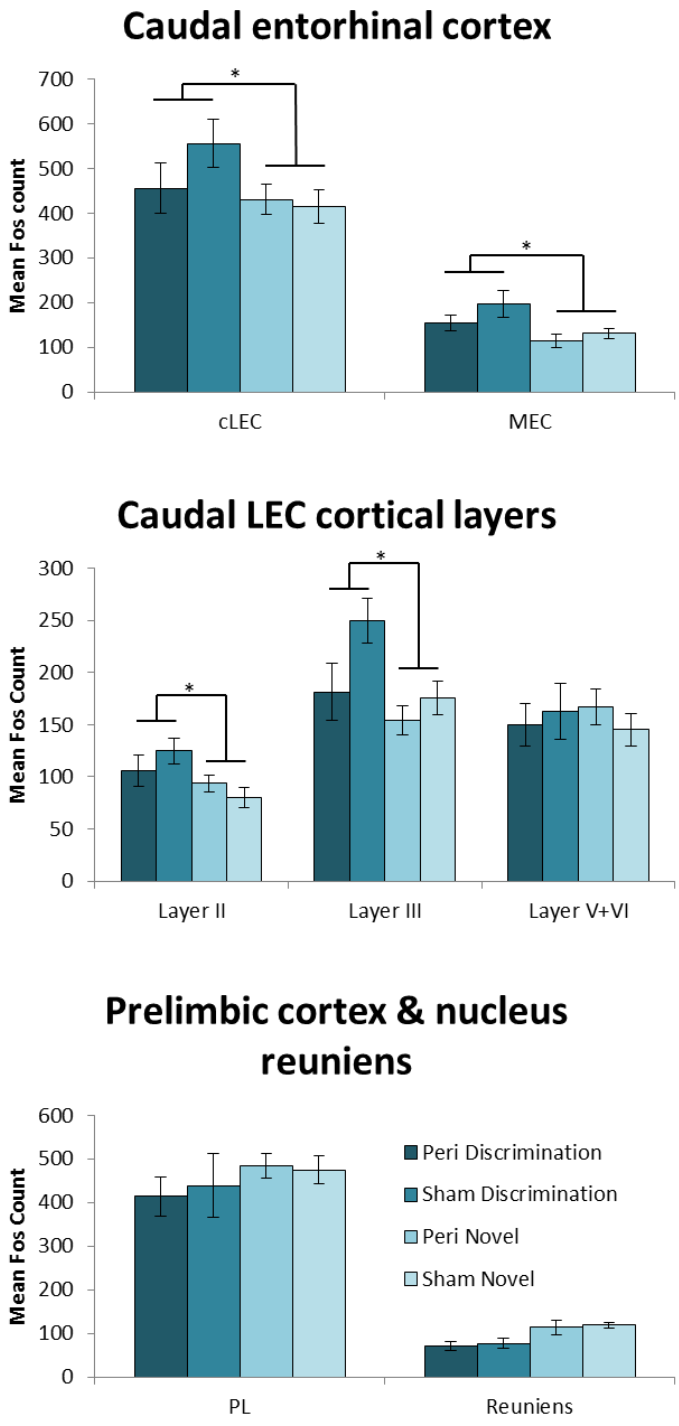

Figure 6.8. Mean counts of Fos-positive cells in caudal entorhinal cortex, prelimbic cortex and nucleus reuniens.

Graphs depict mean counts of Fos-positive cells in all four behavioural groups in: 1) the caudal entorhinal cortex (upper panel), 2) individual cortical layers of caudal lateral entorhinal cortex (LEC; middle panel) and 3) prelimbic cortex (PL) and nucleus reuniens of the thalamus (lower panel). Data are presented as means ±SEM. * $p < 0.05$.

6.3.3.5 Hippocampal formation subfields – comparison of Fos counts

Based on the various ways in which the hippocampal formation subfields were divided for Fos analysis, each of the subfields was analysed separately to compare for lesion effects and effect of behavioural condition.

CA1 Fos

Perirhinal cortex lesions did not affect the overall level of Fos expression in CA1 ($F < 1$; Figure 6.9A), the effect of the behavioural task, although close, also did not reach the level of significance ($F_{1,41} = 3.74$, $p = 0.06$) nor did the interaction between these terms ($F < 1$). Septal CA1 contained fewer Fos cells than the other CA1 levels ($F_{2,82} = 108$, $p < 0.001$), but this difference did not interact with lesion status ($F < 1$). There was, however, a significant interaction between septotemporal level and behaviour ($F_{2,82} = 14.0$, $p < 0.001$) as Novel-Novel object exploration resulted in relatively increased Fos expression over Novel-Familiar discrimination in temporal CA1 ($F_{1,41} = 17.6$, $p < 0.001$), but not in the septal or intermediate levels ($F_{1,41} = 1.02$, $p = 0.32$; $F < 1$ respectively; Figure 6.9A).

The septal-temporal level of CA1 differentially influenced the proximal-distal distribution of Fos counts ($F_{2,82} = 68.6$, $p < 0.001$; Figure 6.9A). At septal and intermediate levels of CA1, the proximal region had the higher Fos counts ($F_{1,41} = 84.1$, $p < 0.001$; $F_{1,41} = 19.3$, $p < 0.001$, respectively) while in temporal CA1 the opposite pattern was seen ($F_{1,41} = 70.2$, $p < 0 .001$). This interaction between the proximal-distal and septotemporal dimensions was not modified by perirhinal cortex lesions ($F_{2,82} = 1.12$, $p = 0.34$), though it was altered by the behavioural condition ($F_{2,82} = 5.28$, $p = 0.007$). There were no behavioural differences observed for proximal-distal CA1 at septal and intermediate levels ($F < 1$), whereas at the temporal level of CA1 both the proximal and distal regions displayed higher Fos expression when the rats explored novel objects as compared to the discrimination condition (proximal: $F_{1,41} = 8.52$, $p = 0.006$ and distal: $F_{1,41} = 25.8$, $p<0.001$). The four-way interaction was not significant ($F < 1$).

CA3 Fos

The level of Fos expression in CA3 was not affected by the behavioural task the rats were given ($F_{1,41} = 1.01$, $p = 0.32$), their lesion status ($F < 1$), nor was there an interaction between these two factors ($F < 1$; Figure 6.9B). Differences were seen in the

different septotemporal levels of CA3 ($F_{2,82}$ = 21.3, p < 0.001) but again, these were not altered by the behavioural task ($F_{2,82}$ = 1.51, p = 0.23) or the presence of perirhinal cortex lesions (F < 1), with no interaction of these conditions ($F_{2,82}$ = 2.40, p = 0.097).

Dentate gyrus Fos

The number of Fos-positive cells in the dentate gyrus was also unaffected by the behavioural condition (F < 1), the presence of perirhinal lesions ($F_{1,41}$ = 1.41, p = 0.24), with again no interaction between these two conditions (F < 1; Figure 6.9C). Additionally, there was no difference in Fos counts between the septal and intermediate levels of the dentate gyrus (F < 1), nor were these levels differently modified by the behavioural task (F < 1), the presence of perirhinal cortex lesions (F<1). There was no interaction between these factors ($F_{1,41}$ = 1.21, p = 0.28).

Subicular Fos

As with all other regions analysed within the hippocampal formation, there was no overall effect of perirhinal cortex lesions on the level of Fos expression in the subiculum ($F_{1,41}$ = 1.63, p = 0.21; Figure 6.9D). There was, however, a behavioural effect as exploration of novel objects produced higher subicular Fos counts than discriminating novel from familiar objects ($F_{1,41}$ = 8.98, p = 0.005; Figure 6.9D). This behavioural effect was not differently affected by perirhinal lesions (F < 1). Although the ventral subiculum had higher Fos counts than the dorsal subiculum ($F_{1,41}$ = 73.4, p < 0.001), this difference was not affected by the behavioural task ($F_{1,41}$ = 2.16, p = 0.15) or by lesion status (F < 1), with no three-way interaction (F < 1; Figure 6.9D).

The distal subiculum had higher Fos counts than the proximal subiculum ($F_{1,41}$ = 85.5, p < 0.001), but this difference was not affected by the behavioural condition (F < 1) or lesion status of the rats ($F_{1,41}$= 2.37, p=0.13; Figure 6.9D). There was, however, a three-way interaction ($F_{1,41}$ = 4.62, p = 0.037). In the surgical control animals, the novel object exploration condition induced higher Fos counts than the discrimination condition in both the proximal ($F_{1,41}$ = 10.7, p = 0.002) and distal ($F_{1,41}$ = 6.03, p = 0.018) regions of the subiculum. While in the perirhinal lesion groups, higher Fos counts were associated with the proximal ($F_{1,41}$ = 8.01, p = 0.007) but not the distal region (F < 1), indicating that perirhinal lesions affected the distal subiculum when rats were exploring novel objects.

Additionally, the proximal-distal dimension was differentially affected by Fos counts in the dorsal and ventral levels of the subiculum ($F_{1,41} = 38.1$, $p < 0.001$; Figure 6.9D). This interaction was modified by the behavioural condition ($F_{1,41} = 5.88$, $p = 0.02$) but not by the lesion status of the rats ($F < 1$). It was found that exploration of novel objects increased Fos expression over that induced by discriminating novel from familiar objects in proximal dorsal subiculum ($F_{1,41} = 19.4$, $p < 0.001$), distal dorsal subiculum ($F_{1,41} = 15.2$, $p < 0.001$) and proximal ventral subiculum ($F_{1,41} = 8.03$, $p = 0.007$) but not distal ventral subiculum ($F < 1$). Thus, the distal ventral subiculum did not increase Fos expression when exposed to only novel objects regardless of lesion status. Finally, the four-way interaction was not significant ($F < 1$).

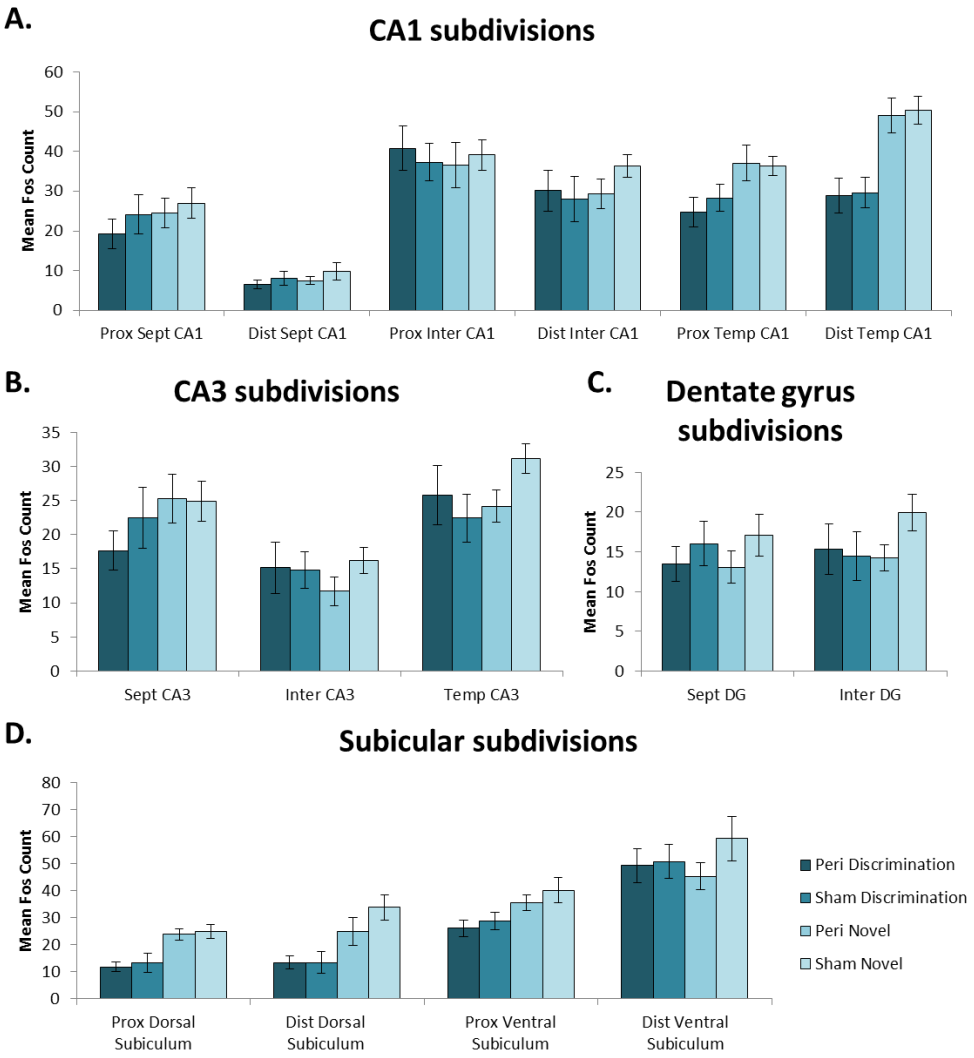

Figure 6.9. Mean counts of Fos-positive cells in hippocampal formation.

Graphs depict mean counts of Fos-positive cells in all four groups in septal (sept), intermediate (inter) and temporal (temp) regions of CA1 (A), CA3 (B), as well as septal and intermediate dentate gyrus (C) and dorsal and ventral subiculum (D). CA1 and subiculum are further divided into proximal (prox) and distal (dist) sub-regions. Data are presented as means ±SEM.

6.3.4 Correlation tables

Pearson product moment correlation coefficients were calculated between all regions of interest based on the raw Fos counts for both the rats in the novel-familiar discrimination condition (Table 6.3) and the novel-novel exploration condition (Table 6.4). These were calculated to give an indication of how the activity of the different brain regions was associated. These tables of correlations present probability levels that are not corrected for multiple comparisons, as the individual correlations are of limited significance. More importantly, these same correlations provide the source data for structural equation modelling, in which the fit of the overall model helps to compensate for Type 1 errors in the individual correlations that comprise the model. Because of this, it is important that any model must conform to known patterns of anatomical connectivity between the regions of interest, i.e., the number of potential models is constrained. Interestingly, many more of the possible inter-area correlations reached an uncorrected significance level ($p < 0.05$) in the novel-familiar discrimination groups than the groups in the novel-novel exploration condition. In the discrimination groups, approximately 69% (Sham Discrimination) and 38% (Peri Discrimination) of the possible inter-region correlations reached significance. In contrast, for the Sham Novel and Peri Novel groups approximately 13% of all of the possible correlations reached significance ($p < 0.05$).

Table 6.3. Inter-region correlations of Fos-positive cell counts in the novel-familiar discrimination condition.

Sham Novel																																Sham Novel		
		Te2	Area 35	Area 36	PRH	rLEC	rLEC layer II	rLEC layer III	rLEC layer V+VI	POR	cLEC	cLEC layer II	cLEC layer III	cLEC layer V+VI	MEC	Prox Septal CA1	Dist Septal CA1	Septal CA3	Septal DG	Prox inter CA1	Dist Inter CA1	Inter CA3	Inter DG	Prox Temp CA1	Dist Temp CA1	Temp CA3	Dist Dorsal Sub	Prox Dorsal Sub	Dist Ventral Sub	Prox Ventral Sub	PL	Reuniens			
Te2	r-value		0.415	**.663***	**.593***	0.249	0.189	0.222	0.263	**.733****	0.373	0.036	0.540	0.340	0.081	0.155	-0.030	-0.142	-0.233	-0.060	0.035	-0.248	0.055	0.260	0.477	0.266	0.152	-0.007	0.479	0.446	0.169	0.134	r-value	Te2	
	p-value		0.180	**0.019**	**0.042**	0.435	0.555	0.488	0.409	**0.007**	0.232	0.911	0.070	0.280	0.803	0.631	0.927	0.659	0.466	0.854	0.914	0.438	0.866	0.415	0.117	0.404	0.638	0.982	0.115	0.146	0.600	0.679	p-value		
Area35	r-value			**.591***	**.908****	0.129	0.070	0.078	0.243	**.731****	0.249	0.072	0.324	0.239	-0.388	-0.032	-0.281	0.143	-0.242	-0.461	-0.144	-0.086	-0.008	0.209	0.229	-0.162	-0.156	-0.346	0.092	0.209	0.342	-0.045	r-value	Area35	
	p-value			**0.043**	**<0.001**	0.689	0.828	0.809	0.447	**0.007**	0.434	0.823	0.304	0.455	0.213	0.921	0.376	0.657	0.449	0.131	0.655	0.790	0.980	0.514	0.474	0.616	0.627	0.270	0.777	0.515	0.277	0.889	p-value		
Area36	r-value				**.874****	0.031	-0.002	0.050	0.026	**.746****	0.484	0.217	0.510	0.537	0.094	0.149	-0.033	0.104	-0.333	-0.337	-0.258	-0.305	-0.225	0.022	0.369	0.015	0.159	-0.170	0.117	0.189	0.158	0.078	r-value	Area36	
	p-value				**<0.001**	0.923	0.995	0.877	0.935	**0.005**	0.111	0.498	0.090	0.072	0.771	0.644	0.918	0.747	0.291	0.284	0.419	0.336	0.482	0.945	0.237	0.964	0.621	0.597	0.716	0.555	0.623	0.810	p-value		
PRH	r-value					0.094	0.041	0.073	0.160	**.827****	0.401	0.156	0.460	0.422	-0.185	0.058	-0.186	0.140	-0.318	-0.452	-0.220	-0.210	-0.121	0.138	0.329	-0.090	-0.012	-0.297	0.116	0.224	0.288	0.013	r-value	PRH	
	p-value					0.772	0.899	0.821	0.620	**0.001**	0.197	0.628	0.133	0.172	0.566	0.858	0.562	0.664	0.314	0.140	0.492	0.513	0.707	0.670	0.296	0.782	0.971	0.349	0.720	0.484	0.365	0.968	p-value		
rLEC	r-value						**.940*****	**.886*****	**.867*****	0.368	**.677***	0.569	**.617***	**.597***	0.497	0.465	0.442	0.568	0.405	0.252	0.491	-0.335	0.170	0.451	0.487	-0.218	-0.040	0.152	**.604***	0.410	0.473	0.389	r-value	rLEC	
	p-value						**<0.001**	**<0.001**	**<0.001**	0.239	**0.016**	0.053	**0.032**	**0.041**	0.101	0.128	0.151	0.054	0.192	0.430	0.105	0.288	0.597	0.141	0.108	0.497	0.901	0.638	**0.038**	0.186	0.120	0.212	p-value		
rLEC layer II	r-value							**.718*****	**.867*****	0.270	**.633***	**.607***	0.530	0.563	0.534	**.612***	0.354	**.723****	0.332	0.371	**.648***	-0.486	0.212	**.596***	0.569	-0.027	-0.025	0.202	**.636***	0.446	0.409	0.489	r-value	rLEC layer II	
	p-value							**0.009**	**<0.001**	0.396	**0.027**	**0.036**	0.076	0.057	0.074	**0.034**	0.259	**0.008**	0.292	0.235	**0.023**	0.109	0.508	**0.041**	0.054	0.933	0.938	0.529	**0.026**	0.146	0.187	0.106	p-value		
rLEC layer III	r-value								0.566	0.322	**.695***	0.454	**.714****	**.598***	0.387	0.211	**.639***	0.376	0.495	0.240	0.239	-0.134	0.136	0.283	0.457	-0.303	0.080	0.242	0.532	0.401	0.483	0.359	r-value	rLEC layer III	
	p-value								0.055	0.307	**0.012**	0.138	**0.009**	**0.040**	0.214	0.510	**0.025**	0.229	0.102	0.452	0.454	0.678	0.673	0.373	0.136	0.338	0.805	0.448	0.075	0.196	0.112	0.251	p-value		
rLEC layer V+VI	r-value									0.410	0.453	0.485	0.351	0.423	0.427	0.534	0.081	0.501	0.209	0.075	0.548	-0.340	0.137	0.403	0.290	-0.207	-0.246	-0.097	0.472	0.253	0.363	0.185	r-value	rLEC layer V+VI	
	p-value									0.185	0.139	0.110	0.264	0.171	0.166	0.073	0.803	0.097	0.514	0.817	0.065	0.279	0.672	0.194	0.361	0.520	0.440	0.763	0.121	0.427	0.247	0.564	p-value		
POR	r-value										0.568	0.303	**.642***	0.575	0.006	0.243	-0.071	0.075	-0.196	-0.330	-0.135	-0.314	-0.236	0.200	0.388	-0.096	-0.007	-0.129	0.136	0.090	**.605***	0.291	r-value	POR	
	p-value										0.054	0.339	**0.024**	0.051	0.986	0.446	0.826	0.817	0.543	0.295	0.676	0.321	0.460	0.533	0.213	0.766	0.983	0.689	0.673	0.781	**0.037**	0.358	p-value		
cLEC	r-value											**.771****	**.938*****	**.836****	**.638***	0.491	0.416	0.430	0.201	0.348	0.291	-0.518	0.181	0.330	**.652***	-0.179	0.117	0.264	0.324	0.300	0.424	0.531	r-value	cLEC	
	p-value											**0.003**	**<0.001**	**0.001**	**0.025**	0.105	0.179	0.163	0.532	0.267	0.360	0.084	0.572	0.296	**0.022**	0.577	0.718	0.408	0.304	0.344	0.170	0.076	p-value		
rLEC layer II	r-value										**.868****		**.579***	0.434	**.602***	0.506	0.243	0.427	0.131	0.172	0.360	-0.574	0.293	0.203	0.353	-0.062	0.282	0.456	0.015	-0.020	0.226	0.474	r-value	rLEC layer II	
	p-value										**0.002**		**0.048**	0.159	**0.038**	0.093	0.446	0.166	0.685	0.593	0.251	0.051	0.355	0.527	0.261	0.847	0.375	0.136	0.962	0.952	0.480	0.119	p-value		
rLEC layer III	r-value										**.845****	**.705***		**.774****	0.470	0.424	0.492	0.291	0.285	0.340	0.237	-0.334	0.208	0.274	**.636***	-0.164	0.057	0.218	0.370	0.350	0.428	0.459	r-value	rLEC layer III	
	p-value										**0.004**	**0.034**		**0.003**	0.123	0.169	0.104	0.358	0.369	0.279	0.457	0.288	0.516	0.389	**0.026**	0.612	0.861	0.496	0.236	0.264	0.165	0.133	p-value		
rLEC layer V+VI	r-value										**.850****	0.623	0.484		0.549	0.488	0.368	0.535	0.137	0.283	0.166	-0.427	-0.217	0.351	**.648***	-0.226	-0.091	-0.017	0.398	0.304	**.579***	0.496	r-value	rLEC layer V+VI	
	p-value										**0.004**	0.073	0.186		0.064	0.107	0.240	0.073	0.671	0.374	0.605	0.166	0.499	0.263	**0.023**	0.480	0.778	0.959	0.200	0.337	**0.049**	0.101	p-value		
MEC	r-value										**.694***	**.683***	0.521	0.604		0.529	0.307	0.268	0.235	0.549	0.440	-0.446	0.191	0.065	0.257	-0.231	-0.059	0.088	0.208	0.106	-0.112	0.201	r-value	MEC	
	p-value										**0.038**	**0.043**	0.151	0.085		0.077	0.332	0.400	0.463	0.065	0.152	0.146	0.552	0.841	0.420	0.471	0.855	0.786	0.518	0.742	0.729	0.532	p-value		
Prox Septal CA1	r-value										-0.442	-0.160	-0.475	-0.377	-0.386		0.429	**.656***	0.476	0.425	**.749****	-0.173	0.190	0.140	0.284	0.013	-0.360	0.088	0.207	-0.029	0.193	0.260	r-value	Prox septal CA1	
	p-value										0.233	0.682	0.197	0.317	0.304		0.165	**0.021**	0.118	0.169	**0.005**	0.590	0.554	0.664	0.371	0.969	0.251	0.785	0.518	0.928	0.548	0.414	p-value		
Dist Septal CA1	r-value										-0.227	-0.111	-0.489	0.075	-0.151	**.670***		0.406	**.847****	0.378	0.336	0.332	0.192	-0.177	0.157	-0.197	-0.072	0.297	0.264	0.096	0.116	0.101	r-value	Dist septal CA1	
	p-value										0.558	0.775	0.181	0.849	0.699	**0.048**		0.190	**0.001**	0.225	0.285	0.292	0.550	0.581	0.627	0.540	0.825	0.348	0.407	0.768	0.719	0.754	p-value		
Septal CA3	r-value										-0.355	-0.226	-0.633	-0.053	-0.507	**.741***	0.616		0.345	0.274	0.571	-0.282	0.062	0.468	0.492	0.031	-0.127	0.104	0.457	0.327	0.333	0.378	r-value	Septal CA3	
	p-value										0.349	0.559	0.067	0.892	0.163	**0.022**	0.077		0.273	0.388	0.053	0.375	0.848	0.125	0.104	0.923	0.693	0.747	0.136	0.299	0.290	0.226	p-value		
Septal DG	r-value										-0.071	-0.232	-0.122	0.078	-0.540	0.392	0.287	0.655		0.378	0.478	0.535	0.303	-0.312	-0.167	-0.446	-0.487	0.003	0.083	-0.108	-0.004	-0.164	r-value	Septal DG	
	p-value										0.857	0.548	0.755	0.842	0.133	0.297	0.455	0.056		0.226	0.116	0.073	0.339	0.323	0.605	0.146	0.108	0.993	0.798	0.738	0.991	0.610	p-value		
Prox Inter CA1	r-value										-0.147	-0.056	-0.276	-0.012	-0.319	**.784***	0.418	**.806****	**.668***		**.684***	-0.167	0.507	0.381	0.462	0.177	-0.118	0.346	0.414	0.382	-0.082	0.334	r-value	Prox Inter CA1	
	p-value										0.705	0.886	0.473	0.975	0.403	**0.012**	0.263	**0.009**	**0.049**		**0.014**	0.603	0.092	0.222	0.130	0.582	0.715	0.271	0.181	0.221	0.801	0.289	p-value		
Dist Inter CA1	r-value										0.237	0.356	0.081	0.256	-0.224	0.497	0.627	0.501	0.431	0.373		-0.086	**.672***	0.376	0.352	0.178	-0.294	0.232	0.498	0.345	-0.085	0.118	r-value	Dist Inter CA1	
	p-value										0.540	0.348	0.836	0.505	0.562	0.173	0.071	0.170	0.247	0.323		0.791	**0.017**	0.229	0.261	0.579	0.354	0.469	0.099	0.273	0.793	0.714	p-value		
Inter CA3	r-value										**.688***	0.530	**.712***	0.455	0.203	-0.400	-0.471	-0.196	0.307	-0.121	0.205		0.085	**-.674***	**-.624***	-0.335	-0.487	-0.297	-0.255	-0.314	-0.283	**-.710****	r-value	Inter CA3	
	p-value										**0.041**	0.142	**0.031**	0.218	0.600	0.285	0.200	0.613	0.422	0.757	0.596		0.793	**0.016**	**0.030**	0.287	0.109	0.348	0.423	0.320	0.372	**0.010**	p-value		
Inter DG	r-value										0.490	0.353	0.465	0.382	0.016	0.110	-0.173	0.268	**.698***	0.512	0.305	**.771***		0.147	0.183	0.152	-0.011	0.328	0.299	0.387	-0.451	-0.170	r-value	Inter DG	
	p-value										0.181	0.352	0.207	0.310	0.966	0.778	0.655	0.486	**0.037**	0.159	0.425	**0.015**		0.649	0.569	0.636	0.974	0.298	0.346	0.213	0.141	0.597	p-value		
Prox Temp CA1	r-value										-0.123	0.051	-0.455	0.149	-0.104	**.709***	0.570	**.811****	0.289	**.825****	0.374	-0.370	0.141		**.847****	0.526	0.313	0.355	**.703***	**.722****	0.443	**.694****	r-value	Prox Temp CA1	
	p-value										0.753	0.896	0.218	0.702	0.789	**0.033**	0.109	**0.008**	0.451	**0.006**	0.321	0.328	0.718		**0.001**	0.079	0.321	0.258	**0.011**	**0.008**	0.149	**0.012**	p-value		
Dist Temp CA1	r-value										0.219	0.467	-0.147	0.366	0.243	0.610	**.675***	0.564	0.038	0.547	0.621	-0.205	0.081	**.824****		0.470	0.381	0.457	**.743****	**.763****	0.455	**.720****	r-value	Dist Temp CA1	
	p-value										0.571	0.205	0.706	0.333	0.529	0.081	**0.046**	0.114	0.922	0.128	0.074	0.598	0.836	**0.006**		0.123	0.222	0.135	**0.006**	**0.004**	0.137	**0.008**	p-value		
Temp CA3	r-value										0.334	0.442	0.022	0.437	**.714***	0.211	0.187	0.150	-0.212	0.332	-0.103	-0.101	0.146	0.557	0.637		**.623***	**.637***	0.327	0.353	-0.001	0.439	r-value	Temp CA3	
	p-value										0.380	0.234	0.954	0.240	**0.031**	0.586	0.630	0.701	0.585	0.383	0.793	0.797	0.709	0.120	0.065		**0.030**	**0.026**	0.299	0.260	0.997	0.153	p-value		
Dist Dorsal Sub	r-value										0.394	0.332	-0.024	0.632	**.707***	-0.216	0.161	0.038	-0.187	-0.114	-0.118	0.130	0.060	0.189	0.356	**.732***		**.739****	0.125	0.241	0.070	0.501	r-value	Dist Dorsal Sub	
	p-value										0.294	0.383	0.951	0.068	**0.033**	0.576	0.680	0.923	0.629	0.770	0.762	0.739	0.878	0.626	0.347	**0.025**		**0.006**	0.700	0.450	0.829	0.097	p-value		
Prox Dorsal Sub	r-value										0.509	0.590	0.255	0.514	**.862****	0.022	0.174	-0.129	-0.375	-0.035	0.030	0.105	0.089	0.217	0.545	**.860****	**.799****		0.169	0.160	0.197	**.634****	r-value	Prox Dorsal Sub	
	p-value										0.162	0.095	0.507	0.157	**0.003**	0.954	0.654	0.740	0.320	0.929	0.938	0.787	0.821	0.575	0.129	**0.003**	**0.010**		0.599	0.620	0.539	**0.027**	p-value		
Dist Ventral Sub	r-value										0.066	-0.138	-0.066	0.323	-0.018	-0.329	0.286	-0.164	-0.247	-0.441	0.203	-0.228	-0.491	-0.115	0.033	-0.267	0.092	-0.051		**.924*****	0.149	0.260	r-value	Dist Ventral Sub	
	p-value										0.865	0.723	0.866	0.397	0.964	0.387	0.455	0.673	0.521	0.235	0.600	0.555	0.180	0.769	0.932	0.487	0.814	0.896		**<0.001**	0.643	0.414	p-value		
Prox Ventral Sub	r-value										0.043	-0.060	-0.372	0.444	-0.225	-0.110	0.281	0.502	0.226	0.107	0.297	-0.034	-0.053	0.409	0.293	-0.048	0.281	-0.159	0.526		0.010	0.215	r-value	Prox Ventral Sub	
	p-value										0.913	0.878	0.324	0.232	0.560	0.778	0.464	0.168	0.559	0.784	0.438	0.931	0.893	0.275	0.445	0.902	0.464	0.682	0.146		0.976	0.503	p-value		
PL	r-value										0.375	0.578	0.206	0.284	0.594	-0.361	-0.108	-0.418	**-.839*****	-0.525	-0.045	-0.111	-0.511	-0.057	0.299	0.292	0.327	0.444	0.320	0.139		**.696****	r-value	PL	
	p-value										0.320	0.103	0.594	0.459	0.092	0.340	0.783	0.263	**0.005**	0.147	0.908	0.775	0.160	0.884	0.435	0.446	0.390	0.231	0.400	0.722		**0.012**	p-value		
Reuniens	r-value										-0.069	0.069	-0.428	0.238	0.156	0.402	0.465	0.485	-0.192	0.395	0.177	-0.487	-0.226	**.822*****	**.769***	0.626	0.409	0.439	0.266	0.468	0.333		r-value	Reuniens	
	p-value										0.860	0.861	0.250	0.538	0.688	0.283	0.207	0.186	0.621	0.293	0.649	0.184	0.559	**0.007**	**0.015**	0.071	0.274	0.237	0.490	0.204	0.381		p-value		
Peri Novel																																Peri Novel		

Correlations absent due to perirhinal lesion

The top right diagonal matrix (darker grey) displays correlational data from the Sham Discrimination group while the bottom left diagonal matrix displays data from the Peri Discrimination group (lighter grey); the blank cells are due to regions not analysed in the rats with perirhinal lesions. The r-values are the Pearson coefficients. * $p < 0.05$, ** $p < 0.01$, *** $p < 0.001$, for two-tailed correlations (uncorrected for multiple comparisons – see main text). Sites included: area 35 and area 36 of the perirhinal cortex (PRH); CA fields –distal (dist), intermediate (inter), proximal (prox), septal and temporal (temp); dentate gyrus (DG); lateral entorhinal cortex (LEC) – caudal (c), rostral (r); medial entorhinal cortex (MEC); nucleus reuniens of the thalamus (Reuniens); prelimbic cortex (PL); postrhinal cortex (POR); area Te2 (Te2); subiculum (Sub) –distal (dist), proximal (prox).

Table 6.4. Inter-region correlations of Fos-positive cell counts in the novel-novel exploration condition.

Sham Discrimination																																	Sham Discrimination		
		Te2	Area 35	Area 36	PRH	rLEC	rLEC layer II	rLEC layer III	rLEC layer V+VI	POR	cLEC	cLEC layer II	cLEC layer III	cLEC layer V+VI	MEC	Prox septal CA1	Dist septal CA1	Septal CA3	Septal DG	Prox inter CA1	Dist Inter CA1	Inter CA3	Inter DG	Prox Temp CA1	Dist Temp CA1	Temp CA3	Dist Dorsal Sub	Prox Dorsal Sub	Dist Ventral Sub	Prox Ventral Sub	PL	Reuniens			
Te2	r-value		.783**	.852***	.826**	.819***	0.380	.744**	.896***	.749**	.700*	0.371	0.499	.791**	0.522	.813**	.734**	.896***	.786**	.873***	.883***	0.370	.765**	.796**	.812**	0.540	.596*	.628*	0.518	.700*	.908***	.782**	r-value	Te2	
	p-value		0.003	<0.001	0.001	<0.001	0.223	0.006	<0.001	0.005	0.011	0.235	0.099	0.002	0.082	0.001	0.007	<0.001	0.002	<0.001	<0.001	0.236	0.004	0.002	0.001	0.070	0.041	0.029	0.084	0.011	<0.001	0.003	p-value		
Area35	r-value			.914***	.988***	.890***	.587*	.866***	.736**	.788**	.821**	.599*	.693*	.763**	0.562	.836**	.755**	.636*	0.513	.670*	.808**	0.093	.666*	.779**	.810**	0.272	.736**	.680*	0.554	.776**	.839**	.642**	r-value	Area35	
	p-value			<0.001	<0.001	<0.001	0.045	<0.001	0.006	0.002	0.001	0.040	0.012	0.004	0.057	0.001	0.005	0.026	0.088	0.017	0.001	0.775	0.018	0.003	0.001	0.392	0.006	0.015	0.062	0.003	0.001	0.024	p-value		
Area36	r-value				.966***	.876***	0.528	.846**	.793**	.876***	.820**	0.407	.663*	.869***	.659*	.812**	.798**	.726**	.685*	.701*	.877***	0.304	.813**	.767**	.776**	0.489	.713**	.686*	0.497	.825**	.917***	.688**	r-value	Area36	
	p-value				<0.001	<0.001	0.078	0.001	0.002	<0.001	0.001	0.189	0.019	<0.001	0.020	0.001	0.002	0.007	0.014	0.011	<0.001	0.337	0.001	0.004	0.003	0.107	0.009	0.014	0.100	0.001	<0.001	0.013	p-value		
PRH	r-value					.903***	.576*	.877***	.773**	.838**	.838**	0.538	.696*	.819**	.610*	.844**	.787**	.683*	.589*	.696*	.852***	0.175	.736**	.790**	.814**	0.360	.743**	.697*	0.544	.811**	.886***	.673**	r-value	PRH	
	p-value					<0.001	0.050	<0.001	0.003	0.001	0.001	0.071	0.012	0.001	0.035	0.001	0.002	0.014	0.044	0.012	<0.001	0.586	0.006	0.002	0.001	0.250	0.006	0.012	0.068	0.001	<0.001	0.017	p-value		
rLEC	r-value						.757**	.977***	.721**	.753**	.916***	.591*	.857***	.816**	.709**	.695*	.638*	.709**	0.503	.729**	.841**	0.123	.713**	.856***	.896***	0.482	.643*	.629*	.629*	.797**	.798**	0.476	r-value	rLEC	
	p-value						0.004	<0.001	0.008	0.005	<0.001	0.043	<0.001	0.001	0.010	0.012	0.026	0.010	0.095	0.007	0.001	0.704	0.009	<0.001	<0.001	0.112	0.024	0.028	0.028	0.002	0.002	0.118	p-value		
rLEC layer II	r-value							.715**	0.112	0.487	.829**	.749**	.942***	0.509	.727**	0.235	0.366	0.259	0.018	0.338	0.416	-0.104	0.287	.685*	.584*	0.495	0.308	0.283	.588*	.583*	0.385	0.135	r-value	rLEC layer II	
	p-value							0.009	0.729	0.108	0.001	0.005	<0.001	0.091	0.007	0.461	0.242	0.417	0.957	0.283	0.179	0.747	0.365	0.014	0.046	0.102	0.329	0.373	0.045	0.047	0.217	0.675	p-value		
rLEC layer III	r-value								.694*	.720**	.884***	0.554	.839**	.784**	.639*	.651*	0.557	.644*	0.437	.625*	.807**	0.084	.702*	.779**	.862***	0.403	.640*	.601*	0.536	.742**	.726**	0.392	r-value	rLEC layer III	
	p-value								0.012	0.008	<0.001	0.061	0.001	0.003	0.025	0.022	0.060	0.024	0.156	0.030	0.002	0.796	0.011	0.003	<0.001	0.194	0.025	0.039	0.072	0.006	0.007	0.207	p-value		
rLEC layer V+VI	r-value									.650*	0.531	0.119	0.302	.732**	0.369	.826**	.658*	.853***	.821**	.814**	.856***	0.334	.786**	.602*	.740**	0.263	.657*	.688*	0.379	.622*	.864***	.636**	r-value	rLEC layer V+VI	
	p-value									0.022	0.076	0.713	0.340	0.007	0.237	0.001	0.020	<0.001	0.001	0.001	<0.001	0.288	0.002	0.039	0.006	0.408	0.020	0.013	0.225	0.031	<0.001	0.026	p-value		
POR	r-value										.835**	0.316	.640*	.960***	.804**	.800**	.869***	.764**	.640*	.714**	.922***	0.508	.876***	.789**	.752**	.583*	.761**	.776**	.626*	.898***	.891***	.746**	r-value	POR	
	p-value										0.001	0.317	0.025	<0.001	0.002	0.002	<0.001	0.004	0.025	0.009	<0.001	0.091	<0.001	0.002	0.005	0.047	0.004	0.003	0.030	<0.001	<0.001	0.005	p-value		
cLEC	r-value											.687*	.941***	.867***	.854***	.640*	.738**	.596*	0.397	.638*	.803**	0.082	.656*	.862***	.843**	0.498	.720**	.705*	.700*	.836**	.743**	0.442	r-value	cLEC	
	p-value											0.014	<0.001	<0.001	<0.001	0.025	0.006	0.041	0.202	0.026	0.002	0.800	0.021	<0.001	0.001	0.099	0.008	0.010	0.011	0.001	0.006	0.150	p-value		
rLEC layer II	r-value										.949***		.734**	0.290	0.340	0.300	0.398	0.067	-0.126	0.219	0.257	-0.463	-0.025	0.553	0.505	0.042	0.410	0.323	0.395	0.313	0.272	0.186	r-value	rLEC layer II	
	p-value										<0.001		0.007	0.360	0.280	0.344	0.200	0.835	0.697	0.495	0.421	0.129	0.939	0.062	0.094	0.898	0.186	0.306	0.204	0.323	0.392	0.562	p-value		
rLEC layer III	r-value										.949***	.921***		.682*	.798**	0.415	0.506	0.379	0.152	0.463	.600*	-0.107	0.460	.789**	.747**	0.463	0.530	0.494	.661*	.717**	0.517	0.186	r-value	rLEC layer III	
	p-value										<0.001	<0.001		0.015	0.002	0.180	0.093	0.225	0.638	0.130	0.039	0.741	0.132	0.002	0.005	0.130	0.076	0.102	0.019	0.009	0.086	0.563	p-value		
rLEC layer V+VI	r-value										.728**	0.452	0.491		.857***	.767**	.842**	.827**	.708*	.762**	.956***	0.464	.914***	.783**	.802**	.580*	.773**	.813**	.648*	.903***	.905***	.636**	r-value	rLEC layer V+VI	
	p-value										0.007	0.140	0.105		<0.001	0.004	0.001	0.001	0.010	0.004	<0.001	0.129	<0.001	0.003	0.002	0.048	0.003	0.001	0.023	<0.001	<0.001	0.026	p-value		
MEC	r-value										.673*	0.490	0.453	.859***		0.467	.684*	.590*	0.444	.605*	.727**	0.339	.696*	.732**	.659*	.651*	0.564	.631*	.748**	.859***	.686*	0.360	r-value	MEC	
	p-value										0.017	0.106	0.139	<0.001		0.125	0.014	0.044	0.148	0.037	0.007	0.280	0.012	0.007	0.020	0.022	0.056	0.028	0.005	<0.001	0.014	0.251	p-value		
Prox septal CA1	r-value										0.537	0.373	0.368	.699*	.636*		.860***	.791**	.742**	.831**	.878***	0.308	.729**	.740**	.715**	0.298	.831**	.807**	0.459	.691*	.833**	.739**	r-value	Prox septal CA1	
	p-value										0.072	0.233	0.240	0.011	0.026		<0.001	0.002	0.006	0.001	<0.001	0.330	0.007	0.006	0.009	0.347	0.001	0.001	0.133	0.013	0.001	0.006	p-value		
Dist septal CA1	r-value										0.465	0.444	0.333	0.486	0.501	.622*		.689*	.686*	.721**	.819**	0.334	.660*	.671*	.600*	0.350	.882***	.895***	0.471	.712**	.839**	.695**	r-value	Dist septal CA1	
	p-value										0.128	0.149	0.290	0.109	0.097	0.031		0.013	0.014	0.008	0.001	0.289	0.020	0.017	0.039	0.265	<0.001	<0.001	0.122	0.009	0.001	0.012	p-value		
Septal CA3	r-value										0.388	0.244	0.126	.744**	.779**	.672*	0.509		.873***	.902***	.917***	.627*	.883***	.723**	.726**	.640*	0.553	.632*	0.526	.712**	.865***	.745**	r-value	Septal CA3	
	p-value										0.212	0.444	0.697	0.006	0.003	0.017	0.091		<0.001	<0.001	<0.001	0.029	<0.001	0.008	0.008	0.025	0.062	0.027	0.079	0.009	<0.001	0.005	p-value		
Septal DG	r-value										0.108	0.001	-0.087	0.451	0.561	.727**	.611*	.711**		.732**	.768**	0.557	.791**	0.473	0.454	0.521	0.514	0.566	0.250	0.543	.778**	.657**	r-value	Septal DG	
	p-value										0.739	0.997	0.788	0.142	0.058	0.007	0.035	0.009		0.007	0.004	0.060	0.002	0.121	0.138	0.082	0.087	0.055	0.433	0.068	0.003	0.020	p-value		
Prox Inter CA1	r-value										0.477	0.386	0.360	0.510	.583*	.669*	.689*	0.576	.745**		.880***	0.423	.749**	.846**	.817**	0.529	.617*	.696*	.687*	.749**	.840**	.673**	r-value	Prox Inter CA1	
	p-value										0.117	0.215	0.251	0.090	0.047	0.017	0.013	0.050	0.005		<0.001	0.170	0.005	0.001	0.001	0.077	0.032	0.012	0.014	0.005	0.001	0.017	p-value		
Dist Inter CA1	r-value										0.404	0.383	0.278	0.431	0.508	.737**	.702*	.603*	.732**	.924***		0.480	.928***	.832**	.862***	0.547	.773**	.809**	.634*	.870***	.932***	.711**	r-value	Dist Inter CA1	
	p-value										0.192	0.219	0.382	0.162	0.091	0.006	0.011	0.038	0.007	<0.001		0.114	<0.001	0.001	<0.001	0.065	0.003	0.001	0.027	<0.001	<0.001	0.010	p-value		
Inter CA3	r-value										0.448	0.469	0.274	0.529	0.555	0.521	.705*	.698*	.679*	.819**	.791**		.633*	0.197	0.126	.631*	0.103	0.228	0.129	0.358	0.480	.604**	r-value	Inter CA3	
	p-value										0.144	0.124	0.388	0.077	0.061	0.082	0.010	0.012	0.015	0.001	0.002		0.027	0.540	0.696	0.028	0.750	0.476	0.691	0.253	0.114	0.038	p-value		
Inter DG	r-value										0.269	0.323	0.132	0.329	0.447	.591*	0.471	.636*	.701*	.823**	.907***	.838**		.687*	.737**	.628*	.576*	.628*	0.568	.857***	.877***	.673**	r-value	Inter DG	
	p-value										0.398	0.306	0.684	0.297	0.145	0.043	0.122	0.026	0.011	0.001	<0.001	0.001		0.014	0.006	0.029	0.050	0.029	0.054	<0.001	<0.001	0.016	p-value		
Prox Temp CA1	r-value										0.302	0.195	0.112	0.507	.662*	0.551	0.463	.661*	0.530	.707*	.780**	0.552	.714**		.919***	.619*	.577*	.586*	.833**	.860***	.769**	.616**	r-value	Prox Temp CA1	
	p-value										0.340	0.544	0.730	0.092	0.019	0.063	0.130	0.019	0.076	0.010	0.003	0.063	0.009		<0.001	0.032	0.049	0.045	0.001	<0.001	0.003	0.033	p-value		
Dist Temp CA1	r-value										0.445	0.274	0.210	.722**	.813***	.623*	0.521	.786**	.637*	.773**	.765**	.689*	.715**	.936***		0.417	.620*	.638*	.820**	.862***	.805**	0.543	r-value	Dist Temp CA1	
	p-value										0.147	0.389	0.513	0.008	0.001	0.031	0.082	0.002	0.026	0.003	0.004	0.013	0.009	<0.001		0.177	0.031	0.026	0.001	<0.001	0.002	0.068	p-value		
Temp CA3	r-value										0.271	0.327	0.134	0.306	.619*	0.511	0.405	0.514	0.548	.642*	.748**	0.553	.783**	.835**	.745**		0.054	0.120	0.459	0.573	0.504	0.516	r-value	Temp CA3	
	p-value										0.395	0.300	0.678	0.333	0.032	0.090	0.191	0.087	0.065	0.024	0.005	0.062	0.003	0.001	0.005		0.867	0.711	0.134	0.051	0.095	0.086	p-value		
Dist Dorsal Sub	r-value										0.321	0.166	0.063	.695*	.764**	.761**	0.411	.760**	.694*	.604*	.647*	0.562	.668*	.791**	.846**	.764**		.974***	0.366	.607*	.690*	0.418	r-value	Dist Dorsal Sub	
	p-value										0.308	0.607	0.845	0.012	0.004	0.004	0.185	0.004	0.012	0.037	0.023	0.057	0.018	0.002	0.001	0.004		<0.001	0.242	0.036	0.013	0.176	p-value		
Prox Dorsal Sub	r-value										0.142	0.141	-0.005	0.291	0.408	.613*	0.399	0.442	.589*	.695*	.819**	0.563	.833**	.813**	.721**	.873***	.803**		0.437	.646*	.740**	0.448	r-value	Prox Dorsal Sub	
	p-value										0.661	0.663	0.987	0.359	0.188	0.034	0.198	0.150	0.044	0.012	0.001	0.057	0.001	0.001	0.008	<0.001	0.002		0.155	0.023	0.006	0.144	p-value		
Dist Ventral Sub	r-value										0.345	0.197	0.273	0.371	0.497	0.510	0.362	0.539	0.333	0.409	0.447	0.139	0.257	.633*	0.567	0.367	0.407	0.272		.859***	.626*	0.431	r-value	Dist Ventral Sub	
	p-value										0.273	0.540	0.390	0.235	0.100	0.091	0.248	0.071	0.290	0.187	0.145	0.666	0.420	0.027	0.055	0.241	0.189	0.393		<0.001	0.029	0.162	p-value		
Prox Ventral Sub	r-value										0.208	-0.084	0.069	0.513	.596*	0.541	0.359	.605*	.599*	0.542	0.473	0.211	0.273	.620*	.662*	0.309	0.483	0.266	.800**		.869***	.616**	r-value	Prox Ventral Sub	
	p-value										0.517	0.796	0.832	0.088	0.041	0.069	0.252	0.037	0.040	0.069	0.120	0.510	0.391	0.031	0.019	0.329	0.111	0.403	0.002		<0.001	0.033	p-value		
PL	r-value										0.302	0.098	0.205	0.435	0.533	0.277	0.294	0.459	0.308	.639*	0.501	0.357	0.389	.692*	.666*	0.452	0.419	0.389	0.528	.668*		.809***	r-value	PL	
	p-value										0.339	0.761	0.523	0.158	0.074	0.384	0.354	0.133	0.331	0.025	0.097	0.254	0.211	0.013	0.018	0.140	0.176	0.211	0.077	0.018		0.001	p-value		
Reuniens	r-value										-0.291	-0.193	-0.393	-0.072	0.122	0.063	-0.048	0.369	0.437	0.366	0.407	0.463	.681*	0.390	0.334	0.571	0.415	0.566	-0.154	0.001	0.328		r-value	Reuniens	
	p-value										0.360	0.549	0.206	0.823	0.706	0.847	0.881	0.238	0.155	0.242	0.189	0.129	0.015	0.209	0.289	0.052	0.180	0.055	0.633	0.999	0.298		p-value		
Peri Discrimination																																Peri Discrimination		

Correlations absent due to perirhinal lesion surgeries

The top right diagonal matrix (darker grey) displays correlational data from the Sham Novel group while the bottom left diagonal matrix displays data from the Peri Novel group (lighter grey); the blank cells are due to regions not analysed in the rats with perirhinal lesions. The r-values are the Pearson coefficients. * $p < 0.05$, ** $p < 0.01$, *** $p < 0.001$, for two-tailed correlations (uncorrected for multiple comparisons – see main text). Sites included: area 35 and area 36 of the perirhinal cortex (PRH); CA fields –distal (dist), intermediate (inter), proximal (prox), septal and temporal (temp); dentate gyrus (DG); lateral entorhinal cortex (LEC) – caudal (c), rostral (r); medial entorhinal cortex (MEC); nucleus reuniens of the thalamus (Reuniens); prelimbic cortex (PL); postrhinal cortex (POR); area Te2 (Te2); subiculum (Sub) –distal (dist), proximal (prox).

6.3.5 Structural equation modelling

6.3.5.1 Refining previously derived novelty-related models - Sham animals only

The first network models to be tested were intended to confirm, and anatomically refine, the network model derived in a preceding experiment of novel object recognition memory (described in Chapter 3). This previously derived model was centred on the rostral region of the parahippocampal cortex and the septal level of the hippocampus (Chapter 3), and so was initially tested in the Sham Discrimination group. It is known that the LEC preferentially projects to distal CA1 and proximal subiculum, as well as CA3 (Amaral, 1993; Witter, 1993); this information was used to improve the anatomical resolution of the model.

Well-fitting network models involving area Te2, as described in Chapter 3, could not be derived and so perirhinal cortex was divided into its composite areas (areas 35 and 36). Aside from this modification, the network model as hypothesised (based on the model depicted in Figure 3.12E) had good indices of fit (χ^2_9 = 11.0, p = 0.27; CFI = 0.97; RMSEA = 0.14; Figure 6.10A). The resulting model that best fit the Fos activity data involved two parallel projections between area 36 of the perirhinal cortex and the rostral LEC; one direct pathway and the other indirect, via area 35. Thereafter, the route of functional activity through the hippocampus was as hypothesised; rostral LEC projected to septal CA3, which proceeded to the distal region of septal CA1 and, finally, onto the proximal region of the dorsal subiculum (Figure 6.10A). The same network model structure was also found to have good fit for group Sham Novel (χ^2_9 = 4.71, p = 0.86; CFI = 1.0; RMSEA = 0.0; Figure 6.10B). Quantitatively, the model differed between the two behavioural tasks; in the Sham Discrimination model, all pathways were significant except that between area 36 and rostral LEC, whereas in the Sham Novel group only the path between area 36 and area 35, and the path from rostral LEC to CA3 reached significance level.

The network models involving the complementary pattern in CA1 and subiculum were also tested; i.e., the parahippocampal to CA3 component of the model was held constant but subsequently, CA3 projected to the proximal region of septal CA1 and dorsal distal subiculum. This network model was found to have non-acceptable fit for group Sham Discrimination (χ^2_9 = 18.3, p = 0.032; CFI = 0.87; RMSEA = 0.31) but retained acceptable for group Sham Novel (χ^2_9 = 5.85, p = 0.76; CFI = 1.0; RMSEA = 0.0).

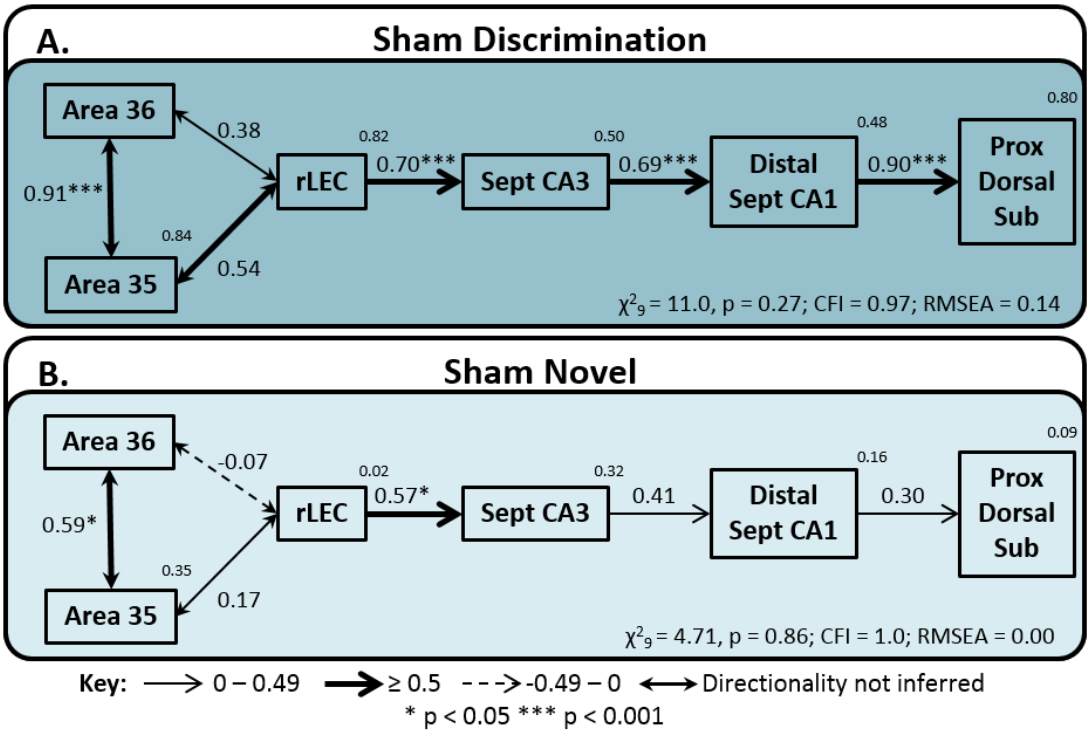

Figure 6.10. Rostral parahippocampal – hippocampal interactions in Sham animals.

Depictions of the optimal parahippocampal - hippocampal interactions derived from structural equation modelling for groups; Sham Discrimination (A) and Sham Novel (B). The fit is noted under each model (CFI, comparative fit index; RMSEA, root mean square error of approximation). The strength of the causal influence of each path is denoted both by the thickness of the arrow and by the path coefficient next to that path. The number above each region is the proportion of its variance that can be explained by its inputs. Sites depicted: area 35 and area 36 of the perirhinal cortex, rostral lateral entorhinal cortex (rLEC), septal CA3, distal septal CA1 and dorsal proximal subiculum. * $p < 0.05$; *** $p < 0.001$.

6.3.5.2 Novel-familiar discrimination vs. novel-novel object exploration

One of the main aims of this study was to investigate if the network for novel object recognition derived in Chapter 3 (Figure 3.12E) reflected the rats discriminating a novel from a familiar object, or if novel objects *per se* are sufficient to induce the same pattern of functional connectivity. SEM data described above indicated indirectly that the latter is true, as the data from both behavioural conditions fit the same network models.

In order to more directly address this question, data from groups Sham Discrimination and Sham Novel were stacked onto the model depicted in Figure 6.10. This first involved constraining the path coefficients of all of the pathways that make up the model to have the same value in both groups (structural weights model). This constrained model was then compared to a model in which the path coefficients were free to vary. This comparison revealed an overall difference between the groups ($\chi^2_{6\ Diff} = 17.4$; p =

0.008). The individual pathways that comprise the model were then allowed to vary individually in order to establish if this group difference was specific to a particular pathway. Allowing the path between area 36 and area 35 to vary significantly improved the fit of the model ($\chi^2_{1\ Diff} = 5.11$, $p = 0.024$), as did unconstraining the path between distal septal CA1 and dorsal proximal subiculum ($\chi^2_{1\ Diff} = 8.11$, $p = 0.004$). There were no other path differences between the two behavioural conditions (path between area 36 and rostral LEC: $\chi^2_{1\ Diff} = 3.13$, $p = 0.077$; all other paths $\chi^2_{1\ Diff} \leq 2$). Figure 6.10 illustrates that these path differences are due to a stronger effective connection in these two pathways when the rats are discriminating novel from familiar objects. Unsurprisingly, as the model fits the data from both groups separately, when the data from the two groups were collapsed and tested on the same network model, it had acceptable fit ($\chi^2_9 = 10.1$, $p = 0.35$; CFI = 0.98; RMSEA = 0.07). This reinforces the assertion that the differences between these groups on this model are predominantly related to the strength of specific connections within the network rather than the overall structure.

6.3.5.3 Testing the novel object network after perirhinal cortex lesions

The network models tested above for the surgical control groups involved regions that could not be analysed in all four groups due to the perirhinal cortex lesions. Thus, the next set of models to be investigated began with the caudal region of the LEC, while keeping the hippocampal component as described. This produced a simple linear model that projected from caudal LEC to septal CA3, then to distal septal CA1 and finally onto the proximal region of the dorsal subiculum (Figure 6.11). This model had good levels of fit for groups Peri Novel ($\chi^2_3 = 2.37$, $p = 0.50$; CFI = 1.0; RMSEA = 0.0), Sham Novel ($\chi^2_3 = 1.33$, $p = 0.72$; CFI = 1.0; RMSEA= 0.0) and Peri Discrimination ($\chi^2_3 = 2.55$, $p = 0.47$; CFI = 1.0; RMSEA = 0.0). Group Sham Discrimination displayed a slightly elevated RMSEA, but all of the other goodness of fit indices indicated a well-fitting model ($\chi^2_3 = 4.44$, $p = 0.21$; CFI = 0.95; RMSEA = 0.21). As seen in Table 6.3, the Fos activity in all of the regions included in this model are highly inter-correlated; this creates redundancy of information that can then inflate the RMSEA (Tabachnick & Fidell, 2001). Surprisingly, this indicates that information flow through the hippocampus, elicited by novel object exploration is not affected by the loss of the perirhinal cortex. This assertion will be tested more directly in a subsequent section.

The models for each group were then tested with cortical layers II, III or V+VI of caudal LEC in place of the Fos counts from the whole caudal LEC. All other aspects of the

network were kept constant. It was found that all three of the cortical layers fit in place of the whole caudal LEC in groups Peri Discrimination and Sham Novel, while only cortical layers II and III fit in groups Sham Discrimination and Peri Novel (Table 6.5).

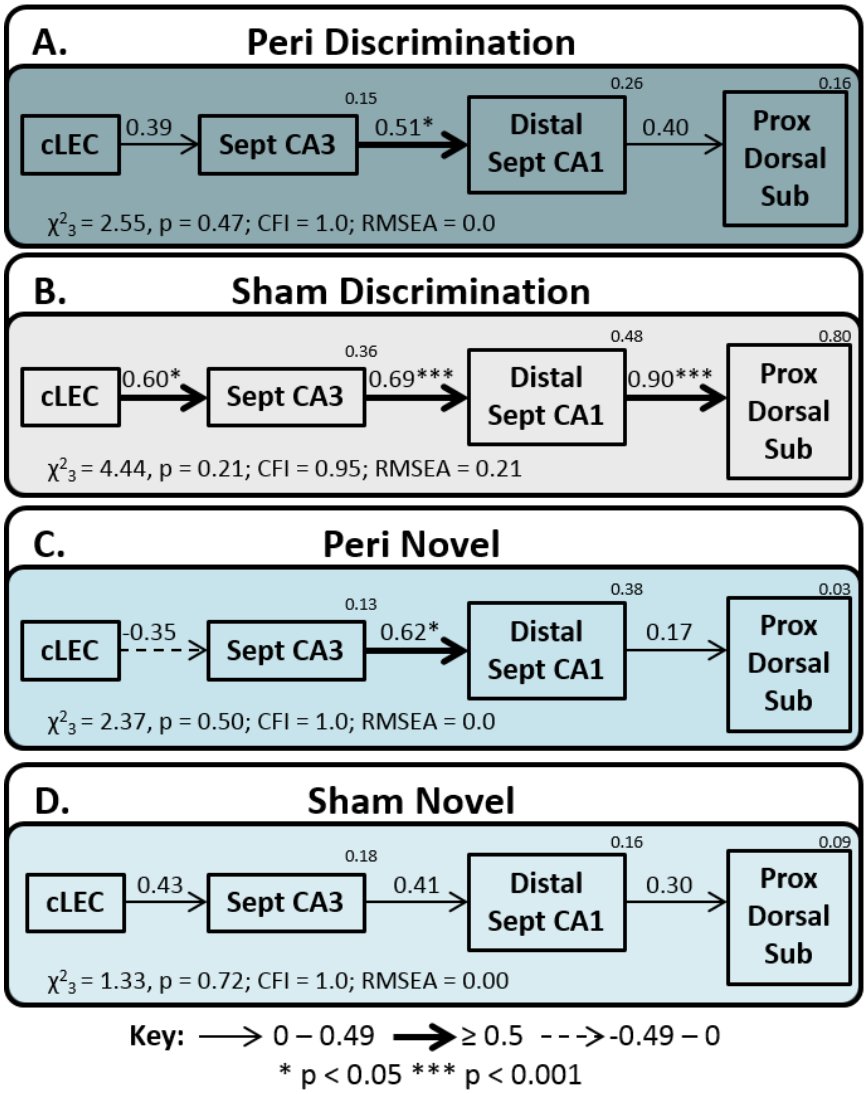

Figure 6.11. Caudal parahippocampal – hippocampal interactions in all groups.

Depictions of the caudal parahippocampal - hippocamapal interactions derived by structural equation modelling for groups; Peri Discrimination (A), Sham Discrimination (B), Peri Novel (C) and Sham Novel (D). The fit is noted under each model (CFI, comparative fit index; RMSEA, root mean square error of approximation) and models with unacceptable fit are represented with a pale grey background. The strength of the causal influence of each path is denoted both by the thickness of the arrow and by the path coefficient next to that path. The number above each region is the proportion of its variance that can be explained by its inputs. Sites depicted: caudal lateral entorhinal cortex (cLEC), septal CA3, distal septal CA1 and dorsal proximal subiculum. * $p < 0.05$; *** $p < 0.001$.

Table 6.5. Model fit when cortical layers II, III or V+VI replace whole cLEC counts in the models depicted in Figure 6.11.

	χ^2-value	df	p-value	CFI	RMSEA	Acceptable model fit
Peri Discrimination						
Cortical layer II	2.83	3	0.42	1.0	0.0	✓
Cortical layer III	2.46	3	0.48	1.0	0.0	✓
Cortical layers V+VI	1.58	3	0.66	1.0	0.0	✓
Sham Discrimination						
Cortical layer II	3.01	3	0.38	0.99	0.04	✓
Cortical layer III	1.72	3	0.63	1.0	0.0	✓
Cortical layers V+VI	9.75	3	0.021	0.83	0.45	x
Peri Novel						
Cortical layer II	1.90	3	0.59	1.0	0.0	✓
Cortical layer III	0.50	3	0.92	1.0	0.0	✓
Cortical layers V+VI	4.14	3	0.25	0.49	0.22	x
Sham Novel						
Cortical layer II	2.62	3	0.45	1.0	0.0	✓
Cortical layer III	2.31	3	0.51	1.0	0.0	✓
Cortical layers V+VI	0.7	3	0.88	1.0	0.0	✓

CFI, comparative fit index; df, degrees of freedom; RMSEA, root mean square error of approximation

A further refinement was made to the network which also generated well-fitting models. A feedback pathway from the dorsal proximal subiculum to rostral LEC was added to the network (Figure 6.12). This generated models of good fit for groups Sham Discrimination ($\chi^2_2 = 0.85$, p = 0.65; CFI = 1.0; RMSEA = 0.0) and Sham Novel ($\chi^2_2 = 0.79$, p = 0.67; CFI = 1.0; RMSEA = 0.00). In group Peri Novel this modification produced a model of good fit ($\chi^2_2 = 0.52$, p = 0.77; CFI = 1.0; RMSEA = 0.0), but the direction of effect could not be inferred. Testing this network on data from group Peri Discrimination generated a model that was just outside the acceptable fit criteria ($\chi^2_2 = 2.49$, p = 0.29; CFI = 0.86; RMSEA = 0.15).

The data presented thus far indicate that perirhinal cortex lesions had little impact on the parahippocampal-hippocampal interactions (Figure 6.12). In order to test this preliminary conclusion directly, the data from all four groups were stacked on the network depicted in Figure 6.11. Allowing the coefficients of all paths to vary between all four groups did not significantly improve the fit over the structural weights model ($\chi^2_{9\ Diff}$ = 15.7, p = 0.074), indicating no overall difference between the four groups. Supporting this conclusion, the Fos data from all four groups were collapsed to create a single group on which the model could be tested. These combined data produced fit indices that just reached acceptable levels (χ^2_3 = 5.74, p = 0.13; CFI = 0.92; RMSEA = 0.14).

Next, the Fos data were collapsed across the behavioural conditions to allow for comparison between lesion status regardless of behavioural task. There was no difference between the structural weights model and the model in which the weights of all paths were free to fluctuate ($\chi^2_{3\ Diff}$ = 2.61, p = 0.46) implying no functional difference between the rats with perirhinal lesions and their surgical controls. To probe this effect further, and to ensure that collapsing across the behavioural condition did not mask an effect of the lesions, group comparisons were made within the behavioural conditions. Again, there was no overall improvement of fit when the paths were allowed to vary as compared to when they were constrained to be the same between groups Sham Novel and Peri Novel ($\chi^2_{3\ Diff}$ = 3.19, p = 0.37). This was also the case when groups Sham Discrimination and Peri Discrimination were compared ($\chi^2_{3\ Diff}$ = 5.66, p= 0.13). This indicates that lesions to the perirhinal cortex did not cause dysfunction in hippocampal activity related to the processing novel objects.

It was found that the data from group Peri Discrimination did not fit the model depicted in Figure 6.12, which involved an additional path from the subiculum back to the caudal LEC. This would indicate that perirhinal cortex lesions alter the reciprocal relationship between the hippocampal formation and the LEC when rats are discriminating novel from familiar objects. However, when the data were collapsed across the behavioural condition there was no improvement in fit by allowing the paths to differ between the lesion and sham groups ($\chi^2_{4\ Diff}$ = 2.42, p = 0.66), nor was there a difference found when the lesion animals were stacked against their surgical control groups within each behavioural condition (Discrimination: $\chi^2_{4\ Diff}$ = 5.38, p = 0.25 and Novel: $\chi^2_{4\ Diff}$ = 4.12, p = 0.39). Thus, when tested directly, the pathway between subiculum and LEC was not affected by the perirhinal lesions.

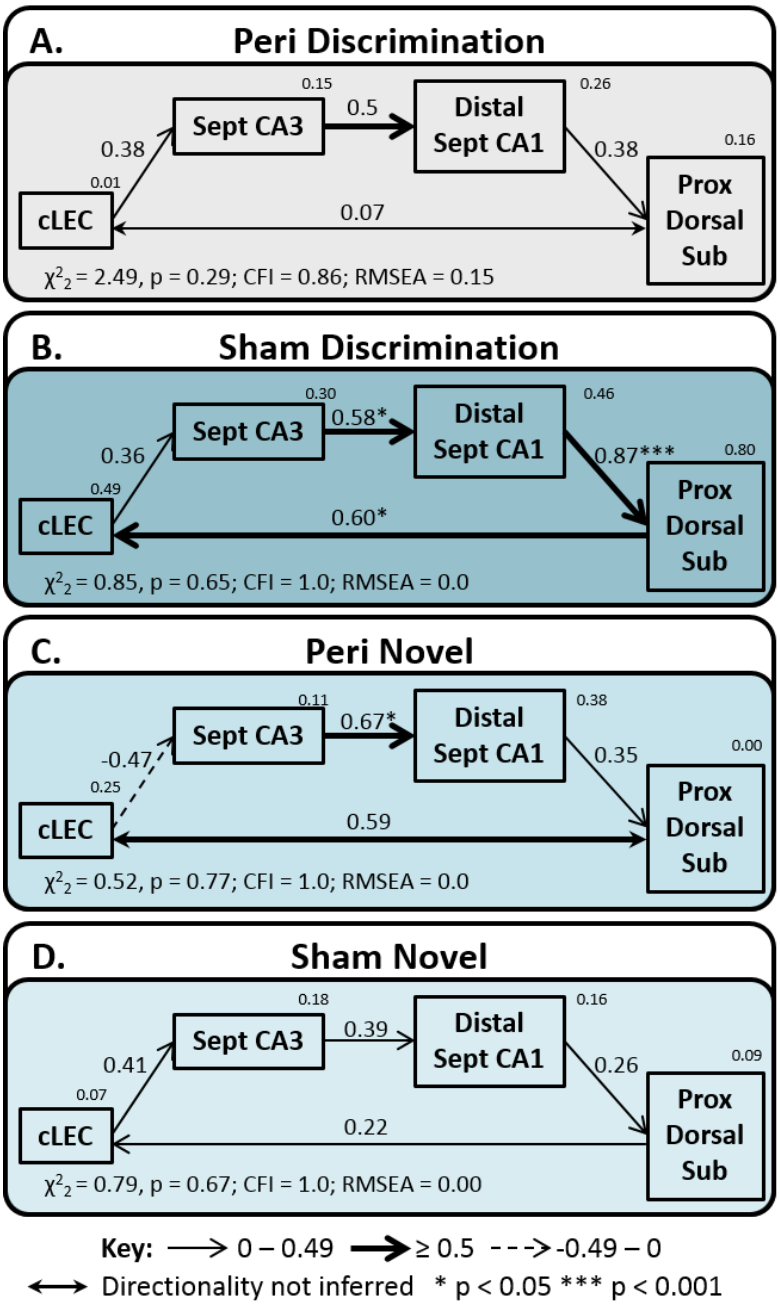

Figure 6.12. Additional parahippocampal – hippocampal interactions in all groups.

Depictions of the caudal parahippocampal - hippocampal interactions derived by structural equation modelling for groups; Peri Discrimination (A), Sham Discrimination (B), Peri Novel (C) and Sham Novel (D). The fit is noted under each model (CFI, comparative fit index; RMSEA, root mean square error of approximation) and models with unacceptable fit are represented with a pale grey background. The strength of the causal influence of each path is denoted both by the thickness of the arrow and by the path coefficient next to that path. The number above each region is the proportion of its variance that can be explained by its inputs. Sites depicted: caudal lateral entorhinal cortex (cLEC), septal CA3 (sept CA3), distal septal CA1 (sept CA1) and dorsal proximal subiculum (prox sub). * $p < 0.05$; *** $p < 0.001$.

6.3.5.4 Novel-familiar discrimination vs. novel-novel object exploration – all four groups

The Fos data were subsequently collapsed across the lesion status of the groups to compare all rats in the novel-novel exploration condition with all rats in the novel-familiar discrimination condition. Allowing the weights of the paths to be different yielded a model of significantly better fit than the structural weights model ($\chi^2_{3\ Diff}$ = 8.39, p = 0.039), indicating a difference between these behavioural conditions. When the paths were individually unconstrained, the only one to significantly improve fit was the path between distal septal CA1 and the dorsal proximal subiculum (χ^2_{1v}= 7.35, p = 0.007), there were no differences between the conditions in the other paths ($\chi^2_{1\ Diff} \leq 1$). Subsequent pairwise stacking between the groups on this network model revealed a difference between groups Sham Discrimination and Sham Novel ($\chi^2_{3\ Diff}$ = 8.38, p = 0.039) that was again due to a difference in the path between distal septal CA1 and the dorsal proximal subiculum ($\chi^2_{1\ Diff}$ = 8.11, p = 0.004) and not in the other paths ($\chi^2_{1\ Diff} \leq$ 1). This difference, based on behavioural condition, appears to be driven by the surgical control animals, as there was no overall difference when groups Peri Discrimination and Peri Novel were stacked on the same model ($\chi^2_{3\ Diff}$ = 2.27, p = 0.52). This suggests that there is a stronger connection between distal CA1 and proximal subiculum in the discrimination condition than in the novel-novel exploration condition in intact rats. The difference is not observed in rats with perirhinal lesions, indicating that perirhinal lesions may affect this connection. However, this implied lesion difference does not reach significance when Peri Discrimination and Sham Discrimination were compared directly in previous section.

The same pattern of differences was found when the stacking procedure was undertaken for the model depicted in Figure 6.12; there was no differential effect of the additional pathway. Thus, the stronger effective connection between distal septal CA1 and the dorsal proximal subiculum seen in the novel-familiar discrimination condition is due to a strong functional connection between these regions only in the surgical control group (Sham Discrimination).

6.3.5.5 Prelimbic cortex models – Sham animals only

Additional models of good fit were derived that involved prelimbic cortex. Prelimbic cortex has been shown to be reciprocally connected to the deep cortical layers of the perirhinal cortex and LEC (Conde et al., 1995; Vertes, 2004; Jones & Witter, 2007), as well as to the temporal region of CA1 via the nucleus reuniens of the thalamus (Vertes et

al, 2007; Prasad & Chudasama, 2013). The first models were tested in the surgical control groups as the prelimbic– perirhinal link was of potential interest (Figure 6.13A, B).

Several of the pathways that compose the optimal network models for these two groups were the same. Both networks involved a path between prelimbic cortex and nucleus reuniens of the thalamus with a further connection with distal temporal CA1, while caudal LEC also connected with the same region of CA1. An interesting dissociation was found in the pathways between prelimbic cortex and areas of the rhinal cortex. The optimal model for the Sham Discrimination group involved a path between prelimbic cortex and area 36 of the perirhinal cortex ($\chi^2_9 = 7.09$, $p = 0.63$; CFI = 1.0; RMSEA = 0.0; Figure 6.13A). In comparison, for the Sham Novel group, prelimbic cortex was functionally connected with area 35 of the perirhinal cortex and caudal LEC ($\chi^2_8 = 7.75$, $p = 0.46$; CFI = 1.0; RMSEA = 0.0; Figure 6.13B). Testing the Fos data from the Sham Discrimination group on the optimal network model for the Sham Novel group yielded a model of inadequate fit ($\chi^2_8 = 13.9$, $p = 0.083$; CFI = 0.92; RMSEA = 0.26; Figure 6.13C). Poor indices of fit were also generated when the data from group Sham Novel were tested on the optimal model for Sham Discrimination ($\chi^2_9 = 13.0$, $p = 0.16$; CFI = 0.82; RMSEA = 0.20; Figure 6.13D).

These data suggest a functional connection between the prelimbic cortex and the more dorsal area 36 in the novel-familiar discrimination condition, while during novel object exploration the prelimbic cortex is functionally connected to the more ventral regions of area 35 and LEC (Figure 6.13A, B). When the two groups were stacked on these models, no differences emerged (analyses not shown). Subsequently, the inter-regional Fos correlations between prelimbic cortex and perirhinal cortex were compared directly between groups Sham Novel-Familiar discrimination and Sham Novel-Novel using Fisher's r-to-z transformation (Zar, 2010). The connection between prelimbic cortex and area 36 was significantly different between the two groups ($z = 2.99$, $p = 0.003$), with a stronger correlation in the Novel-Familiar discrimination group (Figure 6.13A).

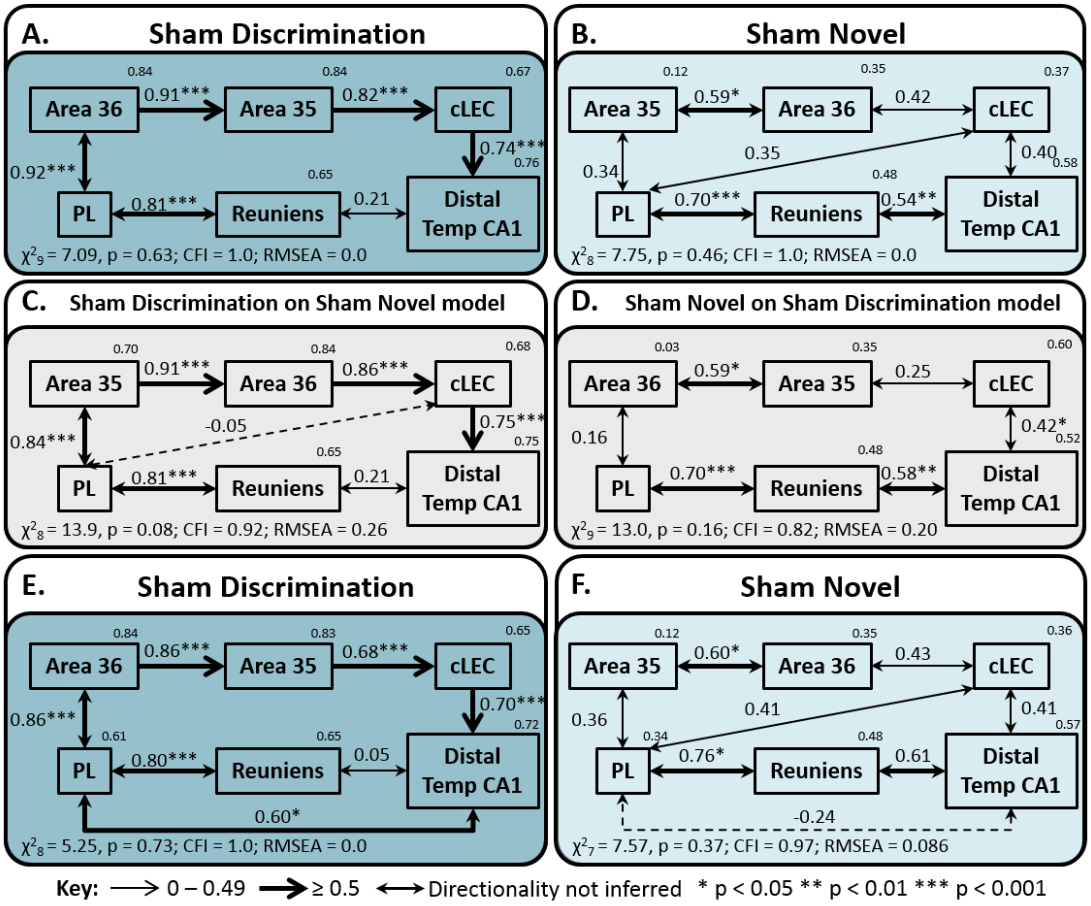

Figure 6.13. Prelimbic cortex interactions in Sham animals only

The upper panels are depictions of the optimal interactions between prelimbic cortex, the rhinal cortex and temporal hippocampus derived by structural equation modelling for the surgical control groups; Sham Discrimination (A), and Sham Novel (B). The middle panels illustrate the same network models tested with data from the other group: group Sham Discrimination tested on the optimal model for Sham Novel with poor fit (C) and Sham Novel tested on the optimal model for Sham Discrimination (D), also with poor fit. The lower panels depict the optimal models illustrated above with an additional feedback pathway in Sham Discrimination (E), and Sham Novel (F).The fit is noted under each model (CFI, comparative fit index; RMSEA, root mean square error of approximation) and models with unacceptable fit are represented with a pale grey background. The strength of the causal influence of each path is denoted both by the thickness of the arrow and by the path coefficient next to that path. The number above each region is the proportion of its variance that can be explained by its inputs. Sites depicted: Areas 35 and 36 of the perirhinal cortex, caudal lateral entorhinal cortex (cLEC), distal temporal CA1, prelimbic cortex (PL) and nucleus reuniens of the thalamus. * $p < 0.05$; ** $p < 0.01$; *** $p < 0.001$.

It should be noted that when data from the two groups were stacked on these models, no improvement in fit was seen by allowing the groups to be different (Sham Discrimination optimal model: $\chi^2_{6\ Diff} = 10.6$, $p = 0.10$; Sham Novel optimal model: $\chi^2_{7\ Diff} = 4.57$, $p = 0.71$). In addition, when the Fos data from both Sham Discrimination and Sham Novel were collapsed to form a single 'Sham' dataset and then tested on the

optimal network model for the Sham Discrimination group, depicted in Figure 6.13A, analysis yielded fit indices that were just within the acceptable limit (χ^2_9 = 16.4, p = 0.059; CFI = 0.91; RMSEA = 0.19). The same was true when the collapsed 'Sham' dataset was tested on the optimal network model for the Sham Novel group depicted in Figure 6.13B (χ^2_8 = 9.35, p = 0.31; CFI = 0.98; RMSEA = 0.09). This is perhaps not surprising based on the overall similarity of the two models. Nonetheless, in both cases the fit indices are poorer when the data are collapsed. Also, as detailed above, when tested in isolation the Fos data from each group did not fit the optimal model for the other group, indicating a non-homogeneous dataset.

Based on the optimal models for each group, two additional models of acceptable fit were also derived that involved an additional pathway between the distal region of temporal CA1 and the prelimbic cortex (Sham Discrimination: χ^2_8 = 5.25, p = 0.73; CFI = 1.0; RMSEA = 0.0; Figure 6.13E and Sham Novel: χ^2_7 = 7.57, p = 0.37; CFI = 0.97; RMSEA = 0.086; Figure 6.13F). Although this pathway appears quantitatively different in each group when the data were stacked on each network model, no group differences were uncovered (Sham Discrimination based model: $\chi^2_{7\ \text{Diff}}$ = 11.5, p = 0.12; Sham Novel based model: $\chi^2_{8\ \text{Diff}}$ = 12.5, p= 0.13).

6.3.5.6 Prelimbic cortex models – all four groups

The final set of models to be tested were a subset of those described in the previous section but involved brain regions that were present in all four animal groups. The perirhinal regions were eliminated creating a network model of two parallel pathways between prelimbic cortex and the distal region of temporal CA1; the first via the nucleus reuniens of the thalamus and the other by way of the caudal region of the LEC (Figure 6.14). This network generated models of good fit for both groups in the novel-novel exploration condition (Peri Novel: χ^2_2 = 0.55, p = 0.76; CFI = 1.0; RMSEA = 0.0; and Sham Novel: χ^2_2 =1.81, p = 0.41; CFI = 1.0; RMSEA = 0.0; Figure 6.14C, D) but poor fit for both groups in the novel-familiar discrimination condition (Peri Discrimination: χ^2_2 = 5.49, p = 0.064; CFI = 0.57; RMSEA = 0.40; and Sham Discrimination: χ^2_2 = 3.70, p = 0.16; CFI = 0.95; RMSEA = 0.29; Figure 6.14A, B).

Additional evidence for behavioural condition differences was seen when the data from all four groups were collapsed to create a single group; these data were tested on the same network creating a model of poor fit (χ^2_2 = 6.71, p = 0.035; CFI = 0.92; RMSEA = 0.23) indicating differences among the datasets. However, when the structural weights of all of the paths in the model were constrained to have the same value for all four

groups the fit was no different from when the structural weights were free to differ between the groups ($\chi^2_{12\ Diff} = 5.49$, $p = 0.94$). Subsequent pairwise stacking procedures yielded no differences in the network based on the behavioural condition when all rats in the novel-familiar discrimination condition were stacked against all rats in the novel-novel exploration condition ($\chi^2_{4\ Diff} = 1.54$, $p = 0.82$). Additionally, there were also no differences when surgical control rats in the novel-familiar discrimination condition were stacked against their counterparts in the novel-novel exploration condition ($\chi^2_{4\ Diff} = 2.61$, $p = 0.63$) or when perirhinal lesion rats in the novel-familiar discrimination condition were stacked against lesion rats from the novel-novel exploration condition ($\chi^2_{4\ Diff} < 1$). Further, no lesion differences in this model were seen when all perirhinal lesions were stacked against surgical controls regardless of the behavioural condition ($\chi^2_{4\ Diff} = 2.27$, $p = 0.69$). Finally, differences between rats with lesions and their surgical controls were not found in rats of the novel-familiar discrimination condition ($\chi^2_{4\ Diff} = 2.24$, $p = 0.66$) or rats in the novel-novel exploration condition ($\chi^2_{4\ Diff} < 1$).

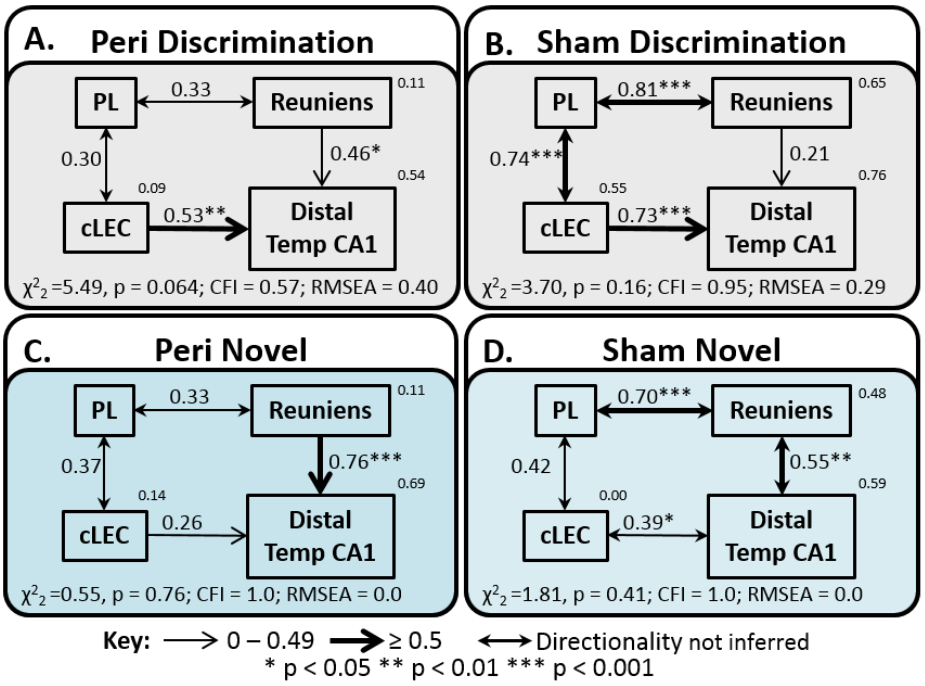

Figure 6.14. Prelimbic cortex interactions in all groups.

Depictions of the interactions between prelimbic cortex, lateral entorhinal cortex and temporal hippocampus derived by structural equation modelling for groups; Peri Discrimination (A), Sham Discrimination (B), Peri Novel (C) and Sham Novel (D). The fit is noted under each model (CFI, comparative fit index; RMSEA, root mean square error of approximation) and models with unacceptable fit are represented with a pale grey background. The strength of the causal influence of each path is denoted both by the thickness of the arrow and by the path coefficient next to that path. The number above each region is the proportion of its variance that can be explained by its inputs. Sites depicted: caudal lateral entorhinal cortex (cLEC), distal temporal CA1 prelimbic cortex (PL) and nucleus reuniens of the thalamus. * $p < 0.05$; ** $p < 0.01$; *** $p < 0.001$.

6.4 Discussion

The present study had two broad sets of goals; the first set was in relation to preceding work on novelty induced c-*fos* activity data presented in this thesis. The second aim was to investigate the behavioural effects of lesions to the perirhinal cortex and the implications of these effects on models of perirhinal cortex function; the behavioural effects will be addressed first.

6.4.1 False memories and interference due to perirhinal cortex lesions

The overall objective of this section was to test specific predictions of the perceptual mnemonic feature conjunction model of perirhinal cortex function (Bussey et al., 2005; McTighe et al., 2010; Romberg et al., 2012). The first prediction to be tested was that rats with lesions to the perirhinal cortex display false memories by treating novel stimuli as if they are familiar; exhibited by reduced exploration times of novel objects in a spontaneous exploration task (McTighe et al., 2010; Romberg et al., 2012). The second prediction to be tested was that perirhinal lesions cause rats to be highly sensitive to interference, such that objects encountered in one trial cause subsequently encountered objects to appear familiar due to feature ambiguity (Cowell et al., 2010; McTighe et al., 2010; Romberg et al., 2012). Feature ambiguity occurs when a particular feature is encountered multiple times on different stimuli; as the number of encountered objects increases the more likely the objects are to share overlapping features (Bussey et al., 2005). While the present study did not intentionally present overlapping features, as each test involved 20 trials it seems inevitable that test objects shared some features. As the test session progressed, objects should become increasingly familiar due to increased likelihood of feature ambiguity. This should manifest itself as a progressive reduction in exploration time dedicated to novel stimuli across the test session as they seem more familiar.

It should be noted that the studies presenting evidence for false memories (McTighe et al., 2010; Romberg et al., 2012) involved exposing rats to pairs of objects in which both objects are either novel or both objects are familiar, so creating indirect tests of recognition memory. If perirhinal lesions cause false memories, evidence of a reduction in total exploration should also be seen in direct tests of object recognition memory and, as described above, this reduction in object exploration should become more marked with increased number of trials.

Rats in Experiment 1 were given a novel-familiar object discrimination task; lesions in the perirhinal cortex impaired the rats' ability to successfully discriminate novel objects from familiar ones when measured across the whole test session. The lesions did not, however, abolish recognition memory completely. Discrimination performance in the group Peri Discrimination was above chance levels; a pattern that has been observed previously with the very short retention intervals employed in the current study (Albasser et al., 2011a; 2015). When the total exploration data from Experiment 1 are examined, there is no evidence that this recognition deficit is due to an overall reduction in exploration of objects. Inspection of the upper left panel of Figure 6.5 shows that the amount of exploration was remarkably similar for both groups along the progression of the 20 trials. Rats with lesions did not show a tendency to reduce exploration of objects, even though interference presumably increased. This null result contradicts the prediction that rats with perirhinal lesions should show an enhanced susceptibility to treat all objects as familiar, thereby reducing total exploration (McTighe et al., 2010).

These predictions are specifically based around exploration of novel objects (McTighe et al., 2010; Romberg et al., 2012) and so mean exploration times from Experiment 1 were separated based on time dedicated to either novel or familiar objects. There was no overall main effect of perirhinal cortex lesions on mean exploration of either novel or familiar objects. These exploration data were divided into four blocks of five consecutive trials in order to examine if novel object exploration reduced as the test session progressed. The only reduction seen in novel object exploration due to perirhinal lesions was across trials 6-10. If this reduction was due to interference effects, it would be expected that the deficit would become progressively worse as the rats progressed through blocks, but this was not the case.

As mentioned above, evidence for false memories comes from behavioural studies in which trials consist of pairs of either novel or familiar objects rather than one of each (McTighe et al., 2010; Romberg et al., 2012). It could be argued that by pairing a novel with a familiar object they are placed in direct competition, as they cannot be explored simultaneously. Based on the fact that the mean amount of exploration per trial in the discrimination task was approximately six seconds, while the total amount of time available for exploration was one minute, this proposition seems unlikely. Nonetheless, this possibility was addressed in Experiment 2 by presenting only novel stimuli, thereby, removing time competition between the classes of objects. In this behavioural condition the rats were presented with 20 pairs of non-identical novel objects; by the end of the

test they had encountered 40 novel objects. However, even upon removal of object class competition, the results of Experiment 2 do not appear to support predictions relating to perirhinal lesions causing false memories or increased susceptibility to interference.

In Experiment 2, the total amount of time rats spent exploring the novel objects over the whole test session was not different between the sham and lesion conditions, indicating that loss of the perirhinal cortex did not induce novel objects to be perceived as familiar. Additionally, there was no evidence of progressive interference effects caused by perirhinal lesions. When the data were divided into four blocks of five trials, exploration levels for the two groups were highly comparable. One shortcoming of the design of Experiment 2 was that a concurrent impairment in recognition memory was not demonstrated in the rats with perirhinal lesions. However, it has been shown previously that when rats with perirhinal lesions are exposed to either pairs of novel or pairs of familiar objects they exhibit exploration levels equivalent to their surgical controls, while displaying a simultaneous recognition deficit (Mumby et al., 2007; Albasser et al., 2009, 2011a).

Comparison of the total exploration times across Experiments 1 and 2 yielded further evidence of at least partially intact novelty detection in rats with perirhinal lesions. Both groups in the novel-novel exploration condition displayed equivalently higher exploration than the two groups in the discrimination condition. Interestingly, the mean exploration time in the novel-novel exploration condition was approximately 80% higher than that of the discrimination condition (see Figure 6.4), a condition in which only half the number of novel objects were encountered. Also, when the mean amount of exploration per novel object was compared, again no difference was observed between the rats with perirhinal lesions and their surgical controls in either behavioural condition.

Further, if perirhinal lesions cause novel objects to appear familiar, the related reduction in exploration of novel objects should also be apparent in the sample phase of any test of object recognition, which is not the case (Ennaceur et al., 1996; Aggleton et al., 1997; Winters et al., 2004; Barker et al., 2007; Mumby et al., 2007; Bartko et al., 2007a, b; Albasser et al., 2009; McTighe et al., 2010; Barker et al., 2011). Romberg et al. (2012) suggested that the home-cage could act as a non-arousing low-interference environment prior to the sample phase. As such, performance on the sample phase is free from interference; however in the same study they used the home-cage as their “high-interference” environment during the retention interval. This implies that a single stimulus presentation followed by time spent in a highly familiar but non-sensory

deprived environment is sufficient to cause significant interference. The results of Experiment 2 would appear to contradict this.

In a set of experiments that sought to modify feature ambiguity, perirhinal cortex lesions did not impair rats ability to recognise novel objects under zero–delay conditions in the low feature-ambiguity conditions; such impairments were only seen when feature ambiguity between the test stimuli was intentionally high (Bartkto et al., 2007a,b). Similar results have been demonstrated in monkeys (Buckley et al, 2001). This could suggest that the objects used in the present study did not have sufficiently overlapping features and so did not induce interference. Yet, rats in the studies proposing evidence for feature ambiguity (Bartkto et al., 2007a,b), as well as the reports seemingly supporting false memories (McTighe et al., 2010; Romberg et al., 2012), following perirhinal lesions were presented with only two pairs of objects. Rats in the present study encountered 20 or 40 pairs of objects, making the absence of feature ambiguity unlikely. Particularly as it has been demonstrated that perirhinal lesions magnify impairment in visual discrimination tasks in monkeys when stimulus set size is increased (Eacott et al., 1994; Buckley & Gaffin, 1997). It should be noted that increasing object set size was not interpreted as inducing a lesion deficit *per se*; rather that an increase in the number of stimuli will increase feature ambiguity by chance overlap of stimulus features (Norman & Eacott, 2004; Bussey et al., 2005). Nevertheless, the main difference between the current study and those of McTighe et al., (2010) and Romberg et al., (2012), is the lack of a delay between sample and test phases.

There is evidence in both monkeys and rats that the imposition of a delay exacerbates recognition memory deficits caused by perirhinal cortex lesions (Eacott et al., 1994; Mumby & Pinel; 1994; Buffalo et al., 1999, 2000; Mumby et al., 2007). Some have cited this as evidence that the perirhinal cortex has only mnemonic functions and does not participate in perception (Buffalo et al., 1999, 2000). However, proponents of the dual role for the perirhinal cortex in memory and perception suggest that perirhinal lesions induce a recognition deficit in conditions that do not involve a retention delay when the task is perceptually hard (Eacott et al., 1994; Murray & Richmond, 2001; Bussey & Saksida, 2007). That is, when feature ambiguity is intentionally high (Buckley et al, 2001; Norman & Eacott, 2004; Bartko et al., 2007a). Thus, perhaps the sensitivity to interference that rats with perirhinal cortex lesions may show is more evident following a discrete intervening event, while the remaining perceptual processing is affected by this interference to a lesser degree. As discussed above, based on the number of stimuli

used in the present experiments, it seems unlikely that interference due to feature ambiguity would not have occurred at all. Nonetheless, the stimuli were not intentionally designed to have overlapping features. Also, the current rats did not have to retain attributes of a particular stimulus for more than a minute, nor was retention required beyond the test environment. Conceivably, only the perceptual properties of the loss of the perirhinal cortex were tested, and if the stimuli were not similar enough to induce immediate feature ambiguity, then it may be that they were less susceptible to misidentification. Perhaps the interference was not sufficient to cause an appreciable effect without the imposition of a delay, unless novel and familiar objects were placed in direct competition with one another. This is supported by the fact that the only behavioural impairment observed in the present study was that rats with perirhinal lesions discriminated novel from familiar objects less efficiently than their surgical controls. The suggestion of reduced interference without a delay is compatible with the finding that sensory deprivation during the retention interval restores performance (McTighe et al., 2010; Romberg et al., 2012). This interpretation would predict that rats with perirhinal lesions exposed to multiple objects during a sample phase would be significantly more impaired at detecting novelty following a delay than those exposed to only one object. An impairment would also be expected without a delay if the test objects were perceptually very similar. It should be noted, however, that recognition impairments due to perirhinal lesions have been observed after just one trial in the bow-tie maze, when interference is least (Albasser et al., 2015).

To summarise the behavioural results, rats with perirhinal lesions were impaired on novel-familiar object discriminations but exhibited normal levels of exploration for novel stimuli when they were not placed in direct competition with familiar objects. This suggests that there are mechanisms beyond the perirhinal cortex that indicate perceptual novelty at short retention intervals, but which are not as efficient or specific as that provided by the perirhinal cortex. As a consequence this information cannot guide the rat when directly choosing between a novel and a familiar object (Zhu, et al, 1995; Brown & Aggleton, 2001). If delay dependent interference does indeed occur then based on previous studies, this novelty signal would be predicted to be fast, transient and/or susceptible to this delayed interference (McTighe et al., 2010; Romberg et al., 2012); however, the results presented here suggest this novelty signal it is relatively stable and not susceptible to interference within a single session. There are potential regions beyond the perirhinal cortex in which this signal could be generated; one example is the association cortex, Te2 (Buffalo et al., 1999, 2000; Albasser et al., 2011a; Ho et al.,

2011). If novelty could be considered an intrinsic feature of a particular stimulus, as the perirhinal cortex is proposed to function in object identification (Bussey et al., 2005), then perhaps loss of the perirhinal cortex prevents attribution of the novelty signal to the correct object. This is consistent with theories relating pattern separation to the perirhinal cortex (Saksida et al., 2006, 2007; Bartko et al., 2007a).

6.4.2 Fos imaging

The initial Fos-positive cell count comparisons were made individually for the novel-familiar discrimination condition and the novel-novel exploration condition to assess the functional impact, on regional neuronal activity, of lesions to the perirhinal cortex following these behavioural tasks. No differences were found in Fos-related activity in any of the regions examined when rats were tested on a 20 trial novel object discrimination task. Similarly, in the novel-novel exploration condition, there was only one lesion difference that reached significance level (discussed below).

One potential short-coming of this study is that the two behavioural tasks were completed by two separate cohorts of rats. The behavioural experiments described here were designed very carefully to match each other as closely as possible. Testing took place in the same maze, in the same room with many of the same test objects, by the same experimenter and they were placed in the same dark room both before and after testing. Additionally, both cohorts of animals were approximately three months old and had very similar weight ranges at the time of the lesion surgeries. The only distinction was the differences in prior learning opportunities between the cohorts. The rats from Experiment 1 were pre-trained in the bow-tie maze and were tested once on a novel object discrimination task before they received surgery. The rats of Experiment 2 were experimentally naive before surgery and were pre-trained in the bow-tie maze following recovery. Both groups of rats received object based tests in the bow-tie maze prior to the ones described here, but the rats of Experiment 1 took part in a greater amount of testing with the addition of a water-maze experiment. It is difficult to predict the impact of these prior learning experiences on the Fos-related activity between these animal groups. Importantly, the rats were similar ages (11-12 months) when behavioural testing for the current experiment began and neither experimental group had undergone a bow-tie maze experiment in approximately three months before that point. Furthermore, there were no differences seen in the level of Fos expression between groups Sham Discrimination and Sham Novel in auditory or motor cortices (areas where a null result might be expected if

the behavioural tasks are well matched) and thus, comparisons were made between the regional Fos counts of these two behavioural conditions.

With respect to the foregoing c-*fos* imaging experiments presented in this thesis, the current investigation had five main objectives. These were to: 1) assess the differences in Fos related activity associated with novel-familiar object discrimination as compared with novel-novel exploration; 2) further examine the functional effects of perirhinal cortex lesions on the hippocampus; 3) validate and anatomically refine the novelty related network derived in Chapter 3; 4) test if the previously derived networks of novelty related activity are generated by the rats actively discriminating between a novel and a familiar object or simply by the presence of novel stimuli in the environment; and 5) determine the extent to which the hippocampal component of this previously derived network depends on the integrity of the perirhinal cortex. These aims will be discussed in turn.

6.4.2.1 Activity induced Fos changes between novel-novel object exploration and novel-familiar object discrimination

Overall, the numbers of Fos-positive cells in the rostral parahippocampal cortex were highly comparable between rats in the novel-familiar discrimination condition and those exploring only novel objects. A relative increase in Fos expression in the perirhinal cortex of the Sham Novel group compared to Sham Discrimination was not observed. This might have been predicted based on the fact that Sham Novel rats encountered twice as many novel objects as those in the discrimination condition (Zhu et al., 1995b, 1996; Wan et al., 1999; Aggleton & Brown, 2005; Albasser at al., 2010b). But the present results are consistent with those of Chapter 3, in which a perirhinal Fos increase was not observed when rats were presented with two familiar objects as compared to one novel and one familiar object. The only difference detected in the rostral parahippocampal cortex was the region of LEC that lies adjacent to the perirhinal cortex. A relative increase in Fos expression was seen in the rats that discriminated novel from familiar objects. Correspondingly, a more caudal region of LEC exhibited a similar result; both groups that were discriminating novel from familiar had higher Fos counts in the entorhinal cortex than those exploring only novel objects regardless of their lesion status. This result suggests a greater level of activation along the whole rostral-caudal extent of the LEC when animals were discriminating novel from familiar stimuli. Lesions to the LEC have been shown to spare novel object recognition while impairments were seen when the task demands required object information to be

associated with context or location (Wilson et al., 2013a,b). Although not absolutely required to complete the task, perhaps the greater demands of the novel-familiar object discrimination task engaged the associative properties of the LEC beyond that when the task demands were essentially null in the novel-novel exploration condition. Further, this effect of higher Fos-related activity in the LEC in rats performing recognition discriminations when compared to experiencing just novel objects was specific to cortical layers II and III (not V+VI). This effect could arise if the perirhinal cortex signals both novelty and familiarity as the familiarity responsive neurons could account for this increased activation of the lateral entorhinal cortex. This interpretation would be more consistent with the perirhinal lesion effects on behaviour and c-*fos* than the supposition that it signals only novelty (Brown & Aggleton, 2001).

In chapter 3, the switch between different modes of hippocampal engagement, based on the behavioural task, was proposed to occur in the connection between the perirhinal cortex and LEC. The increased Fos-activity observed here upon discrimination could be a reflection of that. The superficial cortical layers of the LEC are known to preferentially project to the hippocampus while the deeper layers predominantly receive hippocampal output (Steward & Scoville, 1976; Amaral, 1993; Tamamaki & Nojyo, 1995). At both analysed levels of the LEC, discrimination was associated with increases in Fos-related activity in the superficial layers compared to novel object exploration. No differences were seen in the deeper layers. This suggests active discrimination between novel and familiar stimuli leads to greater activity in the hippocampal input layers, providing evidence that discrimination occurs in the cortex prior to its involvement in altering hippocampal activity patterns even in the absence of the perirhinal cortex.

The main difference observed in the CA1 subfield of the hippocampus was an increase in Fos expression in the novel-novel object exploration condition when compared to discrimination condition at the temporal level of CA1 in both the proximal and distal regions. However, when CA1 was assessed in its entirety, (i.e., septotemporal level of the hippocampus was ignored), rats exploring novel objects had significantly higher Fos counts in the distal region of CA1 (but not the proximal region) than those discriminating novel from familiar objects. This pattern potentially reflects the preference of LEC projections to terminate in distal CA1 (Amaral, 1993; Witter, 1993). There were no Fos differences observed in CA3 or the dentate gyrus of the hippocampus in either of the behavioural conditions. As seen in CA1, novel-novel object exploration was associated with higher Fos counts in the subiculum when compared to rats in the

novel-familiar discrimination condition, except for the ventral distal subicular region in which the level of Fos-expression was comparable across the two behavioural conditions.

Taken together, these results indicate a situation in which LEC efferents to the hippocampus show increased activity when rats are discriminating novel from familiar stimuli while higher levels of activity in CA1 and the subiculum are associated with novel-novel object exploration. This further suggests that discrimination occurs in the parahippocampal cortex while enhanced hippocampal processing occurs when stimuli are novel; potentially reflecting enhanced learning about attributes associated with novel stimuli (Diana et al., 2007).

6.4.2.2 Functional effects of perirhinal cortex lesions

As outlined in the introduction, several models of medial temporal lobe function imply that the perirhinal cortex has a significant impact on hippocampal processing (Aggleton & Brown, 1999, 2006; Fernández & Tendolkar, 2006; Bussey & Saksida, 2007; Diana et al., 2007; Knierim et al., 2014). Thus, Fos-related activity in the hippocampus was analysed to assess the effects of such lesions. Despite these predictions, the present study provided surprisingly limited evidence for hippocampal dysfunction induced by loss of the perirhinal cortex. No lesion differences were seen in CA1, CA3 or the dentate gyrus of the hippocampus at any level analysed. The only lesion difference observed was a reduction in Fos-related activity in the distal region of the subiculum (ignoring the dorsal-ventral dimension) in rats with perirhinal lesions when they were exploring novel-novel objects rather than discriminating novel from familiar. This replicated the lesion difference obtained when Fos related activity was analysed separately for the two experiments. The perirhinal cortex is reciprocally connected to the subiculum, but preferentially targets the proximal rather than the distal region (Witter el al., 2000; Burwell & Agster 2008); thus it seems unlikely that this deficit is due to direct deafferentation. Additionally, it is difficult to explain why this should affect activity during novel-novel object exploration rather than novel-familiar discrimination. Besides this anomalous result, the Fos-imaging results presented here are similar to those of Chapter 5; perirhinal cortex lesions did not cause wide scale dysfunction in the medial temporal lobe. This result also echoes the results of Chapter 3 in which hippocampal lesions were seen to produce only very restricted effects on Fos expression in the parahippocampal cortex. It should be noted that it has been previously demonstrated that this Fos-imaging technique is sensitive to regional functional changes following lesions,

even in remote regions not directly connected to the lesion site (Vann et al., 2000; Jenkins et al., 2002, 2004; Albasser et al., 2007).

Lesions to the perirhinal cortex did however cause a reduction in Fos-related activity specifically in cortical layer III of the caudal region of the LEC regardless of the behavioural condition. This replicates, albeit in a more specific manner, a result seen in Chapter 5. In the novel context based experiment described in Chapter 5 a reduction in Fos expression was observed in the whole caudal region of LEC of rats with lesions to the perirhinal cortex upon exploration of a novel context. This previous lesion deficit in lateral entorhinal Fos expression was interpreted as a deafferentation due to loss of perirhinal inputs (Burwell & Amaral, 1998b); this is also likely to be the case here as the perirhinal projections preferentially terminate in layers II and III of the LEC (Burwell & Amaral, 1998a). Why cortical layer II should be spared in the present study is unclear but it is interesting to note that the connection between lateral entorhinal cortical layer III and CA1 is the proposed route for familiarity related information (Chapter 3). This type of familiarity information would not be required by the rats in the novel-novel exploration condition but could be useful to rats of the novel-familiar discrimination condition, in which a discrimination deficit was seen.

6.4.2.3 Validation and anatomical refinement of a previously derived novelty related network

Using structural equation modelling on c-*fos* data generated from animals engaged in a novel object recognition task, it was demonstrated that novel object recognition recruited the pathway from LEC (cortical layer II or III) to hippocampal field CA3 and, thence, to CA1 (Chapter 3, Albasser et al., 2010b). The first network model to be tested in the present study was intended to both validate and anatomically refine the network model described for novel object recognition memory in Chapter 3. Thus, this initial analysis involved data from group Sham Discrimination as the behavioural test they received was a replication of that given to group Sham Novel in Chapter 3 (although it should be noted that the rats in the current experiment received only a single test session, rather than 12 prior training sessions in Chapter 3). The models derived in the previous experiment highlighted a role for the connections between the LEC and the hippocampus in this type of task (although this was not a task requirement). Moreover, it is known that the hippocampal afferent projections from the LEC preferentially terminate in the region close to the border between CA1 and subiculum; namely distal CA1 and proximal subiculum (Figure 6.3; Amaral, 1993; Witter, 1993). As such, the

aim was to test if the information flow through the hippocampus followed this path, further strengthening both the anatomical resolution of the network models as well as the plausibility of this functional pathway by testing that it adheres to well-established connections.

Network models involving area Te2 (as described in Chapter 3) did not yield models of high fit for either group. Te2 is proposed to function in visual perception (Buffalo et al., 1999, 2000). Functional activity differences could be due to the differences in prior exposure to the test environment and, perhaps more importantly, to several sets of objects in the days leading up to the final test. The present group received only a single test while for rats of the previous experiment the test was preceded by several training sessions although they were only tested once on the final day.

Nevertheless, elimination of Te2 from the models created an opportunity to divide the perirhinal cortex into its constituent parts (area 35 and area 36) while still adhering to the ratio of at least two subjects for every region specified in a model (Bollen & Long, 1992). The optimal network model involved parallel projections from area 36 to the rostral region of the LEC, one direct pathway and the other indirect; via area 35. Thereafter, the route of functional activity through the hippocampus was as hypothesised; rostral LEC projected to septal CA3 which proceeded to the distal region of septal CA1 and finally onto the proximal region of the dorsal subiculum (Figure 6.9). Thus the aim to replicate and anatomically refine the novelty related model was largely accomplished.

6.4.2.4 Comparison of functional networks for novel-novel object exploration and novel-familiar object discrimination

The next aim was to test if the same network model would also fit the Fos data from a group of rats that were exposed only to novel objects rather than to one novel and one familiar object per trial; this was found to be the case (Figure 6.10). The same network model had good fit for Fos data derived from the Sham Novel group. A direct comparison between the network models of the two groups indicated a quantitative difference in the path strength between area 36 and area 35 as well as the one between distal septal CA1 and dorsal proximal subiculum. Both of these paths had a stronger effective connection in the Sham Discrimination group. Based on the role of the perirhinal cortex in object discrimination (Mumby & Pinel, 1994; Brown & Aggleton, 2001; Bartko et al., 2007a, b; Albasser et al., 2009, 2015) greater functional connectivity between its composite regions during discrimination is unsurprising. What remains

unclear is the significance of the connection between septal CA1 and dorsal proximal subiculum in this condition.

Interestingly, the path from the rostral region of LEC to septal CA3 was significant in both groups Sham Discrimination and Sham Novel (Figure 6.9). This is notable as the major distinction between network models for the novel and familiar conditions (from Chapters 3 and 4) is the inclusion of CA3 in the novelty related models. This suggests that the pattern of functional connectivity observed in Chapter 3 was due to the presence of novel objects in the environment rather than reflecting a choice between novel and familiar objects. Although, as discussed in a previous section, novel-familiar object discrimination was associated with greater Fos activity levels in the LEC than when animals did not have to make a choice between classes of objects. Taken together, this suggests that object class can define functional network structure but task demands can alter the strength or quality of the connections within the network.

6.4.2.5 Comparison of functional networks with and without the perirhinal cortex

The network model described above involved regions that could not be analysed in all four groups due to the perirhinal cortex lesions. Thus, in order to test if the perirhinal lesions altered hippocampal processing, network models consisting of regions that could be analysed in all four groups were compared. In order to avoid any inadvertent neurotoxin induced damage, the models began in a more caudal region of the LEC, while the hippocampal component remained the same. This generated a simple linear feedforward model that projected from caudal LEC to septal CA3, then on to distal septal CA1 and, finally, onto the proximal region of the dorsal subiculum (Figure 6.11). This network model had good fit for all groups except Sham Discrimination; the only index of fit that caused this model to be rejected was an elevated RMSEA, all other indices were well within acceptable range. This is probably a reflection of the fact that all three pathways in the model were highly significant, potentially creating redundancy of information in the network. When the network models for each group were directly compared they were not statistically different. This provided initial indications that the lesions did not cause significant functional differences.

To investigate this further, Fos data were collapsed across the behavioural conditions so the data from all the rats with perirhinal lesions was directly compared with the data from all of their surgical controls using a stacking procedure. This analysis did not reveal any lesion differences. Additional pairwise comparisons between the lesion and sham groups within each condition (i.e. Peri Discrimination vs. Sham Discrimination

and Peri Novel vs. Sham Novel) also revealed no lesion differences. Together, this all suggests that loss of the perirhinal cortex does not significantly impact on hippocampal function. This is surprising as object related information ostensibly reaches the hippocampus from the perirhinal cortex (Aggleton & Brown, 1999, 2006; Fernández & Tendolkar, 2006; Bussey & Saksida, 2007; Diana et al., 2007). However, perhaps the persistent novelty signal that is evident from the behavioural data can also activate the hippocampus at short retention intervals upon removal of the perirhinal cortex. Additionally, the hippocampus is not required to perform object discrimination tasks (Aggleton et al., 1986; Winters et al., 2004; Forwood et al., 2005; O'Brien et al., 2006; Chapter 3), whereas, object-in-place tasks are known to be dependent on both the perirhinal cortex and the hippocampus (Aggleton et al., 1986; Brown & Aggleton, 2001; Warburton & Brown, 2010; Barker & Warburton, 2011b) and so loss of the perirhinal cortex may induce differences in hippocampal activity under those conditions.

In combination with Chapter 3, this study provides evidence of a double dissociation: perirhinal cortex lesions do not cause impairment in hippocampal processing and hippocampal lesions do not cause dysfunction in perirhinal activity when rats are engaged in a novel object discrimination task.

6.4.2.6 An aside

Additional evidence that the presence of novel stimuli, rather than novel-familiar discrimination, governs the structure of the processing network comes from the network models that do not involve the perirhinal cortex. Pairwise comparisons between the groups duplicated the only condition difference described above; there was a stronger effective connection between septal CA1 and dorsal proximal subiculum in the Sham Discrimination group than in the other groups. As a further means of comparison with the results of Chapter 3, the models for each group were tested with Fos counts from cortical layers II or III of the caudal LEC in place of the counts from the whole region, while all other aspects of the network were kept constant. It was found that either of these cortical layers fit in place of the whole region in all four groups – as was observed for the group performing a novel object discrimination task in Figure 3.12F. Indeed, although group Sham Discrimination had an elevated RMSEA when the whole region Fos count was included in the network model, all indices of fit were well within acceptable limits when these superficial cortical layers replaced whole caudal LEC. Overall, these results provide further evidence that the pattern of hippocampal

engagement seen previously is due to the presence of novel objects in the rats' environment, rather than discriminating novel from familiar objects.

6.4.2.7 Prelimbic cortex models

Lesion studies have demonstrated that although the rodent medial prefrontal cortex is not required for object discrimination, tested by delayed-nonmatching to sample or spontaneous novel object exploration paradigms, it is necessary for object associative learning (Poucet, 1989; Shaw & Aggleton, 1993; Ennaceur at al., 1996; Mitchell & Laiacona, 1998; Cross et al., 2013). Not only is it a requirement for object-in-place learning and temporal order recognition memory, crossed hemisphere lesion studies have shown that these tasks specifically require an intact connection between the perirhinal cortex and medial prefrontal cortex (Hannesson et al., 2004b; Barker et al., 2007). Additionally, it is known to have a role in cognitive control tasks; including attentional processing, strategy shifting and reversal learning tasks as well as working memory tasks (Birrell & Brown, 2000; Heidbreder & Groenewegen, 2003; Vertes, 2006). Due to the different task demands of the two behavioural conditions in the present study, differential involvement of the medial prefrontal cortex was a possibility.

Based on crossed-lesion/disconnection studies (Hannesson et al., 2004b; Barker et al., 2007), the connections between medial prefrontal and perirhinal cortices are of particular interest. The prelimbic cortex, a sub-region of the medial prefrontal cortex, has been shown to project directly to the deep cortical layers of the perirhinal cortex and LEC, and so this region was analysed for activity related Fos expression (Vertes, 2004; Jones & Witter, 2007). Also, prelimbic cortex is connected to the temporal region of CA1 (rather than septal hippocampus, used in the preceding models) via nucleus reuniens of the thalamus (Vertes et al, 2007; Prasad & Chudasama, 2013).

Dissociable optimal network models were derived for the two Sham groups; both networks involved a path from prelimbic cortex to nucleus reuniens of the thalamus with a further projection onto the distal region of temporal CA1. The caudal region of LEC also projected to the distal temporal CA1. An interesting condition difference was found in the pathways between prelimbic cortex and areas of the rhinal cortex; when rats were discriminating novel from familiar objects the optimal network model contained a path from prelimbic cortex to area 36 of the perirhinal cortex. Whereas, when rats were exploring novel objects, the prelimbic cortex was functionally connected to area 35 of the perirhinal cortex and caudal LEC.

Additional evidence for a condition difference came from the models derived for all four groups. These models could not include regions of the rostral parahippocampal cortex but involved two parallel pathways from the prelimbic cortex to the distal region of temporal CA1; the first via nucleus reuniens of the thalamus and the other by way of the caudal region of the LEC (Figure 6.13). This network model had good fit when the rats were only exploring novel objects but poor fit when the rats were discriminating novel from familiar objects. This further highlights the apparent difference in the way in which the prelimbic cortex interacts with the rhinal cortex in the two behavioural conditions. In the novel-novel exploration condition, the presence of the perirhinal cortex was not necessary to generate models of good fit involving prelimbic cortex. In contrast, well-fitting models involving prelimbic cortex could not be found in the Sham Discrimination groups without the presence of perirhinal cortex and, as such, no plausible models of good fit could be derived involving the prelimbic cortex in the Peri Discrimination group at all. This suggests a functional dissociation; prelimbic cortex is functionally connected to area 36 of the perirhinal cortex when the task involves a choice between different classes of objects, i.e., in the discrimination condition. Further to this, the connection between prelimbic cortex and area 36 was significantly different between the two groups with a stronger correlation in the novel-familiar discrimination group. This result seems counterintuitive as the crossed-lesion studies demonstrated that the connection between prelimbic and perirhinal cortices is not required for novel object recognition (Hannesson et al., 2004b; Barker et al., 2007). However, the current discrimination task is based on spontaneous exploration, the rats would presumably be spontaneously acquiring associative information (Dix & Aggleton, 1999). Also, the discrimination condition arguably requires greater cognitive control than simple exploration of novel objects.

6.4.3 Summary

These experiments have demonstrated that rats with perirhinal lesions do not display false memories with the short retention delays employed here. Additionally, they are not more susceptible to interference effects created by a relatively large number of test stimuli, at least when presented in a single session. Further, perirhinal cortex lesions cause only minor dysfunctions to hippocampal c-*fos* activity related to the processing of novel objects. Finally, stimulus novelty is sufficient to initiate previously observed interactions between the LEC, CA3, CA1 and the subiculum (with or without the presence of the perirhinal cortex) but task demands alter the strength of specific connections within the network, as well as the involvement of the prelimbic cortex.

7 General Discussion

7.1 Overview

Various models have been proposed to account for the way in which regions of the medial temporal lobe interact to support recognition memory (Squire & Zola-Morgan, 1991; Brown & Aggleton, 2001; Fernández & Tendolkar, 2006; Diana et al., 2007). An overarching aim of the experiments presented in this thesis was to test the functional interdependence of regions within the medial temporal lobe (specifically the perirhinal cortex and hippocampus) for supporting recognition memory. A previous experiment indicated that behavioural tasks involving either, novel and familiar, or, just familiar objects generated different modes of hippocampal-parahippocampal interactions (Albasser et al., 2010b). Following on from this, further aims of the present work were to confirm and anatomically refine these network models of regional activity and, subsequently, assess if they are disrupted by lesions to the perirhinal cortex or hippocampus.

The main findings both confirm and extend this previous work by demonstrating that the network structure of hippocampal-parahippocampal interactions is defined by the class of the stimulus, i.e., whether it is novel or familiar. Further, the strength of the specific connections within these networks, as well as additional regional involvement are modified by task demands. Surprisingly, these object processing networks, defined by object class, are on the whole robust to removal of either the perirhinal cortex or hippocampus. In this final chapter, the recurrent patterns of results observed in several of the experiments presented in this thesis will be considered and some of their implications discussed.

7.2 A network for novel objects with a nested network for familiar objects

The network analyses carried out in all of the experiments presented in this thesis on intact rats converge on the idea that the novelty or familiarity of a stimulus alters network dynamics and defines patterns of parahippocampal-hippocampal interactions. Novel objects generated an integrated pattern of Fos-related activity from the perirhinal cortex to the lateral entorhinal cortex, which subsequently recruited CA3 (the perforant pathway), and then CA1 (Chapters 3 & 6). In contrast, familiar objects were associated

with the more direct route from the lateral entorhinal cortex to CA1 (the temporoammonic pathway; Chapters 3 & 4). This notion is supported by previous IEG imaging studies that modulated the novelty or familiarly of stimulus sets (Poirier et al., 2008; Albasser et al., 2010b). The functional and anatomical evidence for each of the steps in these networks will be discussed here.

The differential patterns of hippocampal subfield recruitment for novel compared to familiar objects imply a functional switch that occurs in the parahippocampal region. In Chapter 3, a network difference was observed specifically in the connection between area 35 of the perirhinal cortex and the lateral entorhinal cortex based on the novelty or familiarity of the presented objects. This indicates that information from the perirhinal cortex can influence subsequent network activity, specifically in the lateral entorhinal cortex.

The next processing step in the models is from the lateral entorhinal cortex to the hippocampus. Of particular relevance is the fact that entorhinal cortex layer III projects to CA1, while layer II projects to the dentate gyrus and CA3 (Steward & Scoville, 1976; Insausti et al., 1997). Based on this anatomical information, it was predicted that perirhinal novelty signals, relating to objects, would bias processing towards entorhinal layer II and, so layer II activity would be associated with the novel object network models. It was further expected that familiarity signals would produce a bias towards entorhinal layer III and so layer III activity should be associated with the familiar object model. This laminar analysis revealed further evidence for the role of the temporoammonic pathway in familiarity processing. Lateral entorhinal cortical layer III generated a model of good fit for familiar object processing, while layers II and V+VI (combined) generated poorly fitting models (Chapter 3). The result that both cortical layers II or III consistently produced models of good fit for novel object processing was a more unanticipated finding (Chapters 3 & 6). This result may indicate that rather than object class inducing a dichotomy between these routes into the hippocampus, the situation is one in which information relating to novel stimuli accesses the hippocampus via both the perforant and temporoammonic pathways. This notion echoes a mechanism recently demonstrated in an electrophysiological study in rats. It was found that simultaneous activation of CA1 pyramidal neurons by inputs originating in both CA3 and cortical layer III of the entorhinal cortex was necessary and sufficient to induce the formation of new place fields and contextual feature selectivity (Bittner et al., 2015).

Based on the importance of entorhinal cortical layers II and III in the present models for novel and familiar object processing, it is worth noting that inputs from across the depth of perirhinal cortex converge on these superficial entorhinal layers (Burwell & Amaral, 1998a,b). This fact, along with the object class differences observed in the pathway between area 35 and lateral entorhinal cortex, described above, provide a means by which novelty/familiarity detection in the perirhinal cortex can have a downstream impact on hippocampal processing (via the superficial layers of the lateral entorhinal cortex). This notion is central to the gatekeeper hypothesis of perirhinal function (Fernandez & Tendulkar, 2006). The assumption here is that parahippocampal and hippocampal regions work together but in sequentially different ways. The perirhinal cortex is proposed to process stimulus identity and, thereby, novelty and familiarity (Brown & Aggleton, 2001; Cowell et al., 2010). Hippocampal contributions are thought to more closely reflect additional information and, thereby, additional learning such as the context, location, relationship to other stimuli in the environment, or temporal information associated with the target object. Evidence to support this notion comes from crossed-lesion studies, which demonstrate that the perirhinal cortex and the hippocampus must be part of an intact functional circuit to ensure that associated information, such as its location, is automatically acquired for a given object, i.e., 'object-in-place' information (Barker et al., 2007; Warburton & Brown, 2010; Barker & Warburton, 2011). The present results extend the gatekeeper model by indicating that novel stimuli are more likely to engage CA3 processing. This engagement could lead to the aforementioned enhanced learning.

In addition to anatomically refining the novelty and familiarity related networks with respect to the inputs from the entorhinal cortex into the hippocampus, a further aim of the experiment presented in Chapter 6 was to improve resolution along the proximal-distal axis of the hippocampus. The lateral entorhinal cortex has a stronger projection to distal CA1 and proximal subiculum, while the medial entorhinal cortex preferentially projects to proximal CA1 and distal subiculum (Amaral, 1993; Witter, 1993). The network models derived for novel object processing in Chapter 6, revealed that those with best fit corresponded to the expected proximal-distal connectivity patterns within CA1 and subiculum. Thus, the results support the idea of a bias towards object-based processing in distal CA1 and proximal subiculum, which potentially contrasts with more spatial-based processing in proximal CA1 and distal subiculum (Aggleton 2012; Ranganath & Ritchey, 2012; Knierim et al., 2014). Recent studies have demonstrated that CA3 also displays functional heterogeneity along its proximal-distal axis (Lee et al.,

2015; Lu et al., 2015); consequently, further work is required to integrate this dimension into the proposed network models.

Other pathways that may also be involved in the mechanism of differentially engaging hippocampal subfields include the direct hippocampal projections from the perirhinal cortex, which preferentially target CA1 and to a lesser extent, the subiculum (Furtak et al., 2007). There are also hippocampal projections that can feedback to parahippocampal regions and these could further bias network activity (Aggleton, 2012). Such dynamic interactions between the perirhinal cortex and the hippocampus have been highlighted in human fMRI and EEG studies, which point to partial divisions of function across these same structures that relate to the recognition and recollection of associated information (Staresina & Davachi, 2008; Staresina et al., 2012; Staresina et al., 2013). These mechanisms, along with that proposed above have the potential to function in an interactive and dynamic manner, defined by the task demands, in order to support a range of cognitive tasks.

It should also be noted that, while there are regions that did not fit into the network models, the absolute level of Fos related activity often did not change between the behavioural groups. This is interpreted here as indicating that they are not involved in the functional network in question, as their activity is not predicted by, nor can it be used to predict, the activity of subsequent regions in the model.

7.2.1 Support for differential processing of novel and familiar stimuli

The prediction of additional hippocampal subfield recruitment induced by stimulus novelty is supported by selective lesion studies of the dentate gyrus and CA3 (Gilbert et al., 2001; Lee et al., 2005; Hunsaker et al., 2007, 2008; Langston et al., 2010) as well as c-*fos* activation studies that demonstrate the activation and engagement of these particular subfields by novel spatial configurations (Jenkins et al., 2004; Poirier et al, 2008). Of particular relevance is the finding that lesions to CA3, but not dentate gyrus or CA1, disrupted learning of object-place and odour-place paired associate tasks (Gilbert & Kesner, 2003), in addition to the fact that CA3 inactivation disrupts visual novelty detection (Hunsaker et al., 2007). In contrast, both lesion studies (Gilbert et al., 2001; Hoge & Kesner, 2007; Kesner et al., 2010) and c-*fos* expression studies (Amin et al., 2006) have highlighted the importance of CA1 for processing the temporal properties of a stimulus, a function that is likely to be especially pertinent for distinguishing familiar stimuli. Indeed, CA1 lesions impaired object recency discriminations that were spared

by CA3 lesions (Hoge & Kesner, 2007). These dissociations match the pattern of data derived from structural equation modelling of the present Fos-related activation.

Further compelling evidence comes from a study that temporarily inactivated the projections from CA3 to CA1, but left the entorhinal cortex layer III to CA1 projection intact in a transgenic mouse model. This manipulation disrupted learning about novel contexts but not familiar ones in a contextual fear conditioning paradigm (Nakashiba et al., 2008). This provides evidence that learning about novel stimuli requires intact projections from CA3 to CA1. The same study also reported that inactivating CA3 led to increased firing rates in CA1, but only in a novel context. The authors suggested that CA3 may also function to maintain appropriate levels of network activity while the animal is experiencing novelty (Nakashiba et al., 2008). In a complementary study, the projections from entorhinal cortex layer III to CA1 were reversibly disrupted in another transgenic mouse model and found to disrupt temporal association memory (Suh et al., 2011).

The significance of a mechanism in which novel stimuli generate greater hippocampal engagement is suggested by reference to learning theory. An influential assumption is that novel stimuli, which have uncertain consequences, attract more attention and enhanced rates of learning about their associated properties than familiar stimuli (Pearce & Hall, 1980; Wagner, 1981). A recent human fMRI study demonstrated that while hippocampal activity was associated with the temporal properties of objects learned in a sequence, perirhinal cortex activity was associated with the objects themselves (Hsieh et al, 2014). Further, electrophysiological recordings in the rodent hippocampus found that hippocampal neurons did not specifically encode a stimulus but they were able to monitor the development of stimulus associations, including stimulus context, location, and related reward value during the course of a learning session (Komorowski et al., 2009; McKenzie et al., 2014).

An alternative, or perhaps complementary, notion is that reduced integration of hippocampal subfield activity on encountering a familiar stimulus could allow the network to remain in a state of readiness to engage with and process a novel event. Similar arguments have been made to explain the repetition suppression effect seen in neurons of the inferotemporal cortex in response to familiar visual stimuli (Meyer et al., 2014). This approach could allow an animal to rapidly detect novel variations in the environment, an efficient mechanism such as this could be particularly important when these changes are subtle or occur quickly.

The importance of novelty in relation to learning is further reinforced by the subjective experience that incidental, insignificant details will subsequently be remembered if they occur in close temporal proximity to a surprising event. This neuropsychological process of novelty enhanced memory has been proceduralized in rats. A target location in a delayed matching-to-place task is remembered for significantly longer if, 30 minutes after the sample session, the rat is placed in a novel context for five minutes (Wang et al., 2010). The plausibility of the underlying neural mechanisms were corroborated by electrophysiological recordings in slice preparations; weak, followed by strong electrical stimulation in slice recordings generated longer lasting long term potentiation (Wang et al., 2010). This procedure has been extended to show that other forms of novelty also induce memory persistence of unrelated events (Salvetti et al., 2014).

It should be noted that the suggestion here is not that the hippocampus is required for all types of recognition memory, particularly familiarity–based memory. However, whether to recollect or to simply be familiar with a particular stimulus is not a conscious choice, and although the evidence suggests that these processes are dissociable, under normal circumstances these two processes could occur simultaneously. The models proposed here provide a framework within which this can occur, while keeping the redundancy of information low. Of potential relevance is a study in which hippocampal lesions led rats to forget objects they had been familiar with prior to surgery, but were unimpaired in learning about new objects (Gaskin et al., 2003). This could indicate that under normal circumstances, the hippocampus and adjacent cortex cooperate to support recognition memory but the perirhinal cortex can do this in isolation if necessary based on the more simple familiarity–based mechanism.

7.2.2 Inclusion of the dentate gyrus in models

Although the dentate gyrus was a component of the previously identified network model derived for novel object processing (depicted in Figure 1.10; Albasser et al., 2010b) it could not be included in any well-fitting network models related to novel object processing in the current work (Chapters 3 & 6). That is not to say the proposal here is that the dentate gyrus does not participate in the processing of attributes relating to novel objects. Indeed, of the five groups of rats with an intact hippocampus, that were engaged in exploring novel objects (Group Sham Novel from Chapter 3; Groups Peri Discrimination, Sham Discrimination, Peri Novel and Sham novel from Chapter 6), three of these groups had significant inter-regional correlations between the dentate gyrus and CA3 (Tables 3.4, 6.3). These strong correlations create mathematical

redundancy of information in the models, which can increase the RMSEA fit index leading to a model to be eliminated (Tabachnick & Fidell, 2001). In fact, the three groups in which this correlation was significant were Group Sham Novel ($r= 0.79$; $p=0.007$) from Chapter 3 and groups Peri Discrimination ($r= 0.71$; $p=0.009$) and Sham Discrimination ($r=0.87$; $p<0.001$) from Chapter 6. All three of these groups were engaged in discriminating novel from familiar objects. Thus, the connection between these regions may be of particular importance when objects of different classes are placed in competition.

Indeed the dentate gyrus and its role in pattern separation during encoding (Gilbert et al., 2001; Leutgeb et al., 2007; Clelland et al., 2009; Schimdt et al., 2012; Hunsaker & Kesner, 2013) could be readily integrated into the model of medial temporal lobe interactions postulated here. Pattern separation is a computational process by which inputs into a system are distributed onto a sparse network, allowing for the creation of divergent patterns of activity, even if the inputs are similar. Pattern separation in the dentate gyrus is thought to be achieved by perforant path inputs from entorhinal layer II being distributed throughout the dentate gyrus, generating random, distinctive representations that markedly reduce the likelihood of similar representations for different events (Leutgeb et al., 2007; Hunsaker & Kesner, 2013). This process is likely to be particularly important when processing novel stimuli in order to disambiguate similar features and determine their unique attributes for associative learning. This further emphasises the role of the perforant pathway when processing stimulus novelty.

A recent electrophysiological recording study demonstrated that the activity of both the dentate gyrus and CA3 tracked changes in the local environment (Neunuebel & Knierim 2014). Dentate activity patterns were markedly altered by relatively small changes in environmental cues that could not be predicted specifically by activity changes in the entorhinal input, thereby, generating distinct neuronal representations; putative pattern separation processing (Hunsaker & Kesner, 2013; Neunuebel et al., 2013; Neunuebel & Knierim 2014). Additionally, CA3 was shown to be involved in pattern completion processing (Neunuebel & Knierim 2014). Pattern completion involves integrating sparse cues to reactivate known representations (Hunsaker & Kesner, 2013) and so it would seem that pattern completion should be more closely linked with familiar stimuli. However, even more recent work has indicated that CA3 displays functional heterogeneity along its proximal-distal axis; the proximal region is suggested to be involved in pattern separation, while the distal region and CA2 are involved in pattern

completion (Lee et al., 2015; Lu et al., 2015). Based on this, perhaps proximal CA3 activity drove the involvement of CA3 in the current models of novel object processing. Additional work will be required to answer this question.

7.3 Testing interdependence of the hippocampus and perirhinal cortex

One of the main aims of the work presented in this thesis was to test the functional interdependence of the hippocampus and perirhinal cortex at multiple levels; behaviourally, as well as at the level of regional activation and systems interactions. In this section these will be discussed in turn.

7.3.1 Behavioural evidence for interdependence

The findings of Chapter 3 corroborate the many previous studies that have found no effect of hippocampal lesions on object recognition memory (Aggleton et al., 1986; Murray & Mishkin, 1998; Glenn & Mumby, 1996; Forwood et al., 2005; Albasser et al., 2012). This result, based on rats in the novel condition (groups HPC Novel and Sham Novel), provides further support for dual-process accounts of recognition memory (Brown & Aggleton, 2001; Yonelinas, 2002). More surprising was the absence of a lesion effect in the familiar condition, as the hippocampus has been shown to support temporal associations (Fortin et al., 2002; Hoge & Kesner, 2007; Barker & Warburton, 2011; DeVito & Eichenbaum, 2011; Albasser et al., 2012). In a previous study of the same design, intact rats in the familiar condition either could not perform this discrimination (Albasser et al., 2010b), although, more in line with the results of Chapter 3 is another study in which rats in the familiar condition discriminated above chance levels but remained significantly inferior to the novel group (Albasser et al., 2013b). Nonetheless, this lack of a behavioural deficit was unexpected for rats with hippocampal lesions (group HPC Familiar).

The main difference between the animals of the present study and those of the previous ones is that in the present study they were around a year old when carrying out the task, whereas in the previous studies they were approximately three to four months old (Albasser et al., 2010b, Albasser et al., 2013b). Thus, an alternative explanation is that as the current rats were older, they found it more difficult to remember the objects that were seen in previous sessions. Memory deficits have been found in aged rodents, particularly in acquiring new information and remembering items following a long retention delay (Dunnett et al., 1988; Aggleton et al., 1989; Wyss et al., 2000). It is

possible that the hippocampal lesion rats were not in fact highly familiar with the set of objects as they were intended to be; although as indexed by the difference in the D1 scores and by structural equation modelling of the regional c-*fos* data the objects were not treated as completely novel. This result may indicate that the parahippocampal cortex can solve simple recency problems under certain circumstances, a view supported by the significant correlations between perirhinal Fos counts and recency performance in group HPC Familiar (Chapter 3), and by the ability of perirhinal units to signal recency differences (Zhu et al., 1995a; Xiang & Brown, 1998). This unanticipated result notwithstanding, the behavioural data from the experiment in Chapter 3 demonstrate that the hippocampus is not required for object recognition memory.

The behavioural results presented in Chapter 6 suggest that, although rats with perirhinal cortex lesions struggle to discriminate the identity of a novel object when it is placed in competition with a familiar object (Group Peri Discrimination), they can still detect the presence of novelty as indexed by exploration times that were not different from their surgical controls (Groups Peri Discrimination and Peri Novel). This evidence is consistent with that of other recent studies (Albasser et al., 2015; Olarte-Sanchez et al., 2015). Implicit within this proposal is the idea that other brain sites detect novelty in the absence of perirhinal cortex, even if that novelty information cannot be used to guide recognition discriminations. These behavioural results do not preclude the possibility that this could be accomplished by the hippocampus but this will be discussed further in a later section. More relevant to the issue of structural independence is if the behavioural results of Chapter 6 are taken together with those of Chapter 3, they create a behavioural dissociation in which the perirhinal cortex is a requirement for successful and efficient object recognition memory while the hippocampus is not (Chapters 3 & 6).

7.3.2 Regional activation evidence for interdependence

Limited Fos-related activity differences were observed due to the lesion status of the rats in the lesions studies described here (Chapters 3, 5 & 6). In Chapter 3, the effects of hippocampal lesions were restricted to area Te2, with an additional effect in the mid rostral-caudal level of the perirhinal cortex that was dependent on the behavioural condition. In both regions the lesions induced a reduction in Fos-related activity. The effect on the perirhinal cortex was presumably due to the loss of CA1 efferents and was restricted to the rats performing recency discriminations. This result echoes findings of disconnection studies in which functional perirhinal-hippocampal interactions are required to support associative learning about objects (Warburton & Brown, 2010; Jo &

Lee, 2010; Barker & Warburton, 2011). This conclusion is potentially undermined by the fact that the hippocampal lesions did not have behavioural consequences (Chapter 3) but may simply provide further evidence that the caudal region of the perirhinal cortex is more important for these kind of object based discriminations (Zhu et al., 1995; Wan et al., 1999, 2004; Warburton et al., 2003, 2005; Albasser et al., 2009, 2010b). The result suggests that under normal circumstances, during temporal discriminations, CA1 sends a signal to mid-perirhinal cortex. The signal could be related to additional learning about the associative properties of the familiar object. Indeed, recent single unit recording studies have demonstrated that over time the perirhinal cortex can encode stimulus-outcome associations for highly familiar objects (Ahn & Lee, 2015; Eradath et al., 2015). Nevertheless, this information is evidently not a requirement for the type of discriminations tested here (Chapter 3), providing further evidence for the ability of the perirhinal cortex, particularly the caudal region, to function in a manner that is not dependent on the hippocampus.

Although the context-based behavioural task utilised in Chapter 5 did not provide an actual measure of learning, the hippocampus is known to be critical when learning about contexts (Philips & LeDoux, 1992; Honey & Good, 1993; Good & Bannerman, 1997; Mumby et al., 2002; Lee & Kesner, 2004). One of the main aims of this study was to examine the functional effects of perirhinal lesions on hippocampal activity during a hippocampal dependent task. There was no evidence of any lesion induced Fos-related activity deficits in the hippocampal formation; this provides yet more evidence for independence (Chapter 5).

In the novel object based tasks described in Chapter 6, perirhinal cortex lesions did not affect the patterns of c-*fos* activity observed in the hippocampus proper. There was, however, a restricted effect observed in the distal region of the subiculum that was only evident when the rats were exploring novel objects rather than discriminating novel from familiar objects. The subiculum does receive direct inputs from the perirhinal cortex, however, this is a quite a minor connection and it preferentially terminates in the proximal region of the subiculum (Burwell & Amaral, 1998b; Furtak et al., 2007). The more typical finding was that hippocampal interactions, as measured by Fos, are insensitive to the loss of perirhinal cortex. This apparent independence complements the object recognition experiment in Chapter 3 which showed that hippocampal lesions spare parahippocampal c-*fos* interactions, creating a double dissociation.

At first glance, these results could be taken to indicate that the Fos-imaging procedure is not sensitive to lesion effects; however, this is not the case. Lesion induced deficits in regional Fos counts haven been reported, even in regions that are not directly connected to the lesion site (Vann et al., 2000; Jenkins et al., 2002, 2004). Of particular relevance is a study that demonstrated in several separate cohorts of rats, each engaged in different behavioural paradigms, that hippocampal lesions reduce Fos expression in other brain regions such as the retrosplenial cortex (Albasser et al., 2007). Thus, it is all the more striking that lesions to either the hippocampus or perirhinal cortex did not affect one another more generally (Chapters 3, 5 & 6).

7.3.3 Network dynamics following removal of the hippocampus or perirhinal cortex

If these two regions were indeed permanently part of the same functional system, then a network level analysis should be the most sensitive to dysfunction induced by loss of one of the network components. Again, the most striking result in all of the lesions studies presented here is the lack of network differences induced by lesions to the perirhinal cortex or hippocampus.

The parahippocampal network that ostensibly supported both object recognition and object recency memory in Chapter 3 was not altered following removal of the hippocampus. This was evident in the overall network structure, in that the best fitting parahippocampal model was the same for all four groups of rats. Moreover, this consistency in the network was robust to direct testing. Stacking the Fos data from the rats with hippocampal lesions and their surgical controls on the same network model revealed that there no overall differences between these networks that were induced by hippocampal loss (Chapter 3). A complementary result was obtained in Chapter 6. Removal of the perirhinal cortex did not cause alterations in the network structure of lateral entorhinal - hippocampal interactions induced by either discriminating novel objects from familiar ones or exploration of novel objects. Further, direct comparison by stacking the group data on the same model revealed there were no differences (Chapter 6). This indicates that lesions to the perirhinal cortex did not cause dysfunction in hippocampal processing related to novel objects. Together, these studies create a double dissociation; hippocampal lesions spare parahippocampal c-*fos* interactions while perirhinal lesions spare hippocampal c-*fos* interactions when rats are engaged in novel object based tasks (Chapters 3 & 6). This network dissociation complements evidence of double dissociations between perirhinal and hippocampal function despite their

interconnections, in both amnesic patients and behavioural effects on rodents with lesions (Graham & Hodges, 1997; Winters et al., 2004; Aggleton et al., 2010; Bowles et al., 2007, 2010).

Unlike the object based experiments, network modelling revealed that lesions to the perirhinal cortex caused alterations in the network models related to novel context exploration. However, this difference was identified between the medial entorhinal cortex and CA1 at intermediate and temporal levels. Intrinsic hippocampal interactions were unaffected by the perirhinal lesions. More work is required to distinguish if the perirhinal cortex is directly implicated in these kinds of contextual tasks by deafferentation of the medial entorhinal cortex or if the effect is indirect due to loss of the inputs to the medial entorhinal cortex by deafferentation of regions more heavily connected to the perirhinal cortex such as the lateral entorhinal and postrhinal cortices (Burwell & Amaral, 1998b; Burwell, 2000).

In isolation, based on the paucity of lesion differences, it could be suggested that structural equation modelling is not sensitive to alterations in network dynamics. However, another prominent pattern of results that emerged from the present experiments was that network alterations were observed based on modified behavioural task demands (discussed above). It seems probable that removing a vital component of a functional network would manifest in greater alterations to that network than the changes initiated by variations in the psychological processes underlying network activity. Thus, based on the fact that SEM is sensitive to alterations in task demands, further credibility is conferred upon the technique. Together, these results suggest that the hippocampus and perirhinal cortex are not functionally dependent on one another, particularly in relation to object processing.

Based on the nature of the network models proposed for novel and familiar object processing, it might be expected that hippocampal activity may be sensitive to removal of the perirhinal cortex if a behavioural paradigm were used that is known to more directly involve the hippocampus, for example, an object-in-place task. Indeed, this is a direct prediction of the work presented here. As mentioned in Chapter 1, object-in-place task variants of the bow-tie maze have been carried out (Nelson & Vann, 2014) however, this paradigm is more akin to open-field testing as it is based on single rather than multiple trials. As outlined in Chapter 1, c-*fos* imaging is more suitable for use in conjunction with multiple-trial behavioural tests in which the animal does not have to be handled by the experimenter between trials, in order to ensure a robust Fos signal that is

above baseline levels and also to reduce the impact of individual stimuli (Albasser et al., 2010b, 2013b). Future work will need to establish an appropriate behavioural method in order to test this prediction.

Overall, the evidence presented here provides further support for the idea of functional heterogeneity among regions of the medial temporal lobe as well as for the existence of multiple systems that can function independently to support distinct memory processes. The debate regarding the consequences of hippocampal lesions on rodent object recognition memory is longstanding (Squire & Zola-Morgan, 1991; Brown & Aggleton, 2001; Yonelinas, 2002). Hippocampal lesions have been shown to cause impairments in some studies (Clark et al., 2000; Broadbent et al., 2004, 2010; Cohen et al., 2013) with an absence of deficits reported in others (Aggleton et al., 1986; Glenn & Mumby, 1996; Forwood et al., 2005; Albasser et al., 2012). The model of parahippocampal-hippocampal interactions presented above may provide a potential explanation for these inconsistencies. The models suggest that, although the hippocampus is not required to solve simple recognition memory tasks, it is activated incidentally, particularly during the encoding of novel stimuli. For some spontaneous tests of object recognition, associated item information that depends on the hippocampus, for example, context, location in time or place, may (unbeknownst to the experimenter) contribute to the normal pattern of object discrimination and so may affect exploration levels in intact animals. Consequently, hippocampal lesions may, in some cases, alter levels of exploration without disrupting the underlying ability to initially detect the novelty or familiarity of the test stimuli. In normal intact animals, exploration of novel objects may prove to be prolonged by the engagement of hippocampal subfields that help to determine whether any prior learning about the stimulus has occurred and to ensure the effective learning of new associated information (Zeamer et al., 2011). The loss of this initial exploration could be interpreted as a recognition memory deficit, despite the animal being able to discriminate novel from familiar stimuli.

7.3.4 Implications of lack of perirhinal lesion effects on novelty detection

The earlier IEG findings predicted that perirhinal signals of novelty bias network activity towards the indirect dentate/CA3 pathway (Albasser et al., 2010b; Chapter 3). To test this prediction, the study in Chapter 6 focussed on the impact of perirhinal lesions on responses to novel stimuli, using two different behavioural conditions. The failure to find evidence of a switch to the direct CA1 pathway along with the behavioural evidence that rats with perirhinal lesions can detect novelty in the

environment but not identify the source, implies that extra-perirhinal sites can signal the novelty of objects.

Further evidence for such extra-perirhinal signals comes from behavioural studies in which rats with perirhinal lesions demonstrate sample phase exploration equivalent to their surgical controls (Ennaceur et al., 1996; Aggleton et al., 1997; Winters et al., 2004; Barker et al., 2007; Bartko et al., 2007a, b; McTighe et al., 2010; Barker et al., 2011; Olarte-Sanchez et al., 2015). Additionally, rats with perirhinal lesions repeatedly exposed to either pairs of novel or pairs of familiar objects exhibit exploration levels equivalent to their surgical controls, including the expected decline in exploration of the familiar objects, while also displaying a simultaneous recognition deficit (Mumby et al., 2007; Albasser et al., 2009, 2011a). Results demonstrating intact habituation to multimodal stimuli in rats with perirhinal lesions converge on the same notion (Robinson et al., 2009; Jones et al., 2012). An alternative candidate region for processing familiarity information is the temporal association area, TE/Te2 as this region has been shown to respond to stimulus novelty in both the monkey and the rat (Brown et al., 1987; Buffalo et al., 1999, 2000; Naya et al., 2003; Ho et al., 2011; Meyer et al., 2014). Although it should be pointed out that in many of the rats that received lesions to the perirhinal cortex, small amounts of damage encroached on area Te2, potentially weakening this hypothesis.

As mentioned above, the behavioural results of Chapter 6 do not exclude the possibility that the extra perirhinal novelty detection mechanisms could be generated within the hippocampus. However, the absence of differences in the hippocampal component of the network models between groups of animals with and without perirhinal cortex would argue against the hippocampus generating this signal itself. Consequently, the question remains as to how this signal reaches the hippocampus.

Dopamine signalling from the ventral tegmental area, has been linked to novelty dependent changes in hippocampal activity (Lisman & Grace, 2005). A recent human fMRI study demonstrated that the ability to remember new information is enhanced when a person is curious about the topic (Gruber et al., 2014). This improved memory effect was associated with increased activity in both the ventral tegmental area-substantia nigra complex and the hippocampus, as well as by increased functional connectivity between these regions. Brain activity in these regions, specifically during the anticipation period before an answer was given to a trivia question predicted subsequent recall, predominantly when the subject were curious about the answer.

Curiosity can be thought of as novelty seeking behaviour, implicating novelty associated behaviour in humans with this connection between ventral tegmental area-substantia nigra complex and the hippocampus.

Lisman et al., (2011) proposed a model in which novelty dependent dopamine release from the ventral tegmental area and/or the substantia nigra pars compacta into the hippocampus is driven by the pedunculopontine tegmentum. This brainstem nucleus receives afferent fibres from the perirhinal cortex and prefrontal cortex. The model suggests that, under normal circumstances, the initial novelty signal originates in the perirhinal cortex and this initiates the cascade of activity that ultimately leads to novelty dependent dopamine release in the hippocampus (Lisman et al., 2011). However, when the perirhinal cortex is damaged, perhaps the prefrontal cortex could assume this role. The medial prefrontal cortex is known to be involved in object associative learning (Barker et al., 2007; Warburton & Brown, 2010) as well as other cognitive tasks (Vertes et al., 2006; Heidbreder & Groenewegen, 2003). Indeed, the prelimbic cortex was considered as a site of interest in Chapter 6, however, the Fos-related activity data did not fit the anatomical route to the hippocampus (via the nucleus reuniens of the thalamus) that was tested in that experiment. The dopamine-related evidence discussed above suggests that further multi-synaptic connections between the prefrontal cortex and the hippocampus should be explored.

Another possible alternative for an extra-perirhinal novelty signal is the amygdala. Human imaging studies have demonstrated that the amygdala is sensitive to novel stimuli as it reduces its response to repeated stimuli (Blackford et al., 2010; Weierich et al., 2010), even when emotionally neutral images are used (Balderston et al., 2011). In the rodent, disruption of amygdala activity by the GABA-A antagonist, picrotoxin, prevented the increased Fos expression in the hippocampus that usually occurs when rats explore a novel environment. However, this disruption did not cause any changes in the exploratory behaviour of the rats (Sheth et al., 2008). Additionally, using the odour-based receiver operating characteristic paradigm (outlined in Section 1.3.7.2), amygdala lesions were found to selectively impair familiarity, while not altering overall recognition memory (Farovik et al., 2012). Further, it has been demonstrated in slice preparations that, when stimulating the ventral region of area 36 of the perirhinal cortex, coincident signals from the lateral amygdala are required for the signal to propagate into the hippocampus and activate the dentate gyrus (Koganezawa et al., 2008). Although far from conclusive, these studies do implicate the amygdala in modulating the hippocampal

response to novelty. The amygdala is also known to functionally interact with the substantia nigra in relation to the processing of stimulus-outcome relationships (Lee et al., 2006). Thus, the amygdala could be involved in novelty detection in the absence of the perirhinal cortex through its direct connections with the hippocampus or by indirect connections with the dopamine system described above. Disconnection studies in which lesions are created in different brain structures in opposite hemispheres may aid in elucidating these relationships. Alternatively, virus-based lesion techniques, in which a retrograde virus could be injected into the amygdala and a drug subsequently infused into regions that project to it, such as the substantia nigra, may also provide relevant data.

A very different standpoint on the ostensibly intact novelty detection in the rats with perirhinal lesions (Chapter 6) comes from the parallels between the present pattern of results and those from repetition priming in human amnesia. Priming is a form of implicit, rather than explicit, memory. Generally, priming tasks involve presenting a subject with items, the subject is then given a non-memory based task in which the previously encountered item are intermingled with new ones. Success in the task is facilitated (i.e., accuracy improved or response time reduced) by the prior exposure to the stimuli, even when the subject does not remember encountering them (Voss et al., 2012). It has been demonstrated in amnesic patients, with damage to the medial temporal lobe, that repetition priming effects can remain intact even when recognition memory is severely impaired (Hamann & Squire, 1997; Stark & Squire, 2000). The behavioural results presented in Chapter 6 echo the findings of those patient studies; the subjects display behavioural changes based on prior experience but cannot use this information to identify the prior occurrence of a particular stimulus. Further evidence for this view comes from the demonstration, in rats, of facilitation of visual discrimination problems following priming (Tafozoli et al., 2012).

7.3.5 Time since lesion surgery

Of the lesion studies described in this thesis, all of the rats underwent surgery between four and nine months before beginning the IEG-imaging experiments described here. More specifically, the rats from the experiment in Chapter 3 were approximately nine months post-surgery at the start of the present study. JAR166 rats and JAR169 rats, described in Chapter 5, were eight and four months post-surgery respectively. While the two cohorts of rats from Chapter 6, JAR172 and JAR177 received their surgeries, nine and eight months respectively, before the present IEG imaging experiment. This may

have allowed time for compensatory mechanisms to develop. However, it is worth noting that amnesic patients with damage to the medial temporal lobe present with memory deficits many years after the initial insult occurred (Scoville & Milner, 1957; Baddeley et al., 2001; Mayes et al., 2004; Aggleton et al., 2005; Barbeau et al., 2005; Bowles et al., 2010; Dede et al., 2013). Mnemonic testing in monkeys with lesions can go on for several years after the lesion surgery (Zola-Morgan et al., 1992; Nemanic et al, 2004). Furthermore, lesions studies in rats, in line with the present experiments, often behaviourally test for many months after the lesion surgery and find persistent deficits (Aggleton et al., 1986; Albasser et al., 2013a, 2015). Thus, the experiments described here were carried out in accordance with the norms of the field.

7.4 Testing models of medial temporal lobe interactions

Another aim of the work presented here was to test and anatomically refine models from the literature of how regions of the medial temporal lobe interact to support memory. The behavioural results of Chapter 3, that is, the lack of a deficit in novel object discrimination induced by hippocampal lesions provides evidence for a parahippocampal–prefrontal network that is concerned with discriminating the familiarity and recency of occurrence of objects (Aggleton & Brown, 1999; Aggleton, 2012). Further support for this system comes from the network modelling results of Chapter 4 as many of the regions proposed to be part of the network were involved in the present functional network models, including; area Te2, the perirhinal cortex and lateral entorhinal cortex, as well as the medial prefrontal cortex and medial dorsal nucleus of the thalamus.

The lack of a hippocampal lesion deficit in recognition memory (Chapter 3) along with the considerable evidence for the functional independence of the hippocampus and perirhinal cortex (discussed in the previous section) provides evidence against a hierarchical medial temporal lobe memory system which involves the perirhinal cortex and hippocampus, particularly in relation to recognition memory (Squire & Zola-Morgan, 1991).

The work presented across all experiments of this thesis provide evidence to support both the binding of item and context model (Diana et al., 2007) and the local vs. global reference frames model (Knierim et al., 2014). These models are in fact very similar, although Knierim's model is more specific in terms of anatomy. The main difference between these models is the manner in which they conceptualise the stimuli that should

differentially engage the two routes through the parahippocampal cortices to the hippocampus. The former model distinguishes items and contexts, while the later model describes local cues and global cues. The interpretation here is that the present object based experiments map on to both items and local cues and the context experiment can also be thought of as involving global cues. Nomenclature notwithstanding, the present object based experiments were found to engage connections from the perirhinal cortex to lateral entorhinal cortex and on to the hippocampus (Chapters 3, 4 & 6), the putative 'what' pathway. While the context based experiment described in Chapter 5 found evidence for the 'where' pathway as the optimal network models involved the postrhinal cortex, medial entorhinal cortex and the hippocampus. As mentioned above, the local vs. global reference frames model is more anatomically precise; this model proposes that the 'what'/'local cues' pathway should specifically involve the distal region of CA1 and the proximal region of the subiculum. Indeed, this was found to be the case (Chapter 6). Additionally, the present results extend these models to distinguish the contributions of different cortical layers of the lateral entorhinal cortex (Chapter 6).

7.5 Patterns of Fos expression

In the experiments presented here there were some general patterns of Fos expression that were seen across several experiments. These patterns will be discussed in this section.

7.5.1 Group differences in perirhinal Fos counts

Previous studies that assessed Fos expression following modulation of stimulus class found that exposure to novel objects was associated with increased Fos expression in the perirhinal cortex and various other regions (Zhu et al., 1995b, 1996, 1997; Wan et al., 1999; Albasser et al., 2010, 2013; see Table 1.1). The fact that the current object-based behavioural manipulations engendered very few group differences in the absolute number of neurons in the perirhinal cortex (Chapters 3, 4 & 6) may seem at odds with those studies. However, in all but one of those previous studies (Zhu et al., 1997) that reported condition differences, these differences were based on normalised Fos counts. The Fos immunohistochemical staining was carried out simultaneously for control-pairs in order to reduce the experimental variance between conditions introduced by the DAB visualisation step of the protocol. Normalised scores were calculated for each rat individually by dividing the mean number of Fos-positive cells in a particular region by the sum of the Fos-positive cells for both rats in each control pair (e.g., novel count /

novel + familiar counts). That proportion was then expressed as a percentage and as a consequence the normalised scores for each pair summed to 100. These normalised scores were compared between groups using an ANOVA. However, one of the assumptions underlying an ANOVA is the independence of observations (or more correctly, the independence of the error component of the observations; Howell, 2011) and the normalisation procedure violates this assumption. As a consequence, all of the Fos comparisons made in the present experiments were carried out using absolute Fos counts.

In the recognition memory experiment presented in Chapter 3, Fos counts in the perirhinal cortex of the rats in the novel condition were higher than the corresponding paired rat in the familiar condition. However, due to the variance between the control pairs the differences did not reach statistical significance. Thus, the present results are perhaps not as divergent from previous studies as they first appear. Consequently, greater emphasis is placed on the inter-regional correlations. Further, in the study by Albasser et al., (2010b), on which the experiment in Chapter 3 was based, the rats in the familiar condition could not discriminate between objects that were last encountered on the previous trial and those last encountered in the previous session (Albasser et al., 2010b). In contrast, the rats in the familiar condition of Chapter 3 discriminated above chance level, albeit to a lesser degree than the rats in the novel condition. Perhaps this behavioural feature is the basis of this lack of absolute differences in Fos-related activity between the novel and familiar conditions.

The absence of Fos expression differences due to the behavioural condition was also seen in the recency based experiment described in Chapter 4. This result is perhaps less surprising than that of Chapter 3 based on the fact that the rats in the Recency Test and Recency Control groups had exactly the same amount of exposure to the test objects and all that differed was the order of object presentation at test.

In Chapter 6 there were some specific alterations in regional Fos expression attributable to the different behavioural conditions. Increased lateral entorhinal Fos expression was associated with recognition memory, while increased CA1 and subicular Fos was associated with exploration of novel objects. The lack of perirhinal Fos differences were again unexpected based on the fact that rats in the novel-novel exploration condition encountered twice as many novel objects as those in the novel object discrimination condition. However, to my knowledge, little is known about the relationship between the number of stimuli to be encoded, and the number of active neurons involved in an

encoding ensemble in the perirhinal cortex. The evidence presented here suggests that this relationship is not linear. For example, if overlapping ensembles of neurons encode different stimuli then an overall increase in the number of active neurons would not necessarily be expected simply based on increasing the number of stimuli.

Group differences in perirhinal Fos-related activity were observed in the novel context based experiment described Chapter 5. This is consistent with studies that report lesions to the perirhinal cortex disrupt contextual learning (Corodimas & LeDoux, 1995; Bucci et al., 2000, 2002; Kent & Brown, 2012). However, based on the fact that the comparison was against home-cage controls, rather than a fully matched behavioural condition, the significance of the result is difficult to interpret.

7.5.2 Interregional correlations

A pattern from the Fos data in Chapter 5 was that the groups of rats that served as home-cage controls for the experiment (groups Peri Baseline and Sham Baseline) had far more significant inter-regional correlations than any of the groups that were engaged in a learning paradigm (Table 7.1). The Fos counts in these groups were very low, potentially at floor level, and so the number of significant inter-regional correlations potentially reflected the fact that the basal level of activity for a particular rat is similar in all of its brain regions, but slightly different to that of other rats. These animals had not experienced any learning opportunities and so the Fos expression observed could only reflect the resting state of the rodent brain. This, along with other unpublished observations of very similar findings led to a tentative proposal that this could reflect the rodent equivalent of a default mode network (Lu et al., 2012).

This interpretation was complicated by the fact that group Sham Discrimination from Chapter 6 was calculated to have an equivalent number of significant correlations as the two baseline groups (Table 7.1). It is worth pointing out that with the exception of the two home-cage control groups, the groups of rats with the fewest significant inter-regional correlations were those with the lowest object-based behavioural task demands; group Peri Novel and Sham Novel from Chapter 6. This is particularly striking when compared to the groups in the discrimination condition; groups Peri Discrimination and Sham Discrimination have three times and almost six times as many significant inter-regional correlations respectively than the groups in the novel-novel object condition. Of potential significance is the that fact that the animals in Chapter 6 had the shortest training protocol in the bow-tie maze, just prior to the final test session, of all of the

experiments described in this thesis. Further, the rats in the discrimination condition had higher task demands than their novel-novel condition counterparts. Taken together, this pattern could suggest a dynamic situation in which the regional activity of the resting-state brain is highly inter-correlated. Learning opportunities cause a desynchronisation of activity in the medial temporal lobe until threshold is reached based on task demands and all regions become engaged in the task. Evidently, more work is required to elucidate these relationships.

Table 7.1. Number of significant interregional correlations

Chapter	Group	Number of possible interregional correlations	Number of significant (<0.05) interregional correlations	% significant correlations
3	HPC Novel	33	16	49%
	HPC Familiar	33	15	46%
	Sham Novel	63	24	38%
	Sham Familiar	63	14	22%
4	Recency Test	322	123	38%
	Recency Control	322	98	30%
5	Peri Novel	105	25	23%
	Peri Baseline	105	74	**70%**
	Sham Novel	153	35	22%
	Sham Baseline	153	114	**74%**
6	Peri Novel	231	29	12%
	Peri Discrimination	231	89	38%
	Sham Novel	465	63	13%
	Sham Discrimination	465	320	**68%**

7.6 Proof of principle: Pilot tracer study

A prediction of all of the experiments presented in this thesis was that the lateral entorhinal neurons identified as active by Fos-imaging were indeed the populations that project directly to the hippocampus. In order to test this prediction a pilot tracer study was carried out (not fully presented). Initially 16 rats were pre-trained in the bow-tie maze (Figure 2.2) as described in Section 2.3.3. Subsequently, the fluorescent retrograde axonal tracer, Fast Blue, was injected unilaterally into the septal region of the hippocampus while Cholera toxin subunit B conjugated to Alexa fluor 488 was injected into the contralateral hippocampus (Figure 7.1). The septal region of the hippocampus

was chosen as the network models derived in the preceding experiments that involved object recognition testing were based in this region of the hippocampus (Chapters 3 & 6). Two different neuroanatomical tracers were utilised as this would allow for analysis of ipsilateral and contralateral projections separately. In addition, tracers can have different neuronal uptake efficiencies based on the uptake method by which they enter the axons (Lanciego & Wouterlood, 2011), thus, it has been recommended that where possible more than one tracer should be employed to confirm reliability of results (Schofield, 2008).

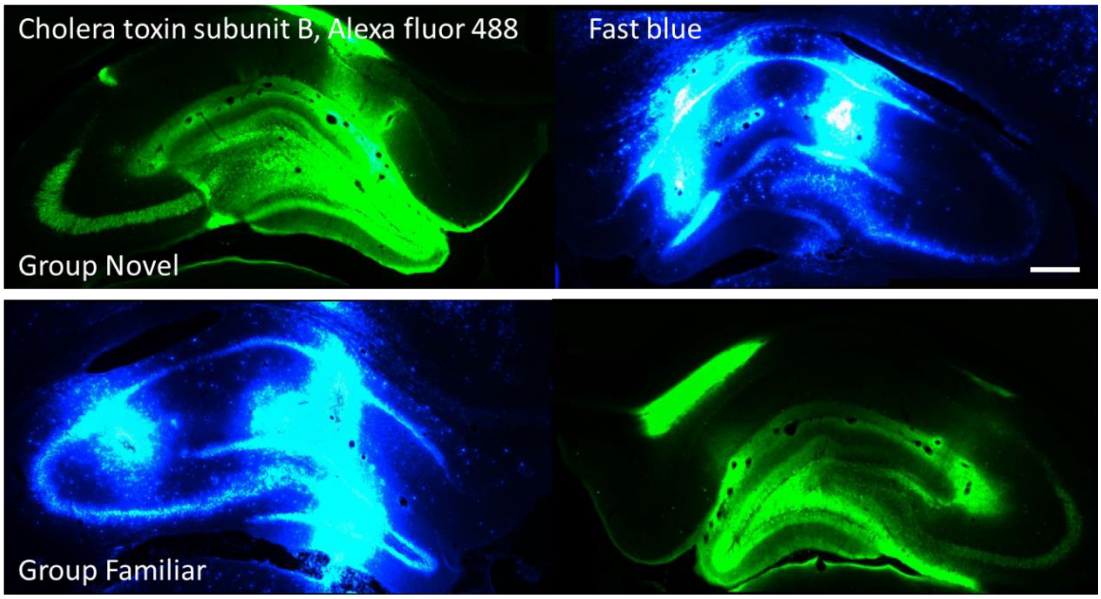

Figure 7.1. Representative fluorescent retrograde tracer injection sites.

These coronal sections depict representative injection sites of the fluorescent retrograde tracers injected into the septal region of the hippocampus for Group Novel (top row) and Group Familiar (bottom row). Scale bar: 500µm.

Following recovery, the rats were divided into two behavioural conditions; Group Novel (n = 8) and Group Familiar (n = 8). They were behaviourally tested in the bow-tie maze according to the novel and familiar protocols described in Chapter 3 (Section 3.2.5) with two modifications. Firstly, the protocol was shortened such that each animal received two sessions per day for three days. Crucially, this allowed the rats in Group Familiar to explore the objects that should be highly familiar in the morning session of the third day before the final test session was administered in the same afternoon. Secondly, the rats in Group Novel were presented with a different set of objects to their Group Familiar counterparts until the final test session on the afternoon of the third day, wherein, they were presented with the same set of objects that the rats in Group Familiar had explored

in all sessions. Consequently, the test objects were the same for both groups but were previously unexperienced by the rats in Group Novel. These modifications allowed for robust group differences in the discrimination measures (Figure 7.2). The rats in Group Novel discriminated novel objects from familiar ones significantly better than those in Group Familiar (Figure 7.2). Yet, both groups discriminated significantly above chance level. This pattern of behavioural results parallels those obtained in Chapter 3.

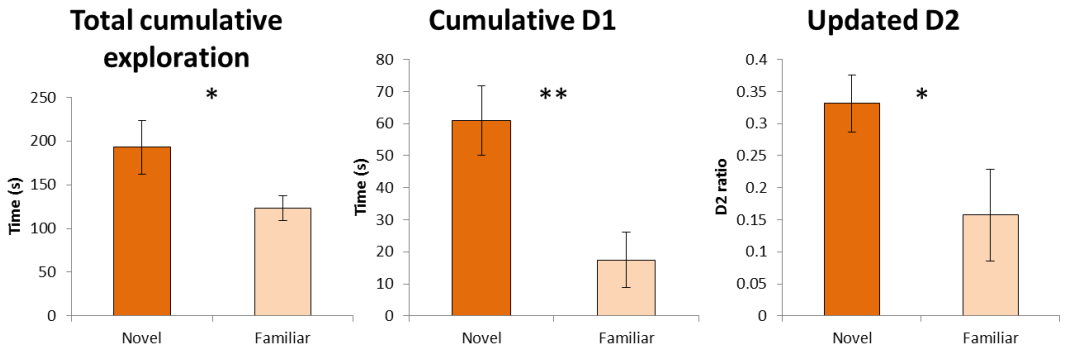

Figure 7.2. Behavioural measures from the final session of the object recognition test.

The graphs depict mean group performance after 20 trials as measured by: the cumulative exploration time for all objects (left panel), the cumulative D1 recognition index (middle panel), and the updated D2 ratio (right panel). For D1 and D2, a score of zero indicates a failure to discriminate. Group Novel, D1 and D2 scores were significantly above zero (one-sample t tests, both $p<0.001$) as were those for Group Familiar (one-sample t tests, both $p<0.05$). *$p<0.05$; ** $p<0.01$ for Group Novel compared to Group Familiar. Data are presented as means ±SEM.

Following the final test session, rats were perfused as described in the General Methods section 2.4, the brains were sectioned and a Fos immunofluorescence protocol was carried out. This allowed for simultaneous quantification in the lateral entorhinal cortex of neurons that were labelled for both an anatomical marker and an activity marker. Initially the tracer positive neurons were identified and then the number of these tracer positive neurons that were also positive for Fos were quantified separately in cortical layers II and III of the lateral entorhinal cortex (Figure 7.3A-D). The number of tracer labelled neurons in these cortical layers was defined by the efficiency of the retrograde tracers and so can be thought of as a random sample of the neurons in the lateral entorhinal cortex that project to the septal region of the hippocampus. Accordingly, the number of these tracer positive neurons that were also Fos-positive were expressed as a percentage of the total number of tracer positive neurons (Figure 7.3E). Approximately 60% of neurons in layer II and 50% of neurons in layer III of the lateral entorhinal cortex that project to the septal region of the hippocampus were assessed to be active

during the discrimination task. Further, this result did not differ between the two tracers used, indicating that this result is reliable. This finding demonstrated that the ensemble of neurons that are active in lateral entorhinal cortex during these object-based tasks include the population that project directly to the hippocampus. This provides evidence for the prediction on which the foregoing experiments presented in this thesis were based.

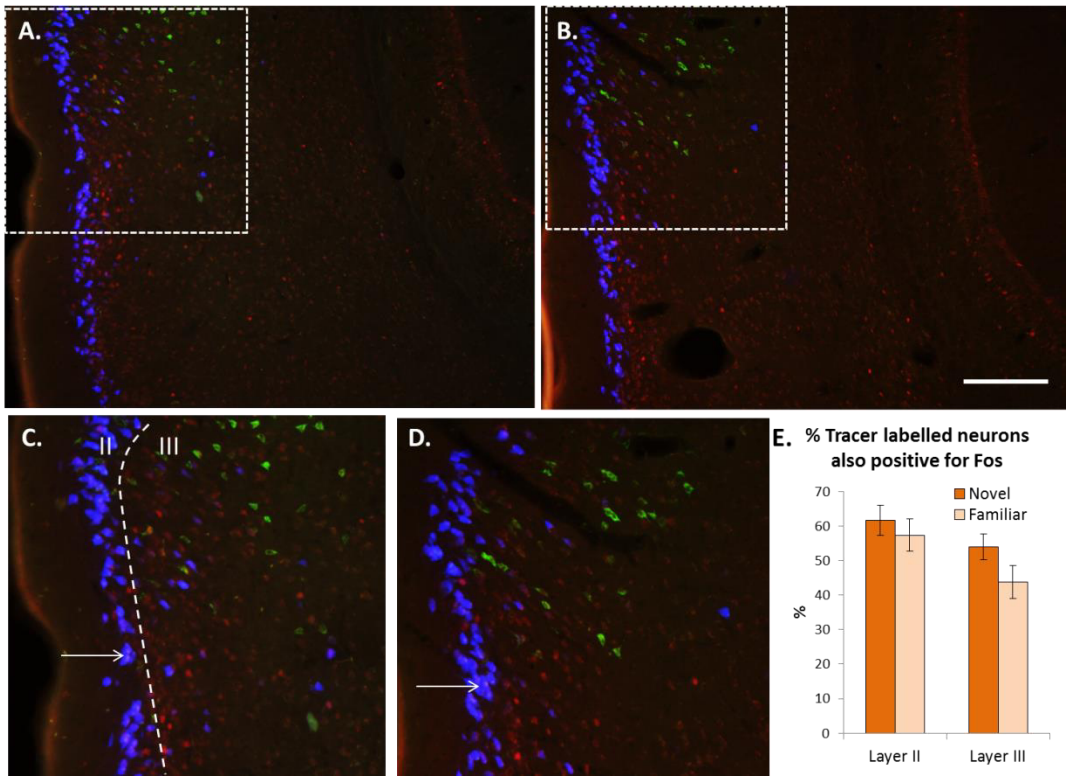

Figure 7.3. Representative photomicrographs of the lateral entorhinal cortex.

These coronal sections depict the lateral entorhinal cortex from rats in Group Novel (A) and Group Familiar (B). Inset in A and B are shown at higher magnification in C and D respectively. Fast Blue (blue) labelled neurons project to the ipsilateral septal hippocampus. Cholera toxin subunit B - Alexa fluor 488 (green) labelled neurons project to the contralateral septal hippocampus. Fos-labelled neurons (red) were the neurons active during the behavioural task. Arrows indicate examples of neurons double-labelled for anatomical and activity marker. Scale bar: 200µm. Graph depicts the mean percentage per animal of tracer positive neurons in cortical layers II and III that were also positive for Fos for rats in Groups Novel and Familiar. Data are presented as means ±SEM.

It should be noted that the proportion of double-labelled neurons did not differ significantly between the behavioural conditions. Based on the results of the preceding experiments, it would have been predicted that the proportion of double-labelled neurons would be higher in Group Novel than Group Familiar, particularly in layer II. Further work is required to derive structural models for this data set in order to test if the

population of double labelled neurons in layers II and III fit the previously derived models of novel and familiar object processing.

There is also a population of Fos-positive neurons that are not tracer positive (Figure 7.3A-D). These neurons could in fact also project to the hippocampus but did not take up the tracer. Alternatively, the neurons may project to other regions of the parahippocampal cortex or the basal ganglia, as these are the strongest efferent connections of the lateral entorhinal cortex (Kerr et al., 2007).

7.7 Summary

To summarise, the main findings of the experiments presented here indicate that in the rat, the perirhinal cortex and hippocampus can function as part of a single network in order to support learning, however this interaction is not a requirement. Both of these regions have the surprising capacity to maintain their activity in the absence of the other. Additionally, when both the perirhinal cortex and the hippocampus are present, their interaction is defined by the novelty or familiarly of the stimuli to be explored. The network engaged by familiar objects is nested within that recruited by novel objects, creating an efficient mechanism for learning about novel stimuli with low redundancy of information. The effective strength of the individual connections within these networks can be modified by the behavioural relevance of the stimuli. Finally, evidence was generated in support of certain models that postulate how regions of the medial temporal lobe interact to support memory, namely Aggleton and Brown's parahippocampal–prefrontal network for discriminating the familiarity and recency of occurrence of objects (Aggleton & Brown, 1999; Aggleton, 2012), the binding of item and context model (Diana et al., 2007) and the local vs. global reference frames model (Knierim et al., 2014). However, this work also raises interesting questions relating to how novelty signals and regional activity can be maintained despite the loss of regions thought to be vital for their maintenance. Future work involving anatomically specific temporary neuronal inactivation techniques will be invaluable in answering these outstanding questions.

References

Abraham, W.C., Dragunow, M., & Tate, W.P. (1991). The role of immediate early genes in the stabilization of long-term potentiation. Molecular Neurobiology, 5, 297-314.

Adlam, A-L. R., Malloy, M., Mishkin, M., & Vargha-Khadem, F. (2009). Dissociation between recognition and recall in developmental amnesia. Neuropsychologia, 47, 2207–2210.

Aggleton, J.P. (1985). One - trial object recognition by rats. Quarterly Journal of Experimental Psychology B, 37, 279-294.

Aggleton, J.P. (2012). Multiple anatomical systems embedded within the primate medial temporal lobe: Implications for hippocampal function. Neuroscience Biobehavioural Reviews, 36, 1579–1596.

Aggleton, J.P., Albasser, M.M., Aggleton, D.J., Poirier, G.L., & Pearce, J.M. (2010). Lesions of the rat perirhinal cortex spare the acquisition of a complex configural visual discrimination yet impair object recognition. Behavioral Neuroscience, 124, 55-68.

Aggleton, J.P., Blindt, H.S., & Candy, J.M. (1989). Working memory in aged rats. Behavioral Neuroscience, 103, 975-983.

Aggleton, J.P., & Brown, M.W. (1999). Episodic memory, amnesia and the hippocampal - anterior thalamic axis. Behavioural and Brain Sciences, 22, 425-444.

Aggleton, J.P., & Brown, M.W. (2006). Interleaving brain systems for episodic and recognition memory. Trends in Cognitive Sciences, 10, 455-63.

Aggleton, J.P., & Brown, M.W. (2005). Contrasting hippocampal and perirhinal cortex function using immediate early gene imaging. Quarterly Journal of Experimental Psychology B, 58, 218-233.

Aggleton, J.P., Brown, M.W., & Albasser, M.M. (2012). Contrasting brain activity patterns for item recognition memory and associative recognition memory: Insights from immediate-early gene imaging. Neuropsychologia, 50, 3141-3155.

Aggleton, J.P., Dumont, J.R., & Warburton, E.C. (2011). Unravelling the contributions of the diencephalon to recognition memory: A review. Learning & Memory, 18, 384-400.

Aggleton, J.P. Hunt, P.R., & Rawlins, J.N.P. (1986). The effects of hippocampal lesions upon spatial and non-spatial tests of working memory. Behavioural Brain Research, 19, 133-146.

Aggleton, J.P., Hunt, P.R., & Shaw, C. (1990). The effects of mammillary body and combined amygdalar-fornix lesions on tests of delayed nonmatching-to-sample. Behavioural Brain Research, 40, 145-157.

Aggleton, J.P., Keen, S., Warburton, E.C., & Bussey, T.J. (1997). Extensive cytotoxic lesions involving both the rhinal cortices and area TE impair recognition but spare spatial alternation in the rat. Brain Research Bulletin, 43, 279–87.

Aggleton, J.P., Kyd R., & Bilkey, D. (2004). When is the perirhinal cortex necessary for the performance of spatial memory tasks? Neuroscience and Biobehavioural Reviews, 28, 611-624.

Aggleton, J.P., Neave, N.J., Nagle, S., & Hunt, P.R. (1995). A comparison of the effects of anterior thalamic, mamillary body and fornix lesions on reinforced spatial alternation. Behavioural Brain Research, 68, 91-101.

Aggleton, J.P., Nicol, R.M., Huston, A.E., & Fairbairn, A.F. (1988). The performance of amnesic subjects on tests of experimental amnesia in animals: delayed matching-to-sample. Neuropsychologia, 26, 265-272.

Aggleton, J.P., & Shaw, C. (1996). Amnesia and recognition memory: A re-analysis of psychometric data. Neuropsychologia, 34, 51–62.

Aggleton, J.P., Vann, S.D., Denby, C., Dix, S., Mayes, A.R., Roberts, N., & Yonelinas, A.P. (2005). Sparing of the familiarity component of recognition memory in a patient with hippocampal pathology. Neuropsychologia, 43, 1810-1823.

Agster, K.L., & Burwell, R.D. (2009). Cortical efferents of the perirhinal, postrhinal, and entorhinal cortices of the rat. Hippocampus, 19, 1159–1186.

Agster, K.L., Fortin, N.J., & Eichenbaum, H. (2002). The hippocampus and disambiguation of overlapping sequences. Journal of Neuroscience, 22, 5760-5768.

Ahn, J.R., & Lee, I. (2015). Neural correlates of object-associated choice behaviour in the perirhinal cortex of rats. Journal of Neuroscience, 35, 1692-1705.

Ainge, J.A., Heron-Maxwell, C., Theofilas, P., Wright, P., de Hoz, L., & Wood, E.R. (2006). The role of the hippocampus in object recognition in rats: Examination of the influence of task parameters and lesion size. Behavioural Brain Research, 167, 183-195.

Albasser, M.M., Amin, E., Iordanova, M.D., Brown, M.W., Pearce, J.M., & Aggleton, J.P. (2011a). Perirhinal cortex lesions uncover subsidiary systems in the rat for the detection of novel and familiar objects. European Journal of Neuroscience, 34, 331-342

Albasser, M.M., Amin, E., Iordanova, M.D., Brown, M.W., Pearce, J.M., & Aggleton, J.P. (2011b). Separate but interacting recognition memory systems for different senses: The role of the rat perirhinal cortex. Learning & Memory, 18, 435-443.

Albasser, M.M., Chapman, R.J., Amin, E., Iordanova, M.D., Vann, S.D., & Aggleton, J.P. (2010a). New behavioural protocols used to extend our knowledge of rodent object recognition memory. Learning & Memory, 17, 407-419.

Albasser, M.M., Davies, M., Futter, J.E., & Aggleton, J.P. (2009). Magnitude of the object recognition deficit associated with perirhinal cortex damage in rats: Effects of varying the lesion extent and the duration of the sample period. Behavioral Neuroscience, 123, 115-124.

Albasser, M.M., Dumont, J.R., Amin, E., Holmes, J.D., Horne, M.R., Pearce, J.M., & Aggleton, J.P. (2013a). Association rules for rat spatial learning: The importance of the hippocampus for binding item identity with item location. Hippocampus, 23, 1162-1178.

Albasser, M.M., Lin, T-C. E., Iordanova, M.D., Amin, E., & Aggleton, J.P. (2012). Evidence that the rat hippocampus has contrasting roles in object recognition memory and object recency memory. Behavioral Neuroscience, 126, 659-669.

Albasser, M.M., Olarte-Sánchez, C.M., Amin, E., Brown, M.W., Kinnavane, L, & Aggleton, J.P. (2015). Perirhinal cortex lesions in rats: novelty detection and sensitivity to interference. Behavioral Neuroscience, 129, 227-243.

Albasser, M.M., Olarte-Sánchez, C.M., Amin, E, Horne, M., Newton, M.J., Warburton, E.C., & Aggleton, J.P. (2013b). The neural basis of nonvisual object recognition memory in the rat. Behavioral Neuroscience, 127, 70-85.

Albasser, M.M., Poirier, G.L., & Aggleton, J.P. (2010b). Qualitatively different modes of perirhinal-hippocampal engagement when rats explore novel vs. familiar objects as revealed by c-fos imaging. European Journal of Neuroscience, 31, 134-147.

Albasser, M.M., Poirier, G.L., Warburton, E.C., & Aggleton, J.P. (2007). Hippocampal lesions halve immediate–early gene protein counts in retrosplenial cortex: distal dysfunctions in a spatial memory system. European Journal of Neuroscience, 26, 1254–1266.

Albrechet-Souza, L., Borelli, K.G., Almada, R.C., & Brandão, M.L., (2011). Midazolam reduces the selective activation of the rhinal cortex by contextual fear stimuli. Behavioural Brain Research, 216, 631–638.

Alvarez, P., Zola-Morgan, S., Squire, L.R., (1995). Damage limited to the hippocampal region produces long lasting memory impairment in monkeys. Journal of Neuroscience, 15, 3796-3807.

Amaral, D.G. (1993). Emerging principles of intrinsic hippocampal organization. Current opinion in Neurobiology, 3, 225-229.

Amaral, D.G., & Lavenex, P. (2007). Hippocampal Neuroanatomy. In: The Hippocampus Book (Andersen, P., Morris, R., Amaral, D., Bliss, T., & O'Keefe. J., eds), pp 37-109. New York: Oxford UP.

Ameen-Ali, K.E., Eacott, M.J., & Easton, A. (2012). A new behavioural apparatus to reduce animal numbers in multiple types of spontaneous object recognition paradigms in rats. Journal of Neuroscience Methods, 211, 66-76.

Ameen-Ali, K.E., Easton, A., & Eacott, M.J. (2015). Moving beyond standard procedures to assess spontaneous recognition memory. Neuroscience and Biobehavioral Reviews, 53, 37-51.

Amin, E., Pearce, J.M., Brown, M.W., & Aggleton, J.P. (2006). Novel temporal configurations of stimuli produce discrete changes in immediate early gene expression in the rat hippocampus. European Journal of Neuroscience, 24, 2611-2621.

Arbuckle, J.L. (2011). IBM SPSS AMOS 20 user's guide. AMSO Development Corporation, Chicago.

Bachevalier, J., & Nemanic, S. (2008). Memory for spatial location and object-place associations are differently processed by the hippocampal formation, parahippocampal areas TH/TF and perirhinal cortex. Hippocampus, 18, 64-80.

Bachevalier, J., Saunders, R.C., & Mishkin, M., (1985). Visual recognition in monkeys: effects of transection of fornix. Experimental Brain Research 57, 547–553.

Baddeley, A.D., Emslie, H., & Nimmo-Smith, I. (1994). The Doors and People Test. Bury St Edmunds, UK: Thames Valley Test Company.

Baddeley, A.D., Vargha-Khadem, F., & Mishkin, M. (2001). Preserved recognition in a case of developmental Amnesia: Implications for the acquisition of semantic memory? Journal of Cognitive Neuroscience, 13, 357-369.

Balderston, N.L., Schultz, D.H., & Helmstetter, F.J. (2011). The human amygdala plays a stimulus specific role in the detection of novelty. NeuroImage, 55, 1559-1898.

Bannerman, D.M., Rawlins, J.N.P., McHugh, S.B., Deacon, R.M.J., Yee, B.K., Bast, T., Zhang, W.-N., Pothuizen, H.H.J., Feldon, J. (2004). Regional dissociations within the hippocampus-memory and anxiety. Neuroscience and Biobehavioral Reviews, 28, 273–283.

Barbeau, E.J., Felician, O., Joubert, S., Sontheimer, A., Ceccaldi, M., & Poncet, M. (2005). Preserved visual recognition memory in an amnesic patient with hippocampal lesions. Hippocampus, 15, 587-596.

Barense, M.D., Bussey, T.J., Lee, A.C., Rogers, T.T., Davies, R.R., Saksida, L.M., Murray, E.A., & Graham, K.S. (2005). Functional specialization in the human medial temporal lobe. Journal of Neuroscience, 25, 10239-10246.

Barker, G.R.I., & Warburton, E.C. (2011a). Evaluating the neural basis of temporal order memory for visual stimuli. European Journal of Neuroscience, 33, 705-716.

Barker, G.R.I., & Warburton, E.C. (2011b). When is the hippocampus involved in recognition memory? Journal of Neuroscience, 31, 10721-10731.

Barker, G.R.I., Bird, F., Alexander, V., & Warburton, E.C. (2007). Recognition memory for objects, places, and temporal order: A disconnection analysis of the role of the medial prefrontal cortex and perirhinal cortex. Journal of Neuroscience, 27, 2948-2957.

Bartko, S.J., Winters, B.D., Cowell, R.A., Saksida, L.M., & Bussey, T.J. (2007a). Perceptual functions of perirhinal cortex in rats: Zero-delay object recognition and simultaneous oddity discriminations. The Journal of Neuroscience, 27, 2548–2559.

Bartko, S.J., Winters, B.D., Cowell, R.A., Saksida, L.M., & Bussey, T.J. (2007b). Perirhinal cortex resolves feature ambiguity in configural object recognition and perceptual oddity tasks. Learning & Memory, 14, 821–832.

Bast, T., (2007). Toward an integrated perspective on hippocampal function: From a rapid encoding of experience to adaptive behaviour. Reviews in Neuroscience, 18, 253-281.

Bast, T., Wilson, I.A., Witter, M.P., & Morris, R.G. (2009). From Rapid Place Learning to Behavioral Performance: A Key Role for the Intermediate Hippocampus. PLoS Biol 7: e1000089.

Baxter, M.G., & Murray, E.A. (2001). Opposite relationship of hippocampal and rhinal cortex damage to delayed nonmatching-to-sample deficits in monkeys. Hippocampus, 11, 61-71.

Beason-Held, L.L., Rosene, D.L., Killiany, R.J., & Moss, M.B. (1999). Hippocampal formation lesions produce memory impairment in the rhesus monkey. Hippocampus, 9, 562-574.

Berlyne, D.E. (1950). Novelty and curiosity as determinants of exploratory behaviour. British Journal of Psychology General Section, 41, 68-80

Bird, C.M., Vargha-Khadem, F., Burgess, N. (2008). Impaired memory for scenes but not faces in developmental hippocampal amnesia: A case study. Neuropsychologia, 46, 1050–1059.

Birrell, J.M., & Brown, V.J. (2000). Medial frontal cortex mediates perceptual attentional set shifting in the rat. Journal of Neuroscience, 20, 4320–4324.

Bisler, S., Schleicher, A., Gass, P., Stehle, J., Zilles, K., & Staiger, J.F. (2002). Expression of c-Fos, ICER, Krox-24 and JunB in the whisker-to-barrel pathway of rats: time course of induction upon whisker stimulation by tactile exploration of an enriched environment. Journal of Chemical Neuroanatomy, 23, 187-198.

Bittner, K.T., Grienberger, C., Vaidya, S.P., Milstein, A.D., Macklin, J.J., Suh, J., Tonegawa, S., & Magee, J.C. (2015). Conjunctive input processing drives feature selectivity in hippocampal CA1 neurons. Nature Neuroscience, 18, 1133-1142.

Blackford, J.U., Buckholtz, J.W., Avery, S.N., & Zald, D.H. (2010). A unique role for the human amygdala in novelty detection. NeuroImage, 50, 1188–1193.

Bliss, T.V P., & Lomo, T. (1973). Long-lasting potentiation of synaptic transmission in the dentate area of the anaesthetized rabbit following stimulation of the perforant path. Journal of Physiology, 232, 331-356.

Bollen, K.A., & Long, J.S. (1992). Tests for structural equation models: Introduction. Sociological Methods & Research, 21, 123–131.

Boucard, A., Marchand, A., Nogues. X. (2007). Reliability and validity of structural equation modeling applied to neuroimaging data: A simulation study. Journal of Neuroscience Methods, 166, 278–292.

Bowles, B., Crupi, C., Mirsattari, S.M., Pigott, S.E., Parrent, A.G., Pruessner, J.C., Yonelinas, A.P., & Kohler, S. (2007). Impaired familiarity with preserved recollection

after anterior temporal-lobe resection that spares the hippocampus. Proceedings of the National Academy of Sciences of the United States of America, 41, 16382-16387.

Bowles, B., Crupi, C., Pigott, S., Parrent, A.,Wiebe, S., Janzen, L., & Kohler, S. (2010). Double dissociation of selective recollection and familiarity impairments following two different surgical treatments for temporal-lobe epilepsy. Neuropsychologia, 48, 2640–2647.

Bowles, B., O'Neil, E.B., Mirsattari, S.M., Poppenk, J. ,& Kohler, S. (2011). Preserved hippocampal novelty responses following anterior temporal-lobe resection that impairs familiarity but spares recollection. Hippocampus, 21, 847–854.

Broadbent, N.J., Squire, L.R., & Clark, R.E. (2004). Spatial memory, recognition memory and the hippocampus. Proceedings of the National Academy of Science, 101, 14515-14520

Broadbent, N.J., Gaskin, S., Squire, L.R., & Clark, R.E. (2010). Object recognition memory and the rodent hippocampus. Learning & Memory, 17, 5-11.

Brown, M.W., & Aggleton, J.P. (2001). Recognition memory: What are the roles of the perirhinal cortex and hippocampus? Nature Reviews Neuroscience, 2, 51-61.

Brown, M.W., Warburton, E.C., & Aggleton, J.P. (2010). Recognition memory: Material, processes, and substrates. Hippocampus, 20, 1228-124.

Brown, M.W., Wilson, F.A.W., & Riches, I.P. (1987). Neuronal evidence that inferomedial temporal cortex is more important than hippocampus in certain processes underlying recognition memory. Brain Research, 204, 158-162.

Brown, M.W., & Xiang, J-Z. (1998). Recognition memory: neuronal substrates of the judgement of prior occurrence, Progress in Neurobiology, 55, 149-189.

Brown, M.W., Warburton, E.C., & Aggleton, J.P. (2010). Recognition memory: material, processes, and substrates. Hippocampus, 20, 1228-1244.

Bucci, D.J., Phillips, R.G., & Burwell, R.D. (2000). Contributions of postrhinal and perirhinal cortex to contextual information processing. Behavioral Neuroscience, 114, 882-894.

Bucci, D.J., Saddoris, M.P., & Burwell, R.D. (2002). Contextual fear discrimination is impaired by damage to the postrhinal or perirhinal cortex. Behavioral Neuroscience, 116, 479–488.

Buckley, M. J., & Gaffan, D. (1997). Impairment of visual object-discrimination learning after perirhinal cortex ablation. Behavioral Neuroscience, 111, 467–475.

Buckley, M.J., Booth, M.C.A, Rolls, E.T., & Gaffan, D. (2001). Selective perceptual impairments after perirhinal cortex ablation. Journal of Neuroscience, 21, 9824–9836.

Buffalo, E.A., Reber, P.J., & Squire, L.R. (1998). The human perirhinal cortex and recognition memory. Hippocampus, 8, 330–339.

Buffalo, E.A., Ramus, S.J., Clark R.E., Teng, E., Squire, L.R., & Zola, S.M. (1999). Dissociation between the effects of damage to perirhinal cortex and area TE. Learning & Memory, 6, 572-99.

Buffalo, E.A., Ramus, S.J., Squire, L.R., & Zola, S.M. (2000). Perception and recognition memory in monkeys following lesions of area TE and perirhinal cortex. Learning & Memory, 7, 375–382.

Bullmore, E., Horwitz, B., Honey, G., Brammer, M., Williams, S., & Sharma, T. (2000). How good is good enough in path analysis of fMRI data? NeuroImage, 11, 289–301.

Burke, S.N., Maurer, A.P., Hartzell, A.L., Nematollahi, S., Uprety, A., Wallace, J.L., & Barnes, C.A. (2012). Representation of three-dimensional objects by the rat perirhinal cortex. Hippocampus, 22, 2032-2044.

Burwell, R.B., Saddoris, M.P., Bucci, D.J., & Wiig, K.A. (2004). Corticohippocampal Contributions to Spatial and Contextual Learning. Journal of Neuroscience, 24, 3826-3836.

Burwell, R.D. (2000). The Parahippocampal Region: Corticocortical Connectivity. Annals of the New York Academy of Sciences, 911, 25-42.

Burwell, R.D. (2001). Borders and cytoarchitecture of the perirhinal and postrhinal cortices in the rat. Journal of Comparative Neurology, 437, 17-41.

Burwell, R.D., & Amaral, D.G. (1998a). Perirhinal and postrhinal cortices of the rat: Interconnectivity and connections with the entorhinal cortex. Journal of Comparative Neurology, 391, 293-321.

Burwell, R.D., & Amaral, D.G. (1998b). Cortical afferents of the perirhinal, postrhinal and entorhinal cortices of the rat. Journal of Comparative Neurology, 398, 179-205.

Burwell, R. D., & Agster, K. L. (2008). Anatomy of the Hippocampus and the Declarative Memory System. In: Memory Systems, vol. 3 (H. Eichenbaum ed.) of

Learning and Memory: A Comprehensive Reference, 4 vols. (Byrne, J. Ed.), pp. 47-66. Oxford: Elsevier.

Bussey, T.J., Duck, J., Muir, J.L., & Aggleton, J.P. (2000). Distinct patterns of behavioural impairments resulting from fornix transection or neurotoxic lesions of the perirhinal and postrhinal cortices in the rat. Behavioural Brain Research, 111, 187–202.

Bussey, T.J., Muir, J.L., & Aggleton, J.P. (1999). Functionally dissociating aspects of event memory: The effects of combined perirhinal and postrhinal cortex lesions on object and place memory in the rat. Journal of Neuroscience, 19, 495–502.

Bussey, T.J., Saksida, L.M., & Murray, E.A. (2002). Perirhinal cortex resolves feature ambiguity in complex visual discriminations. European Journal of Neuroscience, 15, 365-374.

Bussey, T.J., Saksida, L.M., & Murray, E.A. (2003). Impairments in visual discrimination after perirhinal cortex lesions: testing 'declarative' vs. 'perceptual-mnemonic' views of perirhinal cortex function. European Journal of Neuroscience, 17, 649-660.

Bussey, T.J., Saksida, L.M., & Murray, E.A. (2005). The perceptual-mnemonic feature conjugation model of perirhinal cortex function. The Quarterly Journal of Experimental Psychology B: Comparative and Physiological Psychology, 58, 269 –282.

Bussey, T.J., Saksida, L.M., & Murray, E.A. (2007). Memory, perception, and the ventral-perirhinal-hippocampal stream: Thinking outside of the boxes. Hippocampus, 17, 898-908.

Carlesimo, G.A., Lombardi, M.G., & Caltagirone, C. (2011). Vascular thalamic amnesia: A reappraisal. Neuropsychologia, 49, 777-789.

Cassaday, H.J., & Rawlins, J.N.P. (1997). The hippocampus, objects, and their contexts. Behavioral Neuroscience, 111, 1228-1244.

Chaudhuri, A. (1997). Neural activity mapping with inducible transcription factors. NeuroReport, 8, 3-7.

Chen, C., Kim, J.J., Thompson, R.F., & Tonegawa, S. (1996). Hippocampal lesions impair contextual fear conditioning in two strains of mice. Behavioral Neuroscience, 110, 1177-1180.

Cipolotti, L., Bird, C., Good, T., Macmanus, D., Rudge, P., & Shallice, T. (2006). Recollection and familiarity in dense hippocampal amnesia: A case study. Neuropsychologia, 44, 489–506.

Clark, R.E., Zola, S.M., & Squire, L.R. (2000). Impaired recognition memory in rats after damage to the hippocampus. Journal of Neuroscience, 20, 8853-8860.

Clelland, C.D., Choi, M., Romberg, C., Clemenson, G.D., Fragniere, A., Tyers, P., Jessberger, S., Saksida, L.M., Barker, R.A., Gage, F.H., & Bussey, T.J. (2009). A functional role for adult hippocampal neurogenesis in spatial pattern separation. Science, 325, 210-213.

Cohen, J.S., Munchow, A.H., Rios, L.M., Zhang G., Asgeirsdottir, H.N., & Stackman, Jr., R.W. (2013). The rodent hipocampus is essential for nonspatial object memory. Current Biology, 23, 1685-1690.

Conde, F., Marie-Lepoivre, E., Audinat, E., & Crepel, F. (1995). Afferent Connections of the Medial Frontal Cortex of the Rat II: Cortical and Subcortical Afferents. Journal of Comparative Neurology, 352, 567-593.

Corodimas, K.P., & LeDoux, J.E., (1995). Disruptive effects of post training perirhinal cortex lesions on conditioned fear: Contributions of contextual cues. Behavioral Neuroscience, 109, 613-619.

Countryman, R.A., Orlowski, J.D., Brightwell, J.J., Oskowitz, A.Z., & Colombo, P.J. (2005). CREB phosphorylation and c-Fos expression in the hippocampus of rats during acquisition and recall of a socially transmitted food preference. Hippocampus, 15, 56-67.

Cowell, R.A., Bussey, T.J., & Saksida, L.M. (2010). Components of recognition memory: Dissociable cognitive processes or just differences in representational complexity? Hippocampus, 20, 1245-1262.

Cross, L. Aggleton, J.P., Brown, M.W., & Warburton, E.C. (2013). The medial dorsal thalamic nucleus and the medial prefrontal cortex of the rat function together to support associative but not item recognition. Learning & Memory, 20, 41-50.

Daselaar, S.M., Fleck, M.S., & Cabeza, R. (2006). Triple dissociation in the medial temporal lobes: recollection, familiarity, and novelty. Journal of Neurophysiology, 96, 1902–1911.

Davachi, L., Mitchell, J.P., & Wagner, A.D. (2003). Multiple routes to memory: distinct medial temporal lobe processes build item and source memories. Proceedings of the National Academy of Science, 100, 2157-2162.

Davies, R.R., Graham, K.S., Xuereb, J.H., Williams, G.B., & Hodges, J.R. (2004). The human perirhinal cortex and semantic memory. European Journal of Neuroscience, 20, 2441–2446.

Davies, M., Machin, P. E., Sanderson, D. J., Pearce, J. M., & Aggleton, J. P. (2007). Neurotoxic lesions of the rat perirhinal and postrhinal cortices and their impact on biconditional visual discrimination tasks. Behavioural Brain Research, 176, 274 –283.

Dede, A.J.O., Wixted, J.T., Hopkins, R.O., & Squire, L.R. (2013). Hippocampal damage impairs recognition memory broadly, affecting both parameters in two prominent models of memory. Proceedings of the National Academy of Science, 110, 6577-6582.

de Lima, M.N., Luft, T., Roesler, R., & Schroder, N (2006). Temporary inactivation reveals an essential role of the dorsal hippocampus in consolidation of object recognition memory. Neuroscience Letters, 405, 142–146.

Dember, W.N. (1956). Response by the rat to environmental change. Journal of Comparative and Physiological Psychology, 49, 93-95.

Deshmukh, S.S., Johnson, J.L., & Knierim, J.J. (2012). Perirhinal cortex represents nonspatial, but not spatial, information in rats foraging in the presence of objects: comparison with lateral entorhinal cortex. Hippocampus, 22, 2045–2058.

Dere, E., Huston, J.P., & De Souza Silva, M.A. (2005). Episodic-like memory in mice: Simultaneous assessment of object, place and temporal order memory. Brain Research Protocols, 16, 10-19.

DeVito, L.M., & Eichenbaum, H. (2011). Memory for the order of events in specific sequences: contributions of the hippocampus and medial prefrontal cortex. Journal of Neuroscience, 31, 3169-3175.

Diana, R.A., Yonelinas, A.P., & Ranganath, C. (2007). Imaging recollection and familiarity in the medial temporal lobe: a three-component model. Trends in Cognitive Sciences, 11, 379-386.

Diana, R.A., Yonelinas, A.P., & Ranganath, C. (2010). Medial temporal lobe activity during source retrieval reflects information type, not memory strength. Journal of Cognitive Neuroscience, 22, 1808-1818.

Dix, S.L., & Aggleton, J.P. (1999). Extending the spontaneous preference test of recognition: evidence of object - location and object - context recognition. Behavioral Brain Research, 99, 191-200.

Dolorfo, C.L., & Amaral, D.G. (1998). Entorhinal cortex of the rat: Topographic organization of the cells of origin of the perforant path projection to the dentate gyrus. Journal of Comparative Neurology, 398, 25-48.

Dudchenko, P.A., Wood, E.R., & Enchenbaum, H. (2000). Neurotoxic hippocampal lesions have no effect on odor span and little effect on odor recognition memory but produce significant impairments on spatial span, recognition, and alternation. Journal of Neuroscience, 20, 2964–2977.

Dumont, J.R., & Aggleton, J.P. (2013). Dissociation of recognition and recency memory judgments after anterior thalamic nuclei lesions in rats. Behavioral Neuroscience, 127, 415-431.

Dunnett, S.B., Evenden, J.L. & Iversen, S.D. (1988). Delay-dependent short-term-memory deficits in aged rats. Psychopharmacology, 96, 174-180.

Duva, C.A., Floresco, S.B., Wunderlich, G.R., Lao, T.L., Pinel, J.P., & Phillips, A.G. (1997). Disruption of spatial but not object-recognition memory by neurotoxic lesions of the dorsal hippocampus in rats. Behavioral Neuroscience 111, 1184–1196.

Eacott, M. J., Gaffan, D., & Murray, E. A. (1994). Preserved recognition memory for small sets, and impaired stimulus identification for large sets, following rhinal cortex ablations in monkeys. European Journal of Neuroscience, 6, 1466–1478.

Eacott, M. J., & Easton, A. (2007). On familiarity and recall of events by rats. Hippocampus, 17, 890-897.

Eacott, M.J., & Easton, A. (2010). Episodic memory in animals: Remembering which occasion. Neuropsychologia, 48, 2273-2280.

Eacott, M.J., Easton, A., & Zinkivskay, A. (2005). Recollection in an episodic-like memory task in the rat. Learning & Memory, 12, 221-223.

Eacott, M.J., & Norman, G. (2004). Integrated memory for object, place, and context in rats: A possible model of episodic-like memory? Journal of Neuroscience, 24, 1948-1953.

Easton, A., & Eacott, M.J. (2010). Recollection of episodic memory within the medial temporal lobe: behavioural dissociations from other types of memory. Behavioral Brain Research, 215, 310-317.

Easton, A., Zinkivskay, A., & Eacott, M.J. (2009). Recollection is impaired, but familiarity remains intact in rats with lesions of the fornix. Hippocampus 19, 837–843.

Eichenbaum, H., Fortin N., Sauvage, M., Robitsek, R.J., & Farovik, A. (2010). An animal model of amnesia that uses Receiver Operating Characteristics (ROC) analysis to distinguish recollection from familiarity deficits in recognition memory. Neuropsychologia, 48, 2281-2289.

Eichenbaum, H., Sauvage, M., Fortin N., Komorowski, R., & Lipton, P. (2012). Towards a functional organization of episodic memory in the medial temporal lobe. Neuroscience and Biobehavioral Reviews, 36, 1597–1608.

Eichenbaum, H., Yonelinas, A.P., & Ranganath, C. (2007). The medial temporal lobe and recognition memory. Annual Review of Neuroscience, 30, 123-152.

Ennaceur, A., & Aggleton, J.P. (1994). Spontaneous recognition of object configurations in rats: effects of fornix lesions. Experimental Brain Research, 100, 85-92.

Ennaceur, A., & Aggleton, J.P. (1997). The effects of neurotoxic lesions of the perirhinal cortex combined to fornix transection on object recognition memory in the rat. Behavioral Brain Research, 88, 181–193.

Ennaceur, A., & Delacour, J. (1988). A new one-trial test for neurobiological studies of memory in rats. 1: Behavioral data. Behavioral Brain Research, 31, 47-59.

Ennaceur, A., (2010). One-trial object recognition in rats and mice: Methodological and theoretical issues. Behavioural Brain Research, 215, 244-254.

Ennaceur, A., Neave, N., & Aggleton, J.P. (1996). Neurotoxic lesions of the perirhinal cortex do not mimic the behavioural effects of fornix transection in the rat. Behavioral Brain Research, 80, 9-25.

Eradath, M.K., Mogami, T., Wang, G., & Tanaka, K. (2015). Time context of cue-outcome associations represented by neurons in perirhinal cortex. Journal of Neuroscience, 35, 4350-4365.

Fahy, F.L., Riches, I.P., & Brown, M.W., (1993). Neuronal activity related to visual recognition memory: long-term memory and the encoding of recency and familiarity

information in the primate anterior and medial inferior temporal and rhinal cortex. Experimental Brain Research, 96, 457-472.

Fan, X., & Wang, L. (1998). Effects of Potential Confounding Factors on Fit Indices and Parameter Estimates for True and Misspecified SEM Models. Educational and Psychological Measurement, 58, 701-735.

Fan, X., Wang, L., Thompson, B., & Wang, L. (1999). Effects of sample size, estimation methods, and model specification on structural equation modeling fit indexes. Structural Equation Modeling: A Multidisciplinary Journal, 6, 56-83.

Farovik, A., Place, R., Miller, D., & Eichenbaum, H. (2012). Amygdala lesions selectively impair familiarity in recognition memory. Nature Neuroscience, 14, 1416–1417.

Fernández, G., & Tendolkar, I. (2006). The rhinal cortex: 'gatekeeper' of the declarative memory system. Trends in Cognitive Sciences, 10, 358-362.

Flegal, K.E., Marín-Gutiérrez, A., Ragland, J.D., & Ranganath, C. (2014). Brain mechanisms of successful recognition through retrieval of semantic context. Journal of Cognitive Neuroscience, 26, 1694–1704.

Fortin, N.J., Agster, K.L., & Eichenbaum, H.B. (2002). Critical role of the hippocampus in memory for sequences of events. Nature Neuroscience, 5, 458-462.

Fortin, N.J., Wright, S.P., & Eichenbaum, H. (2004). Recollection-like memory retrieval in rats is dependent on the hippocampus. Nature, 431, 188-191.

Forwood, S.E., Winters, B.D., & Bussey, T.J. (2005). Hippocampal lesions that abolish spatial maze performance spare object recognition memory at delays of up to 48 hours. Hippocampus, 15, 347-355.

Friston, K.J. (1994). Functional and effective connectivity in neuroimaging: A synthesis. Human Brain Mapping, 2, 56-78.

Friston, K.J., Frith, C.D., & Frackowiak, R.S.J. (1993). Time-dependent changes in effective connectivity measured with PET. Human Brain Mapping, 1, 69-79.

Furtak, S.C., Wei, S-M., Agster, K.L., & Burwell, R.D. (2007). Functional neuroanatomy of the parahippocampal region in the rat: The perirhinal and postrhinal cortices. Hippocampus, 17, 709-722.

Gaffan, D. (1974). Recognition impaired and association intact in the memory of monkeys after transection of the fornix. Journal of Comparative and Physiological Psychology, 86, 1100-110.

Gaffan, D. (1994). Dissociated effects of perirhinal cortex ablation, fornix transection and amygdalectomy: evidence for multiple memory systems in the primate temporal lobe. Experimental Brain Research, 99, 411–422.

Gaffan, E.A., & Eacott, M.J. (1997). Spatial memory impairments in rats with fornix transection is not accompanied by a simple encoding deficit for directions of objects in visual space. Behavioral Neuroscience, 111, 937-954.

Gaffan, E.A., & Murray, E.A, (1992). Monkeys (*Macaca fascicularis*) with rhinal cortex ablations succeed in object discrimination learning despite 24-hr intertrial intervals and fail at matching to sample despite double sample presentations. Behavioral Neuroscience, 106, 30-38.

Gaskin, S., Tremblay, A., & Mumby, D.G. (2003). Retrograde and anterograde object recognition in rats with hippocampal lesions. Hippocampus, 13, 962–969.

Gilbert, P.E., Kesner, R.K., & DeCoteau, W.E. (1998). Memory for spatial location: Role of the hippocampus in mediating spatial pattern separation. Journal of Neuroscience, 18, 804-810.

Gilbert, P.E., Kesner, R.P., & Lee, I. (2001). Dissociating hippocampal subregions: A double dissociation between dentate gyrus and CA1. Hippocampus, 11, 626-636.

Gilbert, P.E., & Kesner, R.P. (2003). Localization of function within the dorsal hippocampus: The role of the CA3 subregion in paired-associate learning. Behavioral Neuroscience, 117, 1385–1394.

Glenn, M.J., & Mumby, G.D. (1998). Place memory is intact in rats with perirhinal cortex lesions. Behavioral Neuroscience, 6, 1353-1365

Gold, J.J., Smith, C.N., Bayley, P.J., Brewer, J.B., Stark, C.E., Hopkins, R.O., & Squire, L.R. (2006). Item memory, source memory, and the medial temporal lobe: Concordant findings from fMRI and memory-impaired patients. Proceedings of the National Academy of Science, 103, 9351-9356.

Gonsalves, B.D. Kahn, I., Curran, T., Norman, K.A., & Wagner, A.D. (2005). Memory strength and repetition suppression: Multimodal imaging of medial temporal cortical contributions to recognition. Neuron 47, 751–761.

Good, M., & Bannerman, D. (1997). Differential effects of ibotenic acid lesions of the hippocampus and blockade of N-methyl-D-aspartate receptor-dependent long-term potentiation on contextual processing in rats. Behavioral Neuroscience, 111, 1171-1183.

Good, M.A., Barnes, P., Staal, V., McGregor, A., & Honey, R.C. (2007). Context- but not familiarity-dependent forms of object recognition are impaired following excitotoxic hippocampal lesions in rats. Behavioral Neuroscience, 121, 218-223.

Good, M., & Honey, R.C. (1997). Dissociable effects of selective lesions to hippocampal subsystems on exploratory behavior, contextual learning, and spatial learning. Behavioral Neuroscience, 111, 487–493.

Goulet, S., Dore, F.Y., & Murray, E.A. (1998). Aspiration lesions of the amygdala disrupt the rhinal corticothalamic projection system in rhesus monkeys. Experimental Brain Research, 119, 131-140.

Graham, K.S., Beckler, J.T., Hodges, J.R. (1997). On the relationship between knowledge and memory for pictures: Evidence from the study of patients with semantic dementia and Alzheimer's disease. Journal of the International Neuropsychological Society, 3, 534–544.

Graham, K.S., & Hodges, J.R. (1997). Differentiating the roles of the hippocampus complex and the neocortex in long-term memory storage: Evidence from the study of semantic dementia and Alzheimer's disease. Neuropsychology, 11, 77-89.

Graham, K.S., Simons, J.S., Pratt, K.H., Patterson, K., & Hodges, J.R. (2000). Insights from semantic dementia on the relationship between episodic and semantic memory. Neuropsychologia, 38, 313–324.

Groenewegen, H.J. (1988). Organization of the afferent connections of the mediodorsal thalamic nucleus in the rat, related to the mediodorsal-prefrontal topography. Neuroscience, 24, 379–431.

Gruber, M.J., Gelman, B.D., & Ranganath, C. (2014). States of curiosity modulate hippocampus-dependent learning via the dopaminergic circuit. Neuron, 84, 486–496.

Guedj, E., Aubert, S., McGonigal, A., Mundler, O., & Bartolomei, F. (2010). Déjà-vu in temporal lobe epilepsy: Metabolic pattern of cortical involvement in patients with normal brain MRI. Neuropsychologia, 48, 2174–2181.

Guzowski, J.F. (2002). Insights into immediate-early gene function in hippocampal memory consolidation using antisense oligonucleotide and fluorescent imaging approaches. Hippocampus, 12, 86-104.

Guzowski, J.F., Timlin J.A., Roysam,B., McNaughton B.L., Worley P.F., & Barnes C.A. (2005). Mapping behaviourally relevant neural circuits with immediate-early gene expression. Current Opinion in Neurobiology, 15, 599-606.

Hamann, S.B., & Squire, L.R. (1997). Intact perceptual memory in the absence of conscious memory. Behavioral Neuroscicnce, 111, 850-854.

Hammond, R.S., Tull, L.E., & Stackman, R.W. (2004). On the delay-dependent involvement of the hippocampus in object recognition memory. Neurobiology of Learning and Memory, 82, 26–34.

Hannesson, D.K., Vacca, G., Howland, J.G., & Phillips, A.G. (2004a). Medial prefrontal cortex is involved in spatial temporal order memory but not spatial recognition memory in tests relying on spontaneous exploration in rats. Behavioural Brain Research, 153, 273-285.

Hannesson, D.K., Howland, J.G., & Phillips, A.G. (2004b). Interaction between perirhinal and medial prefrontal cortex is required for temporal order but not recognition memory for objects in rats. Journal of Neuroscience, 24, 4596-4604.

He, J., Yamada, K., & Nabeshima, T. (2002). A role of Fos expression in the CA3 region of the hippocampus in spatial memory formation in rats. Neuropsychopharmacology, 26, 259 –268.

Heidbreder, C.A., & Groenewegen, H.J. (2003). The medial prefrontal cortex in the rat: evidence for a dorso-ventral distinction based upon functional and anatomical characteristics. Neuroscience and Biobehavioral Reviews, 27, 555–579.

Henson, R.N.A., Cansino, S., Herron, J.E., Robb, W.G.K., & Rugg, M. D. (2003). A familiarity signal in human anterior medial temporal cortex? Hippocampus, 13, 301-304.

Herdegen, T. (1996). Jun, Fos, and CREB/ATF transcription factors in the brain: control of gene expression under normal and pathophysiological conditions. The Neuroscientist, 2, 153-161.

Herrera, D.G., & Robertson, H.A. (1996). Activation of c-fos in the brain. Progress in Neurobiology, 50, 83-107.

Ho, J.W-T., Narduzzo, K.E., Outram, A., Tinsley, C.J., Henley, J.M., Warburton, E.C., & Brown, M.W. (2011). Contributions of area Te2 to rat recognition memory. Learning & Memory, 18, 493-501.

Hoge, J., & Kesner, R.P. (2007). Role of CA3 and CA1 subregions of the dorsal hippocampus on temporal processing of objects. Neurobiology of Learning and Memory 88, 225-231.

Holdstock, J.S., Mayes, A.R., Gong, Q.Y., Roberts, N., & Kapur, N. (2005). Item recognition is less impaired than recall and associative recognition in a patient with selective hippocampal damage. Hippocampus, 15, 230-215.

Honey, R.C., & Good, M. (1993). Selective hippocampal lesions abolish the contextual specificity of latent inhibition and conditioning. Behavioral Neuroscience, 107, 23-33.

Howell, D.C. (2011). Statistical Methods for Psychology, 8th ed: Wadsworth Cengage Learning.

Hoyle, R.H. (2012) Handbook of structural equation modeling. The Guilford Press, New York.

Hsieh, L.-T., Gruber, M.J., Jenkins, L.J., & Ranganath, C. (2014). Hippocampal activity patterns carry information about objects in temporal context. Neuron, 81, 1165–1178.

Hu, L., & Bentler, P.M. (1998). Fit indices in covariance structure modeling: Sensitivity to underparameterized model misspecification. Psychology Methods, 3, 424-453.

Hunsaker, M.R., & Kesner, R.P. (2013). The operation of pattern separation and pattern completion processes associated with different attributes or domains of memory. Neuroscience and Biobehavioral Reviews, 37, 36-58.

Hunsaker, M.R., Chen, V., Tran, G.T., & Kesner, R.P. (2013). The Medial and Lateral Entorhinal Cortex Both Contribute to Contextual and Item Recognition Memory: A Test of the Binding of Items and Context Model. Hippocampus, 23, 380-391.

Hunsaker, M.R., Rogers, J.L., & Kesner, R.P. (2007). Behavioural characterization of a transection of dorsal CA3 subcortical efferents: Comparison with scopolamine and physostigmine infusions into dorsal CA3. Neurobiology of Learning and Memory, 88, 127-136.

Hunsaker, M.R., Rosenberg, J.S., & Kesner, R.P. (2008). The role of the dentate gyrus, CA3a,b, and CA3c for detecting spatial and environmental novelty. Hippocampus 18, 1064-1073.

Inhoff, M.C., & Ranganath, C. (2015). Significance of objects in the perirhinal cortex. Trends in Cognitive Sciences. 19, 302-303.

Insausti, R., Herrero, M.T., & Witter, M.P. (1997). Entorhinal cortex of the rat: Cytoarchitectonic subdivisions and the origin and distribution of cortical efferents. Hippocampus, 7, 146-183.

Iordanova, M.D., Burnett, D.J., Aggleton, J.P., Good, M.A., & Honey, R.C. (2009). The role of the hippocampus in mnemonic integration and retrieval: complementary evidence from lesion and inactivation studies. European Journal of Neuroscience, 30, 2177-2189.

Jackson-Smith, P., Kesner, R.P., & Chiba, A.A. (1993). Continuous recognition of spatial and nonspatial stimuli in hippocampal-lesioned rats. Behav. Neural Biol. 59, 107–119.

Jenkins, T.A., Amin, E., Harold, G.T., Pearce, J.M., & Aggleton, J.P. (2003). Different patterns of hippocampal formation activity associated with different spatial tasks: a Fos imaging study in rats. Experimental Brain Research, 151, 514-523.

Jenkins, T.A., Amin, E., Pearce, J.M., Brown, M.W., & Aggleton, J. P. (2004). Novel spatial arrangements of familiar stimuli promote activity in the rat hippocampal formation but not the parahippocampal cortices; a c-fos expression study. Neuroscience, 124, 43-52.

Jenkins, T.A., Dias, R., Amin, E., Brown, M.W., & Aggleton, J.P. (2002). Fos imaging reveals that lesions of the anterior thalamic nuclei produce widespread limbic hypoactivity in rats. Journal of Neuroscience, 22, 5230–523.

Jenkins, T.A., Vann, S.D., Amin, E., & Aggleton, J.P. (2004). Anterior thalamic lesions stop immediate early gene activation in selective laminae of the retrosplenial cortex: evidence of covert pathology in rats? European Journal of Neuroscience, 19, 3291-3304.

Jeneson, A., Kirwan, C.B., Hopkins, R.O., Wixted, J.T., & Squire, L.R. (2010). Recognition memory and the hippocampus: A test of the hippocampal contribution to recollection and familiarity. Learning & Memory, 17, 852-859.

Jo, Y.S., & Lee, I. (2010). Disconnection of the hippocampal–perirhinal cortical circuits severely disrupts object–place paired associative memory. Journal of Neuroscience, 30, 9850 –9858.

Jones, P.M., Whitt, E.J., Robinson, J. (2012). Excitotoxic perirhinal cortex lesions leave stimulus-specific habituation of suppression to lights intact. Behavioural Brain Research, 229, 365–371.

Jones, B.F., & Witter, M.P. (2007). Cingulate cortex projections to the parahippocampal region and hippocampal formation in the rat. Hippocampus, 17, 957-976.

Katche, C., Bekinschtein, P., Slipczuk, L., Goldin, A., Izquierdo, I.A., Cammarota, M., & Medina, J.H. (2010). Delayed wave of c-Fos expression in the dorsal hippocampus involved specifically in persistence of long-term memory storage. Proceedings of the National Academy of Science, 107, 349-354.

Kent, B.A., & Brown, T.H. (2012). Dual Functions of Perirhinal Cortex in Fear Conditioning. Hippocampus, 22, 2068–2079.

Kesner, R.P., Bolland, B.L., & Dakis, M. (1993). Memory for spatial locations, motor responses, and objects: triple dissociation among the hippocampus, caudate nucleus, and extrastriate visual cortex. Experimental Brain Research 93, 462–470.

Kesner, R.P., Gilbert, P.E., & Barua, L.A. (2002). The role of the hippocampus in memory for the temporal order of a sequence of odors. Behavioral Neuroscience, 116, 286-290.

Kesner, R.P., Hunsaker, M.R., & Ziegler, W. (2010). The role of the dorsal CA1 and ventral CA1 in memory for the temporal order of a sequence of odors. Neurobiology of Learning and Memory, 93, 111-116.

Kensinger, E.A., & Schacter, D.L. (2006). Amygdala activity is associated with the successful encoding of item, but not source, information for positive and negative stimuli. Journal of Neuroscience, 26, 2564 –2570.

Kholodar-Smith, D.B., Boguszewski, P., Brown, T.H. (2008a). Auditory trace fear conditioning requires perirhinal cortex. Neurobiology of Learning and Memory, 90, 537–543.

Kholodar-Smith, D.B., Allen, T.A., & Brown, T.H. (2008b). Fear conditioning to discontinuous auditory cues requires perirhinal cortical function. Behavioral Neuroscience, 5, 1178-1185.

Kim, J., & Horwitz, B. (2009). How well does structural equation modeling reveal abnormal brain anatomical connections? An fMRI Simulation Study. NeuroImage, 45, 1190–1198.

King, J.A., Trinkler, I., Hartley, T., Vargha-Khadem, F., & Burgess, N. (2004). The hippocampal role in spatial memory and the familiarity–recollection distinction: A case study. Neuropsychology, 18, 205-417.

Kinnavane, L., Amin, E., Horne, M., & Aggleton, J.P. (2014). Mapping parahippocampal systems for recognition and recency memory in the absence of the rat hippocampus. European Journal of Neuroscience, 40, 3720–3734.

Kirwan, C.B., Wixted, J.T., & Squire, L.T. (2010). A demonstration that the hippocampus supports both recollection and familiarity. Proceedings of the National Academy of Science, 107, 344-348.

Kivy, P., Earl, R.W., & Walker, E.L. (1956). Stimulus context and satiation. Journal of Comparative and Physiological Psychology, 49, 90-92.

Knierim, J.J., Lee, I., & Hargreaves, E.L. (2006). Hippocampal place cells: Parallel input streams, subregional processing and implications for episodic memory. Hippocampus 16, 755-764.

Knierim, J.J., Neunuebel, J.P., & Deshmukh, S.S. (2014). Functional correlates of the lateral and medial entorhinal cortex: objects, path integration and local-global reference frames. Philosophical Transactions of the Royal Society B: Biological Sciences, 369, 20130369.

Koganezawa, N., Taguchi, A., Tominaga, T., Ohara, S., Tsutsui, K.-I., Witter, M.P., & Iijima, T. (2008). Significance of the deep layers of entorhinal cortex for transfer of both perirhinal and amygdala inputs to the hippocampus. Neuroscience Research, 61, 172–181.

Komorowski, R.W., Manns, J.R., Eichenbaum, H. (2009). Robust conjunctive item-place coding by hippocampal neurons parallels learning what happens where. Journal of Neuroscience, 29, 9918–9929.

Kovacs, K.J. (2008). Measurement of immediate-early gene activation- c-fos and beyond. Journal of Neuroendocrinology, 20, 665-672.

Kraus, B.J., Robinson II, R.J., White, J.A., Eichenbaum, H., & Hasselmo, M.E., (2013). Hippocampal “time cells”: Time versus path integration. Neuron, 78, 1090-1101.

Lanahan, A., & Worley P. (1998). Immediate-early genes and synaptic function. Neurobiology of Learning and Memory, 70, 37-43.

Lanciego, J.L., & Wouterlood, F.G (2011). A half century of experimental neuroanatomical tracing. Journal of Chemical Neuroanatomy, 42, 157–183.

Langston, R.F., Stevenson, C.H., Wilson, C.L., Saunders, I., & Wood, E.R. (2010). The role of hippocampal subregions in memory for stimulus associations. Behavioural Brain Research, 215, 275-291.

Langston, R.F., & Wood, E.R. (2010). Associative recognition and the hippocampus: Differential effects of hippocampal lesions on object-place, object-context and object-place-context memory. Hippocampus, 20, 1139-1153.

Lee, A.C., Buckley, M.J., Pegman, S.J., Spiers, H., Scahill, V.L., Gaffan, D., Bussey, T.J., Davies, R.R., Kapur, N., Hodges, J.R., & Graham, K.S. (2005a). Specialization in the medial temporal lobe for processing of objects and scenes. Hippocampus, 15, 782–797.

Lee, A.C.H., Buckley, M.J., Gaffan, D., Emery, T., Hodges, J.R., & Graham, K.S. (2006). Differentiating the roles of the hippocampus and perirhinal cortex in processes beyond long-term declarative memory: A double dissociation in dementia. Journal of Neuroscience, 26, 5198 –5203.

Lee, A.C., Bussey, T.J., Murray, E.A., Saksida, L.M., Epstein, R.A., Kapur, N., Hodges, J.R., & Graham, K.S. (2005b). Perceptual deficits in amnesia: challenging the medial temporal lobe 'mnemonic' view. Neuropsychologia, 43, 1–11.

Lee, I., & Kesner, R.P. (2004). Differential contributions of dorsal hippocampal subregions to memory acquisition and retrieval in contextual fear-conditioning. Hippocampus, 14, 301-310.

Lee, A.C.H., Levi, N., Davies, R.R., Hodges, J.R., & Graham, K.S. (2007). Differing profiles of face and scene discrimination deficits in semantic dementia and Alzheimer's disease. Neuropsychologia, 45, 2135–2146.

Lee, I., Hunsaker, M.R., & Kesner, R.P. (2005). The role of hippocampal subregions in detecting spatial novelty. Behavioral Neuroscience, 119, 145-153.

Lee, H., Wang, C., Deshmukh, S.S., Knierim, J.J. (2015). Neural population evidence of functional heterogeneity along the CA3 transverse axis: Pattern completion versus pattern separation. Neuron, 87, 1093‑1105.

Lee, H.J., Youn, J.M., O, M.J., Gallagher, M., & Holland, P.C. (2006). Role of substantia nigra–amygdala connections in surprise-induced enhancement of attention. The Journal of Neuroscience, 26, 6077-6081.

Leutgeb, J.K., Leutgeb, S., Moser, M.B., & Moser, E.I. (2007). Pattern separation in the dentate gyrus and CA3 of the hippocampus. Science, 315, 961-966.

Lindquist, D.H., Jarrard, L.E., & Brown, T.H. (2004). Perirhinal cortex supports delay fear conditioning to rat ultrasonic social signals. Journal of Neuroscience, 24, 3610 – 3617.

Lisman, J.E., & Grace, A.A. (2005). The hippocampal-VTA loop: Review controlling the entry of information into long-term memory. Neuron, 46, 703-713.

Lisman, J.E., Grace, A.A., & Duzel, E. (2011). A neoHebbian framework for episodic memory; role of dopamine-dependent late LTP. Trends in Neurosciences, 34, 536-547.

Liu, P., & Bilkey, D. K. (1998a). Excitotoxic lesions centered on perirhinal cortex produce delay- dependent deficits in a test of spatial memory. Behavioral Neuroscience, 112, 512–524.

Liu, P., & Bilkey, D. K. (1998b). Lesions of perirhinal cortex produce spatial memory deficits in the radial maze. Hippocampus, 8, 114–121.

Liu, P., & Bilkey, D.K. (2001). The effect of excitotoxic lesions centred on the hippocampus or perirhinal cortex in object recognition and spatial memory tasks. Behavioral Neuroscience, 115, 94–111.

Liu, X., Ramirez, S., Pang, P., Puryear, C., Govindarajan, A., Deisseroth, K., & Tonegawa, S. (2012). Optogenetic stimulation of a hippocampal engram activates fear memory recall. Nature, 484, 381–385.

Lu, L., Igarashi, K.M., Witter, M.P., Moser, E.I., & Moser, M.-B. (2015). Topography of place maps along the CA3-to-CA2 axis of the hippocampus. Neuron, 87, 1078‑1092.

Lu, H., Zou, Q., Gu, H., Raichle, M.E., Stein, E.A., & Yang, Y. (2012). Rat brains also have a default mode network. Proceedings of the National Academy of Science, 109, 3979–3984

Machin, P., Vann, S.D., Muir, J.L., & Aggleton, J.P. (2002). Neurotoxic lesions of the rat perirhinal cortex fail to disrupt the acquisition or performance of tests of allocentric spatial memory. Behavioral Neuroscience, 116, 232-240.

Mandler, G. (1980). Recognizing - the Judgment of Previous Occurrence. Psychological Review, 87, 252-271.

Manns, J.R., & Eichenbaum, H. (2009). A cognitive map for object memory in the hippocampus. Learning & Memory, 16, 616–624.

Manns, J.R., Howard, M.W., & Eichenbaum, H. (2007). Gradual changes in hippocampal activity support remembering the order of events. Neuron, 56, 530–540.

Manns, J.R., Hopkins, R.O., Reed, J.M., Kitchener, E.G., & Squire, L.R. (2003). Recognition Memory and the Human Hippocampus. Neuron, 37, 171-180.

Maren, S., & Fanselow M.S. (1997). Electrolytic lesions of the fimbria/fornix, dorsal hippocampus, or entorhinal cortex produce anterograde deficits in contextual fear conditioning in rats. Neurobiology of Learning and Memory, 67, 124-149.

Martin, C.B., Bowles, B., Mirsattari, S.M., & Kohler, S. (2011). Selective familiarity deficits after left anterior temporal-lobe removal with hippocampal sparing are material specific. Neuropsychologia, 49, 1870–1878.

Martin, C.B., Mirsattari, S.M., Pruessner, J.C., Pietrantonio, S., Burneo, J.G., Hayman-Abello, B., & Kohler, S. (2012). Déjà vu in unilateral temporal-lobe epilepsy is associated with selective familiarity impairments on experimental tasks of recognition memory. Neuropsychologia, 50, 2981–2991.

Mayes, A.R., Holdstock, J.S., Isaac, C.L., Hunkin, N.M., & Roberts, N. (2002). Relative sparing of item recognition memory in a patient with adult-onset damage limited to the hippocampus. Hippocampus, 12, 325–340.

Mayes, A. R., Holdstock, J. S., Isaac, C. L., Montaldi, D., Grigor, J., Gummer, A., Cariga, P., Downes, J.J., Tsivilis, D., Gaffan, D., Gong, Q., & Norman, K.A. (2004). Associative recognition in a patient with selective hippocampal lesions and relatively normal item recognition. Hippocampus, 14, 763–784.

Mayes, A., Montaldi, D., & Migo, E. (2007). Associative memory and the medial temporal lobes. Trends in Cognitive Sciences, 11, 126-135.

McIntosh, A.R. (2002). Application of covariance structural equation modeling to the exploration of neurocognitive networks. In: Handbook of brain theory and neural networks, 2nd Edition (Arbib M.A., ed.). pp. 300-304. Cambridge, Massachusetts: MIT Press.

McIntosh, A.R., & Gonzalez-Lima, F. (1991). Structural modeling of functional neural pathways mapped with 2-deoxyglucose: effects of acoustic startle habituation on the auditory system. Brain Research, 547, 295-302.

McIntosh, A.R., Gonzalez-Lima, F. (1994). Structural equation modelling and its application to network analysis in functional brain imaging. Human Brain Mapping, 2, 2-22.

McKenzie, S., Frank, A.J., Kinsky, N.R., Porter, B., Riviere, P.D., & Eichenbaum, H. (2014). Hippocampal representation of related and opposing memories develop within distinct, hierarchically organized neural schemas. Neuron, 83, 202–215.

McNaughton, B.L., Battaglia, F.P., Jensen, O., Moser E.I.,& Moser, M.B. (2006). Path integration and the neural basis of the 'cognitive map'. Nature Review Neuroscience, 7, 663–678.

McTighe, S. M., Cowell, R. A., Winters, B. D., Bussey, T. J., & Saksida, L. M. (2010). Paradoxical false memory for objects after brain damage. Science, 330, 1408–1410.

Meunier, M., Bachevalier, J., Mishkin, M., & Murray, E. A. (1993). Effects on visual recognition of combined and separate ablations of the entorhinal and perirhinal cortex in rhesus monkeys. Journal of Neuroscience, 13, 5418–5432.

Meyer, T., Walker, C., Cho, R.Y., & Olson, C.R. (2014). Image familiarization sharpens response dynamics of neurons in inferotemporal cortex. Nature Neuroscience, 17, 1388-1394.

Mishkin, M. (1978). Memory in monkeys severely impaired by combined but not by separate removal of amygdala and hippocampus. Nature, 273, 297-298.

Mishkin, M., & Delacour, J. (1975). An analysis of short-term visual memory in the monkey. Journal of Experimental Psychology: Animal Behavior Processes 1, 326-334.

Mitchell, J.B., & Laiacona, J., (1998). The medial frontal cortex and temporal memory: tests using spontaneous exploratory behaviour in the rat. Behavioural Brain Research, 97, 107-113.

Mitchell, J.B., & Dalrymple-Alford, J.C. (2005). Dissociable memory effects after medial thalamus lesions in the rat. European Journal of Neuroscience, 22, 973–985.

Montaldi, D., Spencer, T.J., Roberts, N., & Mayes, A.R. (2006). The neural system that mediates familiarity memory. Hippocampus, 16, 504-520.

Morris, R.G.M., Garrud, P., Rawlins, J.N.P., & O'Keefe, J. (1982). Place navigation impaired in rats with hippocampal lesions. Nature, 297, 681-683.

Moser, E., Moser, M.B., & Andersen, XXX. (1993). Spatial learning impairment parallels the magnitude of dorsal hippocampal lesions, but is hardly present following ventral lesions. Journal of Neuroscience, 13, 3916-3925.

Moser, E.I., Kropff, E., & Moser, M.B. (2008). Place cells, grid cells, and the brain's spatial representation system. Annual Review of Neuroscience, 31, 69-89.

Mumby, D.G. (2001). Perspectives on object-recognition memory following hippocampal damage: lessons from studies in rats. Behavioral Brain Research, 127, 159–181.

Mumby, D.G., Gaskin, S., Glenn, M.J., Schramek, T.E., & Lehmann, H. (2002). Hippocampal damage and exploratory preferences in rats: Memory for objects, places, and contexts. Learning & Memory, 9, 49-57.

Mumby, D.G., Pinel, J.P.J., & Wood, E.R. (1990). Nonrecurring-items delayed nonmatching-to-sample in rats: A new paradigm for testing nonspatial working memory. Psychobiology, 18, 321-326.

Mumby, D.G., & Pinel, J.P. (1994). Rhinal cortex lesions and object recognition in rats. Behavioral Neuroscience, 108, 11-18.

Mumby, D.G., Pinel, J.P.J., Kornecook, T.J., Shen, M.J., & Redlia, V.A. (1995). Memory deficits following lesions of hippocampus or amygdala in rat object recognition: Assessment by an object-memory test battery. Psychobiology, 23, 26-36.

Mumby, D.G., Piterkin, P., Lecluse, V., & Lehmann, H. (2007). Perirhinal cortex damage and anterograde object-recognition in rats after long retention intervals. Behavioural Brain Research, 185, 82–87.

Mumby, D.G., Wood, E.R., Duva, C.A., Kornecook, T.J., Pinel, J.P., & Phillips, A.G., (1996). Ischemia-induced object-recognition deficits in rats are attenuated by hippocampal ablation before or soon after ischemia. Behavioral Neuroscience 110, 266–281.

Mumby, D.G., Wood, E.R., & Pinel, J.P.J. (1992). Object-recognition memory is only mildly impaired in rats with lesions of the hippocampus and amygdala. Psycholobiology, 20, 18-27.

Mura, A., Murphy, C.A., Feldon, J., & Jongen-Relo, A.L. (2004). The use of stereological counting methods to assess immediate early gene immunoreactivity. Brain Research, 1009, 120–128.

Murray, E.A. (1996). What have ablation studies told us about the neural substrates of stimulus memory? Seminars in Neuroscience, 8, 13-22.

Murray, E.A., & Bussey, T.J. (1999). Perceptual-mnemonic functions of the perirhinal cortex. Trends in Cognitive Sciences. 3, 142-151.

Murray, E.A., & Mishkin, M. (1985). Amygdalectomy impairs crossmodal association in monkeys. Science, 228, 604-606.

Murray, E.A., & Mishkin, M. (1986). Visual recognition in monkeys following rhinal cortical ablations combined with either amygdalectomy or hippocampectomy. Journal of Neuroscience, 6, 1991-2003.

Murray, E.A., & Mishkin, M. (1998). Object recognition and location memory in monkeys with excitotoxic lesions of the amygdala and hippocampus. Journal of Neuroscience, 18, 6568-6582.

Murray, E. A., & Richmond, B.J. (2001). Role of perirhinal cortex in object perception, memory, and associations. Current Opinion in Neurobiology, 11, 188-193.

Murray, E. A., Bussey, T. J., & Saksida, L. M. (2007). Visual perception and memory: A new view of medial temporal lobe function in primates and rodents. Annual Review of Neuroscience, 30, 99–122.

Murray, E.A., & Wise, S.P. (2012). Why is there a special issue on perirhinal cortex in a journal called Hippocampus? The perirhinal cortex in historical perspective. Hippocampus, 22, 1941–1951.

Naber, P.A., Caballero-Bleda, M., Jorritsma-Byham, B., & Witter, M.P. (1998). Parallel input to the hippocampal memory system through peri- and postrhinal cortices. Neuroreport, 8, 2617–2621.

Nakashiba, T., Young, J.Z., McHugh, T.J., Buhl, D.L., Tonegawa, S. (2008). Transgenic Inhibition of Synaptic Transmission Reveals Role of CA3 Output in Hippocampal Learning. Science, 319, 1260-1264.

Nelson, A.J.D., & Vann, S.D. (2014). Mammillothalamic tract lesions disrupt tests of visuo-spatial memory. Behavioral Neuroscience, 128, 494-503.

Nemanic, S., Alvarado, M.C., & Bachevalier, J. (2004). The hippocampal/parahippocampal regions and recognition memory: Insights from visual paired comparison versus object-delayed nonmatching in monkeys. Journal of Neuroscience, 24, 2013-2026.

Neunuebel, J.P., & Knierim, J.J. (2014). CA3 retrieves coherent representations from degraded input: Direct evidence for CA3 pattern completion and dentate gyrus pattern separation. Neuron, 81, 416–427.

Neunuebel, J.P., Yoganarasimha, D., Rao, G., & Knierim, J.J. (2013). Conflicts between local and global spatial frameworks dissociate neural representations of the lateral and medial entorhinal cortex. Journal of Neuroscience, 33, 9246-9258.

Norman, G., & Eacott, M.J. (2004). Impaired object recognition with increasing levels of feature ambiguity in rats with perirhinal cortex lesions. Behavioural Brain Research 148, 79–91.

Norman, G., & Eacott, M.J. (2005). Dissociable effects of lesions to the perirhinal cortex and the postrhinal cortex on memory for context and objects in rats. Behavioral Neuroscience, 119, 557-566.

Norman, K.A., & O'Reilly, R.C. (2003). Modeling hippocampal and neocortical contributions to recognition memory: A complementary learning-systems approach. Psychological Review, 110, 611-646.

Naya, Y., Yoshida, M., Miyashita, Y. (2003). Forward processing of long-term associative memory in monkey inferotemporal cortex. Journal of Neuroscience, 23, 2861-2871.

O'Brien, N., Lehmann, H., Lecluse, V., & Mumby, D.G. (2006). Enhanced context-dependency of object recognition in rats with hippocampal lesions. Behavioral Brain Research, 170, 156-162.

O'Keefe, J., & Burgess, N. (1996). Geometric determinants of the place fields of hippocampal neurons. Nature 381, 425-428.

O'Keefe, J., & Dostrovsky, J. (1971). The hippocampus as a spatial map. Preliminary evidence from unit activity in the freely-moving rat. Brain Research 34, 171–75.

Ohara, S., Sato, S., Tsutsui, K., Witter, M.P., & Iijima, T. (2013). Organization of multisynaptic inputs to the dorsal and ventral dentate gyrus: retrograde trans-synaptic tracing with rabies virus vector in the rat. PLoS One, 8, e78928.

Olarte-Sánchez, C.M., Kinnavane, L., Amin, A., & Aggleton, J.P. (2014). Contrasting networks for recognition memory and recency memory revealed by immediate-early gene imaging in the rat. Behav Neurosci, 128, 504-522.

Olarte-Sánchez, C.M., Amin, A., Warburton, E.C., & Aggleton, J.P. (2015). Perirhinal cortex lesions impair object recognition memory yet spare novelty detection and landmark discriminations. European Journal of Neuroscience. Manuscript under review.

Olton, D.S., Becker, J.T., & Handelmann, G.E. (1979). Hippocampus, space and memory. Behavioral and Brain Sciences, 2, 313-365.

Pascalis, O., Hunkin, N.M., Holdstock, J.S., Isaac, C.L., & Mayes, A.R. (2004). Visual paired comparison performance is impaired in a patient with selective hippocampal lesions and relatively intact item recognition. Neuropsychologia, 42, 1293-1300.

Paxinos, G., & Watson, C. (2005). The Rat Brain in Stereotaxic Coordinates, 5th edn. Elsevier Academic Press, San Diego.

Pearce, J.M., & Hall, G. (1980). A model for Pavlovian learning: Variations in the effectiveness of conditioned but not unconditioned stimuli. Psychological Review, 82, 532-552.

Peters, J., Thoma, P., Koch, B., Schwarz, M., & Daum, I. (2009). Impairment of verbal recollection following ischemic damage to the right anterior hippocampus. Cortex, 45, 592-601.

Phillips, R.G., & LeDoux, J.E. (1992). Differential contribution of amygdala and hippocampus to cued and contextual fear conditioning. Behavioral Neuroscience, 106, 274-285.

Poirier, G.L., Amin, E., & Aggleton, J.P. (2008). Qualitatively different patterns of hippocampal subfield engagement emerge with mastery of a spatial memory task: a study of Zif268 activity in rats. Journal of Neuroscience, 28, 1034-1045.

Prasad, J.A., & Chudasama, Y. (2013). Viral tracing identifies parallel disynaptic pathways to the hippocampus. Journal of Neuroscience, 33, 8494–8503.

Poucet, B., Chapuis, N., Durup, M., & Thinus-Blanc, C. (1986). A study of exploratory behavior as an index of spatial knowledge in hamsters. Animal Learning and Behavior, 14, 93-100.

Poucet, B. (1989). Object exploration, habituation, and response to a spatial change in rats following septal or medial frontal cortical damage. Behavioral Neuroscience, 103, 1009-1016.

Protzner, A.B., & McIntosh, A.R. (2006). Testing effective connectivity changes with structural equation modeling: What does a bad model tell us? Human Brain Mapping, 27, 935-947.

Prusky, G.T., Douglas, R.M., Nelson, L., Shabanpoor, A., & Sutherland, R.J., (2004). Visual memory task for rats reveals an essential role for hippocampus and perirhinal cortex. Proceedings of the National Academy of Sciences of the United States of America. 101, 5064–5068.

Ramirez, S., Liu, X., Lin,P.-A., Suh, J., Pignatelli, M. Redondo, R.L., Ryan, T.J., & Tonegawa, S. (2013). Creating a false memory in the hippocampus. Science, 341, 387-391.

Ranganath, C. (2010). Binding items and contexts: The cognitive neuroscience of episodic memory. Current Directions in Psychological Science, 19, 131-137.

Ranganath, C., & Ritchey, M. (2012). Two cortical systems for memory guided behaviour. Nature Reviews Neuroscience, 13, 713-726.

Ranganath, C., Yonelinas, A.P., Cohen, M.X., Dy, C.J., Tom, S.M., & D'Esposito, M. (2003). Dissociable correlates of recollection and familiarity within the medial temporal lobes. Neuropsychologia, 42, 2-13.

Rawlins, J.N., Lyford, G.L., Seferiades, A., Deacon, R.M., & Cassaday, H.J. (1993). Critical determinants of nonspatial working memory deficits in rats with conventional lesions of the hippocampus or fornix. Behavioral Neuroscience 107, 420–433.

Richmond, M.A., Yee, B.K., Pouzet, B., Veenman, L., Rawlins, J.N.P., Feldon, J., & Bannerman, D.M. (1999). Dissociating context and space within the hippocampus: Effects of complete, dorsal, and ventral excitotoxic hippocampal lesions on conditioned freezing and spatial learning. Behavioral Neuroscience, 113, 1189-1203.

Robinson, J., Sanderson, D.J., Aggleton, J.P., Jenkins, T.A. (2009). Suppression to visual, auditory, and gustatory stimuli habituates normally in rats with excitotoxic lesions of the perirhinal cortex. Behavioral Neuroscience, 123, 1238–1250.

Robitsek, R.J., Fortin, N.J., Koh, M.T., Gallagher, M., & Eichenbaum, H. (2008). Cognitive aging: A common decline of episodic recollection and spatial memory in rats. Journal of Neuroscience, 28, 8945–8954.

Rolls, E.T., Cahusac, P.M.B., Feigenbaum, J.D., & Miyashita, Y. (1993). Responses of single neurons in the hippocampus of the macaque related to recognition memory. Experimental Brain Research 93, 299–306.

Romberg, C., McTighe, S.M., Heath, C.J., Whitcomb, D.J., Cho, K., Bussey, T.J., & Saksida, L.M. (2012). False recognition in a mouse model of Alzheimers disease: Rescue with sensory restriction and memantine. Brain: A Journal of Neurology, 135, 2103–2114.

Rossato, J.I., Bevilaqua, L.R., Myskiw, J.C., Medina, J.H., Izquierdo, I., & Cammarota, M. (2007). On the role of hippocampal protein synthesis in the consolidation and reconsolidation of object recognition memory. Learning & Memory, 14, 36–46.

Rothblat, L.A., & Kromer, L.F. (1991). Object recognition memory in the rat: the role of the hippocampus. Behavioural Brain Research 42, 25–32.

Rudebeck, S.R., Scholz, J., Millington, R., Rohenkohl, G., Johansen-Berg, H., & Lee, A.C. (2009). Fornix microstructure correlates with recollections but not familiarity memory. Journal of Neuroscience, 29, 14987-14992.

Ruth, R.E., Collier, T.J., & Routtenberg, A. (1988). Topographical relationship between the entorhinal cortex and the septotemporal axis of the dentate gyrus in rats: II. Cells projecting from lateral entorhinal subdivisions. Journal of Comparative Neurology, 270, 506-516.

Rutishauser, U., Mamelak, A.N., & Schuman, E.M. (2006). Single-trial learning of novel stimuli by individual neurons of the human hippocampus-amygdala complex. Neuron, 49, 805-813.

Sacchetti, B., Ambrogi Lorenzini, C., Baldi, E., Tassoni, G., & Bucherelli, C. (1999). Auditory thalamus, dorsal hippocampus, basolateral amygdala, and perirhinal cortex role in the consolidation of conditioned freezing to context and to acoustic conditioned stimulus in the rat. Journal of Neuroscience, 19, 9570–9578.

Saksida, L.M., Bussey, T.J., Buckmaster, C.A., & Murray, E.A. (2006). No effect of hippocampal lesions on perirhinal cortex-dependent feature-ambiguous visual discriminations. Hippocampus, 16, 421–430.

Saksida, L.M., Bussey, T.J., Buckmaster, C.A., & Murray, E.A. (2007). Impairment and facilitation of transverse patterning after lesions of the perirhinal cortex and hippocampus, respectively. Cerebral Cortex, 17, 108—115.

Salvetti, B., Morris, R.G.M., Wang, S.-H. (2014). The role of rewarding and novel events in facilitating memory persistence in a separate spatial memory task. Learning & Memory, 21, 61–72.

Sauvage, M.M., Beer, B., & Eichbaum, H. (2010). Recognition memory: Adding a response deadline eliminates recollection but spares familiarity. Learning & Memory, 17, 104-108.

Sauvage, M.M., Fortin, N.J., Owens, C.B., Yonelinas, A.P., & Eichbaum, H. (2008). Recognition memory: opposite effects of hippocampal damage on recollection and familiarity. Nature Neuroscience, 11, 16-18.

Save, E., Poucet, B., Foreman, N., & Buhbot, M-C. (1992). Object exploration and reactions to spatial and nonspatil changes in hooded rats following damage to parietal cortex or hippocampal formation. Behavioral Neuroscience, 106, 447-456.

Schimdt, B., Marrone, D.F., & Markus, E.J. (2012). Disambiguating the similar: The dentate gyrus and pattern separation. Behavioural Brain Research, 226, 56– 65.

Schofield, B.R. (2008). Retrograde axonal tracing with fluorescent markers. Current Protocols in Neuroscience, 43:1.17:1.17.1–1.17.24.

Schumacker, R.E., & Lomax, R.G. (2010). A Beginners Guide to Structural Equation Modelling, 3rd edn. Routledge, Taylor & Francis Group, New York.

Scoville, W.B., & Milner, B (1976). Loss of recent memory after bilateral hippocampal lesions. Journal of Neurology Neurosurgery Psychiatry, 20, 11-21.

Seoane, A., Tinsley, C.J., &. Brown, M.W. (2012). Interfering with Fos expression in rat perirhinal cortex impairs recognition memory. Hippocampus, 22, 2101-2113.

Shaw, C., & Aggleton, J.P. (1993). The effects of fornix and medial prefrontal lesions on delayed nonmatching-to-sample by rats. Behavioural Brain Research, 54, 91-102.

Sheth, A., Berretta, S., Lange, N., & Eichenbaum, H. (2008). The amygdala modulates neuronal activation in the hippocampus in response to spatial novelty. Hippocampus, 18, 169-181.

Shrager, Y., Gold, J.J., Hopkins, R.O., & Squire, L.R. (2006). Intact visual perception in memory impaired patients with medial temporal lobe lesions. Journal of Neuroscience, 26, 2235–2240.

Shrager, Y., Kirwan, C.B., & Squire, L.R. (2008). Activity in both hippocampus and perirhinal cortex predicts the memory strength of subsequently remembered information. Neuron 59, 547–553.

Simons, J.S., Verfaellie, M., Hodges, J.R., Lee, A.C., Graham, K.S., Koutstaal, W., Schacter, D.L., & Budson, A.E. (2005). Failing to get the gist: Reduced false recognition of semantic associates in semantic dementia. Neuropsychology,19, 353-361.

Sikes, R.W., Chronister, R.B., & White, L.E. Jr. (1977). Origin of the direct hippocampus-anterior thalamic bundle in the rat: a combined horseradish peroxidase—Golgi analysis. Experimental Neurology, 57, 379–395.

Smith, C.N. Jeneson, A., Frascinoa, A.C., Kirwan, C.B., Hopkins, R.M., & Squire, L.A. (2014). When recognition memory is independent of hippocampal function. Proceedings of the National Academy of Science, 111, 9935-9940.

Streiner, D.L. (2005) Finding our way: An introduction to path analysis. The Canadian Journal of Psychiatry−Research Methods in Psychiatry, 50, 115-122.

Squire, L.R., Zola-Morgan, S., & Chen, K.S. (1988). Human amnesia and animal models of amnesia: Performance of amnesic patients on tests designed for the monkey. Behavioral Neuroscience, 102, 210-221.

Squire, L.R., & Zola-Morgan, S. (1991). The medial temporal lobe memory system. Science 253, 1380–1386.

Squire, L.R., Stark, C.E.L., & Clark, R.E. (2004). The medial temporal lobe. Annual Review of Neuroscience, 27, 279–306.

Squire, L.R., Wixted, J.T., & Clark, R.E. (2007). Recognition memory and the medial temporal lobe: a new perspective. Nature Review Neuroscience, 8, 872–883.

Staresina, B.P., & Davachi, L. (2008). Selective and shared contributions of the hippocampus and perirhinal cortex to episodic ítem and associative encoding. Journal of Cognitive Neuroscience, 20, 1478-1489.

Staresina, B.P., Fell, J., Do Lam, A.T., Axmacher, N., & Henson, R.N. (2012). Memory signals are temporally dissociated in and across human hippocampus and perirhinal cortex. Nature Neuroscience, 15, 1167-73.

Staresina, B.P., Fell, J., Dunn, J.C., Axmacher, N., & Henson, R.N. (2013). Using state-trace analysis to dissociate the functions of the human hippocampus and perirhinal cortex in recognition memory. Proceedings of the National Academy of Science, 110, 3119-3124.

Stark, C.E.L., Bayley, P.J., & Squire, L.R. (2002). Recognition memory for single items and for associations is similarly impaired following damage to the hippocampal region. Learning & Memory, 9, 238-242.

Stark, C.E.L., & Squire, L.R. (2000). Recognition memory and familiarity judgments in severe amnesia: No evidence for a contribution of repetition priming. Behavioral Neuroscience, 114, 459-467.

Steele, K., & Rawlins, J.N., (1993). The effects of hippocampectomy on performance by rats of a running recognition task using long lists of non-spatial items. Behavioural Brain Research 54, 1–10.

Steward, O., & Scoville, S.A. (1976). Cells of origin of Entorhinal cortical afferents to the hippocampus and fascia dentata of the rat. Journal of Comparative Neurology, 16, 347-370.

Strange, B.A., Witter, M.P., Lein, E., & Moser, E.I. (2014). Functional organization of the hippocampal longitudinal axis. Nature Reviews Neuroscience,10, 655-669.

Strong, E.K. (1913). The effect of time-interval upon recognition memory. The Psychological Review, XX, 339-372.

Strong, M., & Strong, E.K. (1916). The Nature of Recognition Memory and of the Localization of Recognitions. The American Journal of Psychology 27, 341–362.

Suh, J., Rivest, A.J., Nakashiba, T., Tominaga, T., Tonegawa, S. (2011). Entorhinal Cortex Layer III Input to the Hippocampus Is Crucial for Temporal Association Memory. Science, 334, 1415-1420.

Suzuki, W.A., Zola-Morgan, S., Squire, L.R., & Amaral, D.G. (1993). Lesions of the perirhinal and parahippocampal cortices in the monkey produce long-lasting memory impairment in the visual and tactile modalities. Journal of Neuroscience, 13, 2430–2451.

Swank, M.W., Ellis, A.E., & Cochran, B.N. (1996). c-Fos antisense blocks acquisition and extinction of conditioned taste aversion in mice. NeuroReport, 7, 1866-1870.

Swanson, L.W., & Cowan, W.M. (1975). Hippocampo-hypothalamic connections: Origin in subicular cortex, not ammon's horn. Science, 189, 303–304.

Swanson, L.W. (1992). Brain maps: structure of the rat brain, Elsevier, Amsterdam.

Tabachnick, B.G., & Fidell, L.S. (2001). Using Multivariate Statistics, 4th edn. Allyn & Bacon, Needham, MA.

Tafazoli, S., Di Filippo, A., & Zoccolan, D. (2012). Transformation-tolerant object recognition in rats revealed by visual priming. Journal of Neuroscience, 32, 21–34.

Tamamaki, N., & Nojyo, Y. (1995). Preservation of topography in the connections between the subiculum, field CA1, and the entorhinal cortex in rats. Journal of Comparative Neurology, 353, 379-390.

Templer, V.L., & Hampton, R.R. (2013). Cognitive mechanisms of memory for order in rhesus monkeys (Macaca mulatta). Hippocampus, 23, 193-201.

Tischmeyer, W., & Grimm, R. (1999). Activation of immediate early genes and memory formation. Cellular and Molecular Life Science, 55, 564-574.

Tulving, E. (1972). Episodic and semantic memory. In: Organization of Memory (Tulving, E., Donaldson, W., eds), pp. 381-403. New York: Academic Press.

Turriziani, P., Fadda, L., Caltagirone, C., & Carlesimo, G.A. (2004). Recognition memory for single items and for associations in amnesic patients. Neuropsychologia, 42, 426–433.

Uncapher, M.R., Otten, L.J., & Rugg, M.D. (2006). Episodic encoding is more than the sum of its parts: An fMRI investigation of multifeatural contextual encoding. Neuron, 53, 547-556.

van Strien, N.M., Cappaert, N.L.M., & Witter, M.P. (2009). The anatomy of memory: An interactive overview of the parahippocampal–hippocampal network. Nature Review Neuroscience, 10, 272-282.

VanElzakker, M., Fevurly, R.D., Breindel, T., & Spencer, R.L. (2008). Environmental novelty is associated with a selective increase in Fos expression in the output elements of the hippocampal formation and the perirhinal cortex. Learning & Memory, 15, 899-908.

Vann, S.D., Brown, M.W., Erichsen, J.T., & Aggleton, J.P. (2000). Using Fos Imaging in the Rat to Reveal the Anatomical Extent of the Disruptive Effects of Fornix Lesions. Journal of Neuroscience, 20, 8144–8152.

Vann, S.D., Tsivilis, D., Denby, C.E., Quamme, J., Yonelinas, A.P., Aggleton, J.P., Montaldi, D., & Mayes, A.R. (2009). Impaired recollection but spared familiarity in patients with extended hippocampal system damage: convergence across three methods. Proceedings of the National Academy of Science, 106, 5442-5447.

Vertes, R.P. (2004). Differential projections of the infralimbic and prelimbic cortex in the rat. Synapse, 51, 32-58.

Vertes, R.P., Hoover, W.B., Szigeti-Buck, K., & Leranth, C. (2007). Nucleus reuniens of the midline thalamus: Link between the medial prefrontal cortex and the hippocampus. Brain Research Bulletin, 71, 601–609.

Voss, J.L., Lucas, H.D., & Paller, K.A. (2012). More than a feeling: Pervasive influences of memory without awareness of retrieval. Cognitive Neuroscience, 3, 193-207.

Wagner, A.R. (1981). SOP: A model of automatic memory processing in animal behavior. In: Information processing in animals: Memory mechanisms (Spear, N.E. & Miller, R.R. eds.) pp. 5-47. Hillsdale, NJ: Erlbaum.

Wais, P.E., Mickes, L., & Wixted, J.T. (2008). Remember/know judgments probe degrees of recollection. Journal of Cognitive Neuroscience, 20, 400–405.

Wais, P.E., Wixted, J.T., Hopkins, R.O., & Squire, L.R. (2006). The hippocampus supports both the recollection and the familiarity components of recognition memory. Neuron, 49, 459-466.

Wan, H., Aggleton, J.P., & Brown, M.W. (1999). Different contributions of the hippocampus and perirhinal cortex to recognition memory. Journal of Neuroscience, 19, 1142- 1148.

Wan, H., Warburton, E.C., Kusmiereck, P., Aggleton, J P., Kowalska, D.M., & Brown, M.W. (2001). Fos imaging reveals differential neuronal activation of areas of rat temporal cortex by novel and familiar sounds. European Journal of Neuroscience, 14, 118-124.

Wan, H., Warburton, E.C., Zhu, X.O., Koder, T.J., Park, Y., Aggleton, J.P., Cho, K., Bashir, Z.I., & Brown, M.W. (2004). Benzodiazepine impairment of perirhinal cortical plasticity and recognition memory. European Journal of Neuroscience, 20, 2214-2224.

Wang, S.-H., Redondo, R.L., & Morris, R.G.M. (2010). Relevance of synaptic tagging and capture to the persistence of long-term potentiation and everyday spatial memory. Proceedings of the National Academy of Science, 107, 19537–19542.

Warburton, E.C., & Brown, M.W. (2010). Findings from animals concerning when interactions between perirhinal cortex, hippocampus and medial prefrontal cortex are necessary for recognition memory. Neuropsychologia, 48, 2262-2272.

Warburton, E.C., Glover, C.P.J., Massey, P.V., Wan, H., Johnson, B., Bienemann, A., Deuschle, U., Kew, J.N.C., Aggleton, J.P., Bashir, Z.I., Uney, J.B., & Brown, M.W. (2005). CREB phosphorylation is necessary for perirhinal LTP and recognition memory. Journal of Neuroscience, 25, 6296-6303.

Warburton, E.C., Koder, T., Cho, K., Massey, P.V., Duguid, G., Barker, G.R.I., Aggleton, J.P., Bashir, Z.I., & Brown, M.W. (2003). Cholinergic neurotransmission is essential for perirhinal cortical plasticity and recognition memory. Neuron, 38, 987-996.

Weierich, M.R., Wright, C.I., Negreira, A., Dickerson, B.C., Barrett, L.F. (2010). Novelty as a dimension in the affective brain. NeuroImage, 49, 2871–2878.

Wiig, K.A., & Bilkey, D.K. (1994a). Perirhinal cortex lesions in rats disrupt performance in a spatial DNMS task. NeuroReport 5:1405–1408.

Wiig, K.A., & Bilkey, D.K. (1994b). The effects of perirhinal cortical lesions on spatial reference memory in the rat. Behavioural Brain Research, 63, 101–109.

Wilson, D.I.G., Langston, R.F., Schlesiger, M.I., Wagner, M., Watanabe, S., & Ainge, J.A. (2013a). Lateral entorhinal cortex is critical for novel object-context recognition. Hippocampus, 23, 352-366.

Wilson, D.I.G., Watanabe, S., Milner, H., & Ainge, J.A. (2013b). Lateral entorhinal cortex is necessary for associative but not nonassociative recognition memory. Hippocampus, 23, 1280-1290.

Winters, B. D., Forwood, S. E., Cowell, R., Saksida, L. M., & Bussey, T.J. (2004). Double dissociation between the effects of peri-postrhinal cortex and hippocampal lesions on tests of object recognition and spatial memory: Heterogeneity of function within the temporal lobe. Journal of Neuroscience, 24, 5901-5908.

Winters, B.D., & Bussey, T.J. (2005). Transient inactivation of perirhinal cortex disrupts encoding, retrieval and consolidation of object recognition memory. Journal of Neuroscience, 25, 52-61.

Winters, B.D., Saksida, L.M., & Bussey, T.J. (2008). Object recognition memory: Neurobiological mechanisms of encoding, consolidation and retrieval. Neuroscience and Biobehavioral Reviews, 32, 1055-1070.

Witter, M.P. (1993). Organization of the entorhinal-hippocampal system: A review of current anatomical data. Hippocampus, 3, 33-44.

Witter, M. P., Naber, P.A., van Haeften, T., Machielsen, W.C.M., Rombouts, S.A.R.B., Barkhof, F., Scheltens, P., & Lopes da Silva, F.H. (2000). Cortico-hippocampal communication by way of parallel parahippocampal-subicular pathways. Hippocampus, 10, 389-410.

Wixted, J.T., & Squire, L.R. (2011). The medial temporal lobe and the attributes of memory. Trends in Cognitive Sciences, 15, 210–217.

Wolff, M., Gibb, S.J., & Dalrymple-Alford, J.C. (2006). Beyond spatial memory: the anterior thalamus and memory for the temporal order of a sequence of odour cues. Journal of Neuroscience, 26, 2907-2913.

Woloszyn, L., & Sheinnberg, D.L. (2012). Effects of long-term visual experience on responses of distinct classes of single units in inferior temporal cortex. Neuron, 74, 193–205.

Wothke, W. (1993). Nonpositive definite matrices in structural equation modeling. In: Testing structural equation models (Bollen, K.A., & Long, J.S., eds.). pp. 256–93. London: Sage Publications.

Wright, N.F., Vann, S.D., Erichsen, J.T., O'Mara, S., & Aggleton, J.P. (2013). Segregation of parallel inputs to the anteromedial and anteroventral thalamic nuclei of the rat. Journal of Comparative Neurology, 521, 2966-2986.

Wyss, J.M., Chambless, B.D., Kadish, I. & Van Groen, T. (2000). Age-related decline in water maze learning and memory in rats: strain differences. Neurobiology of Aging, 21, 671-681.

Xiang, J.Z., & Brown, M.W. (1998). Differential neuronal encoding of novelty, familiarity and recency in regions of the anterior temporal lobe. Neuropharmacology, 37, 657-676.

Yanike, M., Wirth, S., & Suzuki, W.A. (2004). Representation of well-learned information in the monkey hippocampus. Neuron, 3, 477-487.

Yonelinas, A.P. (2002). The nature of recollection and familiarity: A review of 30 years of research. Journal of Memory Language, 46, 441-517.

Zangenehpour, S., & Chowdhari, A. (2002). Differential induction and decay curves of c-fos and zif268 revealed through dual activity maps. Molecular Brain Research, 109, 221-225.

Yonelinas, A., Kroll, N.E.A., Dobbins, I., Lazzara, M., & Knight, R.T. (1998). Recollection and familiarity deficits in amnesia: Convergence of remember/know, process dissociation and receiver operating characteristic data. Neuropsychology 12, 323–339.

Yonelinas, A., Kroll, N.E., Quamme, J.R., Lazzara,M.M., Sauve, M.J., Widaman, K.F., & Knight, R.T. (2002). Effects of extensive temporal lobe damage or mild hypoxia on recollection and familiarity. Nature Neuroscience 5, 1236–1241.

Yonelinas, A.P., Otten, L.J., Shaw, K.N., & Rugg, M.D. (2005). Separating the brain regions involved in recollection and familiarity in recognition memory. Journal of Neuroscience, 25, 3002–3008.

Yonelinas, A.P., & Parks, C.M. (2007). Receiver operating characteristics (ROCs) in recognition memory: A review. Psychological Bulletin, 133, 800–832.

Zar, J.H. (2010). Biostatistical analysis Prentice-Hall/Pearson.

Zeamer, A., Meunier, M., & Bachevalier, J. (2011). Stimulus similarity and encoding time influence incidental recognition memory in adult monkeys with selective hippocampal lesions. Learning & Memory, 18, 170-180.

Zhu, X.O., Brown, M.W., & Aggleton, J.P. (1995a). Neuronal signalling of information important to visual recognition memory in rat rhinal and neighbouring cortices. European Journal of Neuroscience, 7, 753-765.

Zhu, X.O., Brown, M. W., McCabe, B. J., & Aggleton, J. P. (1995b). Effects of the novelty or familiarity of visual stimuli on the expression of the intermediate early gene c-fos in the rat brain. Neuroscience, 69, 821-829.

Zhu, X.O., McCabe, B.J., Aggleton, J.P. & Brown, M. W. (1996). Mapping recognition memory through the differential expression of the immediate early gene c-fos induced by novel or familiar visual stimulation. NeuroReport, 7, 1871-1875.

Zhu, X. O., McCabe, B. J., Aggleton, J.P., & Brown M. W. (1997). Differential activation of the hippocampus and perirhinal cortex by novel visual stimuli and a novel environment. Neuroscience Letters, 229, 141-143.

Zola, S.M., Squire, L.R., Teng, E., Stefanacci, L., Buffalo, E.A., & Clark, R.E. (2000). Impaired recognition memory in monkeys after damage limited to the hippocampal region. Journal of Neuroscience, 20, 451–463.

Zola, S.M., & Squire, L.R. (2001). Relationship between magnitude of damage to the hippocampus and impaired recognition memory in monkeys. Hippocampus, 11, 92-98.

Zola-Morgan, S., Squire, L.R., & Ramus, S.J. (1994). Severity of memory impairment in monkeys as a function of locus and extent of damage within the medial temporal lobe memory system. Hippocampus, 4, 483–495.

Zola-Morgan, S., Squire, L.R., Amaral, D.G., & Suzuki, W.A. (1989). Lesions of perirhinal and parahippocampal cortex that spare the amygdala and hippocampal formation produce severe memory impairment. Journal of Neuroscience, 9, 4355-4370.

Zola-Morgan, S., Squire, L.R., Clower, R.P., Rempel, N.L., (1993). Damage to the perirhinal cortex exacerbates memory impairment following lesions to the hippocampal formation. Journal of Neuroscience, 13, 251-65.

Zola-Morgan, S., Squire, L.R., Rempel, N.L., Clower, R.P., & Amaral, D.G. (1992). Enduring memory impairment in monkeys after ischemic damage to the hippocampus. Journal of Neuroscience, 12, 2582–2596.